MORE THAN JUST A DIMER:
DETECTION OF G PROTEIN-COUPLED RECEPTOR OLIGOMERS USING FLUORESCENT PROTEIN REASSEMBLY OF STE2P, A YEAST PHEROMONE RECEPTOR

A THESIS SUBMITTED TO
THE GRADUATE SCHOOL OF NATURAL AND APPLIED SCIENCES
OF
MIDDLE EAST TECHNICAL UNIVERSITY

BY

ORKUN CEVHEROĞLU

IN PARTIAL FULFILLMENT OF THE REQUIREMENTS
FOR
THE DEGREE OF DOCTOR OF PHILOSOPHY
IN
BIOTECHNOLOGY

AUGUST 2015

Approval of the thesis:

MORE THAN JUST A DIMER: DETECTION OF G PROTEIN-COUPLED RECEPTOR OLIGOMERS USING FLUORESCENT PROTEIN REASSEMBLY OF STE2P, A YEAST PHEROMONE RECEPTOR

submitted by **ORKUN CEVHEROĞLU** in partial fulfillment of the requirements for the degree of **Doctor of Philosophy in Biotechnology Department**, **Middle East Technical University** by,

Prof. Dr. Gülbin Dural Ünver
Dean, Graduate School of **Natural and Applied Sciences**

Prof. Dr. Filiz Bengü Dilek
Head of Department, **Biotechnology**

Assoc. Prof. Dr. Çağdaş Devrim Son
Supervisor, **Biology Dept., METU**

Prof. Dr. Mahinur Akkaya
Co-Supervisor, **Chemistry Dept., METU**

Examining Committee Members:

Prof. Dr. Engin Umut Akkaya
Chemistry Dept., Bilkent University

Assoc. Prof. Dr. Çağdaş Devrim Son
Supervisor, Biology Dept., METU

Assist. Prof. Dr. Filiz Bakar
Pharmacology Dept., Ankara University

Assoc. Prof. Dr. Mesut Muyan
Biology Dept., METU

Assoc. Dr. Can Özen
Biotechnology Dept., METU

Date: 28.08.2015

I hereby declare that all information in this document has been obtained and presented in accordance with academic rules and ethical conduct. I also declare that, as required by these rules and conduct, I have fully cited and referenced all material and results that are not original to this work.

Name, Last name: ORKUN CEVHEROĞLU

Signature:

ABSTRACT

MORE THAN JUST A DIMER:
DETECTION OF G PROTEIN-COUPLED RECEPTOR OLIGOMERS USING FLUORESCENT PROTEIN REASSEMBLY OF STE2P,
A YEAST PHEROMONE RECEPTOR

Cevheroğlu, Orkun
Ph.D., Department of Biotechnology

Supervisor: Assoc. Prof. Dr. Çağdaş Devrim Son
Co-Supervisor: Prof. Dr. Mahinur Akkaya

August 2015, 185 pages

GPCRs are known to form homo- and hetero-dimers and this interaction could have important roles in internalization, maturation, function and/or pharmacology of these receptors. In the first part of the study bimolecular fluorescence complementation (BiFC) using split enhanced green fluorescent protein (EGFP) was used to determine the interaction and cellular location between various Ste2p constructs. Co-expression of two constructs, one with the N-terminus of EGFP inserted into the full-length receptor at the end of the 7th transmembrane domain and the other with the C-terminus of EGFP inserted at the same position, led to the discovery of dimers both at the cell surface and intracellularly as shown by BiFC. Only cell surface dimerization was observed when truncated receptors with the N-terminus of EGFP or the C-terminus of EGFP attached to the 7th transmembrane domain were co-expressed. Co-expression of EGFP-tagged truncated receptors with tagged full-length receptors showed dimers intracellularly and on the plasma membrane indicating that truncated receptor could interact with full-length receptor. Fluorescence as a result of BiFC requires dimer formation, but whether the receptors were also forming higher order aggregates could not be determined by the method used. Using bimolecular fluorescence complementation, we present the evidence that both full length and C-terminally truncated Ste2p traffics to the membrane as a monomer and forms dimers on the cell membrane. C-terminally truncated receptors do not appear to be internalized. In contrast, full-length receptors can internalize as dimers and/or higher oligomers. This study shows that yeast pheromone receptor, Ste2p dimerize on the plasma membrane and are internalized as dimers or oligomers. The BiFC method provided the first evidence of the localization of dimers of truncated and full-length Ste2p. In the second part of the study, BiFC constructs from the first part and new BiFC constructs; truncated receptors with the N-terminus of mCherry or the C-terminus of mCherry attached to the 7th transmembrane domain; as well as, full length or truncated receptors tagged with full length EGFP or mCherry was used to show three and four receptor oligomerization of Ste2p, taking advantage of endocytosis using colocalization and FRET methods.

Keywords: G protein-coupled receptor (GPCR), receptor trafficking, confocal fluorescence microscopy, bimolecular fluorescence complementation (BiFC), Förster resonance energy transfer (FRET).

ÖZ

DİMERDEN FAZLASI: G PROTEİNE KENETLİ RESEPTÖR ETKİLEŞİMİNİN, STE2P MAYA FEROMON RESEPTÖRÜ'NDE FLORESAN PROTEİN BİRLEŞMESİ İLE GÖSTERİLMESİ

Cevheroğlu, Orkun
Doktora, Biyoteknoloji Bölümü

Tez Yöneticisi: Doç. Dr. Çağdaş Devrim Son
Ortak Tez Yöneticisi: Prof. Dr. Mahinur Akkaya

Ağustos 2015, 185 sayfa

GPKRlerin kendileri ve diğer GPKRler ile eşleştikleri bilinmektedir, bu eşleşmenin reseptör intörnalizasyonu, olgunlaşması, işlev ve farmakolojisi üzerinde önemli rolü olduğu düşünülmektedir. Bu çalışmanın ilk kısmında gelişmiş yeşil protein (EGFP) ve çift moleküllü floresan birleştirme metodu (BiFC) tekniğini kullanarak Ste2p proteinin kendisi ile etkileşimini ve bu etkileşimin hücre içindeki yerini tayin ettik. Yedinci transmembran altyapısından biri N-EGFP diğeri C-EGFP ile işaretlenmiş tam uzunluktaki Ste2p eşzamanlı olarak hücrelere ürettirildiğinde, eşleşmenin hem hücre zarında hem de hücre içerisinde olduğu BiFC metodu ile gösterildi. Yedinci transmembran altyapısından N-EGFP ve C-EGFP ile işaretlenmiş C kuyruğu kesik Ste2p reseptörlerinde ise eşleşme sadece hücre zarında gözlemlendi. EGFP parçalarıyla işaretli tam uzunluktaki ve kuyruğu kesik reseptörler hücrede eşzamanlı üretttirildiğinde ise eşleşmenin hem hücre zarında hem de hücre içerisinde olduğu, dolayısıyla kesik reseptörlerin, tam uzunluktaki reseptörlerle etkileşebildiği gözlemlendi. BiFC metodundaki floresan sadece ikili eşleşmeyi gösterebilmektedir, reseptörlerin ikiden fazla etkileşimlerinin olup olmadığı bu metotla gösterilememektedir. İki moleküllü floresan birleşme (BiFC) metodunu kullanarak, Ste2p reseptörlerinin hücre zarına monomer olarak taşındığını, zarda eşleştiklerini gösterdik. C-kuyruğu kesik reseptör çiftlerinin hücre zarından intörnalize olmadıklarını, tam uzunluktaki reseptör çiftlerininse ikili ya da çoklu eşleşerek intörnalize olduklarını gösterdik. Bu çalışma, maya feromon reseptörü olan Ste2p'nin hücre zarında eşleştiğini ve ikili ya da çoklu olarak intörnalize olduklarını göstermektedir. Kullanılan BiFC metodu kesik ve tam uzunluktaki reseptörlerin nerede eşleştikleri hakkında ilk delilleri sunmaktadır. Çalışmanın ikinci kısmında ise, Yedinci transmembran altyapısından biri N-mCherry diğeri C-mCherry ile işaretlenmiş tam C-kuyruğu kesik Ste2p reseptörleri ve tam uzunluktaki EGFP ve mCherry ile işaretlenmiş, C-kuyruğu kesik ve tam uzunluktaki reseptörler kullanılarak, endositoz, kolokalizasyon ve FRET metodlarıyla üçlü ve dörtlü reseptör etkileşimleri tespit edilmiştir.

Anahtar sözcükler: G proteine kenetli reseptörler, reseptör trafiği, konfokal floresan mikroskobu, iki moleküllü floresan birleşme, Förster enerji transferi (FRET).

In the vast sea of the knowledge,
I feel as blank as this page.

ACKNOWLEDGMENTS

I am aware that I have received more than my fair share when it comes to mentors. I would like to thank Dr. Çağdaş Son, for his continuous support, encouragement and optimism on the challenges of this tedious path, and Dr. Jeffrey Becker for sharing his vast experience, for his guidance and patience. It was a valuable opportunity for me to work with two such distinguished scientists. Their critical suggestions helped me overcome a lot of setbacks throughout this work and I can sincerely admit that this dissertation is a result of their mutual support.

A big thank you also goes to Becker lab and Son lab members that I worked with. I would like to thank Dr. Melinda Hauser for our discussions. Her approach, different perspectives contributed in lots of points to my research that I might have easily missed without her. I would also like to thank Sarah Kauffman for her help with my experiments, for being such a great lab mate and a coffee mate with Elena Ganusova. An acknowledgments section would be missing without thanking Sarah for bringing her awesomely delicious cookies. I also would like to thank Dr. Steven Wright for our scientific discussions and ideas during his visits to Becker lab.

Unfortunately funding is one of the most essential things for the research and for us, the scientists conducting the research. So, I would like to thank Turkish Academy of Sciences (TUBITAK Grant no. 110T414), International Reintegration Grants Marie Curie Actions (Grant no. PIRG07-GA-2010-268336) and National Institute of Health (NIH Grant no. GM112496) for supporting this research. I would also like to thank Turkish Academy of Sciences for supporting me with a 2214/A scholarship (Grant no. B.14.2.TBT.0.06.01-214-83) to conduct part of my PhD research at University of Tennessee.

I could not have gotten here without the unconditional love and support of my family: my mom, Emel Cevheroğlu; my dad, Dr. Şemsettin Cevheroğlu; and of course my grandma, Sezaver Tekçe, who will always live in my memories and in my heart. I love you all very much.

I think love is another thing I have received much more than my fair share in this life. So, last but not least, a huge thank you goes to the love of my life, Burcu Cevheroğlu. Thank you dearly for all your support, understanding and your love. You are the nicest, kindest and most beautiful thing has ever happened to me. I love you.

TABLE OF CONTENTS

ABSTRACT v
ÖZ vii
ACKNOWLEDGMENTS x
TABLE OF CONTENTS xii
LIST OF TABLES xiv
LIST OF FIGURES xv
LIST OF ABBREVIATIONS xxxi

CHAPTERS

1 INTRODUCTION 1
  1.1 G-Protein Coupled Receptors: Structure, Function and Significance 1
  1.2 Yeast GPCRs and Ste2p as a model GPCR 3
    1.2.1 Yeast pheromone signaling pathway: 5
    1.2.2 Yeast glucose sensing mechanism: 9
  1.3 GPCR Oligomerization 11
  1.4 Fluorescence methods for detecting GPCR oligomerization 16
    1.4.1 Fluorescence proteins 16
    1.4.2 Bimolecular fluorescence complementation assay (BiFC): 23
    1.4.3 Förster resonance energy transfer (FRET): 27
  1.5 Aim of the study 34
2 EXPERIMENTAL PROCEDURES 35
  2.1 Materials 35
    2.1.1 Yeast strains, plasmids and media 35
    2.1.2 Bacterial Strains, Media and Growth Conditions 36
    2.1.3 Chemical reagents and other materials 37

2.2 Protocols ... 37
2.2.1 High Efficiency Transformation of chemically competent E.coli Cells . 37
2.2.2 Yeast Transformation ... 38
2.2.3 Insertional PCR protocol for the construction of tagged Ste2p ... 39
2.2.4 Site directed mutagenesis ... 45
2.2.5 Ligation protocol for constructs ... 48
2.3 Growth Arrest (Halo) Assay ... 52
2.4 FUS1-lacZ gene induction assay ... 52
2.5 Binding Assays ... 53
2.6 Membrane Preparation ... 53
2.7 Western Blot Analysis ... 54
2.8 Knocking Out URA3 (YEL021W) gene from LM102 cells ... 55
2.9 Imaging with Laser Scanning Confocal Microscope ... 58
3 RESULTS AND DISCUSSION ... 61
3.1 Construction of plasmids carrying tagged Ste2p ... 61
3.1.1 Construction of plasmid carrying EGFP and mCherry tagged Ste2p ... 62
3.1.2 Construction of Ste2p constructs tagged with EGFP or mCherry fragments ... 65
3.1.3 Removing FLAG^{TM} and His$_6$ epitope tags from Ste2p constructs ... 67
3.1.4 Disturbing G^{56}XXXG^{60} dimerization motif on Ste2p constructs ... 69
3.1.5 Growth arrest assays of Ste2p constructs ... 74
3.1.6 Western blot experiment of Ste2p constructs ... 78
3.1.7 Saturation binding experiments ... 83
3.2 Microscopy of cells expression Ste2p tagged with EGFP or split EGFP 85
3.2.1 Detection of monomers of full-length Ste2p tagged with EGFP ... 85
3.2.2 Detection of dimers of full-length Ste2p tagged with split EGFP ... 87
3.2.3 Detection of monomers of truncated Ste2p tagged with EGFP ... 89
3.2.4 Detection of dimers of truncated Ste2p tagged with split EGFP ... 90

3.2.5 Detection of dimers of full-length and truncated Ste2p with spilt EGFP 91
3.2.6 Conclusion of first part 97
3.3 More than just a dimer: studying oligomerization of Ste2p 98
3.3.1 Construction of galactose inducible double promoter vectors 98
3.3.2 Construction of constitutively active double promoter vectors 106
3.3.3 Growth arrest assays of Ste2p constructs cloned into double promoter plasmids 113
3.3.4 Western blot experiment of Ste2p constructs cloned into double promoter plasmid 116
3.4 Imaging of higher Ste2p oligomers 119
3.4.1 Detection of oligomerization taking advantage of endocytosis 119
3.4.2 Detection of oligomerization using sensitized emission 123
3.4.3 Detection of oligomerization using acceptor photobleaching 125
3.5 Conclusion to the second part 127
REFERENCES 129

APPENDICES

A.YEAST MEDIA PREPARATION 149
B. BACTERIAL MEDIA PREPARATION 153
C. SOLUTIONS AND BUFFERS 155
D. CODING SEQUENCES OF STE CONSTRUCTS 159

LIST OF TABLES

TABLES

Table 1.1 Potential FRET pairs according to their spectral profiles.......................... 31

Table 2.1 Primers for amplifying N-EGFP (1-158) and C-EGFP (159-238) to carry complementary overhanging regions from the 304-305th positions on Ste2p receptor. 41

Table 2.2 Primers designed for amplifying N-EGFP (1-158) and C-EGFP (159-238) to carry complementary overhanging regions from the 304-305th positions on Ste2p receptor and to insert a stop codon right before 305th position.................................. 41

Table 2.3 Primers for amplifying N-mCherry (1-159) and C-EGFP (160-237) carrying complementary overhanging Ste2p sequences upstream and downstream from the 304-305th and inserting a stop codon right before 305th position................ 42

Table 2.4 Primers to remove the FLAG and HIS tags from expressed Ste2p. 46

Table 2.5 Primers to remove the stop codon at 305th position from Ste2p................ 47

Table 2.6 Primers designed to mutate Glycines to Leucine at positions 56 and 60 on Ste2p. 47

Table 2.7 Primers designed to mutate proline to aspartic acid at position 290 on Ste2p. 47

Table 2.8 Primers for cloning Ste2p constructs into pESC vectors........................... 48

Table 2.9 TEF1-PGK1 and PGK1-TEF1 promoter region amplification primers. 50

Table 2.10 Coding sequence of URA3 gene from S288C strain. Obtained from https://wwww.yeastgenome.org. 56

Table 2.11 Primers used to amplify Kan^r gene cassette with flanking URA3 regions. 56

Table 3.1 Plasmids (1st column) constructed for this study and the abbreviated names of the Ste2p construct expressed (2nd column). 67

Table 3.2 The amount of α-factor (μg) that yielded a 25mm halo zone for EGFP constructs. 78

Table 3.3 K_d, B_{max} and number of receptors at the plasma membrane calculated from the B_{max} for the constructs. 84

Table 3.4 Abbreviated names of the Ste2p constructs (1st column) constructed from pESC vectors (2nd column) and the position of inserts (3rd and 4th columns). 103

Table 3.5 Constructed plasmids to study the interaction of 3 or more receptor. G1 stands for TEF1-PGK1 divergent promoter region, G2 stands for PGK1-TEF1 region. 112

LIST OF FIGURES

FIGURES

Figure 1.1 Schematic representation of signaling by heterotrimeric G proteins upon the activation of receptor with its agonist [6]. In their GDP bound inactive state, the G protein α subunit (G_α) stays as a heterotrimeric protein complex associated with the G protein βγ heterodimer ($G_{\beta\gamma}$). Upon agonist binding to a receptor GDP on G_α phosphorylates to GTP, leading the dissociation (or rearrangement) of heterodimeric $G_{\beta\gamma}$ subunits. These dissociated subunits initiate cellular signaling by activating effectors inside the cell. RGS (regulator of G protein signaling) proteins bind to G_α to stimulate GTP hydrolysis, so the GTP molecule on G_α is hydrolyzes back to GDP resulting a reassociation (or rearrangement) of inactive heterotrimeric protein complex. In the inactive heterotrimeric complex $G_{\beta\gamma}$ inhibits guanine nucleotide exchange therefore desensitizes the receptor. $G_{\beta\gamma}$, acts as a dual signal regulator both playing a positive role in signal transduction after the dissociation from G_α; and a negative role by desensitizing the receptor as a result of reassociation with G_α. 2
Figure 1.2 Mating-Pheromone Response Pathway in *S.cerevisiae* (© 2009 QIAGEN, all rights reserved) 6
Figure 1.3 Overview of pheromone and glucose signaling in *S. cerevisiae.* The putative glucose receptor Gpr1 activates the G_α protein Gpa2. Although Gpb1/Krh2 and Gpb2/Krh1 proteins were shown to interact with Gpa2 and act as G_β mimic, still it is not clear that whether these proteins constitute $G_{\beta\gamma}$ subunit, of if any such subunit exists. Rgs2 stimulates the GTPase activity of Gpa2 and thus inhibits glucose-induced cAMP signaling. Gpa2 is thought to activate adenylate cyclase (Cdc35/Cyr1) but direct biochemical evidence for this is still lacking. The basal activity of adenylate cyclase also depends on the Ras1 and Ras2 proteins of which the signaling function, if any, remains unclear. Activation of PKA by cAMP results in stimulation of growth

and pseudohyphal differentiation, loss of stress resistance, mobilization of trehalose and glycogen and in reduced life-span. Pheromone sensing depends on the Ste2 and Ste3 receptors that respectively bind α- and **a**-factor and that transmit the signal to the heterotrimeric G-protein consisting of the G_α protein Gpa1 and the βγ subunit Ste4 and Ste18. The RGS protein Sst2 is able to diminish signaling by stimulating the GTPase activity of Gpa1. Ste4 recruits both the scaffolding protein Ste5 and Ste20 (which can also be stimulated by Cdc42) to the membrane resulting in activation of the mating MAP kinase cascade (Ste11, Ste7 and Fus3). Activation of the MAP kinase pathway results in growth arrest and conjugation [99]....................................... 10

Figure 1.4 Chemical reaction leading to the formation of GFP chromophore [138]. 18

Figure 1.5 *A. victoria* GFP β-barrel structure and approximate dimensions [138]. 18

Figure 1.6 Various fluorescent proteins under white light (top panel) and their fluorescence (bottom panel) purified from *E.coli* [143].. 19

Figure 1.7 Chromophore region structures of (A) EBFP (B) ECFP (C) EGFP and (D) EYFP, each chromophore is shaded according to their spectral properties [138]........... 20

Figure 1.8 Excitation (A) and emission (B) spectra of enhanced GFP derivatives [138]. 21

Figure 1.9 mCherry fluorescent protein β-barrel structure and approximate dimensions [138]. 22

Figure 1.10 Representation of reconstitution of fluorescent protein by bimolecular fluorescence complementation [151].. 23

Figure 1.11 Examples of protein fragments that can be used to study protein interactions. The fragments are shown in red and blue using models based on the X-ray crystal structures of the intact proteins. In b-galactosidase, the overlap between the fragments is shown in magenta. The discontinuity in the polypeptide backbone is shown in translucent grey [155]. 24

Figure 1.12 Jablonski diagram illustrating the coupled transitions between the donor emission (red arrow) and acceptor excitation (dashed green arrow) in FRET. Excitation and emission transitions are presented by straight vertical arrows (green and red, respectively). The coupled transitions are shown with dashed lines. In the presence of a suitable acceptor, the donor fluorophore can transfer excited state energy directly to the acceptor without emitting a photon (blue arrow). The resulting sensitized fluorescence emission has characteristics similar to the emission spectrum of the acceptor... 30

Figure 1.13 Representation of FRET phenomena as a result of two interacting GPCRs. 31

Figure 1.14 Crosstalk and bleed through in FRET measurements. 33

Figure 2.1 The representation of 1st PCR, amplification of EGFP from pEGFP-N2 with primers carrying complementary Ste2p sequences (shown in blue) homologous to the insertion position on STE2 gene. 40

Figure 2.2 The representation of 1st PCR, amplification of EGFP fragments from pEGFP-N2 with primers carrying complementary Ste2p sequences (shown in blue) homologous to the insertion position on STE2 gene. 40

Figure 2.3 Representation of 2nd PCR, inserting the fluorescent tag, or fluorescent protein fragments to the directed position on STE2 gene... 43

Figure 2.4 Representative image for inserting the directed mutation with double primer method.. 45

Figure 2.5 pESC-TRP and pESC-URA (Agilent Technologies, CA, USA) vector maps and their multiple cloning sites (MCS) sequences. 49

Figure 2.6 pSP-G1 (TEF1-PGK1) and pSP-G2 (PGK1-TEF1) vector maps. [172] 49

Figure 2.7 pUG6 vector map. 55

Figure 2.8 Agarose Gel (1%) image of PCR amplified Kan^r gene from pUG6 vector. First lane is the 1kb DNA ladder; PCR reaction was loaded into second and third lanes. The upper and most intense band is the amplified Kan^r gene carrying homologous flanking sequences as expected around 1.5kb band; the lower bands are primers. 57

Figure 3.1 Snake diagram of yeast α-pheromone receptor (Ste2p) with a FLAG™ and His$_6$ tag appended to the C-terminus. We designate this construct as wild type for the purpose of this manuscript. The arrow indicates insertion position 304. EL1, EL2 and EL3 are the extracellular loops, IL1, IL2 and IL3 are the intracellular loops and TM1 – TM7 are the transmembrane residues of Ste2p... 62

Figure 3.2 Agarose gel electrophoresis image of optimization PCR for amplification of EGFP and mCherry from pEGFP-N2 and pmCherry-N1 plasmids. The product size was observed between 800bp-700bp ladder bands in GeneRuler^{TM} 100bp plus DNA ladder. 63

Figure 3.3 For inserting EGFP sequence in Ste2p sequence, a gradient PCR reaction was run at 3 different annealing temperatures. Plasmids isolated from these reactions were digested with BamHI – EcoRI enzymes at 37°C for 3h. Ste2p gene is 1386 bp (lower band at pBEC1 digests); EGFP gene is 714 bp so a correct EGFP insert is 2100 bp together. The bands marked with red asterix on gel photo shows Ste2p-EGFP constructs with expected size. These plasmids were verified by sequencing............ 64

Figure 3.4 mCherry sequence was also inserted with and without a stop codon after 305th position on Ste2p. Plasmids isolated from these reactions were digested with BamHI – EcoRI enzymes at 37°C for 3h. The bands marked with red asterix on gel photo shows Ste2p-mCherry constructs with expected size. These plasmids were verified by sequencing. 64

Figure 3.5 EGFP sequence was also inserted with a stop codon after 305th position on Ste2p. Plasmids isolated from these reactions were digested with BamHI – EcoRI enzymes at 37°C for 3h. The bands marked with red asterix on gel photo shows Ste2p-EGFP constructs with expected size. These plasmids were verified by sequencing... 64

Figure 3.6 Agarose gel electrophoresis image of PCR amplified EGFP and mCherry fragments with and without “TAA” stop codon. The product size for N-EGFP and N-mCherry was observed around 500bp ladder bands in GeneRuler^{TM} 100bp plus DNA ladder.. 65

Figure 3.7 N-EGFP and C-EGFP sequences were inserted between 304-305 positions on Ste2p. Plasmids isolated from these reactions were digested with BamHI – EcoRI enzymes at 37°C for 3h. The bands marked with red asterix on gel photo show constructs with expected size, Ste2p[N-EGFP]305-451 size is 1860 bp, Ste2p[C-EGFP]305-451 size is 1626 bp. These plasmids were verified by sequencing. 66

Figure 3.8 N-mCherry and C-mCherry sequences were inserted between 304-305 positions on Ste2p. Plasmids isolated from these reactions were digested with BamHI – EcoRI enzymes at 37°C for 3h. The bands marked with red asterix on gel photo show constructs with expected size, Ste2p[N-mCherry]305-451 size is 1863 bp, Ste2p[C-mCherry]305-451 size is 1620 bp. These plasmids were verified by sequencing. 66

Figure 3.9 Saturation binding data of DK102 cells expressing the split EGFP tagged receptor. Cells expressing WT Ste2p receptor from pBEC1 vector (■); Cells expressing Ste2p[C-EGFP]; C-EGFP (159-238) attached at position 304 of the Ste2p receptor (▲), Cells expressing Ste2p[N-EGFP]; N-EGFP (1-158) attached at position 304 of the Ste2p receptor (△), Cells expressing Ste2p[C-EGFP]305-451; C-EGFP (159-238) inserted between positions 304-305 of the Ste2p receptor (▼), Cells expressing Ste2p[N-EGFP]305-451; N-EGFP (1-158) inserted between positions 304-305 of the Ste2p receptor (▽). 68

Figure 3.10 Saturation binding data of DK102 cells expressing the split EGFP tagged receptor. (a) Cells expressing Ste2p[C-EGFP]; C-EGFP (159-238) attached at position 304 of the Ste2p receptor (▲), Cells expressing Ste2p[N-EGFP]; N-EGFP (1-158) attached at position 304 of the Ste2p receptor (△). (b) Cells expressing Ste2p[C-EGFP]305-451; C-EGFP (159-238) inserted between positions 304-305 of the Ste2p receptor (▼), Cells expressing Ste2p[N-EGFP]305-451; N-EGFP (1-158) inserted between positions 304-305 of the Ste2p receptor (▽)................................. 68

Figure 3.11 *FUS1-lacZ* gene induction assay of G56/60L constructs. 71

Figure 3.12 β-galactosidase activity of Ste2pG56L, Ste2pG60L and Ste2pG56/60L constructs. 72

Figure 3.13 Western blot of the BJS21 cells expressing the constructs, the first lane is an extract of Ste2Δ cells expressing empty vector, the second lane is an extract of

Ste2Δ cells expressing WT Ste2p receptor (52 kDa), third lane shows protein ladder, the lanes four to seven are extracts from cells expressing Ste2p[C-EGFP]305-451 (calc. ≈57 kDa), Ste2p[N-EGFP]305-451 (calc. ≈66 kDa), Ste2pG56/60L[C-EGFP]305-451 (calc. ≈57 kDa), Ste2pG56/60L[N-EGFP]305-451 (calc. ≈66 kDa) respectively. The last three lanes from eight to ten are extracts of Ste2pG56L (52 kDa), Ste2pG60L (52 kDa) and Ste2pG56/60L (52 kDa) respectively. The proteins from lanes 1 to 10 were detected with antireceptor antiserum directed against the N-terminal domain of the α-factor receptor. 73

Figure 3.14 Representative images of growth inhibition zones (halo) in pheromone induced growth arrest assay. Various amounts of pheromone (10 – 0.625 μg for full length constructs [left image], 1 – 0.0625 μg for truncated constructs [right image]) were absorbed onto filter disks. 74

Figure 3.15 Biological assay of Ste2p constructs expressed from pBEC1. Wild-type Ste2p (●); Ste2p[EGFP]305-431, Ste2p receptor with full-length EGFP (1-238) inserted between positions 304-305 (⦿); Ste2p[N-EGFP]305-431, Ste2p receptor with N-EGFP (1-158) inserted between position 304-305 (○)................................. 75

Figure 3.16 Biological assay of Ste2p constructs expressed from pCL01. Wild-type Ste2p (■); Ste2p[C-EGFP]304-431, Ste2p receptor tagged with C-EGFP (159-238) inserted between positions 304-305 (□). 75

Figure 3.17 Biological assay of Ste2p constructs lacking the C-terminus. Ste2p[EGFP], C-terminally truncated Ste2p-Δ305-431 receptor tagged with full length EGFP (1-238) (▲); Ste2p[N-EGFP], C-terminally truncated Ste2p-Δ305-431 receptor tagged with N-EGFP (1-158) attached at position 304 (△); Ste2p[C-EGFP], C-terminally truncated Ste2p-Δ305-431 receptor tagged with C-EGFP (159-238) attached at position 304 (▼)... 76

Figure 3.18 Biological assay of Ste2p constructs expressed from pBEC1. Wild-type Ste2p (●); Ste2p[EGFP]305-431, Ste2p receptor with EGFP (1-238) inserted between positions 304-305 (■); Ste2p[mCherry]305-431, Ste2p receptor with mCherry (1-237) inserted between positions 304-305 (▲)....................................... 76

Figure 3.19 Biological assay of C-terminally truncated Ste2p constructs expressed from pBEC1. Ste2p-Δ305-431 (●); Ste2p[EGFP], C-terminally truncated Ste2p receptor with full-length EGFP (1-238) attached at position 304 (■); Ste2p[mCherry], C-terminally truncated Ste2p receptor with mCherry (1-237) attached at position 304 (▲).. 77

Figure 3.20 Western blot of the BJS21 cells expressing the constructs, the first lane is an extract of Ste2Δ cells expressing WT Ste2p receptor (52 kDa), the lanes three to six are extracts from cells expressing Ste2p[C-EGFP] (calc. ≈42 kDa), Ste2p[N-EGFP] (calc. ≈51 kDa), Ste2p[C-EGFP]305-431 (calc. ≈57 kDa) and Ste2p[N-EGFP]305-431 (calc. ≈66 kDa) respectively. Lane 7 shows cells co-expressing Ste2p[C-EGFP] and Ste2p[N-EGFP]; Lane 8 shows cells co-expressing Ste2p[C-EGFP]305-431 and Ste2p[N-EGFP]305-431. The proteins from lanes 1 to 8 were detected with antireceptor antiserum directed against the N-terminal domain of the α-factor receptor.. 79

Figure 3.21 Western blot of the BJS21 cells expressing the constructs, the first lane is an extract of Ste2Δ cells, the second lane is an extract of Ste2Δ cells expressing WT Ste2p receptor (52 kDa), the lanes 4 to 7 are extracts from cells expressing Ste2p[C-EGFP] (calc. ≈42 kDa), Ste2p[N-EGFP] (calc. ≈51 kDa), Ste2p[C-EGFP]305-431 (calc. ≈57 kDa) and Ste2p[N-EGFP]305-431 (calc. ≈66 kDa) respectively. Lanes 8 and 9 are extracts of Ste2Δ cells transformed with empty plasmid and extract of Ste2Δ cells expressing WT Ste2p receptor (52 kDa) respectively. The proteins at lanes 1 and 2 were detected with anti-FLAG antibody and proteins from lanes 4 to 9 were detected with GFP Rabbit Serum Polyclonal antibody (Molecular Probes)...... 80

Figure 3.22 Western blot of the BJS21 cells expressing the constructs, the first lane is an extract of Ste2Δ cells expressing WT Ste2p receptor (52 kDa), the lanes three to six are extracts from cells expressing Ste2p[EGFP]305-431 (calc. ≈75 kDa), Ste2p[EGFP] (calc. ≈60 kDa), Ste2p[mCherry] (calc. ≈60 kDa) and Ste2p[mCherry]305-431 (calc. ≈75 kDa) respectively. The proteins from lanes 1 to 6 were detected with antireceptor antiserum directed against the N-terminal domain of the α-factor receptor (green channel), proteins at lanes 5 and 6 are also detected with mCherry monoclonal antibody (16D7, Life Technologies, NY, USA) (red channel) using LI-COR Odyssey CLx Infrared Imaging System. 81

Figure 3.23 Western blot of the BJS21 cells expressing the Ste2p constructs detected at two separate channels (a) left blot shows Ste2p constructs detected with antireceptor antiserum directed against the N-terminal domain of the α-factor receptor primary antibody and IRDye 680CW Goat anti-rabbit IGg secondary antibody detected at 680nm (a) the right blot shows Ste2p constructs detected with mCherry monoclonal antibody and IRDye 800CW Goat anti-rat IGg secondary antibody detected at 800nm. 83

Figure 3.24 Saturation binding data of DK102 cells co-expressing the split EGFP receptor pairs. Cells expressing WT Ste2p receptor from pBEC1 vector (●); Cells co-expressing Ste2p[N-EGFP]305-431/Ste2p[C-EGFP]305-431, N-EGFP (1-158) or C-EGFP (159-238) inserted between positions 304-305 of the Ste2p receptor (■); Cells co-expressing Ste2p[N-EGFP]/Ste2p[C-EGFP], N-EGFP (1-158) or C-EGFP (159-238) attached at position 304 of C-terminally truncated Ste2p receptor (□). 84

Figure 3.25 Cells expressing EGFP tagged full length Ste2p, scale bars correspond 5 μm length. **(a)** Shows cells expressing Ste2p[EGFP]305-431. **(b)** Shows cells expressing Ste2p[EGFP]305-431 treated with latrunculin A. **(c)** Shows cells expressing Ste2p[EGFP]305-431 treated with cycloheximide. 86

Figure 3.26 Cells co-expressing full length Ste2p tagged with either N-EGFP or C-EGFP, scale bars correspond 5 μm. **(a)** Shows cells co-expressing Ste2p[N-EGFP]305-431 / Ste2p[C-EGFP]305-431; Ste2p BiFC pair tagged with either N-EGFP (1-158) or C-EGFP (159-238) inserted between position 304-305. **(b)** Shows cells co-expressing Ste2p[N-EGFP]305-431 / Ste2p[C-EGFP]305-431 treated with latrunculin A, the internal signal arising from dimerization is almost completely lost.

(c) Shows cells co-expressing Ste2p[N-EGFP]305-431 / Ste2p[C-EGFP]305-431 treated with cycloheximide, the internal puncta is shown with red arrows indicative of endocytic vesicles. 88

Figure 3.27 Cells expressing EGFP tagged C-terminally truncated Ste2p, scale bars correspond 5 μm. **(a)** Shows cells expressing Ste2p[EGFP]; C-terminally truncated Ste2p receptor tagged with full length EGFP attached at position 304. **(b)** Shows cells expressing Ste2p[EGFP] treated with cycloheximide. The internal EGFP signal was completely lost after blocking the protein synthesis. 90

Figure 3.28 Cells co-expressing Ste2p[N-EGFP] / Ste2p[C-EGFP]; C-terminally truncated receptor tagged with either N-EGFP (1-158) or C-EGFP (159-238) attached to position 304, scale bars correspond 5 μm.. 91

Figure 3.29 Cells co-expressing full length and C-terminally truncated Ste2p tagged with either N-EGFP or C-EGFP, scale bars correspond 5 μm length. **(a)** Shows cells co-expressing Ste2p[N-EGFP]305-431 / Ste2p[C-EGFP]. **(b)** Shows cells co-expressing Ste2p[C-EGFP]305-431 / Ste2p[N-EGFP]. **(c)** Shows the full length / truncated BiFC pair treated with latrunculin A, resulting with a signal loss intracellularly. **(d)** Shows the full length / truncated BiFC pair treated with cycloheximide, the red arrows show endocytotic vesicles at intracellular region...... 92

Figure 3.30 pESC-TRP and pESC-URA (Agilent Technologies, CA, USA) vector maps and their multiple cloning sites (MCS) sequences. 99

Figure 3.31 Gel image for the amplified Ste2p constructs with either 5’ EcoRI – 3’ NotI primer pair or 5’ BamHI – 3’ NheI primer pair. 99

Figure 3.32 Three colonies were picked from each construct and each colony was digested with EcoRI – NotI (first lane), BamHI – NheI (second lane). Insert sizes were consistent with expected results... 100

Figure 3.33 Digestion control of the inserts after the construction of pESC-URA-Ste2p[N-EGFP] and pESC-URA-Ste2p[C-EGFP] plasmids (left image). Digestion of pESC-URA-STE2[N-EGFP] and pESC-URA-STE2[C-EGFP] vectors for cloning the complementary Ste2p constructs; Ste2p[C-EGFP] and Ste2p[N-EGFP] respectively; into the empty cloning sites. 101

Figure 3.34 Digestion control of double promoter vectors for coexpression of complementary C-terminally truncated Ste2p constructs tagged with C-EGFP and N-EGFP (U12) and C-mCherry and N-mCherry (T67) from one plasmid. Each red box, represents EcoRI – NotI digestion (first lane) and BamHI – NheI digestion (second lane) of same plasmid. The sizes of Ste2p constructs are in accordance with the calculated values. STE2[C-EGFP] (1): 1614 bp, STE2[N-EGFP] (2): 1854 bp, STE2[C-mCherry] (6): 1611 bp, STE2[N-mCherry] (7): 1851 bp. 102

Figure 3.35 Digestion control of double promoter vectors for coexpression of complementary full length Ste2p constructs from one plasmid. In each red box, first lane represents BamHI – NheI digestion, second lane represents EcoRI – NotI digestion. The sizes of Ste2p constructs are in accordance with the calculated values. STE2[C-EGFP]305-431 (3): 1611 bp, STE2[N-EGFP]305-431 (4): 1851 bp, STE2[C-EGFP] (1): 1614 bp, STE2[N-EGFP] (2): 1854 bp. 102

Figure 3.36 Bright field and fluorescent images of pESC-U12 vector, coexpression of Ste2p[N-EGFP] (1) and Ste2p[C-EGFP] (2), scale bars correspond 5 μm. 104

Figure 3.37 Bright field and fluorescent images of pESC-U43 vector, coexpression of Ste2p[N-EGFP]305-431 (3) and Ste2p[C-EGFP]305-431 (4), scale bars correspond 5 μm. 104

Figure 3.38 Bright field and fluorescent images of pESC-U23 vector, coexpression of Ste2p[C-EGFP] (2) and Ste2p[N-EGFP]305-431 (3), scale bars correspond 5 μm. 105

Figure 3.39 Bright field and fluorescent images of pESC-T67 vector, coexpression of Ste2p[N-mCherry] (6) and Ste2p[C-mCherry] (7), scale bars correspond 5 μm...... 105

Figure 3.40 pSP-G1 (TEF1-PGK1) and pSP-G2 (PGK1-TEF1) vector maps. 106

Figure 3.41 Agarose gel image of amplification product for PGK1-TEF1 and TEF1-PGK1 promoter region. 107

Figure 3.42 Agarose gel image of EcoRI – BamHI digested U12 (Ste2p[N-EGFP], Ste2p[C-EGFP]), T67 (Ste2p[N-mCherry], Ste2p[C-mCherry]) constructs and PGK1

– TEF1 and TEF1 – PGK1 PCR products. The constitutively active double promoter region is right below 1.5 kb band as expected. Red box shows dropped Gal1 – Gal10 region. 107

Figure 3.43 EcoRI-BamHI digestion of U1 (Ste2p[N-EGFP]), U2 (Ste2p[C-EGFP]), T6 (Ste2p[N-mCherry]), T7 (Ste2p[C-mCherry]) constructs to drop the Gal1-Gal10 promoter region. 108

Figure 3.44 Agarose gel image of EcoRI – BamHI digestion control pESC-TRP and pESC-URA based constructs to verify correct TEF1-PGK1 (G1) or PGK1-TEF1 (G2) inserts. This new promoter region is expected around 1.5kb band, whereas the Gal1-Gal10 promoter region is approximately 670 base pairs. *(a)* pESC-URA based constructs carrying Ste2p[N-EGFP] (2) and Ste2p[C-EGFP] (1) at both MCS “U12” and pESC-TRP based constructs carrying Ste2p[N-mCherry] (7) and Ste2p[C-mCherry] (6) at both MCS “T67”. (b) pESC-URA based constructs carrying Ste2p[N-EGFP] (2), Ste2p[C-EGFP] (1) at each MCS “U2” and “U1” and pESC-TRP based constructs carrying Ste2p[N-mCherry] (7), Ste2p[C-mCherry] (6) at each MCS “T7” and “T6”. (c) pESC-URA based constructs carrying Ste2p[N-EGFP]305-431 (4), Ste2p[C-EGFP]305-431 (3) at each “U3” and “U4” or both “U34” MCS.............. 109

Figure 3.45 Agarose gel image for NotI – NheI digestion of U12G1 and U34G1 plasmids. The lower bands in first 3 lanes are STE2[C-EGFP]-TEF1-PGK1-STE2[N-EGFP] expected to show ≈ 5 kb DNA ladder band, upper bands are as expected ≈ 6kb. The lower bands in second 3 lanes group is STE2[C-EGFP]305-431-TEF1-PGK1-STE2[N-EGFP]305-431 construct again expected to show ≈ 5 kb DNA ladder band, likewise upper bands are as expected ≈ 6kb. 110

Figure 3.46 Agarose gel image of constitutively active empty plasmids and constitutively active vectors carrying wild type Ste2p (a) EcoRI – BamHI digestion of constitutively active double promoter vectors with empty multiple cloning sites (TG1, TG2, UG1 and UG2) and constitutively active plasmids carrying wild type Ste2p in each MCS. The red asterix shows the correct TEF1 – PGK1 (G1) or PGK1 – TEF1 (G2) inserts as a band expected to be around 1.5kb ladder band. (b) Constitutively active plasmids originating from pESC-TRP plasmid carrying wild type Ste2p in each MCS. EcoRI – NotI (EN) band shows the insert at the 1st MCS, BamHI – NheI (BN) shows the insert at the 2nd MCS and EcoRI – BamHI (EB) shows the TEF1 – PGK1 or PGK1 – TEF1 promoter region. 111

Figure 3.47 Biological assay of Ste2p constructs expressed from constitutively active double promoter plasmids. Wild-type Ste2p expressed from 1st MCS of TG1 plasmid (●), wild-type Ste2p expressed from 2nd MCS of TG1 plasmid (■), wild-type Ste2p expressed from 1st MCS of UG1 plasmid (▲), wild-type Ste2p expressed from 2nd MCS of UG1 plasmid (▼).......... 113

Figure 3.48 Biological assay of C-terminally truncated Ste2p constructs expressed from constitutively active double promoter plasmids. Ste2p-Δ305 expressed from 1st MCS of TG1 plasmid (●), Ste2p[C-EGFP] expressed from 1st MCS of UG1 plasmid (■), Ste2p[N-EGFP] expressed from 2nd MCS of UG1 plasmid (□), Ste2p[C-mCherry] expressed from 1st MCS of TG1 plasmid (▼), Ste2p[N-EGFP] expressed from 2nd MCS of UG1 plasmid (▽). 114

Figure 3.49 Biological assay of Ste2p constructs carrying an intact C-terminus expressed from constitutively active UG1 double promoter plasmids. Ste2p WT expressed from 1st MCS of UG1 plasmid (●), Ste2p[C-EGFP]305-431 expressed from 1st MCS of UG1 plasmid (■), Ste2p[N-EGFP]305-431 expressed from 2nd MCS of UG1 plasmid (□). 115

Figure 3.50 Western blot of the BJS21 cells expressing the constructs, the first lane is an extract of Ste2Δ cells expressing empty vector. The second lane is an extract of Ste2Δ cells expressing WT Ste2p receptor WT Ste2p (52 kDa) from the 1st MCS of T-G1 vector under TEF1 promoter. The third lane represents cells expressing WT Ste2p (52 kDa) from 2nd MCS of T-G1 vector under PGK1 promoter. Fourth lane is the protein marker. Fifth lane represents cells expressing Ste2p[C-EGFP] (calc. ≈42 kDa) under the control of TEF1. Sixth lane represents cells expressing Ste2p[N-EGFP] (calc. ≈51 kDa) under the control of PGK1 promoter. Seventh lane shows the transformants expressing Ste2p[C-EGFP]305-431 (calc. ≈57 kDa) from MCS1 of T-G1 vector, under the control of TEF1 promoter. Eight lane shows the transformants expressing Ste2p[N-EGFP]305-431 (calc. ≈66 kDa) from MCS2 of T-G1 vector, under the control of PGK1. The proteins from lanes 1 to 8 were detected with antireceptor antiserum directed against the N-terminal domain of the α-factor receptor. 116

Figure 3.51 Western blot of the BJS21 cells expressing the constructs; the first lane is an extract of Ste2Δ cells expressing WT Ste2p receptor (52 kDa) from T-G1 vector. Second lane is the protein marker. The third lane represents cells expressing Ste2p[EGFP]305-431 (calc. ≈75 kDa) from pBEC1 vector. Forth lane represents cells expressing Ste2p[EGFP] (calc. ≈60 kDa) from pBEC1 plasmid. Fifth lane represents cells expressing Ste2p[N-EGFP] (calc. ≈51 kDa) from TG1 vector. Sixth lane shows the transformants expressing Ste2p[C-EGFP] (calc. ≈42 kDa) from T-G1 vector. Seventh lane represents cells expressing Ste2p[N-mCherry] (calc. ≈51 kDa) from TG1 vector. Eight lane shows the transformants expressing Ste2p[C-mCherry] (calc. ≈42 kDa) from T-G1 vector. Ninth lane shows the transformants expressing Ste2p[mCherry] (calc. ≈60 kDa) from pBEC1 plasmid. Tenth lane shows the transformants expressing Ste2p[mCherry]305-431 (calc. ≈75 kDa) from pBEC1 plasmid. The proteins from lanes 1 to 10 were detected with antireceptor antiserum directed against the N-terminal domain of the α-factor receptor; lanes 9 and 10 were also detected with mCherry antibody (16D7, Life Technologies, NY, USA).......... 118

Figure 3.52 Cells co-expressing Ste2p[N-EGFP] / Ste2p[C-EGFP]; C-terminally truncated receptor tagged with either N-EGFP (1-158) or C-EGFP (159-238) attached to position 304, scale bars correspond 5 μm.......... 120

Figure 3.53 Cells co-expressing three Ste2p constructs; WT Ste2p and C-terminally truncated BiFC pair; Ste2p WT / Ste2p[N-EGFP] / Ste2p[C-EGFP]; the red arrows show endocytotic vesicles at intracellular region, scale bars correspond 5 μm length. 121

Figure 3.55 First image in both rows was taken at either donor (a) or acceptor (b) settings, the second image corresponds to FRET settings and finally the third image is the FRET image shown in “fire” settings under lookup tables in imageJ software for better visualization of bleed through (a) Yeast cells expressing only the donor; EGFP BiFC Ste2p pair (b) cells expressing only the acceptor; mCherry BiFC Ste2p pair. Scale bars correspond to 5 μm length. 124

Figure 3.56 FRET image acquisition from cells coexpressing Ste2p EGFP BiFC pair and Ste2p mCherry BiFC pair. First column of images represent donor settings, second column represents acceptor settings, third column represents FRET settings, the fourth columns is “fire” representation of FRET image for better visualization of pixels. Scale bars correspond to 5 μm length. 125

Figure 3.57 FRET data acquisition for acceptor photobleaching. First column shows donor signal before acceptor photobleaching; second column shows acceptor signal before photobleaching; third column shows donor after acceptor photobleaching, the forth column shows acceptor after bleaching. Scale bars correspond to 5 μm length. 126

LIST OF ABBREVIATIONS

6'-GNTI	6'-guanidinonaltrindole
A_1R	Adenosine A_1 Receptor
$A_{2A}R$	Adenasione A_{2A} Receptor
ADP	Adenosine diphosphate
AFM	Atomic force microscopy
AMP	Adenosine monophosphate
ATP	Adenosine triphosphate
Bar	Barrier (to α-factor diffusion)
Bem	Bud emergence
BiFC	Bimolecular fluorescence complementation
Bp	Base pair
BRET	Bioluminescence resonance energy transfer
BSA	Bovine serum albumin
cAMP	Cyclic AMP
Cdc	Cell division control
cDNA	Complementary deoxyribonucleic acid
DAG	Diacylglycerol
CFP	Cyan fluorescent protein
D_2R	Dopamine D2 receptor
DHFR	Dihydrofolate reductase
DHFR	dihydrofolate reductase
Dig	Down-regulator of invasive growth
DLS	Dynamic light scattering
DMSO	Dimethyl sulfoxide
DNA	Deoxyribonucleic acid

EDTA	Ethylenediamine tetraacetic acid
EGFP	Enhanced green florescent protein
EL	Extracellular loop
ER	Endoplasmic reticulum
EtBr	Ethidium bromide
Far	Factor arrest
FRET	Fluorescence/Förster resonance energy transfer
G_i	Inhibitory G_α subunit
G_{olf}	Olfactory G_α subunit
G_s	Stimulatory G_α subunit
GABA	γ-Amino butyric acid
GDP	Guanosine diphosphate
GFP	Green fluorescence protein
GPCR	G protein coupled receptors
G_i	Inhibitory G_α subunit
G_{olf}	Olfactory G_α subunit
Gpa1	G-protein alpha subunit
G_s	Stimulatory G_α subunit
GTP	Guanosine triphosphate
IL	Intracellular loop
IP3	Inositol 1,4,5-triphosphate
kb	Kilobase pair
Kss1	Kinase-supressor of Sst2
LB	Luria Bertani
MAP	Mitogen activated protein
mCherry	Monomeric cherry
$MgCl_2$	Magnesium chloride
mGluR	Metabotropic Glutamate Receptor
MAPK	Mitogen Activated Protein Kinase

MLT	Media lack of tryptophan
MLTU	Media lack of tryptophan and uracil
MLU	Media lack of uracil
mRNA	Messenger RNA
Msg5	Multicopy suppressor of *GPA1* deletion
N2A	Neuro2a
NMDAR	N-Methyl D-Aspartate Receptor
PAK	p21-activated protein kinase
PBS	Phosphate buffered saline
PCR	Polymerase Chain Reaction
PLC	Phospholipase C
Ptp	Protein tyrosine phosphatase
RE	Restriction enzyme
Rpm	Revolution per minute
SBT	Spectral bleed-through
SDS-PAGE	Sodium dodecyl sulfate-polyacrylamide gel electrophoresis
SOB	Super optimal broth
SOC	Super optimal broth with catabolite
Sst	Supersensitive
Ste	Sterile
Taq	*Thermus aquaticus*
TAE	Tris Acetate EDTA
TBE	Tris Borate EDTA
TM	Transmembrane
UV	Ultraviolet
YEPD	Yeast extract-peptone-dextrose
YFP	Yellow fluorescent protein

CHAPTER 1

INTRODUCTION

1.1 G-Protein Coupled Receptors: Structure, Function and Significance

G protein-coupled receptors (GPCRs) belong to the largest cell surface receptor family in eukaryotic cells. Considering the role of these receptors in sensing extracellular signals, the GPCR family is one of the most important sensory systems for the detection and transmission of a large assortment of extracellular chemicals (hormones, neurotransmitters, chemoattractants, calcium ions and analgesics) and sensory (light, odorants and taste molecules) signals [1].

The importance of understanding the mechanisms of GPCR signal transduction pathways can be summarized in several main points. Firstly, many of the extracellular signals are detected by cell surface receptors and transmitted inside the cell by G proteins that serve as molecular switches [2]. Second, GPCRs are the targets of ~30-50% of pharmaceuticals on the market hence being a major focus of molecular pharmacology research [3]. Third, mutations and functional problems of these receptors are linked to many human diseases such as diabetes insipidus and mellitus, hypercalcaemia, obesity, hypertension, cancer, hypothyroidism, retinitis pigmentosa and many psychotic disorders [4].

G-protein signaling mechanisms are well established. Upon the activation of the seven-transmembrane receptor on the plasma membrane, the catalysis of GDP to

GTP occurs on its cognate G-protein α subunit. The activation of G_{α} through its receptor causes either dissociation of $G_{\beta\gamma}$ heterodimer or molecular rearrangement [5, 6]. As a result, either G_{α} or $G_{\beta\gamma}$ heterodimer or both become free to activate downstream effectors (Figure 1.1). Furthermore, after activating their cognate G proteins GPCRs can also act as scaffolds to recruit other signaling proteins that result in additional cellular responses [7].

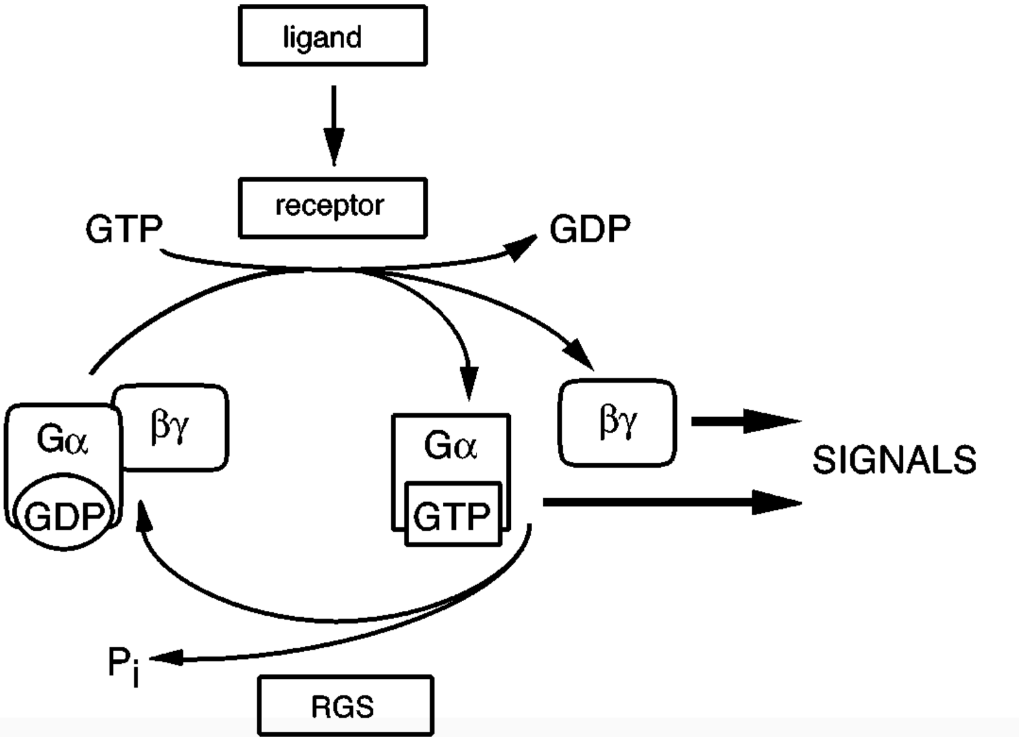

Figure 1.1 Schematic representation of signaling by heterotrimeric G proteins upon the activation of receptor with its agonist [6]. In their GDP bound inactive state, the G protein α subunit (G_{α}) stays as a heterotrimeric protein complex associated with the G protein βγ heterodimer ($G_{\beta\gamma}$). Upon agonist binding to a receptor GDP on G_{α} phosphorylates to GTP, leading the dissociation (or rearrangement) of heterodimeric $G_{\beta\gamma}$ subunits. These dissociated subunits initiate cellular signaling by activating effectors inside the cell. RGS (regulator of G protein signaling) proteins bind to G_{α} to stimulate GTP hydrolysis, so the GTP molecule on G_{α} is hydrolyzes back to GDP resulting a reassociation (or rearrangement) of inactive heterotrimeric protein complex. In the inactive heterotrimeric complex $G_{\beta\gamma}$ inhibits guanine nucleotide exchange therefore desensitizes the receptor. $G_{\beta\gamma}$, acts as a dual signal regulator both playing a positive role in signal transduction after the dissociation from G_{α}; and a negative role by desensitizing the receptor as a result of reassociation with G_{α}.

Adenylyl cyclase isotypes, plasma membrane Na^+/H^+ exchangers, some calcium and potassium channels, phospholipase C isoforms, exchange factors for small GTPases, cytosolic tails of cadherins, and certain protein kinases are examples of direct effectors in mammalian cells [8-10]. These effectors produce secondary messengers or various biochemical changes resulting a stimulation of protein kinase. As a result, changes in phosphorylation occur and this affects the metabolism, gene expression, morphology and cellular development. Signaling continues until the reassociation of receptor, G_α and $G_{\beta\gamma}$ as a result of GTP to GDP catalysis, hence completes the signaling.

One of the most important discoveries since the introduction of G protein initiated signaling is the discovery of RGS protein family. RGS proteins have GTPase activating properties for different classes G_α proteins, making them an important factor for signal desensitization, therefore G protein inactivation [6]. Many RGS proteins also carry certain additional modular domains with known or suspected signaling functions. Existence of such domains suggests that these types of RGS proteins constitute another node that adds to the diversity and complexity of heterotrimeric G proteins which can affect cellular signaling networks [11 12 13].

1.2 Yeast GPCRs and Ste2p as a model GPCR

GPCR structure and function have been studied in many model systems to alleviate the difficulties found in experiments involving complex mammalian systems. The budding yeast, *Saccharomyces cerevisiae* has only three G-protein coupled receptors, in contrast to the human genome, which encodes nearly 1000 GPCRs [14]. In yeast, recognition of the mating pheromone occurs through the action of two GPCRs, Ste2p and Ste3p; glucose sensing occurs through Gpr1p. Basic principles of G protein signaling and regulation were first elucidated by genetic and biochemical assays analyzing the response of yeast to its mating pheromone peptide. Many of the important mechanisms of G protein and mitogen-activated protein (MAP) kinase signaling were first demonstrated in Saccharomyces cerevisiae [6]. The first demonstration of positive signaling role of $G_{\beta\gamma}$ subunits was again shown in yeast [15]. The three tiered structure of MAP kinase module [16] and existence kinase scaffold proteins [17] were also first discovered in yeast. Receptors are known to be targets of desensitization, but the desensitization of G proteins by regulator of G protein signaling (RGS) proteins were shown for the first time using genetic disruption of SST2 in yeast [18]. Homologs of Sst2 also exist in higher eukaryotes and were renamed RGS proteins and shown to accelerate G protein GTPase activity, thus leading to subunit reassociation [6]. Identification of monoubiquitination as a signal for receptor endocytosis was also first shown in yeast cells [19] [20]. Most of the GPCR mediated signaling pathway and its elements in mammalian cells are structurally and functionally similar to yeast pheromone signaling pathway [21], the G protein and kinase components in particular, share extensive sequence similarity with their mammalian counterparts [22]. Therefore making yeast as an ideal and valuable model system for understanding ligand-GPCR and GPCR-GPCR interactions [21, 23]. Furthermore, yeast is the only system in which nearly every open reading frame has been systematically deleted [24]; organized into microarrays [25]; each gene was fused with fluorescent proteins for the global analysis of protein localization [26]; a Saccharomyces cerevisiae fusion library was created where each open reading frame is tagged with a high-affinity epitope and expressed from its natural chromosomal location and each protein was detected through immunodetection [27], purified and analyzed on a proteomic scale [28]. This knowledge database on yeast makes it possible to study gene function, gene transcription, protein localization and intermolecular associations in a systematic way and on genome-wide scale [22].

1.2.1 Yeast pheromone signaling pathway:

Saccharomyces cerevisiae can be found in two different haploid mating types, *MAT**a*** or *MATα*. Two short peptides named pheromones trigger the signaling pathway responsible for mating of these haploid yeast cell types to generate a *MAT**a**/MATα* type diploid cell. Pheromones are defined as "substances that mediate communication between individuals of the same species" and mating pheromones induce the subsequent mating response in haploid yeast cells by enabling communication between cells [29]. *MAT*α cells produce and secrete a 13 amino acid peptide called α-factor (WHWLGLKPGQPMY) [30], whereas *MAT**a*** cells produce and secrete a 12 amino acid peptide called **a**-factor, carrying a carboxymethylated S-farnesyl group on the Cys residue and its C-terminal ([YIIKGVFWDPAC(farnesyl)-OCH3]) [31]. The α-factor binds to Ste2p expressed only on *MAT***a** cells and **a**-factor binds to Ste3p expressed only on *MAT*α cells. Both Ste2p and Ste3p are coupled to same heterotrimeric protein complex G_{α} (Gpa1) and $G_{\beta\gamma}$ (Ste2-Ste18) [32 33].

Followed by the activation of the receptors through their pheromones, signaling starts (Figure 1.2). As a result cytoskeletal structure starts to change for polarized cell growth to prepare them for cell fusion (plasmogamy) [34]. For cell fusion new gene transcriptions are required to produce certain proteins for adhesion and cell fusion induction [35 36 37 38 39]. Rearrangement in nuclear architecture [40] is required to prepare the cells for nuclear fusion (karyogamy) and for the completion of zygote formation [41]. As the signaling starts, cell cycle progression arrest in the G1 phase occurs [42 43]. This growth arrest synchronizes cell cycles for mating with their partners [6].

The agonist, binds to its receptor and causes a conformational change on G_{α} (Gpa1). G_{α} transmits the signal to $G_{\beta\gamma}$ heterodimer (Ste4-Ste18) with a rearrangement or release of this protein. Then effector proteins bind the free $G_{\beta\gamma}$ hence transmits the G protein initiated signaling [6].

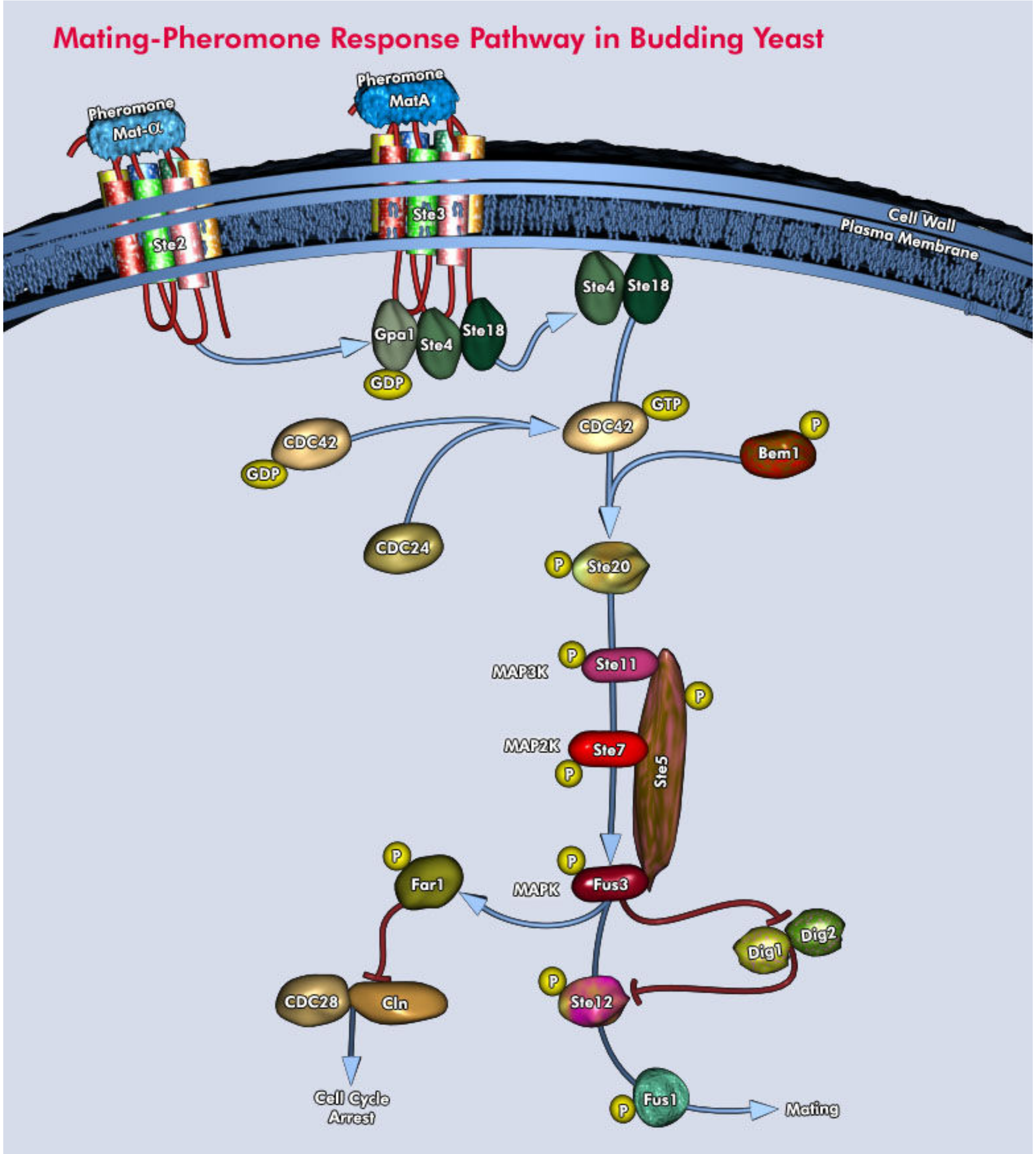
Mating-Pheromone Response Pathway in Budding Yeast
Pheromone
Mat-α
Pheromone
MatA
Ste2
Ste3
Cell Wall
Plasma Membrane
Gpa1
Ste4
Ste18
GDP
Ste4
Ste18
CDC42
GTP
CDC42
GDP
Bem1
P
CDC24
P
Ste20
MAP3K
P
Ste11
P
MAP2K
Ste7
P
Ste5
P
Far1
P
MAPK
Fus3
Dig1
Dig2
P
Ste12
CDC28
Cln
Cell Cycle
Arrest
P
Fus1
Mating

Figure 1.2 Mating-Pheromone Response Pathway in *S.cerevisiae* (© 2009 QIAGEN, all rights reserved)

Cdc24 is an effector protein for $G_{\beta\gamma}$ in the mating pathway. It is a guanine nucleotide exchange factor for Cdc42 [44], which is a GTPase resembling the Rho family of Ras-related small G proteins [45]. Rho and Cdc42 proteins are important components that control the cell morphogenesis in all eukaryotes [46 47 48 49 50]. In yeast, Cdc24 and Cdc42 are required for generation of cell polarity and budding, upon pheromone stimulation, these proteins are required for the formation of projection towards the pheromone source. During polarized growth in response to pheromone stimulation $G_{\beta\gamma}$ interacts with Cdc24 and the "scaffold protein" Far1 [51 52]. In the absence of pheromone, Far1-Cdc24 protein complex is found mainly in the nucleus. One other Far1 function in the nucleus is in the pheromone imposed G1 arrest mechanism by inhibiting cyclin dependent kinase (CDK) Cdc28, which is required for G1 phase of cell cycle [53 54]. Upon stimulation of the cells with pheromone, Far1 carries its bound cargo, Cdc24, to cytosol [55 52], where Far1 acts as a scaffold and generates Cdc24-Far1-$G_{\beta\gamma}$ protein complex that localizes at the tip of mating projection [51 52]. This orienting of cytoskeleton is believed to be mediated by efficient and highly localized generation of the GTP-bound state of Cdc42 with Cdc24 [6].

Cdc42 has many target proteins that play role in the state of assembly of actin microfilaments in yeast [56]. Cdc42-GTP also binds to Ste20, the first p21 activated kinase (PAK) to be identified in any eukaryote [57 58]. Bem1 is another protein acting on actin cytoskeleton in polarized growth of cell. Bem1 binds Cdc24, Ste5 and Ste20, and its function is to connect the mating signal to the proteins that induce the appropriate changes to the actin cytoskeleton [59].

In its GTP-bound state, Cdc42 binds to the N terminus of Ste20 [57 58] and Cla4, a Ste20 homolog, which plays a role in the establishment of cell polarity in yeast [60 61 62]. Since, Cdc42 is tethered to the plasma membrane, its association localizes Ste20 and Ste20 bound $G_{\beta\gamma}$ [63] at the projection tip of pheromone stimulated cells [64, 65].

Ste11 is the substrate of Ste20, which is mitogen-activated protein kinase kinase kinase (MAPKKK) first discovered in any eukaryote and is essential for the activation of transcription and other events in the nucleus [66 67]. Ste11 phosphorylates

MAPK kinase (MAPKK), Ste7 [68]. Ste7 phosphorylates and activates two MAPKs Kss1 [69 70] and Fus3 [69 71]. These kinases, Ste7, Kss1 and Fus3 were first identified in yeast [72 73]. Therefore, MAPK cascade, the three-tiered signal transduction module which is conserved ubiquitously throughout the eukaryotic kingdom, was first identified by genetic and biochemical studies in *S. cerevisiae* [6]. Fus3 has an essential function in mating pathway; Kss1 has an essential function in invasive growth in haploid cells and pseudohyphal growth in diploids cells [74, 75 76].

Ste5 functions as a scaffold protein for Ste11, Ste7 and Fus3 [17, 77, 78]. Similar to Far1, Ste5 also shuttles between nucleus and cytosol and upon pheromone stimulation, exported to cytosol [79-81]. Ste5 also interacts as an effector with $G_{\beta\gamma}$ and localizes at the projection tip [81-83 84]. Ste5 is believed to for oligomers which may have effect on the cross phosphorylation of the kinases and efficiency of Fus3 activation [77, 83 84, 85], yet, whether these oligomers are simple dimers or higher oligomers remains to be unresolved [6]. Nuclear proteins, Far1 [86, 87], Ste5 [88], Ste12 [86, 89, 90], and Ste12 inhibitor proteins Dig1 and Dig2 [91-93] are among the substrates of Fus3.

Thus, as a summary, pheromone-initiated signaling in yeast begins with occupancy of G protein–coupled receptors at the plasma membrane. The extracellular stimuli is transferred inside the cell through the heterotrimeric G proteins by activation of proteins involved in cell morphogenesis, as well as by recruitment and activation of a protein kinase cascade which phosphorylates, therefore activates the nuclear proteins that control cell polarity, transcription, and progression during the cell cycle. All these changes represent a coordinated response to pheromone that permits haploids to differentiate transiently into nonproliferating gamete-like cells that are prepared for cell and nuclear fusion [6].

1.2.2 Yeast glucose sensing mechanism:

Saccharomyces cerevisiae prefers to utilize glucose as a carbon source and the presence of glucose activates a shift to the fermentative state by stimulating cAMP synthesis. The glucose sensing pathway is more recently discovered and remains to be a less studied compared to pheromone sensing pathway. In yeast, Glucose / cAMP pathway has been shown to be Ras-dependent pathway in which Ras proteins controls the elements of adenylate cyclase [94]. Saccharomyces cerevisiae genome encodes 2 RAS genes, RAS1 and RAS2 [95, 96]. They encode proteins with nearly 90% homology to the first 80 positions of the mammalian ras proteins, and nearly 50% homology to the next 80 amino acids [96]. Recently, studies have shown that in yeast there is a second GPCR system is also responsible for the activation of this Glucose / cAMP pathway, composed of a glucose receptor; Gpr1 and associated subunit G_α protein; Gpa2 as main components [97 98]. As in the case of pheromone activation of Ste2p and Gpa1p, the glucose receptor Gpr1p activates its G_α, Gpa2. However, the direct activators of adenylate cyclase are Ras proteins and the exact role of Gpa2 protein is still not very well understood [94]. Activation of Gpa2 and Ras proteins as a result of two different specific signaling pathways is stimulating adenylate cyclase synthesis and therefore activating PKA (cAMP-dependent protein kinase), which ends up with pseudohyphal differentiation, loss of stress resistance (high osmolarity, salinity, heat, freezing, etc.), storage of carbohydrates (trehalose and glycogen), stimulation of growth and lower life-span (Figure 1.3) [99]. In G-protein coupled signal transduction, glucose induced cAMP signaling inhibited by Rgs2, an RGS protein (regulators of G-protein signaling). Rgs2 stimulates the GTPase activity of G_α protein, therefore can be indicated as a negative regulator [99]. In contrast to conventional G_α subunits, Gpa2 forms an atypical G protein complex with the kelch repeat G_β mimic proteins Gpb1 and Gpb2. Gpb1/2 negatively regulate cAMP signaling by inhibiting Gpa2. There has not been any $G_{\beta\gamma}$ dimer identified yet; however, Gpb1/Krh2 and Gpb2/Krh1 proteins bind to Gpa2 by acting together with Gpg1 protein therefore these proteins could be proposed to serve as a $G_{\beta\gamma}$ mimic even if they do not function parallel to the role of $G_{\beta\gamma}$ [100 101].

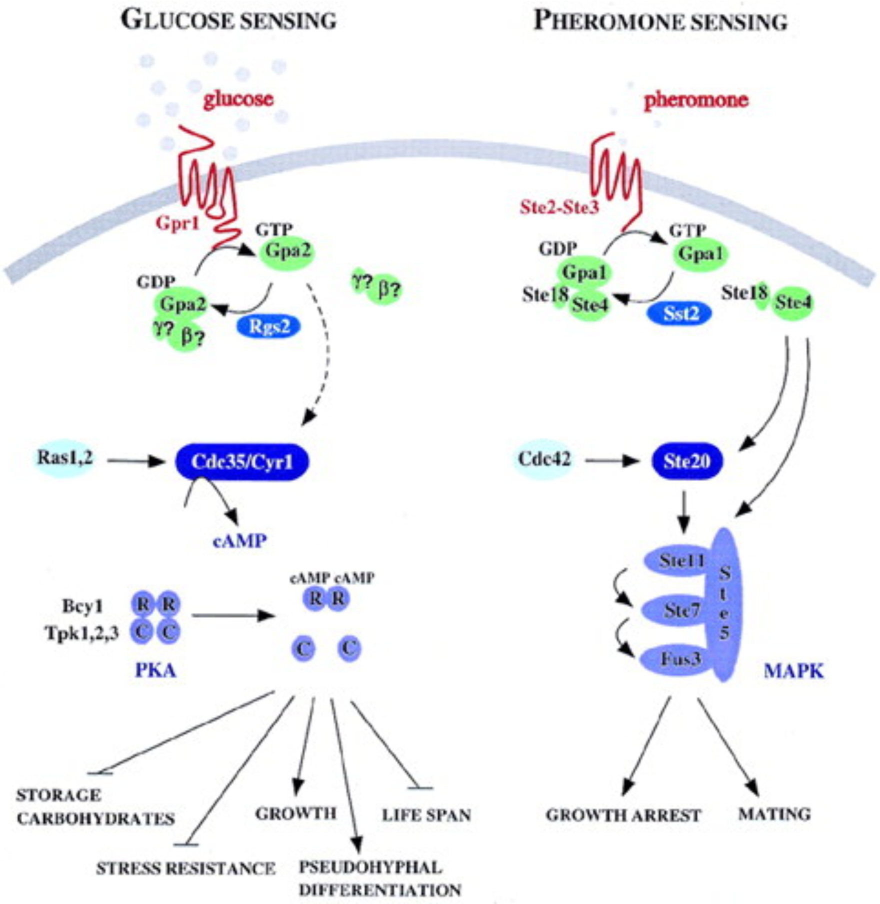
GLUCOSE SENSING
PHEROMONE SENSING
glucose
pheromone
Gpr1
Ste2-Ste3
GTP
Gpa2
GDP
Gpa2
γ? β?
Rgs2
γ? β?
GDP
Gpa1
GTP
Gpa1
Ste18 Ste4
Sst2
Ste18 Ste4
Ras1,2
Cdc35/Cyr1
cAMP
Cdc42
Ste20
Ste11
Ste7
Fus3
Ste5
MAPK
Bcy1
Tpk1,2,3
R R
C C
PKA
cAMP cAMP
R R
C C
STORAGE CARBOHYDRATES
STRESS RESISTANCE
GROWTH
PSEUDOHYPHAL DIFFERENTIATION
LIFE SPAN
GROWTH ARREST
MATING

Figure 1.3 Overview of pheromone and glucose signaling in *S. cerevisiae.* The putative glucose receptor Gpr1 activates the G_{α} protein Gpa2. Although Gpb1/Krh2 and Gpb2/Krh1 proteins were shown to interact with Gpa2 and act as G_{β} mimic, still it is not clear that whether these proteins constitute $G_{\beta\gamma}$ subunit, of if any such subunit exists. Rgs2 stimulates the GTPase activity of Gpa2 and thus inhibits glucose-induced cAMP signaling. Gpa2 is thought to activate adenylate cyclase (Cdc35/Cyr1) but direct biochemical evidence for this is still lacking. The basal activity of adenylate cyclase also depends on the Ras1 and Ras2 proteins of which the signaling function, if any, remains unclear. Activation of PKA by cAMP results in stimulation of growth and pseudohyphal differentiation, loss of stress resistance, mobilization of trehalose and glycogen and in reduced life-span. Pheromone sensing depends on the Ste2 and Ste3 receptors that respectively bind α- and **a**-factor and that transmit the signal to the heterotrimeric G-protein consisting of the G_{α} protein Gpa1 and the βγ subunit Ste4 and Ste18. The RGS protein Sst2 is able to diminish signaling by stimulating the GTPase activity of Gpa1. Ste4 recruits both the scaffolding protein Ste5 and Ste20 (which can also be stimulated by Cdc42) to the membrane resulting in activation of the mating MAP kinase cascade (Ste11, Ste7 and Fus3). Activation of the MAP kinase pathway results in growth arrest and conjugation [99].

1.3 GPCR Oligomerization

Although for many years G protein-coupled receptors were thought to exist as monomers and one ligand-receptor complex was considered the functional unit for signal transduction [1], dimerization of GPCRs became an accepted concept for most of the cell surface receptors. The formation of dimers or higher oligomers offers various properties that a monomer does not possess such as increased ligand specificity, internalization of receptors, trafficking; versatility or affinity; and cell surface mobility [102]. During the last decade, there has been evidence to support the notion that GPCRs form homo- and/or hetero- dimers and even higher-ordered oligomers [103]. In the literature many studies have used techniques such as immunoblot analysis of 5-HT1B receptor in Sf9 insect cells [104], applying covalent cross linkers to verify the existence of homomeric forms of D2 and A1 receptors in brain tissue, *in situ* [105] [104], and saturation and competition binding experiments that provided evidence of a strong interaction between certain glutamate and adenosine receptors [106] to show interactions between these receptors.

With the development of advanced fluorescent microscopy techniques, specifically resonance energy transfer (RET) methods, such as FRET (Fluorescence-RET) and BRET (Bioluminescence-RET), detection of GPCR interactions in living cells have become possible. In 2000, Blumer *et al.* observed homodimers of Ste2p receptor using the FRET methodology [64]. Another study by Angers *et al.* made use of BRET to observe homodimerization of β2-adrenergic receptor in mammalian HEK-293 cells [107]. In a more recent study oxytocin receptor dimers and oligomers have been shown to exist in the mammary gland using time-resolved FRET [108]. The results obtained using a variety of different biochemical and biophysical methodologies, (SDS-PAGE with covalent cross-linking, co-immunoprecipitation, FRET, BRET and functional complementation assays) demonstrate that dimerization of GPCRs occurred not only *in vitro* but also in native tissues. However, many questions remained to be answered regarding the mechanisms underlying GPCR dimerization, oligomerization, and internalization.

GPCRs can be found in various stages in living cells: biosynthesis and modification in ER and Golgi; trafficking to the membrane; activation by ligand and signal transduction; and internalization [109]. The key questions that need to be addressed are "Why and where do GPCRs undergo dimerization?" and "What is the role of dimerization in GPCR biosynthesis and membrane trafficking?". Currently, there is no consensus regarding the answers of these questions.

One other important concept in the receptor dimerization is whether GPCRs exist as preformed dimers in their quiescent state or act as dynamic structures that can be modulated by ligands. Three types of scenario is possible with the current data: (a) Dimers are detected under basal conditions and no change in their amount is observed upon ligand treatment, indicating that they represent stable preformed complexes; (b) dimers are detected under basal conditions, but ligands can modulate the extent of dimers observed; and (c) ligand treatment is a prerequisite to the detection of dimers [110]. So, understanding the true role of ligand in promoting or modulating the oligomeric state of the receptors would be an important contribution to the role of dimerization in receptor function. For many receptor families such as the tyrosine kinase and the cytokine receptors and TNF-α family receptors, agonist-promoted homo- and heterodimerization were shown with various studies and equilibrium between monomer and dimer is accepted to be a part of the receptor activation process [111] [112]. However, with recent crystallographic and protein-protein interaction studies have shown that erythropoietin receptor exists as preformed dimer and agonist binding activates the receptor through conformational changes rather than modulating the dimerization state [113] [114].

Unfortunately, there is no ideal case for investigating the effect of receptor ligand on its oligomerization; methods employed in the literature all need a modification of these proteins. For Western blot and coimmunoprecipitation-based approaches, the accessibility of the specific immunogenic epitopes used to detect the dimers could be either favored or reduced by the conformational changes promoted by the ligands [110]. For energy transfer experiments since the efficacy of energy transfer from donor to acceptor decreases as the 6th power of distance, the observed changes due to the ligand activation may be simply due to the conformational changes bringing fluorescent proteins closer or farther rather than an increase in the overall dimerization state. Depending on the method used to label the desired receptor (antibody vs. GFP) and on the region of labeling (N terminus vs. C terminus), receptor motion imposed by a specific ligand could determine whether a change in signal is detected. In some cases, the signal could go from undetectable to important, whereas in others the large basal signals would cover changes due to small conformation change [110].

A recent description of the crystal structure of the amino-terminal domain of the metabotropic glutamate receptor [115] strongly suggests that, dimers are preformed and that ligand binding simply changes the conformation of the dimer. The large N-terminal ectodomain that carries the ligand-binding pocket of the receptor was found to be dimeric whether it was crystallized alone or cocrystallized with glutamate. Two distinct conformations of the dimer structure corresponding to the ligand-bound and ligand-free receptor were detected indicating that glutamate promoted or stabilized a specific conformation of the dimer.

Where does the receptors form dimers/oligomers is another phenomena remains to be unsolved. The assembly of protein subunits in the endoplasmic reticulum is a common quality control strategy used by the cell to permit the export only of the correctly folded complexes [116]. A role of dimerization on receptor trafficking was first shown in metabotropic GABAb receptors [117] [118] [119] [120]. For functional metabotropic GABAb receptors, it is necessary to coexpress two receptor subtypes, the GABAb R1 and the GABAb R2. When expressed alone, the GABAb R1 receptor is retained in the ER as an immature protein. When GABAb R2 is expressed alone, it is properly targeted to the plasma membrane yet it cannot bind to GABA. When GABAb R1 and GABAb R2 were coexpressed, both receptors reach the plasma membrane as a complex and can bind GABA and inhibit cAMP production through its coupling to G_i/G_o G proteins. Those findings suggests that GABAb R2 serves as a molecular chaperone for the proper targeting of GABAb R1 to the plasma membrane, and the receptor is functional only as a dimer.

The majority of V2 vasopressin receptor mutants associated with nephrogenic diabetes insipidus result in ER retention and lack of cell surface expression of the receptor. Still, many of these mutant receptors can form dimers, suggesting dimerization occurs early after receptor biosynthesis [121]. Another example is when third cytoplasmic loop (D3nf) of D3 dopamine was interrupted it impairs cell surface expression of the wild-type full-length receptor as well, proposed to be likely due to their association in the ER [122].

The ER dimerization for GABAb R1 and GABAb R2 is a special case of heterodimerization involving two different receptors with different individual properties. The other findings in the literature are indirect ways of showing dimerization occurring at the ER, mostly about regaining or shielding the function of a WT receptor with a mutant one. There are also growing number of articles claiming the dimerization of GPCRs occur at the plasma membrane. In one study, β_2-adrenoreceptor (β_2AR) was shown to form oligomers in cellular membranes [123]. In this study, fluorescence resonance energy transfer (FRET) was used to characterize the oligomerization of purified β_2AR labeled with fluorescent proteins from different positions and reconstituted into a model lipid bilayer. The results suggested not only do β_2ARs oligomerize spontaneously inside the reconstructed phospholipid vesicles in the absence of scaffolds or other chaperon proteins, but also the predominant oligomeric state was shown to be a tetramer, hence showing ER transport is not necessary for the receptor oligomerization. In another report, $A_{2A}R/A_{2A}R$ interaction was monitored using bimolecular fluorescence complementation (BiFC) and proper subcellular localization of tagged receptors. In this study, Vidi *et al*., have shown that at least three A_{2A} receptors assemble into higher-order oligomers at the plasma membrane in Cath.A differentiated neuronal cells [124]. Numerous studies in the literature detecting various GPCR oligomers using FRET, reported the dimers to exist on plasma membrane [125 126 127 128].

Homodimerization of the α-factor receptor (Ste2p), a GPCR of *S. cerevisiae,* has been surveyed with some of the methods mentioned above. One of the first examples in support of homodimerization is the restoration of internalization when the endocytosis deficient receptors lacking the regulatory C-terminal carboxyl-terminal cytoplasmic domain, which includes DAKSS endocytosis signal, are co-expressed with wild-type receptors. In this study, co-immunoprecipitation of the influenza HA epitope (Ste2-HA) tagged and GFP tagged (Ste2-GFP) receptors with anti-HA antibody was found to yield both GFP and HA tagged receptors [129]. In another study, Overton and Blumer for the first time demonstrated Ste2p oligomerization in intact cells using FRET, and showed that oligomer formation is independent of agonist or antagonist binding. They indicated that homodimer formation was constitutive [64]. In 2007, another study was conducted using BRET and its results are consistent with the ones obtained by Overton and Blumer [130]. This study also concludes that signaling defective receptors are obtained upon heterodimerization of normal and dominant negative mutant receptors, indicating that two functional receptors are required for proper signaling. In a more recent study, the ligand related dimerization of a recombinant Ste2p receptor was investigated *in vitro* using atomic force microscopy (AFM), dynamic light scattering (DLS) and chemical cross-linking. The dimer form of the receptor was found in the absence of pheromone, but dimerization was enhanced in the presence of pheromone. These studies suggest that GPCR dimerization is constitutive; however ligand binding may induce dimer stability and oligomeric assembly of the receptor [109]. The particular contact sites for homodimer formation have also been investigated. In the yeast GPCR Ste2p TM1 and TM7 were reported to play a role in dimerization [131], which is in agreement with computational studies [132].

1.4 Fluorescence methods for detecting GPCR oligomerization

1.4.1 Fluorescence proteins

The whole fluorescence story dates back to AD77 by the comments of Pliny the Elder from his observations of a “glow” at Bay of Naples (Pulmo marinus). It is now known that many marine organisms produce light through chemiluminescent or fluorescence processes. Osamu Shimomura is the first pioneer in this field to identify the molecular basis of this glow studying Aequorea jellyfish in early 1960’s. He was able to isolate a chemiluminescent protein aequorin [133]. Aequorin is a luciferase that emits blue light as a result of catalyzing the oxidization of the substrate coelenterazine in a calcium-dependent reaction. Shimomura had also observed a protein in the jellyfish extracts “exhibiting a very bright, greenish fluorescence” under ultraviolet (UV) light illumination [133]. Later in 1970’s Shimomura and colleagues purified this autofluorescent protein, which is now one of the most famous proteins in molecular biology, called “Green Fluorescent Protein” (GFP) [134]. In the same study, it was reported that the autofluorescence of GFP is due to an energy transfer process, from the excited state energy of aequorin to GFP and as a result emitting the characteristic green light. Later in 1992, Prasher managed to clone a single full-length (gfp10) gene that encoded the complete Aequorea GFP sequence [135].

Martin Chalfie, expressed GFP in both a prokaryote; *Escherichia coli*; and the sensory neurons of a eukaryote *Caenorhabditis elegans*, using the clone isolated by Prasher. In Chalfie's study, GFP was shown to be functional hence he concluded that "because any exogenous substrates and cofactors (specific to the jellyfish) are not required for this fluorescence, GFP expression can be used to monitor gene expression and protein localization in living organisms" [136]. Later, in numerous studies GFP was demonstrated as a probe for in vivo fluorescence labeling of various proteins in variety of different cellular systems and organisms.

Encoded by the primary amino acid sequence, GFP forms and folds by a self-catalyzed mechanism spontaneously without the need of any additional cofactors or external enzymes in the presence of molecular oxygen. So, genetically fusing the proteins with GFP inside the cell and coupling the fluorescence property with advanced live cell imaging techniques started a revolution for the cell biology research to study protein-protein interactions, conformational changes, protein localization and investigating the mechanisms of signaling molecules to their natural environment within the intact cell.

First structural studies on GFP by Shimomura revealed that a single hexapeptide structure starting at position 64 is responsible for the fluorescence properties of GFP [137]. In the same study it was also shown that chromophore region absorbing the blue light energy from aequorin was formed by the cyclization of Ser65-Tyr66-Gly67 residues within the hexapeptide (Figure 1.4).

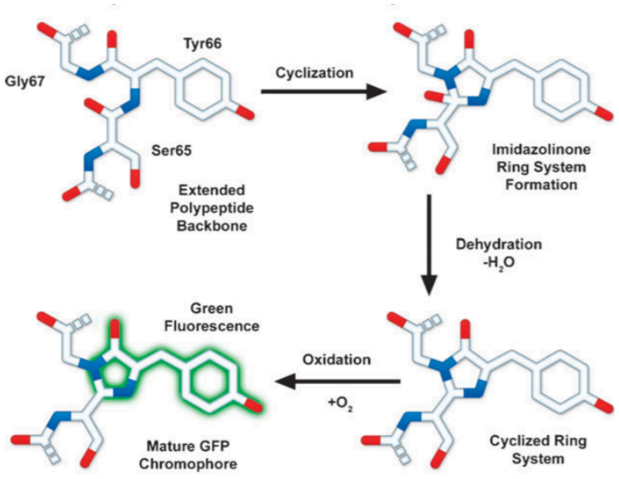
Tyr66
Gly67
Ser65
Extended Polypeptide Backbone
Cyclization
Imidazolinone Ring System Formation
Dehydration
-H₂O
Cyclized Ring System
Oxidation
+O₂
Green Fluorescence
Mature GFP Chromophore

Figure 1.4 Chemical reaction leading to the formation of GFP chromophore [138].

The crystal structure for GFP was resolved in 1996, cyclic tripeptide chromophore region which is responsible for the fluorescence characteristics is found to be caged in the center of a nearly perfect cylinder formed by interwoven eleven-stranded β-barrel structure (Figure 1.5) [139 140].

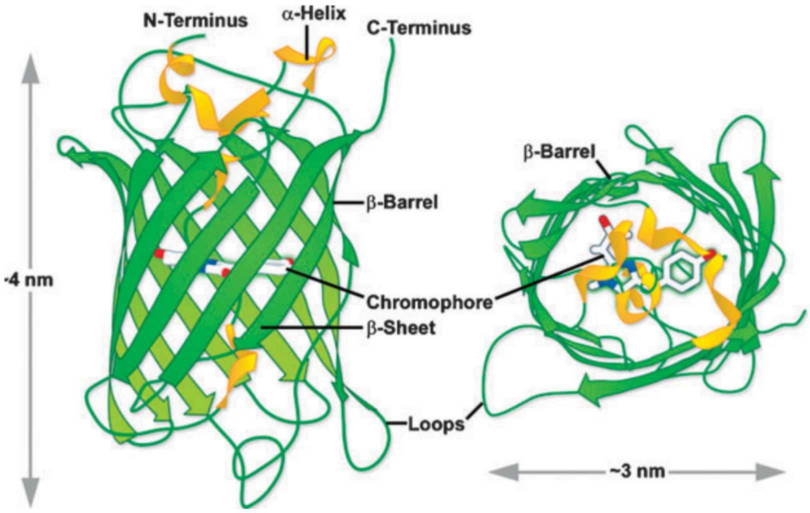
N-Terminus
α-Helix
C-Terminus
β-Barrel
~4 nm
Chromophore
β-Sheet
Loops
β-Barrel
~3 nm

Figure 1.5 *A. victoria* GFP β-barrel structure and approximate dimensions [138].

As the protein folds to create the β-barrel structure, the chromophore region is positioned at the core catalyzing the cyclization and dehydration reactions for the formation of mature fluorophore as well as stabilizing it [141]. This β-barrel structure is a common feature for all the discovered and engineered fluorescent proteins so far.

After the cloning of GFP cDNA, site directed and random mutagenesis approaches have shown that the fluorescence properties are very much dependent on the amino acid residues surrounding the chromophore region [141] [142]. Mutating the amino acid residues around the hexapeptide resulted in a significant effect on the spectral characteristics of the protein. Using these protein engineering approaches, a wide variety of different spectral derivatives of GFP were constructed with superior properties such as improved protein maturation, higher brightness, increased efficiency of folding and maturation of the protein at physiological temperatures resulting a better expression at different mammalian cells. These GFP variants were named as enhanced fluorescent proteins (Figure 1.6).

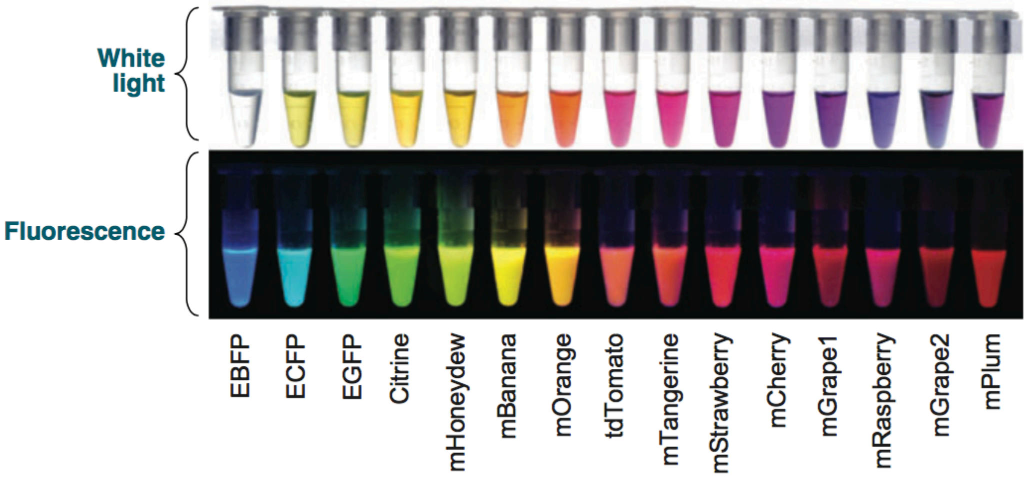
White light
Fluorescence
EBFP
ECFP
EGFP
Citrine
mHoneydew
mBanana
mOrange
tdTomato
mTangerine
mStrawberry
mCherry
mGrape1
mRaspberry
mGrape2
mPlum

Figure 1.6 Various fluorescent proteins under white light (top panel) and their fluorescence (bottom panel) purified from *E.coli* [143].

In the earlier studies in Roger Tsien's laboratory on the chromophore region of GFP, a mutation of serine residue at position 65 to threonine (S65T), resulted a GFP^{S65T} variant, with better absorption profile with only one excitation peak at 489 nm, in contrast to bimodal absorption profile of wtGFP. In addition, GFP^{S65T} is five times brighter than wtGFP and also matures more rapidly [142]. A second mutation on GFP^{S65T}, replacing of phenylalanine at position 64 to leucine (F64L) improved the maturation efficiency at 37°C, and named as EGFP. This new enhanced green fluorescent, has an absorption peak overlaying nicely with the 488 nm argon-ion laser line and commercially available filter sets designed for fluorescein (FITC). Continued engineering of GFP variants resulted in a full palette of fluorescent proteins (Figure 1.6, Figure 1.7, Figure 1.8).

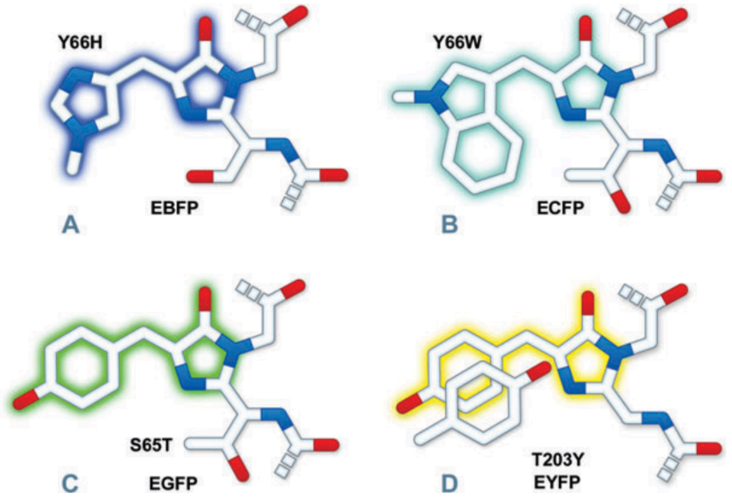

Figure 1.7 Chromophore region structures of (A) EBFP (B) ECFP (C) EGFP and (D) EYFP, each chromophore is shaded according to their spectral properties [138].

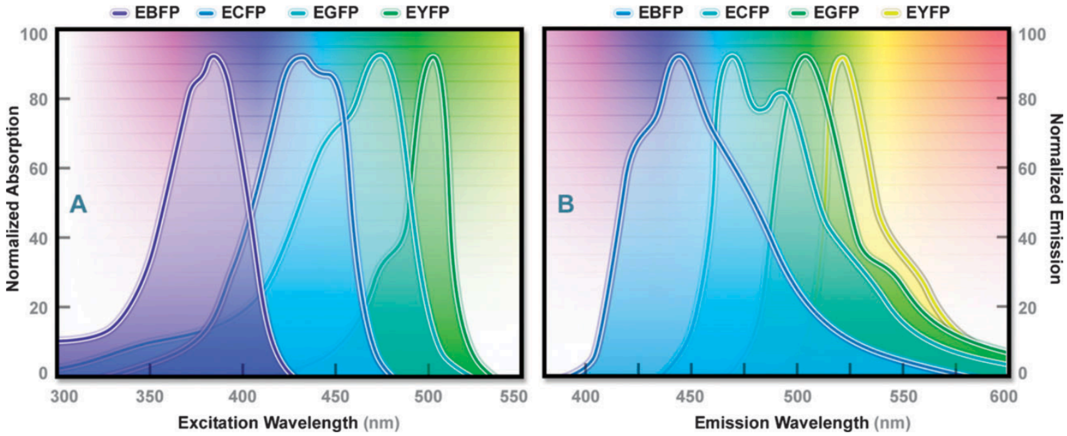

Figure 1.8 Excitation (A) and emission (B) spectra of enhanced GFP derivatives [138].

A new group of fluorescent proteins with spectral profiles at longer wavelengths, as an important tool for multicolor imaging and for generating better FRET sensors was developed from Anthozoa [144]. Another important property of these red fluorescent proteins is the reduced cellular autofluorescence in this spectral region and detection deeper into biological tissues [145].

One of the first red fluorescent proteins to be characterized was isolated from sea anemone *D.striata*. It was named as drFP583, which is now commonly known as dsRed [146]. DsRed protein has an excitation maximum at 558 nm and an emission maximum at 583 nm. However, dsRed has poor maturation characteristics through a “green” emission intermediate state leading to channel crosstalk and in addition dsRed is an obligate tetramer, therefore leading to protein aggregation of linked proteins. To overcome these limitation Tsien and his coworkers inserted 33 amino acid substitutions, hence produced the first monomeric red protein, mRFP1 [147]. This new red fluorescent protein has rapid maturation characteristics compared with dsRed and about 25 nm deeper shift into red spectrum. The tradeoff was almost 4-fold reduced fluorescence emission intensity compared to tetrameric dsRed and this new protein is very sensitive to photobleaching.

Over the years various fluorescent proteins were generated in the orange and red spectral regions from mRFP1 with directed evolution [148]. Targeting the chromophore region amino acids Q66 and Y67 in mRFP1, first group of monomeric fluorescent proteins with emission maxima from 540 nm to 610 nm was generated. These new fluorescent proteins were named mHoneydew, mBanana, mOrange, mTangerine, mStrawberry and mCherry, referencing the fruits that bear the color. The mFruit family proteins have ideal spectral characteristics allowing them to be paired with green and cyan region fluorescent proteins as FRET acceptors or for multicolor imaging. One of the most promising members of this family is mCherry (Figure 1.9), with a similar, but more elliptical β-barrel structure shielding the chromophore region.

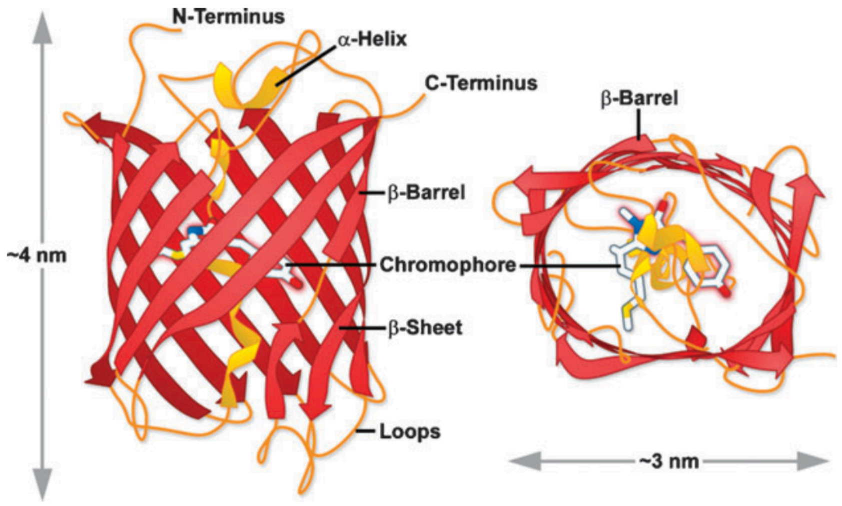

Figure 1.9 mCherry fluorescent protein β-barrel structure and approximate dimensions [138].

Almost forty years ago pioneering work of Osamu Shimomura opened a path of fluorescent proteins in what has often been described now as a ‘‘revolution’’ in cell biology. Douglas Prasher’s and Martin Chalfie’s visions adapted these magical molecules as a tool for live cell imaging. As a result of the enormous contribution of Roger Tsien laboratory fluorescent proteins covering almost the entire visible spectrum from deep blue to deep red is now being used by thousands of scientist as markers for studies in cell biology.

1.4.2 Bimolecular fluorescence complementation assay (BiFC):

Investigation of molecular processes, protein dynamics and interactions should be studied in cells normal cellular environment. The bimolecular fluorescence complementation (BiFC) assay provides a method to visualize protein interactions and modifications in living cells. This assay is based on the facilitated association of complementary fluorescent protein fragments fused to interaction partners. Complex formation by the interaction partners brings the fluorescent protein fragments into close proximity thereby facilitating their complementation (Figure 1.10). The BiFC assay enables sensitive visualization of protein complexes with high spatial resolution, however the temporal resolution may be limited by the time required for fluorophore formation, as well as the stabilization of complexes by association of the fluorescent protein fragments [149 150].

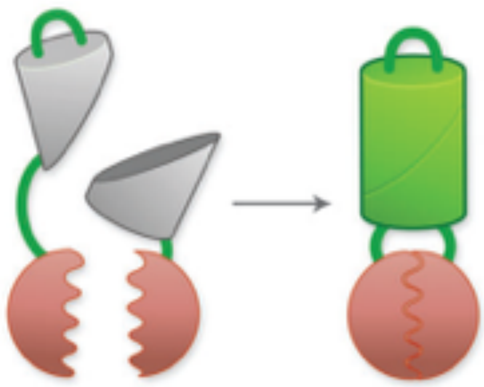

Figure 1.10 Representation of reconstitution of fluorescent protein by bimolecular fluorescence complementation [151].

This method was first defined for ubiquitin in 1994 [152] and subsequently, fragments of dihydrofolate reductase (DHFR), β-lactamase, β-galactosidase, several luciferases and in the case of fluorescent proteins, the method is called bimolecular fluorescent complementation (BiFC) assay (Figure 1.11), which enable the visualization of interactions between proteins *in vivo;* and also measure the effects of extracellular agents such as drugs or agonists on the protein complexes therefore have been used to study protein-protein interactions in bacteria, yeast, mammalian cells, and plants [153] [154]. Based on protein fragment association approaches, bimolecular fluorescence complementation (BiFC) analysis is the most widely used method for the detection of protein interactions [155] [156].

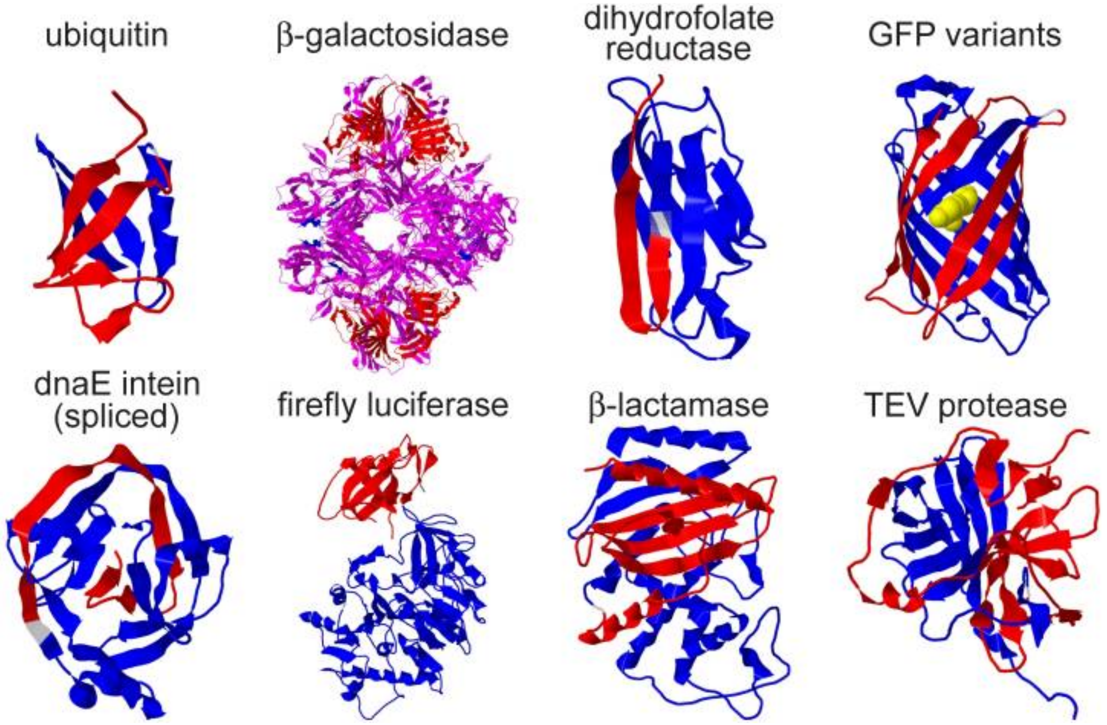
ubiquitin
β-galactosidase
dihydrofolate reductase
GFP variants
dnaE intein (spliced)
firefly luciferase
β-lactamase
TEV protease

Figure 1.11 Examples of protein fragments that can be used to study protein interactions. The fragments are shown in red and blue using models based on the X-ray crystal structures of the intact proteins. In b-galactosidase, the overlap between the fragments is shown in magenta. The discontinuity in the polypeptide backbone is shown in translucent grey [155].

The major advantage of tagging the proteins with fluorescent proteins is to study interactions *in-vivo*, in normal cellular environment, including in the physiological context of multicellular organisms [149]. When compared with other complementation techniques, BiFC's one other important advantage is, it enables detection of proteins without the need of any other exogenous reagents, and in BiFC only the intrinsic fluorescence property is used.

Importantly, only a few fragments of each protein can associate to form a functional complex and neither of these fragments is known to associate either alone or upon association with each other. Therefore, it is unlikely that the individual fragments by themselves fold into a structure resembling the intact protein in the absence of the complementary fragment. Most of these protein fragments are probably unfolded, rapidly interconverting through different conformations. Bringing two protein fragments, N-terminus and C-terminus, into close proximity is expected to be necessary for the association of these fragments, since only certain fragments and conformations allow association and therefore regain of fluorescence. However, since the folding pathways of all the protein fragments used for studies of protein interactions are unknown, this information cannot be used to predict or design protein fragments with enhanced performance characteristics [149] [151].

Although the discontinuity in the peptide backbone may affect the overall structure and dynamics of the proteins, after the association of two fragments, the structure of the constructed protein is expected to be similar to its intact version due to the fact that the spectra of formed complex from fluorescent protein fragments are indistinguishable from the intact fluorescent proteins [157] [158]. These results suggest that the structure and dynamics of complexes formed by fluorescent protein fragments are similar to those of the intact protein.

Regarding the kinetics of BiFC complex fluorescence, the two BiFC fragments do not associate simultaneously with the tagged endogenous proteins interaction. There is a delay between fusion protein interaction and when the complex becomes fluorescent. Fluorescent protein fragment association and construction of the fluorophore requires some time [157] [149]. Nevertheless, BiFC complex fluorescence can often be detected within minutes after fusion protein interaction. In studies of the time course of BiFC complex formation by YFP fragments fused to FKBP and FRB, fluorescence was detected within 10 minutes and continued to increase for at least 8 hours [159].

BiFC analysis has been used to visualize a wide range of cellular processes including non-covalent interactions between proteins of many different structural classes in virtually every subcellular compartment. Fluorescence techniques provide a variety of methods to study molecular characteristics. By combining BiFC with fluorescence recovery after photobleaching (FRAP) or fluorescence loss in photobleaching (FLIP) techniques, mobilities of protein complexes can be visualized [160]. Fluorescence photobleaching can also be used to evaluate if a BiFC complex is associated with a cellular scaffold or if it is free to diffuse within the cell [161]. BiFC and combining this technique with various fluorescence techniques provide powerful tools for studying and characterization of the protein complex dynamics in living cells.

In *Saccharomyces cerevisiae,* several protein-protein interactions have been revealed using the BiFC technique. In one study, a combination of split-GFP and the yeast two hybrid system was applied to detect interaction between Gal4p and Gal11p [162]. Another study utilized homologous recombination to label target proteins on the chromosomal level to identify protein-protein interactions. Sis1p in *MAT***a** yeast cells and Ssa1p in *MATα* yeast cells were labeled with YFP (Yellow Fluorescent Protein) fragments and fluorescence signal was observed in diploid yeast cells [163]. In another study a plasmid based system was used to express tagged proteins, to identify protein-protein interactions in different subcellular compartments including mitochondria and nucleus [153] . In the study reported herein, a split-EGFP method is implemented to detect G-protein coupled receptor dimerization. Enhanced green fluorescent protein [138] is a green fluorescent protein variant with improved properties in terms of folding, efficiency, and brightness, making this molecule one of the brightest and the most photostable among the *Aequorea* based fluorescent proteins [149]. In the BiFC assay, the EGFP molecule was split into two fragments termed N-EGFP (1-158) and C-EGFP (159-238), these fragments are then fused to the proteins whose interaction is being interrogated. Co-expression of these differently tagged fusion proteins results in chromophore maturation and fluorescence signal in the cell.

Although there are numerous studies, showing the dimerization of GPCRs with various methods, none indicate how and where these transmembrane proteins dimerize and/or internalize, hence leaving this issue still under debate. Our aim in this study is to investigate the location of dimerization and internalization of the Ste2p receptor dimers *in vivo* by live cell imaging using confocal laser scanning microscope.

1.4.3 Förster resonance energy transfer (FRET):

The theory of resonance energy transfer was originally developed by Theodor Förster and, in honor of his contribution, has been named after him [164] [165]. RET is a electrodynamic phenomenon that occurs when an excited state "donor" fluorophore transfers its energy to a ground state "acceptor" fluorophore in a non-radiative process through long range dipole-dipole interactions. For such an energy transfer to occur, the donor molecule should be in a close proximity with the acceptor molecule, which is typically ≤10 nm. For an efficient energy transfer, the emission spectrum of donor molecule should have a considerable overlap with the excitation spectrum of the acceptor molecule and in principle donor and acceptor molecules should have proper transition dipole moment orientations with each other but such a result is rare and possibly nonexistent in biomolecules. RET will occur if the spectral properties are suitable and the distance between donor and acceptor is within the RET range or so-called Förster distance. A wide variety of biochemical interactions result in a comparable distance within RET range hence such interactions are measurable using this technique.

Förster distance is defined as the distance at which RET efficiency is 50% [165]. In Förster Theory, rate of energy transfer from donor to acceptor $k_\tau(r)$ is given by:

$$k_\tau(r) = \frac{1}{\tau_D}\left(\frac{R_0}{r}\right)^6 \qquad 164$$

In this equation, τ_D is the decay time of donor in the absence of the acceptor, R_0 is the Förster distance and r is the distance between donor and acceptor. When, Förster distance is equal to the distance between donor and acceptor; $R_0 = r$; then rate of energy transfer should be equal to rate of decay of donor ($1/\tau_D$) and the RET efficiency is 50%. At Förster distance, where $r = R_0$, the donor emission intensity should be decreased to half in the absence of the acceptor.

In Förster Theory, the FRET efficiency (E) is calculated by using the following equation:

$$E_{\text{FRET}} = \frac{R_0^6}{r^6 + R_0^6} \qquad 164$$

Förster distances ranges from 20 to 90 Å, which is far below the spatial resolution of conventional widefield fluorescence optical microscopy, which enables localization of fluorescently labeled molecules within the optical spatial resolution limits defined by Rayleigh criterion, approximately 200 nanometers. Therefore RET is a convenient method for studying the interactions within and between the biological macromolecules. These distances are comparable to the size of biomolecules and/or the distance between sites on multi-subunit proteins and in physiological condition RET can only be observed only when two proteins are interacting since the average molecular distance is far above R_0.

Radiative energy transfer is due to the emission and absorption of photons and it depends on non-molecular optical properties of the sample, such as size of sample container, the path length, optical density of the sample, geometric arrangement of excitation and emission pathways. In contrast, RET phenomena does not involve emission or absorption of photons. The theory of fluorophore is assumed to be an oscillating dipole, which can exchange energy with another dipole with a similar resonance frequency [166]. Therefore, RET provides molecular information independent of solvent relaxation, excited state reactions, fluorescence quenching or fluorescence anisotropy. Such fluorescence phenomena depend on the interaction of fluorophore and the surrounding molecules, such as the solvent. However, these nearby interactions are less important for RET, except for the effects of these surrounding molecules on the spectral properties of donor and acceptor. RET is effective over longer distances, therefore the intervening solvent or macromolecules has little effect on efficiency of energy transfer, which is mostly dependent on the distance between donor and acceptor [167]. When energy transfer occurs, the acceptor molecule quenches the donor molecule fluorescence, and from the acceptor fluorophore, a sensitized fluorescence emission is observed (Figure 1.12).

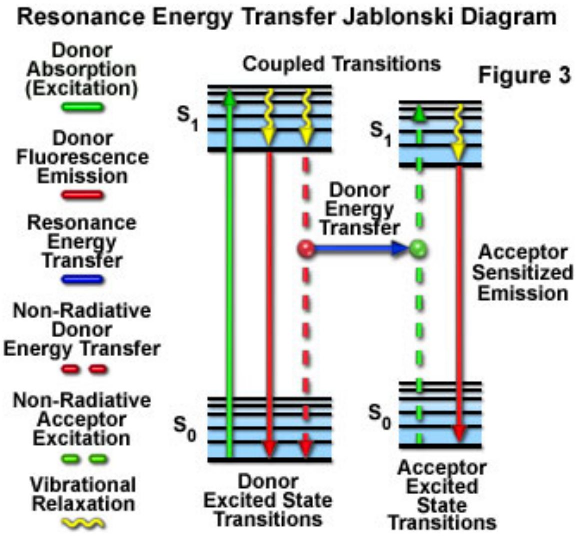
Resonance Energy Transfer Jablonski Diagram
Donor Absorption (Excitation)
Donor Fluorescence Emission
Resonance Energy Transfer
Non-Radiative Donor Energy Transfer
Non-Radiative Acceptor Excitation
Vibrational Relaxation
Coupled Transitions
Figure 3
S_1
S_1
Donor Energy Transfer
Acceptor Sensitized Emission
S_0
S_0
Donor Excited State Transitions
Acceptor Excited State Transitions

Figure 1.12 Jablonski diagram illustrating the coupled transitions between the donor emission (red arrow) and acceptor excitation (dashed green arrow) in FRET. Excitation and emission transitions are presented by straight vertical arrows (green and red, respectively). The coupled transitions are shown with dashed lines. In the presence of a suitable acceptor, the donor fluorophore can transfer excited state energy directly to the acceptor without emitting a photon (blue arrow). The resulting sensitized fluorescence emission has characteristics similar to the emission spectrum of the acceptor.
(source: http://www.olympusmicro.com/primer/techniques/fluorescence/fret/fretintro.html)

In cell biology fluorescent proteins could serve as FRET donors and FRET acceptors. These fluorescent proteins are genetically fused to the proteins of interest, imaging live cells expressing these fusion proteins with confocal fluorescence microscope results in data with high spatiotemporal resolutions. The interactions of proteins bring donor and acceptor fluorescent proteins into close proximity, resulting in a nonradiative energy transfer from donor to acceptor (Figure 1.13).

Over the last decade, the expansion of fluorescent protein color palette has resulted in numerous potential FRET donor and acceptors. Apart from the common FRET pairs such as BFP – GFP or CFP –YFP, especially the latter being almost accepted as an “industrial standard”, which are known to have significant spectral bleed through or channel crosstalk, now we have access to numerous other potential FRET pairs with better spectral profiles. Some of these potential pairs are given in Table 1.1.

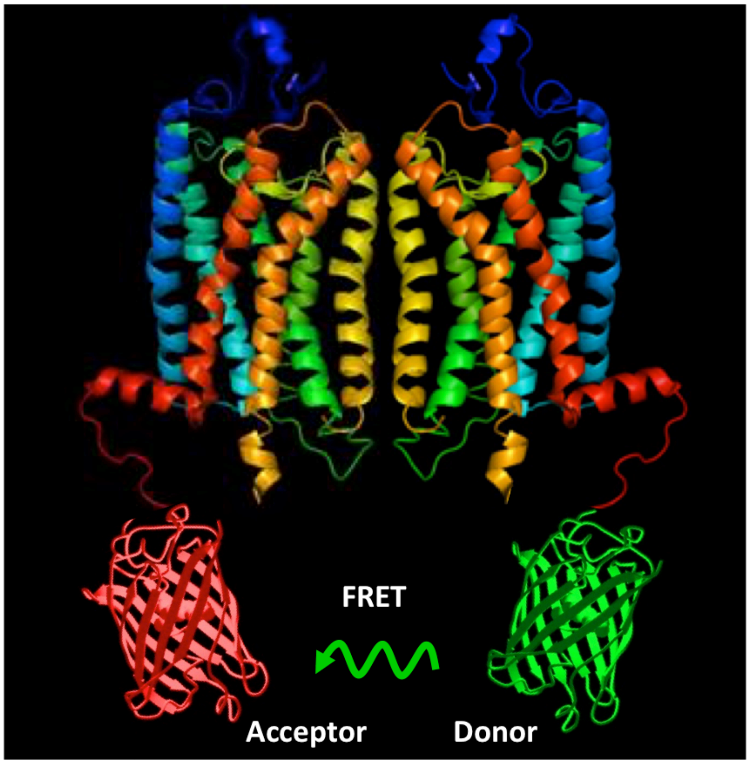

Figure 1.13 Representation of FRET phenomena as a result of two interacting GPCRs.

Table 1.1 Potential FRET pairs according to their spectral profiles.

FRET Pair	Donor excitation maximum (nm)	Acceptor emission maximum (nm)	Donor quantum yield	Acceptor extinction coefficient	Förster Distance (nm)
EBFP2-mEGFP	383	507	0.56	57,500	4.8
ECFP-EYFP	440	527	0.4	83,400	4.9
Cerulean-Venus	440	528	0.62	92,200	5.4
MiCy-mKO	472	559	0.9	51,600	5.3
TFP1-mVenus	492	528	0.85	92,200	5.1
CyPet-YPet	477	530	0.51	104,000	5.1
EGFP-mCherry	507	610	0.6	72,000	5.1
Venus-mCherry	528	610	0.57	72,000	5.7
Venus-tdTomato	528	581	0.57	138,000	5.9
Venus-mPlum	528	649	0.57	41,000	5.2

Ideally, a high degree of spectral overlap between the donor emission and acceptor excitation is required for efficient FRET to occur; yet in reality this overlap also generates a significant level of noise which interferes with the FRET signal. A population of excited donor molecules cannot transfer their energy to the acceptor, yet the relaxation occurs in a radiative manner by emitting photons, some of this emitted light can pass through the FRET filter, detected by the detector therefore leading a noise which is called donor bleed through (Figure 1.14). These bleed-through contributions from the donor result from the overlap of the donor and acceptor fluorescence emission profiles and they are often very broad (up to 100 nanometers) and difficult to separate. Likewise, a population of acceptor molecules is also being excited from the donor excitation channel which results in a noise termed as acceptor bleed through. Also, there is wide variety of other noise sources such as autofluorescence, detector noise, optical noise, filter noise and spectral sensitivity variations in the donor and acceptor channels. So, detection of actual FRET signal requires successful subtraction of these background noises from the detected FRET signal.

The most straightforward technique for measuring FRET is known as "sensitized emission". In this technique, the donor fluorophore is excited with a certain wavelength of light and the signal is detected using two emission filter sets one is tuned for donor emission wavelength (donor filter) and the other is tuned for acceptor emission wavelength (FRET filter). Unfortunately, in sensitized emission bleed-through is an important problem, to overcome this problem extensive control experiments needs to be designed and the collected data needs to be subjected to complicated image processing for subtracting bleed-through (Figure 1.14).

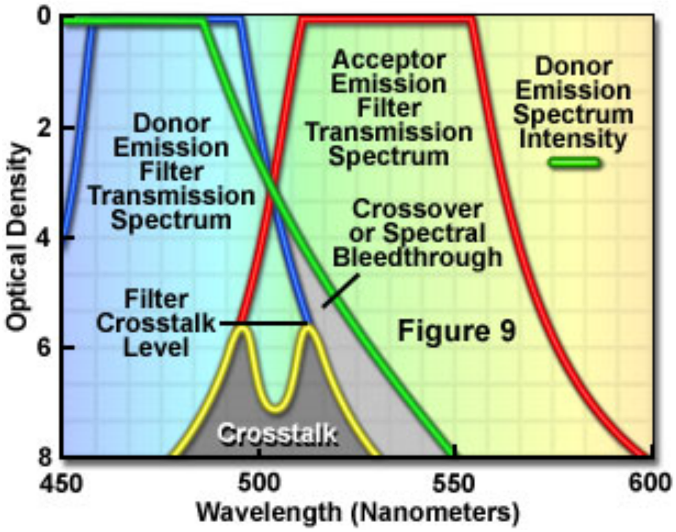

Figure 1.14 Crosstalk and bleed through in FRET measurements.

Using FRET methods such as “acceptor photobleaching” and “fluorescence lifetime imaging microscopy (FLIM)”, bleed-through signals can be significantly avoided. In former technique, FRET efficiency is calculated by using the ratio of quenched donor signal in the presence of the acceptor, and the de-quenched donor signal after the photobleaching of acceptor fluorophore. In the presence of a bleached acceptor molecule, donor molecule cannot transfer its energy through FRET, hence results in an increase in the donor signal. In acceptor photobleaching each cell being investigated are also the control sets, as a result making this technique one of the most accurate ways of measuring FRET. All fluorophores has a nanosecond timescale exponential decay in their fluorescence emission, and this “fluorescence lifetime” can be measured. The rate of this decay is sensitive to any processes that influence the excited state, most importantly to the presence of an acceptor. In FLIM, fluorescence lifetime of donor is measured in the presence of and acceptor, in other word in the presence of FRET; and in the absence of an acceptor, in other words after the photobleaching of the acceptor.

Although there are various methods available for measuring FRET in live cell using confocal microscope, none of these techniques are completely free from disadvantages. To overcome these disadvantages, there are methods and software for with significant corrective calculations or data analysis algorithms for the acquired FRET data. It is certain that FRET analysis is an invaluable tool for studying protein interactions using live cell imaging and without a doubt shows great promise and potential for further development in the instrumentation and software and the scope of biological applications.

1.5 Aim of the study

The first aim of this study was to determine where receptor dimerization of a model GPCR occurs *in vivo*: either at the plasma membrane or during transit to and from the membrane. We used a bimolecular fluorescence complementation assay with Ste2p incorporating split EGFP fragments and confocal laser microscopy. The second aim was to determine whether the model GPCR interacts only as a homodimer or as higher homooligomeric structures with 3 or more proteins *in vivo*. For this, we used bimolecular fluorescence complementation (BiFC) assay with Ste2p incorporating split EGFP and split mCherry fragments, signal colocalization and Förster resonance energy transfer with confocal laser microscopy.

CHAPTER 2

EXPERIMENTAL PROCEDURES

2.1 Materials

2.1.1 Yeast strains, plasmids and media

Saccharomyces cerevisiae strains used were DK102 (*MAT***a** *ura3*-52 *lys*2–801^{am} *ade2*-101^{oc} *trp1*-Δ63 *his3*-Δ200 *leu2*-Δ1 *ste2*::*HIS3 sst1*-Δ5) [168], BJS21 (*MAT***a**, *prc1-407 prb1-1122 pep4-3 leu2 trp1 ura3-52 ste2::Kan*^{R}) [169], LM102 (MATa, bar1, his4, leu2, trp1, met1, ura3, FUS1–lacZ::URA3, ste2–dl) [170] and OM102 (MATa, bar1, his4, leu2, trp1, met1, ura3, FUS1–lacZ, ste2–dl) created from LM102. DK102 was used for alpha-factor induced growth arrest assay and imaging of the constructs. The protease deficient BJS21 strain was employed in western blot analysis due to the decreased receptor degradation. LM102 strain, carrying FUS1-lacZ gene was used for the gene expression assays (*FUS1-lacZ* assay).

The parental plasmids pBEC1 (constructed from p424GPD, a 2µm based shuttle vector with a GPD promoter, CYC1 terminator, and TRP marker) and pCL01 (constructed from p424GPD, a 2µm based shuttle vector with a GPD promoter, CYC1 terminator, and URA marker) expressing the Ste2p receptor which was used as template for our constructs were kindly gifted by Prof. Dr. Jeffrey M. Becker (University of Tennessee Knoxville, USA). pUG6 plasmid [171] possessing a KanMX drug resistance cassette and pESC-TRP (a 2µm based shuttle double promoter vector with a GAL1 promoter - CYC1 terminator, GAL10 promoter - ADH1 terminator and TRP marker) and pESC-URA (a 2µm based shuttle double promoter vector with a GAL1 promoter - CYC1 terminator, GAL10 promoter – ADH1 terminator and URA marker) (Agilent Technologies, CA, USA) were also generously supplied by Prof. Dr. Jeffrey M. Becker (University of Tennessee Knoxville, USA). pSP-G1 and pSP-G2 (2µm based shuttle double promoter vectors, PGK1 – TEF1 promoter region, ADH1 – CYC1 terminator region and URA marker) plasmids [172] were kindly provided by Dr. Jens B. Nielsen (Chalmers University of Technology, Sweden).

pEGFP-N2, enhanced green fluorescence cDNA and pmCherry-N1, mCherry cDNA vectors were generously donated by Prof. Dr. Henry Lester (California Institute of Technology, USA).

Yeast strains were grown in YEPD (yeast extract-peptone-dextrose) broth at 30 °C and were maintained on agar plates at 4 °C for short-term storage. For selection of successful yeast transformants with our constructed plasmids, media lacking tryptophan (MLT) media lacking uracil (MLU) and media lacking both Tryptophan and Uracil (MLTU), respectively were used (Appendix A).

2.1.2 Bacterial Strains, Media and Growth Conditions

DH5α competent E.coli strain (New England Biolabs, USA) was used in this study. Bacterial strains were grown in LB (Luria Bertani) media, both solid agar plates and liquid broth. All ingredients of the media which are given in Appendix B were dissolved in distilled water, and after adjusting the pH to 7.4, media were sterilized by autoclaving at 121°C for 20 minutes. 100 mg/mL of Ampicillin or 50 mg/mL Kanamycin was added to sterile media for bacterial selection. Solid E.coli cultures were grown in incubators and liquid cultures were grown in rotary incubator at 37 °C.

2.1.3 Chemical reagents and other materials

Phusion Hot Start II High-Fidelity DNA Polymerase and LA Taq polymerases were purchased from Takara Bio Inc. (Japan) and Thermo Fisher Scientific (MA, USA), respectively. Restriction enzymes used in this study were purchased from Thermo Fisher Scientific (MA, USA). The peptide pheromone α-factor used in biological activity assays was synthesized and purified by previously published methods [173]. Primers used in this study were purchased from Invitrogen (MA, USA). Paper filter disks were from BD (Franklin Lakes, NJ, USA), microscope slides and cover glass used in imaging experiments were ordered from Fisher Scientific (MA, USA). All other chemicals used in buffers and mediums were obtained from Sigma-Aldrich Inc. (NY, USA) and AppliChem (Darmstadt, Germany). Leica SP2 Laser Scanning Confocal Microscope equipped with a Leica 63x/1.32 HCX PL APO Oil DIC objective (Department of Microbiology and Department of Biochemistry, Cell, and Molecular Biology, University of Tennessee, Knoxville, Tennessee).

2.2 Protocols

2.2.1 High Efficiency Transformation of chemically competent E.coli Cells

10-30 µL of DH5α chemically competent E.coli cells (New England Biolabs, USA), were thawed on ice for 5 minutes. 0.2 µL of plasmid DNA (≈20 ng) on 10 µL of DH5α competent cells or 1.5 µL of PCR mixture; ligation or DpnI digestion mixture was added on 30 µL of DH5α competent E.coli with gently flicking the tube to mix the cells and DNA. Cells were placed on ice for 30 minutes followed by a heat shock at 42 °C for 30 seconds. After the heat shock cells were chilled on ice for 5 minutes and volume was brought to 1000 µL with adding SOC (New England Biolabs, USA). Cells were incubated at 37 °C with constant shaking for 60 minutes. Cells were spinned down at 4,000 rpm for 4 minutes, followed by discarding 800 µL of supernatant without disturbing the pellet. Finally, the cell pellet was resuspended and 200 µL of cell mixture was spreaded on the selective LB plates containing Amp/Kan and plates were incubated overnight at 37 °C.

2.2.2 Yeast Transformation

For high efficiency transformation the LiAc/SS-DNA/PEG transformation method was modified and applied [174]. All solutions were prepared under aseptic conditions and sterilized either by filter or autoclave and the recipes of solutions were listed in the Appendix A. Yeast cells were inoculated in 5 mL of appropriate medium broth and incubated with shaking at 30°C overnight. Following day, cells were counted by hemocytometer and 5×10^6 cells/mL in a total volume of 50 mL were inoculated in sterile Erlenmeyer flask. The culture was incubated at 30°C on a shaker at 200 rpm 3 -5 hours until cell density reaches to 2×10^7 cells/mL. The culture harvested in a sterile 50 mL centrifuge tube at 4000 rpm for 5 minutes, the supernatant was discarded. Cells were washed with 25 ml of sterile water and then resuspended in 1 mL 100 mM Lithium acetate (CH_3COOLi). The suspension was transferred to a 1.5 mL microfuge tube and cells were spinned down for 15 seconds and LiAc was removed using micropipette. Cells were resuspended in 400 µL of 100 mM LiAc and divided into microfuge tubes in 50 µL aliquots. Cells were spinned down again to remove the LiAc, then for each transformation 240 µL PEG (50% w/v), 36 µL 1.0 M. LiAc, 50 µL SS-DNA (2.0 mg/mL), X µL Plasmid DNA (0.1 - 10 µg), 34-X µL Sterile water giving a total volume of 360 µL was added in the given order. Each tube was vigorously vortexed until the disappearance of the cell pellet and yielding a homogeneous solution. The cell solution was incubated at 30°C for 30 minutes with constant shaking followed by a heat shock at 42 °C for 25 minutes. The cells were spinned down at 8000 rpm for 30 seconds, supernatant was removed with micropipette and cells were resuspended in 1 mL of sterile water. 200 µL of cell suspension was placed on selective media plates and incubated at 30 °C for 2 days. From each transformation plate, 4 individual single colonies were picked and streaked on a fresh selective media plate for further analysis.

2.2.3 Insertional PCR protocol for the construction of tagged Ste2p

EGFP and mCherry sequences were both inserted into Ste2p receptor between the 304-305th residues, yielding a full-length receptor carrying a fluorescent protein tag between its 304-305th positions. Additionally these fluorescent proteins (FP) were also appended into C-terminally truncated Ste2p-Δ305-431 receptor. For the *bimolecular fluorescence complementation* (BiFC) *method*, EGFP fragments were dissected between 158-159th positions; mCherry fragments were dissected between 159-160th positions and they were both inserted into Ste2p receptor between the 304-305th residues; additionally these fragments were also appended into C-terminally truncated Ste2p-Δ305-431 receptor.

The strategy for cloning a fluorescent protein (FP) or a fluorescent protein fragment into the Ste2p receptor includes two consecutive PCRs. For cloning the whole FP; EGFP or mCherry sequence into Ste2p; in the first reaction, FP is amplified with primers carrying homologous regions from 5' and 3' ends of FP with 25-30 overhanging bases from STE2 sequence upstream and downstream from 304-305th position (corresponding to 912th position on the cDNA). Likewise, for cloning the FP fragment sequence into Ste2p, N- and C-terminals of FP fragments; N-EGFP (1-158) and C-EGFP (159-238) or N-mCherry (1-159) and C-mCherry (160-237) were amplified with primers carrying homologous sequences from EGFP or mCherry fragments and 25-30 overhanging bases from STE2 sequence from 304-305th position.

The general schematic representation of the amplification of the EGFP sequence from it's vector pEGFP-N2 is given in Figure 2.1. Likewise, the amplification of EGFP fragment sequences from pEGFP-N2 is schematically represented in Figure 2.2.

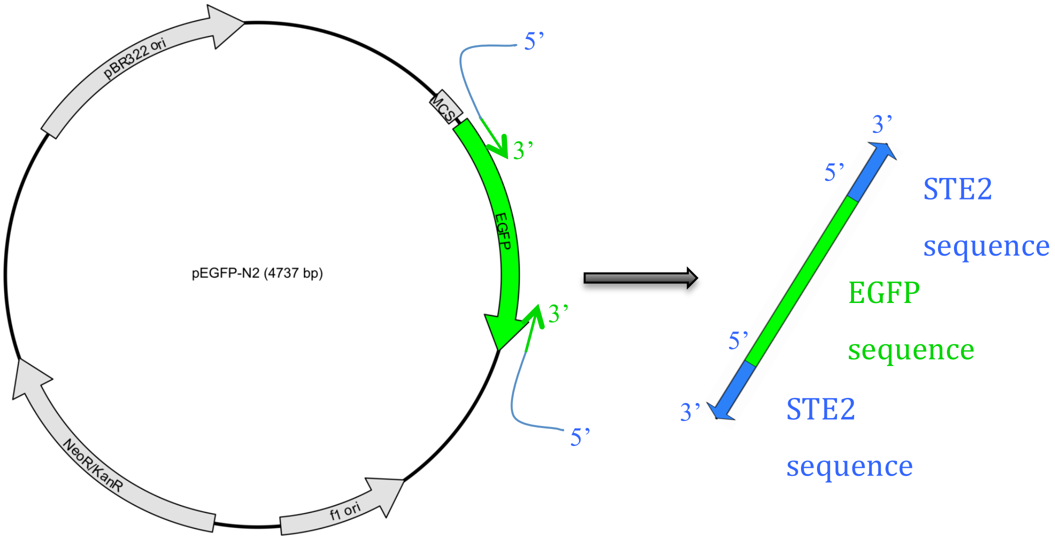
pBR322 ori
MCS
EGFP
pEGFP-N2 (4737 bp)
NeoR/KanR
f1 ori
5'
3'
3'
5'
3'
5'
STE2
sequence
EGFP
sequence
5'
3'
STE2
sequence

Figure 2.1 The representation of 1st PCR, amplification of EGFP from pEGFP-N2 with primers carrying complementary Ste2p sequences (shown in blue) homologous to the insertion position on STE2 gene.

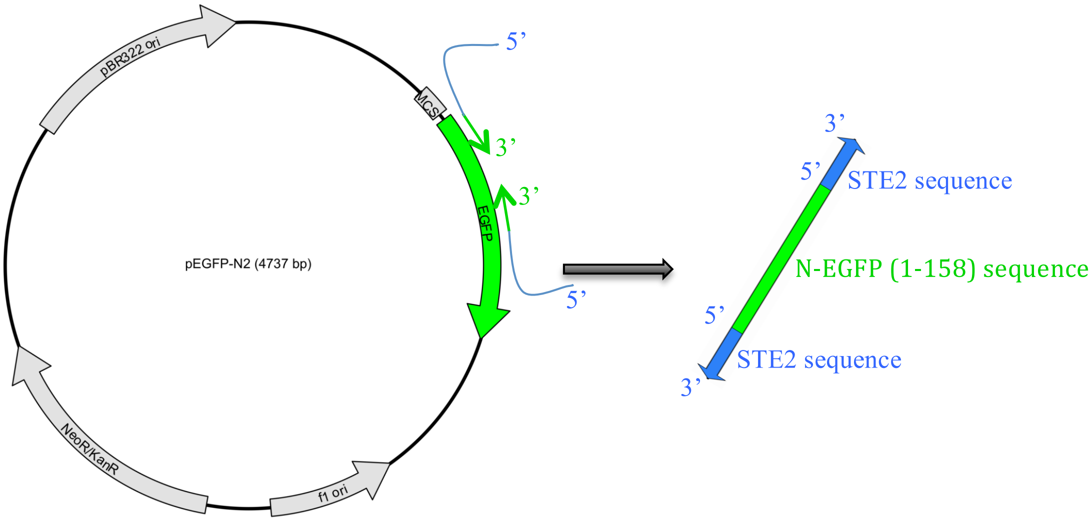
pBR322 ori
MCS
EGFP
pEGFP-N2 (4737 bp)
NeoR/KanR
f1 ori
5'
3'
3'
5'
3'
5'
STE2 sequence
N-EGFP (1-158) sequence
5'
3'
STE2 sequence

Figure 2.2 The representation of 1st PCR, amplification of EGFP fragments from pEGFP-N2 with primers carrying complementary Ste2p sequences (shown in blue) homologous to the insertion position on STE2 gene.

Primers for dissecting EGFP from 158-159th positions, carrying complementary overhanging regions from the 304-305th positions on Ste2p receptor are given in Table 2.1 below.

Table 2.1 Primers for amplifying N-EGFP (1-158) and C-EGFP (159-238) to carry complementary overhanging regions from the 304-305th positions on Ste2p receptor.

Primer	Sequence
N-EGFP (1-158) For	CACGGCTGCTAATAATGCATCCAAAatggtgagcaagggcgaggag
N-EGFP (1-158) Rev	GTAAAGTCTGAAGTAATTGTGTTTGTctgcttgtcggccatgatatagac
C-EGFP (159-238) For	CACGGCTGCTAATAATGCATCCAAAaagaacggcatcaaggtgaacttc
C-EGFP (159-238) Rev	GTAAAGTCTGAAGTAATTGTGTTTGTcttgtacagctcgtccatgcc

To generate C-terminally truncated Ste2p constructs, primers were designed with a “TAA” stop codon right after the FP sequence (EGFP and mCherry) or FP fragments (N-EGFP (1-158), C-EGFP (159-238), N-mCherry (1-159) and C-mCherry (160-237)) at 3’ end.

The primers designed for dissecting EGFP from 158-159th positions; with a 3’ stop codon and complementary overhanging regions from the 304-305th positions on Ste2p receptor are given in Table 2.2.

Table 2.2 Primers designed for amplifying N-EGFP (1-158) and C-EGFP (159-238) to carry complementary overhanging regions from the 304-305th positions on Ste2p receptor and to insert a stop codon right before 305th position.

Primer	Sequence
N-EGFP (1-158) For	CACGGCTGCTAATAATGCATCCAAAatggtgagcaagggcgaggag
N-EGFP (1-158) Rev	GTAAAGTCTGAAGTAATTGTGTTTGT**TTA**ctgcttgtcggccatgatatagac
C-EGFP (159-238) For	CACGGCTGCTAATAATGCATCCAAAaagaacggcatcaaggtgaacttc
C-EGFP (159-238) Rev	GTAAAGTCTGAAGTAATTGTGTTTGT**TTA**cttgtacagctcgtccatgcc

The primers designed for dissecting mCherry from 159-160th positions, with 3' stop codon and complementary overhanging regions from the 304-305th positions on Ste2p receptor are given in Table 2.3.

Table 2.3 Primers for amplifying N-mCherry (1-159) and C-EGFP (160-237) carrying complementary overhanging Ste2p sequences upstream and downstream from the 304-305th and inserting a stop codon right before 305th position.

Primer	Sequence
N-mCherry (1-159) For	GCCACGGCTGCTAATAATGCATCCAAAatggtgagcaagggcgaggag
N-mCherry (1-159) Rev	GTCTGAAGTAATTGTGTTTGT**TTA**gtcctcggggtacatccgctcggaggaggc
C-mCherry (160-237) For	GCCACGGCTGCTAATAATGCATCCAAAggcgccctgaagggcgagatcaag
C-mCherry (160-237) Rev	GTAAAGTCTGAAGTAATTGTGTTTGT**TTA**cttgtacagctcgtccatgcc

The general PCR conditions for a 50 μL reaction mixture using the primers given in Tables 2.1 – 2.3 is given below:

Component	50 μL rxn	Final conc.
Water	30.5	
5X Phusion HF Buffer	10	1X
10 mM dNTPs	5	200 μM each
Primer forward	1.25	0.5 μM
Primer reverse	1.25	0.5 μM
pEGFP-N2 or pmCherry-N1	1.5	150 ng
Phusion Hot Start II DNA Polymerase	0.5	0.02 U/μL

98°C	30s	
98°C	**10s**	
54.1°C	**30s**	**25-35cycles**
72°C	**15-30 s/kb**	
72°C	10m	

Products of "first" PCR were loaded on a 1% low melting point agarose gel and extracted using QIAquick gel extraction kit (Qiagen, MD, USA).

In a "second" PCR, using the products from "first" PCR as tandem primer and pCL01 or pBEC1 as template vector, desired FP or FP fragment sequences were inserted into the targeted position of Ste2p receptor. The complementary regions present on the "first" PCR product constitute the initial hybridization to insert the FP sequence into the targeted position on the template (Figure 2.3).

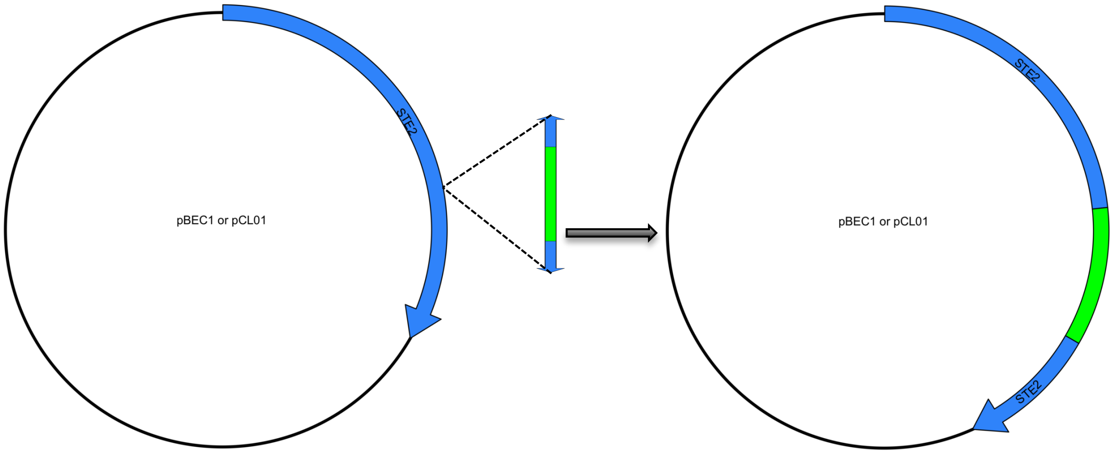

Figure 2.3 Representation of 2nd PCR, inserting the fluorescent tag, or fluorescent protein fragments to the directed position on STE2 gene.

So, in this "second" PCR, whole vector was amplified with choice of high fidelity DNA polymerase enzyme, 1:10 (vector : insert) molar ratio of "first" PCR products (insert) as tandem dimers to insert FPs of FP fragments sequences between the targeted sequences in a Ste2p gene (vector). For a 20 μL reaction mixture:

Component	20 μL rxn	Final conc.
Water	13-X	
5X Phusion HF Buffer	4	1X
10 mM dNTPs	2	200 μM each
pBEC1 or pCL01	0.6	60-100 ng
Insert	X	10X molar ratio to template
Phusion Hot Start II DNA Polymerase	0.4	0.04 U/μL

98°C	30s	
98°C	**10s**	
50-60°C	**30s**	**25-35cycles**
72°C	**8 min**	
72°C	10m	
4°C	hold	

To get rid of the template plasmid, the PCR mixture was digested with DpnI enzyme (Thermo Scientific, MA, USA) for 1 hour to overnight. DpnI recognizes the G_mA/TC sequences and cleaves only when this recognition site is methylated, so template DNA must be purified from a dam$^+$ strain, which would be a substrate for DpnI. The digestion reaction condition is as follows:

20 μL reaction	
PCR mixture	12
Nuclease free water	5
Buffer Tango	2
DpnI (Fermentas)	1

1h – overnight @ 37°C

The digestion mixture was directly used in transformation of E.coli. Transformants were selected on ampicillin LB plates and plasmids were isolated using MiniPrep kit (Fermentas GeneJET^{TM} Plasmid MiniPrep Kit).

The constructs were verified by sequencing and they were used for the transformation of yeast cells. As positive EGFP signal controls, Ste2p receptor tagged with full length EGFP and mCherry between 304-305th positions; and C-terminally truncated

Ste2p-Δ305-451 receptor tagged with full length EGFP and mCherry at 304th position was constructed.

2.2.4 Site directed mutagenesis

For inserting the desired mutation "double primer method" [175] was used (Figure 2.4). In this method two primers, both carrying the targeted mutation at their overlapping region are designed as shown in figure. A "**G**" or "**C**" is left both at 3' and 5' ends of both primers. More than 5 bases are left at 5' end and more than 8 non-overlapping bases are left from the 3' end. Taking into account these properties primers that are 20-30 bases long were used for the insertion the mutation.

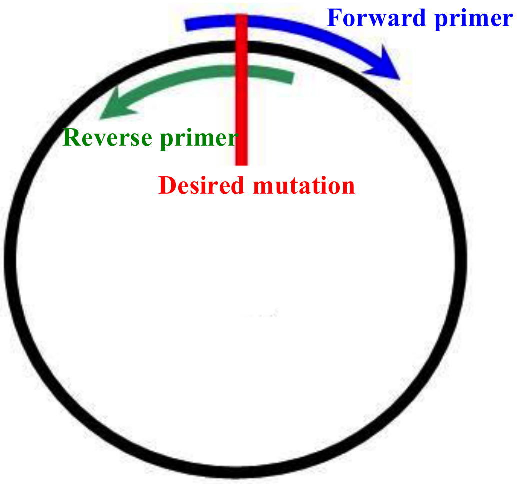

Figure 2.4 Representative image for inserting the directed mutation with double primer method.

In site directed mutagenesis, whole vector is amplified with the primers both carrying directed mutations using Phusion Hot Start II High-Fidelity DNA Polymerase (Thermo Fisher Scientific, MA, USA). For 20 µL reaction, the mixture is:

Component	20 µL rxn	Final conc.
Water	12	
5X Phusion HF Buffer	4	1X
10 mM dNTPs	2	200 µM each
Primer forward	0.5	0.5 µM
Primer reverse	0.5	0.5 µM
Template DNA	0.6	60-100 ng
Phusion Hot Start II DNA Polymerase	0.4	0.04 U/µL

98°C	30s	
98°C	**10s**	
50-60°C	**30s**	**25-35cycles**
72°C	**8 min**	
72°C	10m	
4°C	hold	

To get rid of the template plasmid, the PCR mixture was digested with DpnI enzyme (Thermo Scientific, MA, USA) for 1 hour to overnight.

The digestion mixture was directly used in transformation of E.coli. Transformants were selected on ampicillin LB plates. Selected colonies were inoculated in 5 mL LB/Amp liquid media, after overnight growth plasmids were isolated using MiniPrep kit (Fermentas GeneJET^{TM} Plasmid MiniPrep Kit) and all constructs were confirmed by sequencing.

On all full-length Ste2p constructs originating from pBEC1 and pCL01 plasmids a "TAA" stop codon was inserted right before FLAG & HIS tags using primers given in Table 2.4.

Table 2.4 Primers to remove the FLAG and HIS tags from expressed Ste2p.

Primer	Sequence
Ste2-Stop HT-FT for:	CTGGACTGAAGATAATAATAATTTA**TAA**GACTACAAGGACG
Ste2-Stop HT-FT rev:	GTCATCGTCGTCCTTGTAGTC**TTA**TAAATTATTATTATCTT

Primers designed to remove the "TAA" stop codon from 305th position on Ste2p[EGFP] or Ste2p[mCherry] are given in Table 2.5.

Table 2.5 Primers to remove the stop codon at 305th position from Ste2p.

Primer	Sequence
Ste2-nostop-304 for:	gacgagctgtacaagACAAACACAATTACTTCAGACTTTACAACATCC
Ste2-nostop-304 rev:	GTCTGAAGTAATTGTGTTTGTcttgtacagctcgtccatgcc

Primers designed to insert G56L, G60L and G56/60L mutations on $G^{56}XXXG^{60}$ motif at positions 56 and 60 on Ste2p given in Table 2.6.

Table 2.6 Primers designed to mutate Glycines to Leucine at positions 56 and 60 on Ste2p.

Primer	Sequence
Ste2-G56L for:	GCCATTATGTTTCTTGTCAGATGTGGTGCAGCTGCTTTGACTTTG
Ste2-G56L rev:	CATCTGACAAGAAACATAATGGCCTGAGTAACAGTACTGTTAAC
Ste2-G60L for:	GTCAGATGTCTTGCAGCTGCTTTGACTTTGATTGTCATGTGG
Ste2-G60L rev:	GCAGCTGCAAGACATCTGACACCAAACATAATGGCCTGAGTAAC
Ste2-G60/56L rev:	GCAGCTGCAAGACATCTGACAAGAAACATAATGGCC

Primers designed to insert P290D mutation on Ste2p given in Table 2.7.

Table 2.7 Primers designed to mutate proline to aspartic acid at position 290 on Ste2p.

Primer	Sequence
Ste2-P290D for:	GTCTTTAGATTTATCATCAATGTGGGCCACG
Ste2-P290D rev:	GATGATAAATCTAAAGACAATACAGCAAG

2.2.5 *Ligation protocol for constructs*

The labeling of Ste2p with EGFP, mCherry, N- or C- EGFP and N- or C-mCherry was done on pBEC1 and pCL01 vectors as explained previously. These labeled DNAs were then amplified with primers carrying restriction sites at 5' and 3' ends using Phusion Hot Start II High-Fidelity DNA Polymerase (Thermo Fisher Scientific, MA, USA) for cloning these constructs into any desired vector. Also for constructing constitutively active double promoter vectors, TEF1-PGK1 divergent promoter region was amplified and ligated into the desired vector.

Cloning of Ste2p constructs were done into pESC-TRP and pESC-URA vectors (Agilent Technologies, CA, USA), between EcoRI – NotI restriction regions on multiple cloning site 1 and between BamHI – NheI restriction regions on multiple cloning site 2 (Figure 2.5).

Primers were designed to amplify Ste2p gene carrying either 5' EcoRI – 3' NotI restriction enzyme sites, or 5' BamHI – 3' NheI restriction enzyme sites as given in Table 2.8.

Table 2.8 Primers for cloning Ste2p constructs into pESC vectors.

Primer	Sequence
Ste2-EcoRI-F	GAGAGAGAGGAATTCATGTCTGATGCGGCTCCTTCATTGAGC
Ste2-NotI-R	GAGAGAGAGGCGGCCGCttagccgctgctatgatgatgatgatg
Ste2-BamHI-F	GAGAGAGAGGGATCCATGTCTGATGCGGCTCCTTCATTGAGC
Ste2-NheI-R	GAGAGAGAGGCTAGCttagccgctgctatgatgatgatgatg

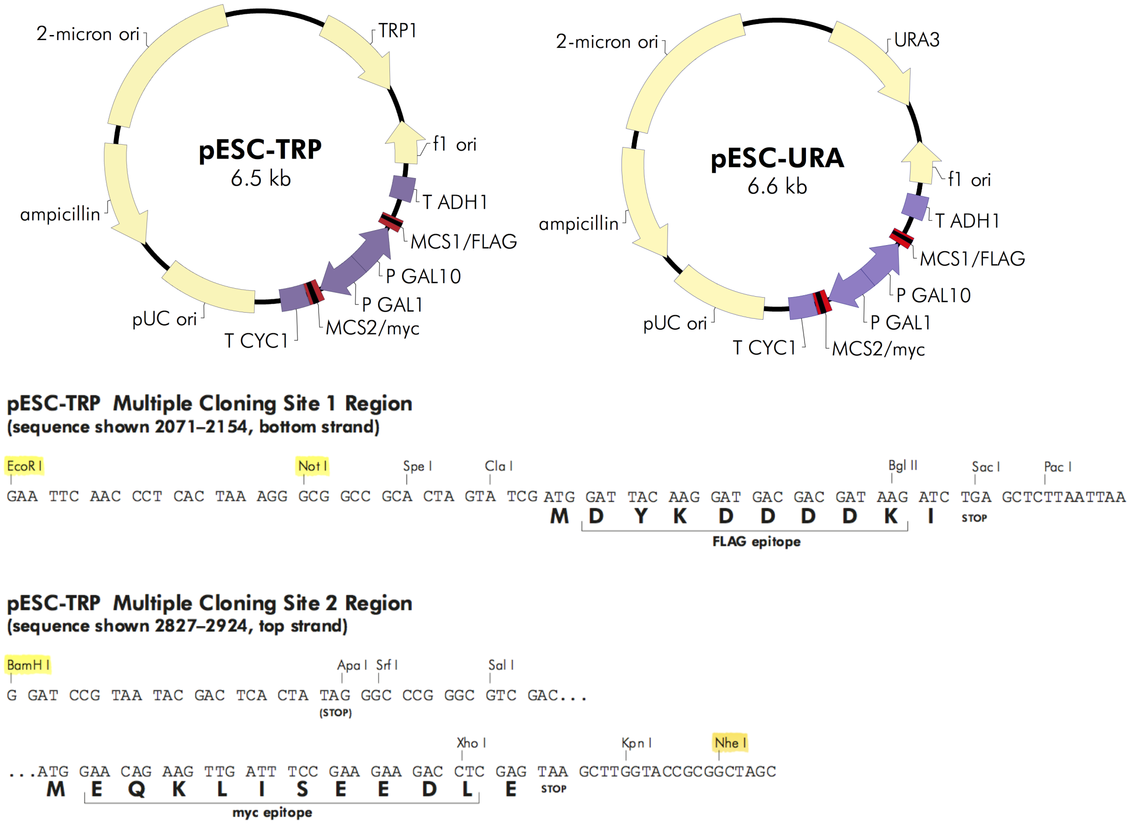
2-micron ori
TRP1
pESC-TRP
6.5 kb
f1 ori
T ADH1
MCS1/FLAG
P GAL10
P GAL1
MCS2/myc
T CYC1
pUC ori
ampicillin
2-micron ori
URA3
pESC-URA
6.6 kb
f1 ori
T ADH1
MCS1/FLAG
P GAL10
P GAL1
MCS2/myc
T CYC1
pUC ori
ampicillin
pESC-TRP Multiple Cloning Site 1 Region
(sequence shown 2071–2154, bottom strand)
EcoR I
Not I
Spe I
Cla I
Bgl II
Sac I
Pac I
GAA TTC AAC CCT CAC TAA AGG GCG GCC GCA CTA GTA TCG ATG GAT TAC AAG GAT GAC GAC GAT AAG ATC TGA GCTCTTAATTAA
M D Y K D D D D K I STOP
FLAG epitope
pESC-TRP Multiple Cloning Site 2 Region
(sequence shown 2827–2924, top strand)
BamH I
Apa I
Srf I
Sal I
G GAT CCG TAA TAC GAC TCA CTA TAG GGC CCG GGC GTC GAC...
(STOP)
Xho I
Kpn I
Nhe I
...ATG GAA CAG AAG TTG ATT TCC GAA GAA GAC CTC GAG TAA GCTTGGTACCGCGGCTAGC
M E Q K L I S E E D L E STOP
myc epitope

Figure 2.5 pESC-TRP and pESC-URA (Agilent Technologies, CA, USA) vector maps and their multiple cloning sites (MCS) sequences.

The Gal1 – Gal10 promoter region on pESC vectors was switched with TEF1 – PGK1 (G1) and PGK1 – TEF1 (G2) promoter regions obtained from pSP-G1 and pSP-G2 plasmids given in Figure 2.6 [172] for constitutive expression of cloned Ste2p constructs Figure 2.6).

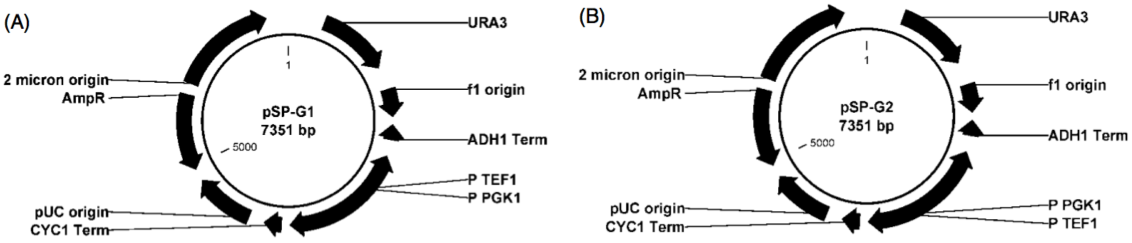
(A)
URA3
1
2 micron origin
AmpR
f1 origin
pSP-G1
7351 bp
5000
ADH1 Term
P TEF1
P PGK1
pUC origin
CYC1 Term
(B)
URA3
1
2 micron origin
AmpR
f1 origin
pSP-G2
7351 bp
5000
ADH1 Term
P PGK1
P TEF1
pUC origin
CYC1 Term

Figure 2.6 pSP-G1 (TEF1-PGK1) and pSP-G2 (PGK1-TEF1) vector maps. [172]

The G1 and G2 promoter regions were amplified by using the primer set given in Table 2.9, to carry EcoRI – BamHI sites on 5’ and 3’ termini respectively.

Table 2.9 TEF1-PGK1 and PGK1-TEF1 promoter region amplification primers.

Primer	Sequence
G1-EcoRI-F	GAGAGAGAGAGAATTCTTGtAATTAAAACTTAgATTAgATTGC
G1-BamHI-R	GAGTCGTATTACGGATCCTTGTTTTATATTTGTTG
G2-EcoRI-F	GAGAGAGAGAGAATTCTTGTTTTATATTTGTTGTAAAAAG
G2-BamHI-R	GTCGTATTACGGATCCTTGTAATTAAAACTTAGATTAGATTGC

The general PCR condition for amplifying Ste2p constructs or PGK1-TEF1 divergent promoter region with desired 5’ – 3’ restriction enzyme sites are as follows:

Component	50 μL rxn	Final conc.
Water	30.5	
5X Phusion HF Buffer	10	1X
10 mM dNTPs	5	200 μM each
Forward primer	1.25	0.5 μM
Reverse primer	1.25	0.5 μM
Template DNA	1.5	150 ng
Phusion Hot Start II DNA Polymerase	0.5	3%

98°C	30s	
98°C	**10s**	
54.1°C	**30s**	**25-35cycles**
72°C	**15-30 s/kb**	
72°C	10m	
4°C	hold	

The PCR product, carrying desired restriction sites on 5’ and 3’ ends, is purified by PCR purification kit (Fermentas GeneJET^{TM} PCR Purification Kit) and left for digestion for 1-3 h with corresponding restriction enzyme pair. The general digestion conditions are as follows:

40 µL reaction	
PCR product	34
FD green buffer	4
E1	1
E2	1

1-3h @37°C

The cloning vector that will be used for ligating the constructed cDNA is also left for digestion with same restriction enzymes. The reaction conditions are as follows:

30 µL reaction	
Vector	23
FD green buffer	3
E1	2
E2	2

1-3 h @37°C

The digestion reaction products were then run on 1% low molecular weight agarose gel and products of digestion reactions were extracted by using QIAquick gel extraction kit (Qiagen, MD, USA).

The ligation reaction was set to be 1:3 (vector : insert), molar ratio using 100 ng of linearized vector unless otherwise is specified. Both the linearized vector and digested PCR product were extracted from agarose gel and were let to ligation with conditions given below:

20 µL reaction	
Vector	100 ng
Insert	3x molar ratio
Water	20–X µL
Buffer Tango (Thermo Fisher Scientific, MA, USA)	2 µL
T4 DNA Ligase (Thermo Fisher Scientific, MA, USA)	1 µL

1 h @RT

1.5 μL of ligation mixture was directly used in transformation of E.coli. Next day transformants were selected on ampicillin LB plates. Three colonies were inoculated in 5 mL LB/Amp liquid media and the plasmids were isolated using Fermentas GeneJET^{TM} Plasmid MiniPrep Kit (Thermo Fisher Scientific, MA, USA). The positive inserts were first confirmed on gel by digesting plasmids with the same restriction enzymes and finally plasmids carrying correct sized inserts were confirmed by sequencing.

2.3 Growth Arrest (Halo) Assay

Solid MLT medium and solid MLU medium was overlaid with 4 mL of *S. cerevisiae* DK102 cell suspension (2,5 x 10^5 cells/mL of Nobel agar) [176]. 10 μL of alpha-factor pheromone at various concentrations were applied on filter disks (BD, Franklin Lakes, NJ) and placed on top of agar. Plates were incubated at 30 °C for 24-36 h and then observed for clear zones (halos) around the disks. The data were expressed as the diameter of the halo including the diameter of the disks versus alpha-factor concentration and analyzed by employing Prism software (GraphPad Software, San Diego, CA). Each assay was carried out at least three times with no more than a 2 mm variation in halo size at an individual amount of alpha-factor. The reported values represent the mean of these tests.

2.4 FUS1-lacZ gene induction assay

LacZ gene induction was determined with a fluorescein-containing galactopyranoside analog [177] using LM102 yeast strain that carries a *FUS1-lacZ* gene inducible by the mating pheromone. Cells were grown in MLT/MLU medium broth overnight at 30°C. Next day, each culture was diluted to an OD_{600} of 0.8 in a total volume of 5 mL of selective media and incubated at 30°C for 4 hours. Aliquots of 450 μL of each cell culture were transferred into siliconized tubes (1.5 mL) and mixed with 50 μL of 10 μM α-factor at various amounts so that the final α-factor concentration ranged from 10^{-11} to 10^{-6} M. Ninety microliters of the cell suspension were added to microtiter plate wells and OD_{600} was measured using a multi-well plate reader. Cells were incubated for 90 min at 30°C with constant shaking and 20 μL of FDG solution (0.25 mM fluorescein di-β-D-galactopyranoside in 2.5% Triton X-100) was added to each well and incubated for an additional 90 min at 37°C. Fluorescence was measured using a multi-well plate reader at an excitation wavelength of 485 nm and an emission wavelength of 530 nm. The *FUS1-lacZ* induction was measured in quadruplicates; values were normalized to the WT level, and expressed as a percentage of the control. Data were plotted and analyzed to determine the EC_{50} values (the concentration of pheromone required to elicit one-half the maximal response) using Prism (GraphPad, Software, CA, USA).

2.5 Binding Assays

Saturation and competition binding assays were performed using tritiated α-factor as previously described [176]. Each experiment was repeated at least four times, and each data point measured in quadruplicate. GraphPad Prism nonlinear regression analysis software was used for fitting data curves with single-site competition. K_d and $B_{\max}$ values were determined from saturation binding assays for WT, N-EGFP (1-158) and C-EGFP (159-238) tagged Ste2p receptors.

2.6 Membrane Preparation

Yeast cells were grown in 50 mL of the selective proper medium (MLT/MLU) at 30 °C overnight. Yeast culture was washed twice with water and resuspended with

HEPES solution (10 mM HEPES and 4 mM EDTA, pH 7.0), cells were homogenized with glass beads followed by a centrifugation for 5 minutes at 2000 g to get rid of cell debris and intact cells. Membranes were harvested by centrifuging supernatant at 15,000 g for 30 minutes at 4 °C. The membrane pellet was resuspended in HEPES solution and protein concentration determined using the BioRad Protein Assay (BioRad, CA, USA).

2.7 Western Blot Analysis

Membrane proteins were solubilized in SDS sample buffer and fractioned by SDS-PAGE and transferred to Immobilon-P membrane (Millipore Corporation, Bedford, MA) for immunoblot analysis Immunoblotting was carried out using anti-FLAG antibody, GFP Rabbit Serum Polyclonal antibody (Molecular Probes), mCherry antibody (16D7, Life Technologies, NY, USA) and affinity-purified antireceptor antiserum directed against the N-terminal domain of the α-factor receptor [178], which were kindly provided by James Konopka, State University of New York, Stony Brook, NY. Bands were observed with West Pico Chemiluminescent Detection System (Pierce) and Odyssey CLx Infrared Imaging System (LI-COR). For coomassie staining another gel was loaded with same protein samples and then 25mL of coomassie stain (0.025% Coomassie Brilliant Blue R-250, 50% Methanol, 10% Acetic Acid) was added and incubated at room temperature for 3h. Following the staining step, gel was washed with distilled water thoroughly and kept in destaining solution (10% Methanol, 10% Acetic Acid, 2% Glycerol) for overnight in order to remove the unbound stain from the gel.

2.8 Knocking Out URA3 (YEL021W) gene from LM102 cells

During the construction of LM102 yeast strain (MATa, bar1, his4, leu2, trp1, met1, ura3, FUS1–lacZ::URA3, ste2–dl) a *FUS1-lacZ*::URA3 gene cassette was integrated into its chromosome, so that it can be used for the gene expression assays to show the functionality Ste2p receptor. Since our methods rely on yeast transformants carrying plasmids with URA marker, URA3 gene was knocked-out from the LM102 Strain.

Kan^r gene cassette was amplified from pUG6 plasmid (Figure 2.7) with primers carrying ~40 bp homologous flanking regions from 5' and 3' ends of the URA3 gene (Table 2.12).

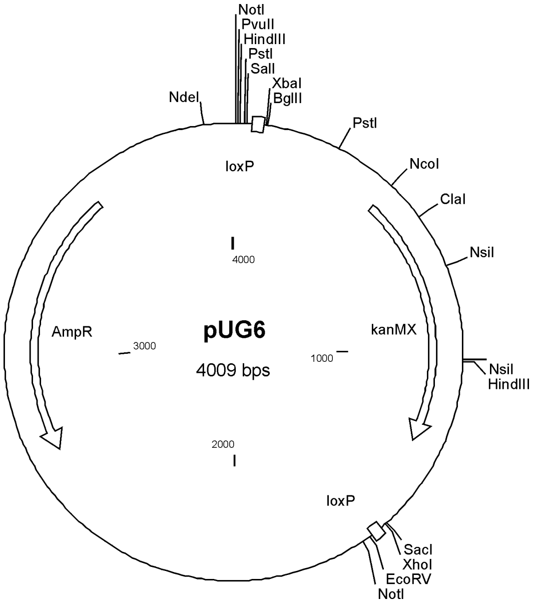
NotI
PvuII
HindIII
PstI
SalI
XbaI
BglII
NdeI
PstI
NcoI
ClaI
NsiI
NsiI
HindIII
loxP
4000
AmpR
3000
pUG6
4009 bps
1000
kanMX
2000
loxP
SacI
XhoI
EcoRV
NotI

Figure 2.7 pUG6 vector map.

The complete URA3 gene sequence for primer design was obtained from Yeast Genome Database (Saccharomyces cerevisiae S288c chromosome V):

Table 2.10 Coding sequence of URA3 gene from S288C strain. Obtained from https://wwww.yeastgenome.org.

URA3 gene coding sequence
atgtcgaaagctacatataaggaacgtgctgctactcatcctagtcctgttgctgccaag ctatttaatatcatgcacgaaaagcaaacaaacttgtgtgcttcattggatgttcgtacc accaaggaattactggagttagttgaagcattaggtcccaaaatttgtttactaaaaaca catgtggatatcttgactgatttttccatggagggcacagttaagccgctaaaggcatta tccgccaagtacaattttttactcttcgaagacagaaaatttgctgacattggtaataca gtcaaattgcagtactctgcgggtgtatacagaatagcagaatgggcagacattacgaat gcacacggtgtggtgggcccaggtattgttagcggtttgaagcaggcggcggaagaagta acaaaggaacctagaggccttttgatgttagcagaattgtcatgcaagggctccctagct actggagaatatactaagggtactgttgacattgcgaagagcgacaaagattttgttatc ggctttattgctcaaagagacatgggtggaagagatgaaggttacgattggttgattatg acacccggtgtgggtttagatgacaagggagacgcattgggtcaacagtatagaaccgtg gatgatgtggtctctacaggatctgacattattattgttggaagaggactatttgcaaag ggaagggatgctaaggtagagggtgaacgttacagaaaagcaggctgggaagcatatttg agaagatgcggccagcaaaactaa

Table 2.11 Primers used to amplify Kan^r gene cassette with flanking URA3 regions.

Primer	Sequence
URA3-KO-For	atgtcgaaagctacatataaggaacgtgctgctactcatcccagctgaagcttcgtacgc
URA3-KO-Rev	ttagttttgctggccgcatcttctcaaatatgcttcccagccgcataggccactagtggatctg

The PCR conditions for the amplification of the Kan^r cassette are given below:

Component	20 µL rxn	Final conc.
Water	30.5	
5X Phusion HF Buffer	10	1X
10 mM dNTPs	5	200 µM each
URA3-KO-For (20 pmols/µL)	1.25	0.5 µM
URA3-KO-Rev (20 pmols/µL)	1.25	0.5 µM
pUG6 (100 ng/µL)	1.5	60-100 ng
Phusion Hot Start II DNA Polymerase	0.5	0.02 U/µL
DMSO	1.5	3%

98°C	30s	
98°C	**10s**	
54.1°C	**30s**	**35cycles**
72°C	**15-30 s/kb**	
72°C	10m	

After the PCR, product was run on an agarose gel (1% agarose) and the bands were purified both with gel extraction kit (QIAquick Gel Extraction Kit) and PCR Purification (Promega Wizard PCR Preps DNA Purification Kit). Kan^r gene; kanMX; is 1612 bp carrying two flanking regions homologous to URA3, so the position of the band was as expected, being little above 1.5 kb band. The gel image is given below.

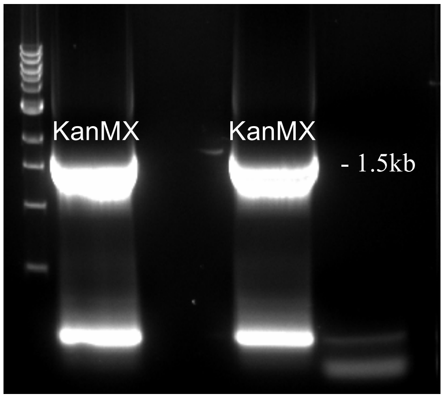

Figure 2.8 Agarose Gel (1%) image of PCR amplified Kan^r gene from pUG6 vector. First lane is the 1kb DNA ladder; PCR reaction was loaded into second and third lanes. The upper and most intense band is the amplified Kan^r gene carrying homologous flanking sequences as expected around 1.5kb band; the lower bands are primers.

The purified knockout cassette was used in the transformation of LM102 strain with the LiAc / SS-DNA / PEG method given previously. During the transformation 500ng, 1000ng and 2000ng of linear DNA was used. Additionally to the LiAc / SS-DNA / PEG transformation method, at the very last step of right after the heat shock, cells were spinned down, supernatant was removed by pipette and cells were resuspended in 1000µL of YEPD and left in incubator @ 30°C with constant shaking for more than 5 hours to let the efficient integration of drug resistance cassette into the targeted locus. The cells were spinned down, 800µL of YEPD was removed, the cell pellet was resuspended in the left 200µL YEPD and applied onto freshly prepared YEPD plates containing G418 (200 mg/L). After incubating the transformants for 4-5 days, significantly larger colonies were observed onto a crowded background. The observed colonies are significantly larger than regular round shaped yeast colonies with colony morphology similar to volcano mountains, hence these colonies were named as volcano colonies. These colonies were picked and streaked onto YEPD/G418, MLU plates and MLU+Uracil plates for the selection. The colonies, grown on YEPD/G418 and MLU+Uracil plates but unable to grow on MLU plates were chosen and streaked onto YEPD/G418 and MLU plates for the last verification. The 2 of best-grown colonies were selected and incubated in 5mL YEPD, for the transformation with p424, pBEC1 and pCL01 plasmids.

Also, overnight grown culture of LM102 cells were harvested and resuspended in 1000 µL of water, 200 µL of this final culture was applied on 5-FOA (5-Fluoroorotic acid) plates to select the cells carrying URA3 gene mutations. URA3 gene encodes an enzyme called orotidine 5-phosphate decarboxylase (ODCase), which catalyzes a reaction involved in the synthesis of pyrimidine ribonucleotides in yeast RNA. When yeast cells are grown in a media containing 5-FOA, cells having an intact URA3 gene in their chromosomes will produce ODCase which converts 5-FOA into 5-fluorouracil. 5-fluorouracil is a toxic compound causing death. Hence, the yeast carrying and intact URA3 gene on their chromosome would die, while cells that lack the gene would survive.

2.9 Imaging with Laser Scanning Confocal Microscope

For image acquisition, yeast cells were grown overnight at 30 °C in 5mL fresh media. Following day, the cells were subcultured and grown to OD_{600} of 1. From this culture 1mL was taken, spinned down and the cells were resuspended again in 200 µL. For detection of fluorescent signal in live cells, yeast cells were observed using a Leica SP2 Laser Scanning Confocal Microscope equipped with an Leica 63x/1.32 HCX PL APO Oil DIC objective and Leica 100x/1.49 Oil DIC objective (Department of Microbiology and Department of Biochemistry, Cell, and Molecular Biology, University of Tennessee, Knoxville, Tennessee). Cells were excited at 488 nm and emission between 505-550nm ranges was collected. All images were collected with the same parameters.

CHAPTER 3

RESULTS AND DISCUSSION

3.1 Construction of plasmids carrying tagged Ste2p

Previous studies have shown that EGFP could be split at residues 128-129 [179] or 158-159 [180] to obtain fluorescence complementation (BiFC) when the two halves of the EGFP were co-expressed. The BiFC method is used to detect interaction between two molecules as a way to determine dimer formation. However, BiFC cannot distinguish between dimers and higher order oligomer formation in the living cell. In this study we use the term dimer formation but this does not preclude the formation of oligomers of Ste2p in the yeast cell.

We made constructs of Ste2p with EGFP, mCherry, EGFP residues 1-158 (N-terminal) and EGFP residues 159-238 (C-terminal); mCherry residues 1-159 (N-terminal) and EGFP residues 160-237 (C-terminal) appended to position 304 of Ste2p or inserted between residues 304 and 305 of Ste2p (Figure 1) and evaluated the BiFC of co-expressed N-terminal and C-terminal constructs.

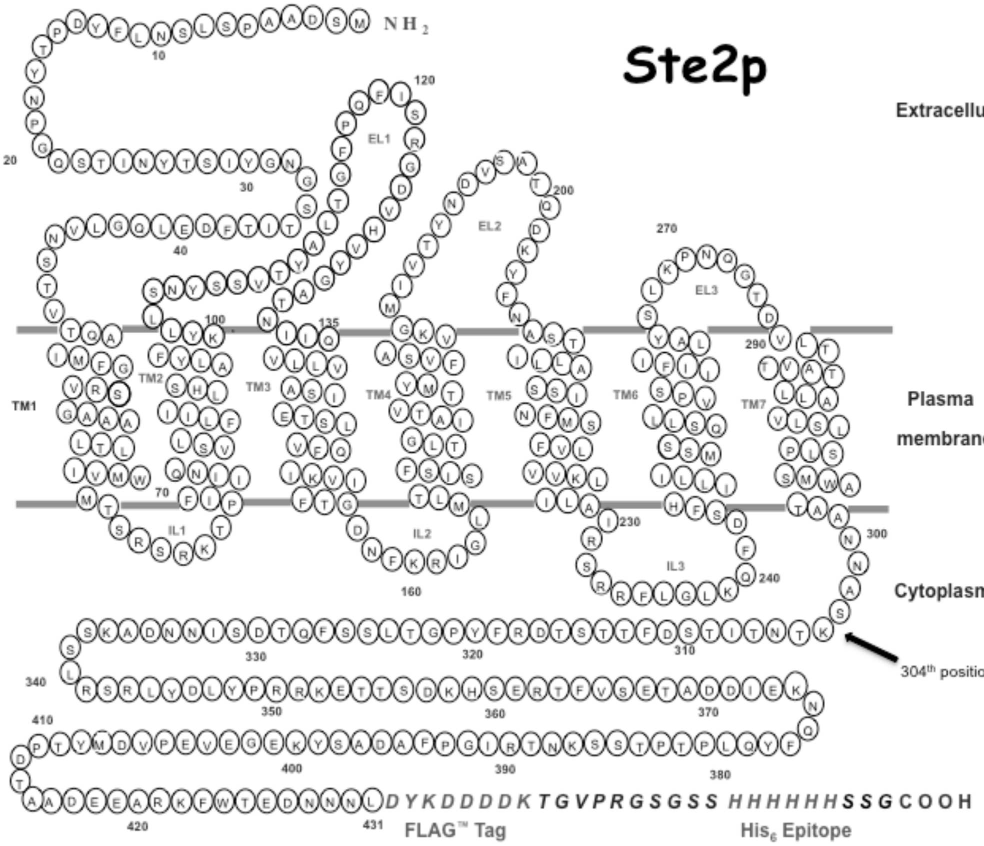
Ste2p
NH2
Extracellular
Plasma membrane
Cytoplasmic
EL1
EL2
EL3
IL1
IL2
IL3
TM1
TM2
TM3
TM4
TM5
TM6
TM7
304th position
DYKDDDDKTGVPRGSGSS HHHHHHSSGCOOH
FLAG™ Tag
His6 Epitope

Figure 3.1 Snake diagram of yeast α-pheromone receptor (Ste2p) with a FLAG™ and His$_6$ tag appended to the C-terminus. We designate this construct as wild type for the purpose of this manuscript. The arrow indicates insertion position 304. EL1, EL2 and EL3 are the extracellular loops, IL1, IL2 and IL3 are the intracellular loops and TM1 – TM7 are the transmembrane residues of Ste2p.

3.1.1 Construction of plasmid carrying EGFP and mCherry tagged Ste2p

EGFP and mCherry genes were amplified from their vectors, pEGFP-N2 and pmCherry-N1, using same primers carrying 21 bases homologous regions from 5' and 3' ends of EGFP and mCherry genes with 25-30 overhanging bases from STE2 sequence upstream and downstream from 912th position corresponds to 304-305th position in the translated protein. First PCR was optimized, running the reaction at different annealing temperature conditions from 53 – 65 °C. PCR products were run on agarose gel (1% w/v), bands were observed in all temperature conditions (Figure

3.2) so the reaction was upscaled to 50 μL reaction setting 54 °C as the annealing temperature.

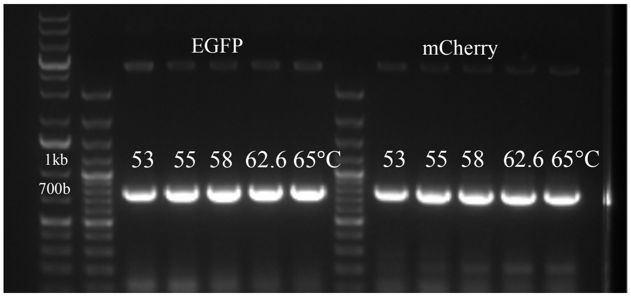

Figure 3.2 Agarose gel electrophoresis image of optimization PCR for amplification of EGFP and mCherry from pEGFP-N2 and pmCherry-N1 plasmids. The product size was observed between 800bp-700bp ladder bands in GeneRuler^{TM} 100bp plus DNA ladder.

Products of "first" PCR were extracted from 1% low melting point agarose gel using QIAquick gel extraction kit (Qiagen, MD, USA). These DNA fragments carry homologous regions upstream and downstream from 912th position on STE2 gene, were used as a tandem primer in a "second" PCR to insert these sequences into the 304th position on Ste2p receptor, using pCL01 and pBEC1 as template vectors. The reaction was run as a gradient PCR with annealing temperatures ranging from 53 – 58 °C.

The PCR mixture was digested with DpnI and digestion mixture was directly used in the transformation DH5α competent E.coli (New England Biolabs, MA, USA). Three colonies were picked for each PCR condition and isolated plasmids were digested with BamHI – EcoRI and run on gel to control the correct insert size (Figures 3.3 – 3.5).

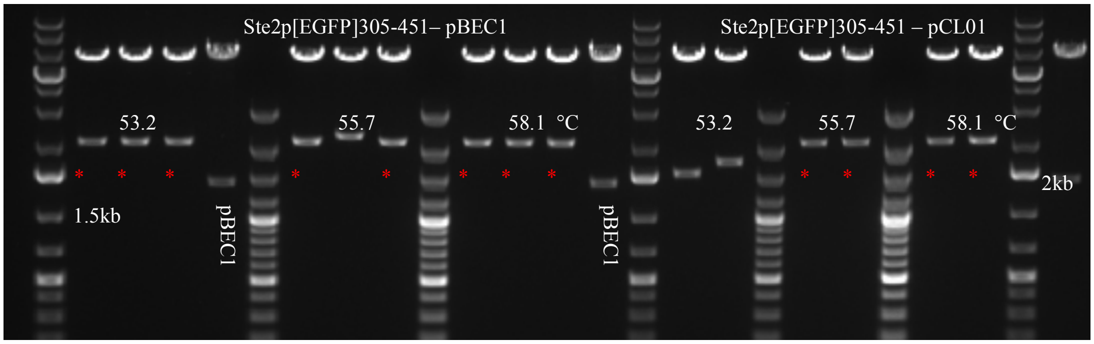
Ste2p[EGFP]305-451– pBEC1
Ste2p[EGFP]305-451 – pCL01
53.2
55.7
58.1 °C
53.2
55.7
58.1 °C
1.5kb
pBEC1
pBEC1
2kb

Figure 3.3 For inserting EGFP sequence in Ste2p sequence, a gradient PCR reaction was run at 3 different annealing temperatures. Plasmids isolated from these reactions were digested with BamHI – EcoRI enzymes at 37°C for 3h. Ste2p gene is 1386 bp (lower band at pBEC1 digests); EGFP gene is 714 bp so a correct EGFP insert is 2100 bp together. The bands marked with red asterix on gel photo shows Ste2p-EGFP constructs with expected size. These plasmids were verified by sequencing.

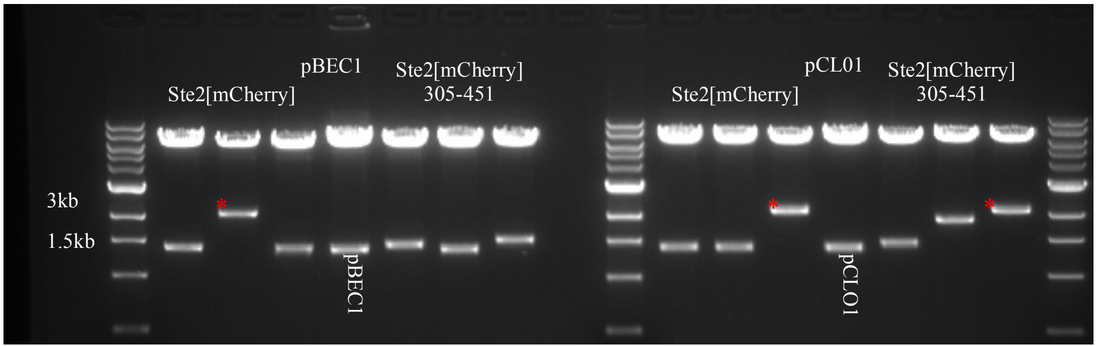
pBEC1
Ste2[mCherry]
Ste2[mCherry]
305-451
pCL01
Ste2[mCherry]
Ste2[mCherry]
305-451
3kb
1.5kb
pBEC1
pCL01

Figure 3.4 mCherry sequence was also inserted with and without a stop codon after 305th position on Ste2p. Plasmids isolated from these reactions were digested with BamHI – EcoRI enzymes at 37°C for 3h. The bands marked with red asterix on gel photo shows Ste2p-mCherry constructs with expected size. These plasmids were verified by sequencing.

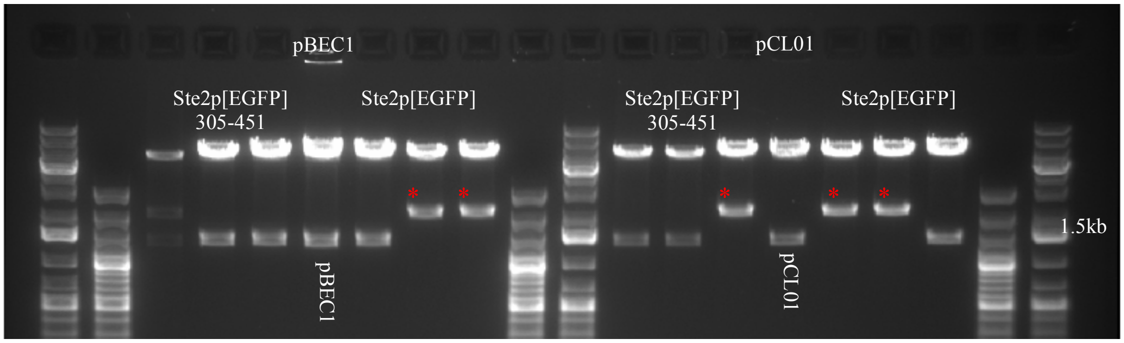
pBEC1
pCL01
Ste2p[EGFP]
305-451
Ste2p[EGFP]
Ste2p[EGFP]
305-451
Ste2p[EGFP]
pBEC1
pCL01
1.5kb

Figure 3.5 EGFP sequence was also inserted with a stop codon after 305th position on Ste2p. Plasmids isolated from these reactions were digested with BamHI – EcoRI enzymes at 37°C for 3h. The bands marked with red asterix on gel photo shows Ste2p-EGFP constructs with expected size. These plasmids were verified by sequencing.

3.1.2 Construction of Ste2p constructs tagged with EGFP or mCherry fragments

N-EGFP (1-158), C-EGFP (159-238), N-mCherry (1-159) and C-mCherry (160-237) fragments were amplified from pEGFP-N2 and pmCherry-N1 plasmids, using primers that split the fluorescent protein from the desired position. These primers were designed to carry 25-30 overhanging bases upstream and downstream of 912th position STE2 sequence, which corresponds to 304th position on translated protein. Same conditions optimized from the amplification of EGFP and mCherry genes were used for amplifying their fragments. After the reaction, products were extracted from low melting point agarose gel (1% w/v), (Figure 3.6).

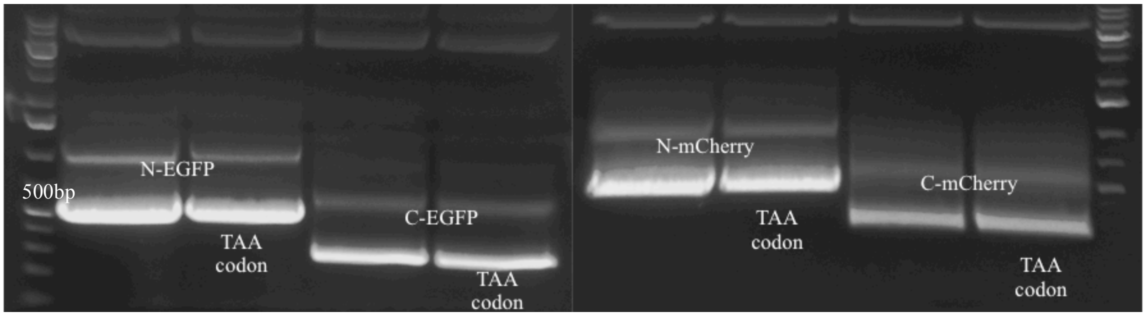

Figure 3.6 Agarose gel electrophoresis image of PCR amplified EGFP and mCherry fragments with and without "TAA" stop codon. The product size for N-EGFP and N-mCherry was observed around 500bp ladder bands in GeneRuler^{TM} 100bp plus DNA ladder.

Likewise, these DNA fragments carrying homologous regions on STE2 gene were used as a tandem primer in a "second" PCR. A gradient PCR was set to insert these fluorescent protein fragments' sequences into the 304th position on Ste2p receptor, using pCL01 and pBEC1 as template vectors.

The PCR mixture was digested with DpnI right after the reaction and digestion mixture was directly used in the transformation DH5α competent E.coli (New England Biolabs, MA, USA). Three colonies were picked for each PCR condition and plasmids were isolated. The isolated plasmids were digested with BamHI – EcoRI and run on gel to control the correct insert size (Figures 3.7, 3.8).

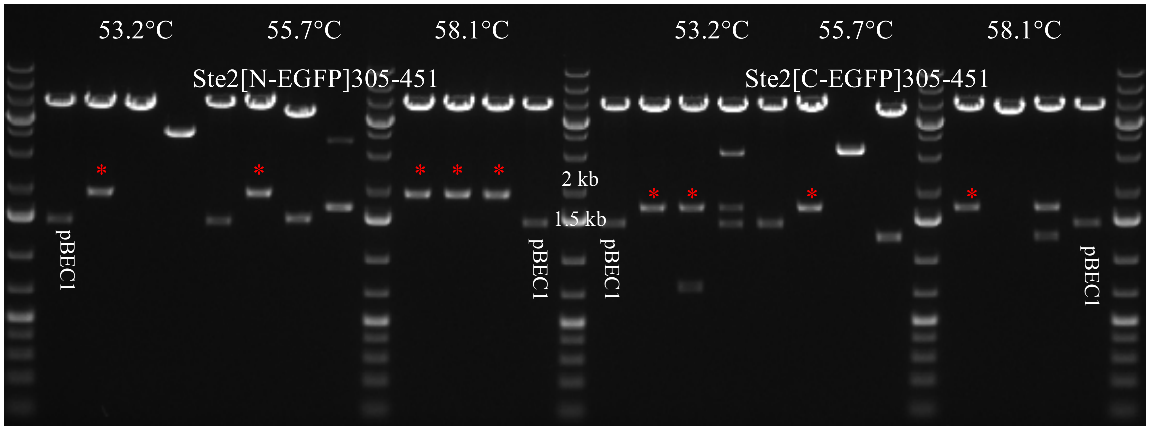
53.2°C
55.7°C
58.1°C
Ste2[N-EGFP]305-451
53.2°C
55.7°C
58.1°C
Ste2[C-EGFP]305-451
2 kb
1.5 kb
pBEC1
pBEC1
pBEC1
pBEC1

Figure 3.7 N-EGFP and C-EGFP sequences were inserted between 304-305 positions on Ste2p. Plasmids isolated from these reactions were digested with BamHI – EcoRI enzymes at 37°C for 3h. The bands marked with red asterix on gel photo show constructs with expected size, Ste2p[N-EGFP]305-451 size is 1860 bp, Ste2p[C-EGFP]305-451 size is 1626 bp. These plasmids were verified by sequencing.

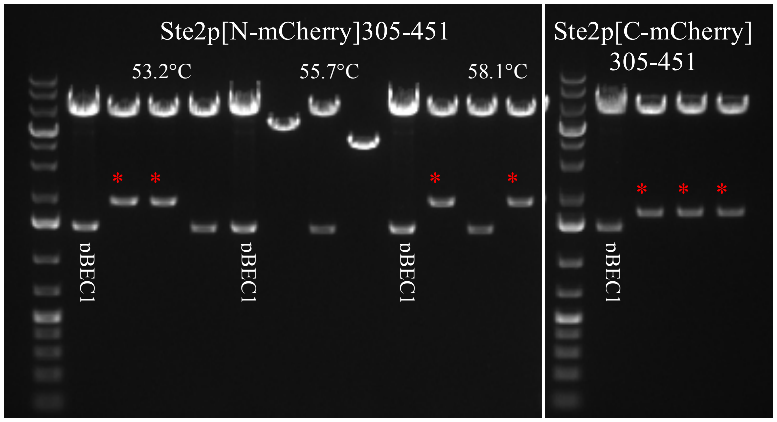
Ste2p[N-mCherry]305-451
53.2°C
55.7°C
58.1°C
Ste2p[C-mCherry]
305-451
pBEC1
pBEC1
pBEC1
pBEC1

Figure 3.8 N-mCherry and C-mCherry sequences were inserted between 304-305 positions on Ste2p. Plasmids isolated from these reactions were digested with BamHI – EcoRI enzymes at 37°C for 3h. The bands marked with red asterix on gel photo show constructs with expected size, Ste2p[N-mCherry]305-451 size is 1863 bp, Ste2p[C-mCherry]305-451 size is 1620 bp. These plasmids were verified by sequencing.

The plasmids constructed as explained above are given in Table 3.1.

Table 3.1 Plasmids (1st column) constructed for this study and the abbreviated names of the Ste2p construct expressed (2nd column).

Plasmid	Ste2p Construct Expressed
pBEC1 [constructed from p424GPD, a 2µm based shuttle vector with a GPD promoter, CYC1 terminator, and TRP marker]	Ste2p (Wild-type)
pCL01 [constructed from p426GPD, a 2µm based shuttle vector with a GPD promoter, CYC1 terminator, and URA marker]	Ste2p (Wild-type)
pBEC1[N-EGFP (1-158) inserted at 304]	Ste2p[N-EGFP]305-431
pCL01[C-EGFP (159-238) inserted at 304]	Ste2p[C-EGFP]305-431
pBEC1[N-EGFP (1-158) attached at 304]	Ste2p[N-EGFP]
pCL01[C-EGFP (159-238) attached at 304]	Ste2p[C-EGFP]
pBEC1[EGFP (1-238) inserted at 304]	Ste2p[EGFP]305-431
pBEC1[EGFP (1-238) attached at 304]	Ste2p[EGFP]
pBEC1[N-mCherry (1-158) attached at 304]	Ste2p[N-mCherry]
pCL01[C-mCherry (159-238) attached at 304]	Ste2p[C-mCherry]
pBEC1[mCherry (1-238) inserted at 304]	Ste2p[mCherry]305-431
pBEC1[mCherry (1-238) attached at 304]	Ste2p[mCherry]
pBEC1[mCherry (1-238) inserted at 304]	Ste2p[EGFP]305-431
pBEC1[mCherry (1-238) attached at 304]	Ste2p[EGFP]

3.1.3 Removing FLAG™ and His$_6$ epitope tags from Ste2p constructs

Although full length Ste2p constructs tagged with EGFP, mCherry or fragments of these fluorescent proteins were shown to be functional with growth arrest assay (data not shown), preliminary saturation binding experiments using tritiated α-factor gave ambiguous binding results (Figure 3.9 and 3.10).

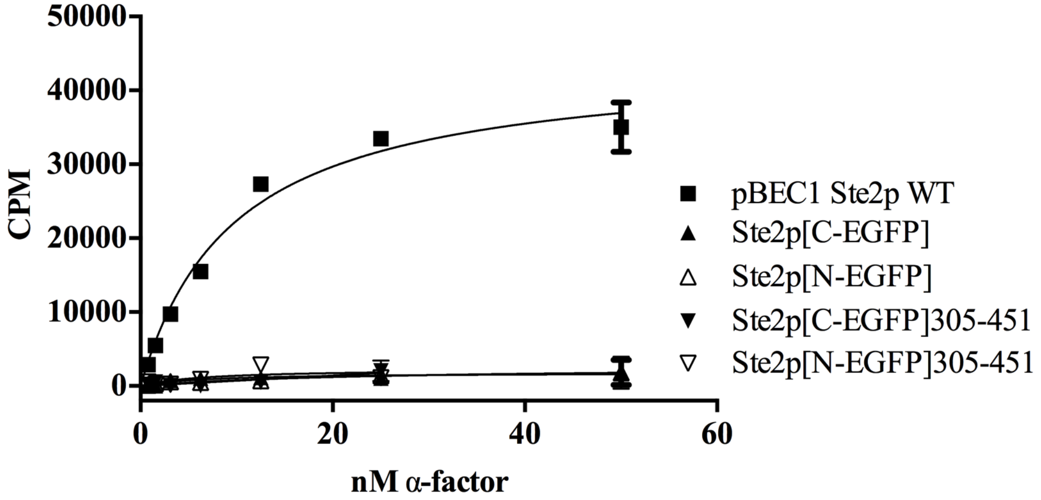

Figure 3.9 Saturation binding data of DK102 cells expressing the split EGFP tagged receptor. Cells expressing WT Ste2p receptor from pBEC1 vector (■); Cells expressing Ste2p[C-EGFP]; C-EGFP (159-238) attached at position 304 of the Ste2p receptor (▲), Cells expressing Ste2p[N-EGFP]; N-EGFP (1-158) attached at position 304 of the Ste2p receptor (△), Cells expressing Ste2p[C-EGFP]305-451; C-EGFP (159-238) inserted between positions 304-305 of the Ste2p receptor (▼), Cells expressing Ste2p[N-EGFP]305-451; N-EGFP (1-158) inserted between positions 304-305 of the Ste2p receptor (▽).

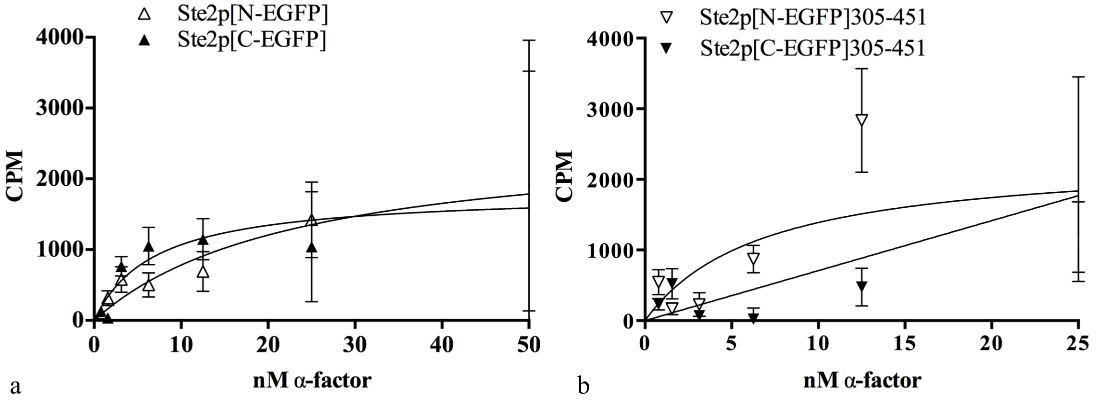

Figure 3.10 Saturation binding data of DK102 cells expressing the split EGFP tagged receptor. (a) Cells expressing Ste2p[C-EGFP]; C-EGFP (159-238) attached at position 304 of the Ste2p receptor (▲), Cells expressing Ste2p[N-EGFP]; N-EGFP (1-158) attached at position 304 of the Ste2p receptor (△). (b) Cells expressing Ste2p[C-EGFP]305-451; C-EGFP (159-238) inserted between positions 304-305 of the Ste2p receptor (▼), Cells expressing Ste2p[N-EGFP]305-451; N-EGFP (1-158) inserted between positions 304-305 of the Ste2p receptor (▽).

The C-terminally truncated Ste2p constructs; Ste2p[C-EGFP] and Ste2p[N-EGFP]; were countable on cell surface and yield an acceptable binding curve, yet Ste2p constructs with an intact C-terminus; Ste2p[C-EGFP]305-451 and Ste2p[N-EGFP]305-451; gave an ambiguous binding curve. So, to prevent possible cell surface expression effects due to the FLAG^{TM} and His$_6$ tags at the C-terminus of receptor, a stop codon right after 431st residue was inserted.

For inserting a stop codon after 431st amino acid, whole vector carrying Ste2p constructs were amplified with "Ste2-Stop HT-FT for" and "Ste2-Stop HT-FT rev" primers given in Materials and Methods section, using Phusion Hot Start II High-Fidelity DNA Polymerase (Thermo Fisher Scientific, MA, USA).

PCR mixture was digested with DpnI enzyme (Thermo Scientific, MA, USA) and digestion mixture was directly used in transformation of E.coli. Constructs that carry stop codon after 431st residue were confirmed by sequencing.

Saturation binding data for new constructs, lacking FLAG^{TM} and His$_6$ tags are presented in Chapter 3.1.7.

3.1.4 Disturbing $G^{56}XXXG^{60}$ dimerization motif on Ste2p constructs

It was reported that Ste2p receptor carries a ($_{52}$AIMF**G**VRC**G**AAL$_{63}$) Glycophorin A-like Dimerization Motif "$G^{56}XXXG^{60}$" in Transmembrane Domain 1 and replacing the glycine residues with a bulkier amino acid such as leucine, substantially disrupting α-factor receptor oligomerization and biogenesis without significantly impairing the ligand binding affinity [181]. In the same study, it was also mentioned that signaling defects observed in these mutant receptors were not as a result of impaired cell surface expression, indicating, "*oligomerization promotes α-factor receptor* *signal transduction*" [181]. In order to test if the constructs developed in this study can be used to identify important residues in dimerization we replaced glycine residues at positions 56 and 60 (one at a time and both at the same time) in the Glycophorin A-like Dimerization Motif "*GXXXG*" in Transmembrane Domain 1 with a bulkier amino acid (leucine). These G56L, G60L and G56/60L mutations were applied to both full length and truncated Ste2p constructs labeled with EGFP fragments at position 304.

Glycine → Leucine mutation was inserted on 56th amino acid using "Ste2-G56L for" and "Ste2-G56L rev" primer pair, and on 60th amino acid using "Ste2-G60L for" and "Ste2-G60L rev" primers. These mutations were verified by sequencing. For constructing G56/60L double mutants, plasmids verified to carry G56L mutation were amplified using "Ste2-G60/56L rev" and "Ste2-G60L for" primer pair.

In site directed mutagenesis PCR, whole vector was amplified with the primers both carrying the mutations using Phusion Hot Start II High-Fidelity DNA Polymerase. PCR mixture was digested with DpnI enzyme and digestion mixture was directly used in transformation. All constructs were confirmed by sequencing.

As our first control set, we imaged the co-expression of G56/60L mutants of full length receptor Ste2pG56/60L[C-EGFP]305-451 - Ste2pG56/60L[N-EGFP]305-451 pair and the truncated receptor pair; Ste2pG56/60L[C-EGFP] - Ste2pG56/60L[N-EGFP] by confocal microscopy. None of these BiFC pairs gave any fluorescent signal, neither intracellularly nor on the membrane (data not shown). These results supported the previous literature saying replacement of glycine residues on $G^{56}XXXG^{60}$ motif impairs dimerization. We did also image the cells co-expressing only G56L mutants, Ste2pG56L[C-EGFP]305-451 - Ste2pG56L[N-EGFP]305-451 pair; Ste2pG56L[C-EGFP] - Ste2pG56L[N-EGFP] pairs and G60L mutants, Ste2pG60L[C-EGFP]305-451 - Ste2pG60L[N-EGFP]305-451 pair; Ste2pG60L[C-

EGFP] - Ste2pG60L[N-EGFP]. Similar to co-expression of G56/60L mutants and consistent with the previous literature, these G56L or G60L single mutant pairs did not show any fluorescent signal due to the dimerization either. These results indicated that either of the Glycines in *GXXXG* motif is enough to impair dimerization of Ste2p (data not shown).

We decided to verify that the constructs are biologically functional by using *FUS1-lacZ* gene induction assay. For this, LM102 and OM102 strains were transformed using Ste2p G56/60L mutant constructs. The β-galactosidase activity of these cells expressing G56/60L mutants is given in Figure 3.11.

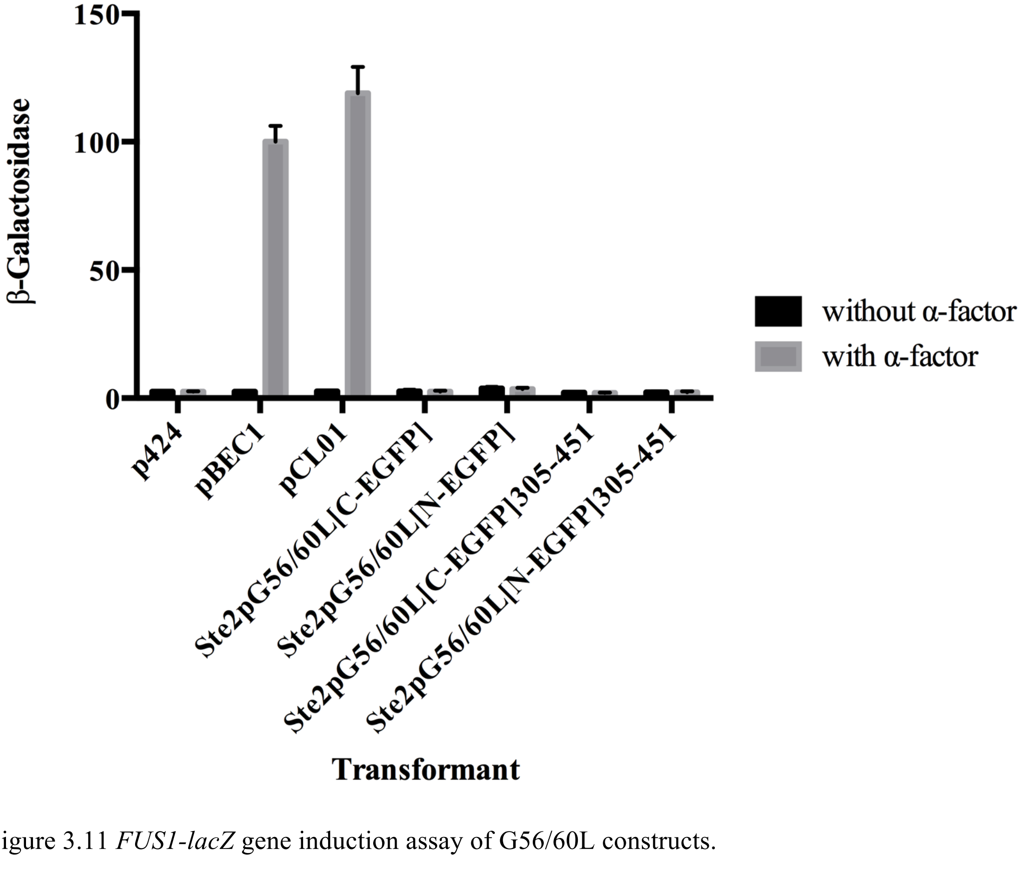

Figure 3.11 *FUS1-lacZ* gene induction assay of G56/60L constructs.

To verify that, the loss of receptor function is not due to the EGFP fragments fused on the Ste2p receptor and to further verify the effects of G56L and G60L mutations on Ste2p, these mutations were inserted into Ste2p WT in pBEC1 plasmid. LM102 cells were transformed using Ste2pG56L, Ste2pG60L and Ste2pG56/60L constructs and β-galactosidase activity of these new constructs were measured. The results are given in Figure 3.12.

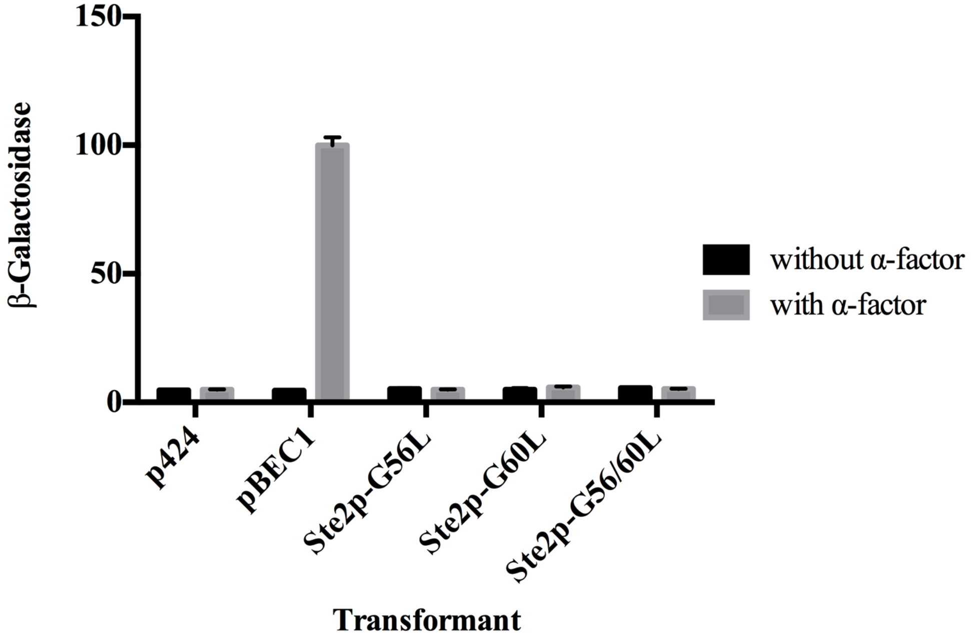

Figure 3.12 β-galactosidase activity of Ste2pG56L, Ste2pG60L and Ste2pG56/60L constructs.

Unfortunately, Ste2p carrying the G56L, G60L or G56/60L mutations were not functionally expressed at the cell surface.

For a longer-term pheromone responsiveness, DK102 strain was transformed to express Ste2pG56L, Ste2pG60L, Ste2pG56/60L, Ste2pG56/60L[N-EGFP], Ste2pG56/60L[C-EGFP], Ste2pG56/60L[N-EGFP]305-451 and Ste2pG56/60L[C-EGFP]305-451 constructs, the biological function of these mutant receptors was measured using pheromone induced growth arrest assay. Unfortunately, neither G56L or G60L single mutants nor G56/60L double mutants produced any halos when subjected to different concentrations of α-factor pheromone. These results indicated that Glycine → Leucine mutants are not properly expressed on the cell membrane.

For whole cell expression of these proteins, BJS21 cells were transformed to express Ste2p[C-EGFP]305-451, Ste2p[N-EGFP]305-451, their G56/60L mutants and StepG56L, Ste2pG60L and Ste2pG56/60L. Transformants were harvested and Ste2p constructs were resolved on SDS Page (Figure 3.13).

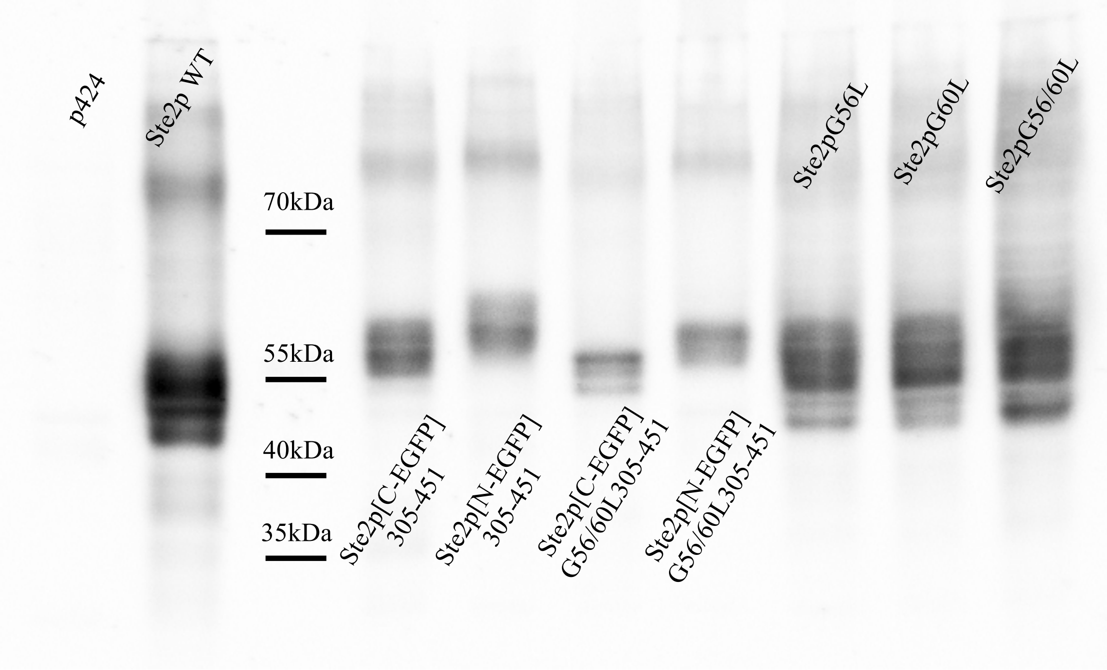
p424
Ste2p WT
70kDa
55kDa
40kDa
35kDa
Ste2p[C-EGFP] 305-451
Ste2p[N-EGFP] 305-451
Ste2p[C-EGFP] G56/60L305-451
Ste2p[N-EGFP] G56/60L305-451
Ste2pG56L
Ste2pG60L
Ste2pG56/60L

Figure 3.13 Western blot of the BJS21 cells expressing the constructs, the first lane is an extract of Ste2Δ cells expressing empty vector, the second lane is an extract of Ste2Δ cells expressing WT Ste2p receptor (52 kDa), third lane shows protein ladder, the lanes four to seven are extracts from cells expressing Ste2p[C-EGFP]305-451 (calc. ≈57 kDa), Ste2p[N-EGFP]305-451 (calc. ≈66 kDa), Ste2pG56/60L[C-EGFP]305-451 (calc. ≈57 kDa), Ste2pG56/60L[N-EGFP]305-451 (calc. ≈66 kDa) respectively. The last three lanes from eight to ten are extracts of Ste2pG56L (52 kDa), Ste2pG60L (52 kDa) and Ste2pG56/60L (52 kDa) respectively. The proteins from lanes 1 to 10 were detected with antireceptor antiserum directed against the N-terminal domain of the α-factor receptor.

These receptors carrying G → L mutations were expressed in lower amounts compared to the wild type receptor. The multiple bands pattern was still observed at approximately 52 kDa due to different glycosylated forms of the receptor as shown previously [182] [183].

3.1.5 Growth arrest assays of Ste2p constructs

For Ste2p-EGFP constructs, EGFP was split at 158-159 and a full length EGFP was appended or inserted at position 304 of Ste2p. These Ste2p proteins were expressed from pBEC1 or pCL01 plasmids carrying different auxotrophic markers in order to co-express the split EGFP constructs. Biological activity of these Ste2p EGFP fusion proteins was studied with "Pheromone Induced Growth Arrest Assay" using DK102 strain. *Growth arrest assays* were performed for Ste2p receptors shown in Table 3.1. Halo assays were repeated at least three times for each of the plasmids and diameters of halos were plotted against logarithm of peptide concentration. The assay was quite reproducible as the variation in the inhibition zones was always within 2 mm for a given concentration. The representative images of the assay are given in Figure 3.14.

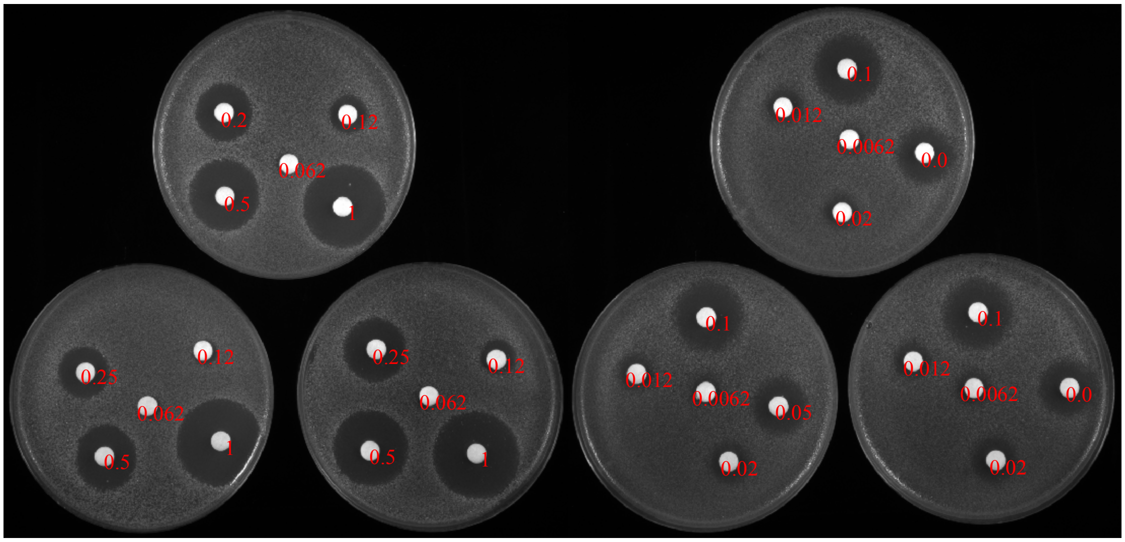

Figure 3.14 Representative images of growth inhibition zones (halo) in pheromone induced growth arrest assay. Various amounts of pheromone (10 – 0.625 μg for full length constructs [left image], 1 – 0.0625 μg for truncated constructs [right image]) were absorbed onto filter disks.

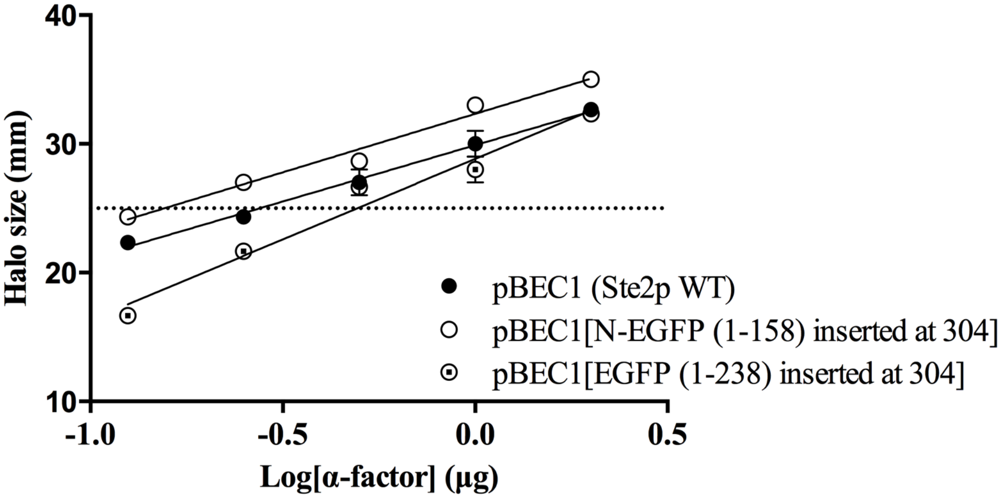

Figure 3.15 Biological assay of Ste2p constructs expressed from pBEC1. Wild-type Ste2p (●); Ste2p[EGFP]305-431, Ste2p receptor with full-length EGFP (1-238) inserted between positions 304-305 (⦿); Ste2p[N-EGFP]305-431, Ste2p receptor with N-EGFP (1-158) inserted between position 304-305 (○).

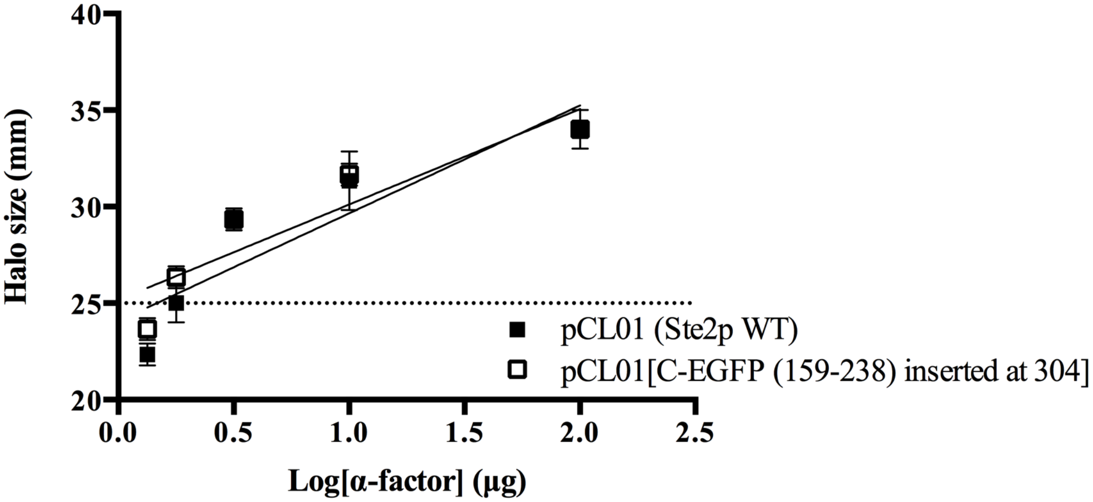

Figure 3.16 Biological assay of Ste2p constructs expressed from pCL01. Wild-type Ste2p (■); Ste2p[C-EGFP]304-431, Ste2p receptor tagged with C-EGFP (159-238) inserted between positions 304-305 (□).

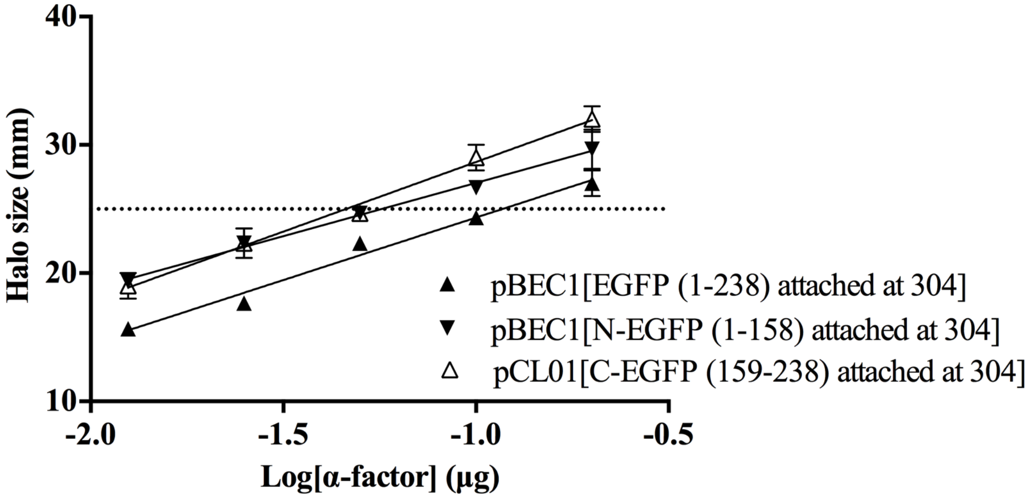

Figure 3.17 Biological assay of Ste2p constructs lacking the C-terminus. Ste2p[EGFP], C-terminally truncated Ste2p-Δ305-431 receptor tagged with full length EGFP (1-238) (▲); Ste2p[N-EGFP], C-terminally truncated Ste2p-Δ305-431 receptor tagged with N-EGFP (1-158) attached at position 304 (△); Ste2p[C-EGFP], C-terminally truncated Ste2p-Δ305-431 receptor tagged with C-EGFP (159-238) attached at position 304 (▼).

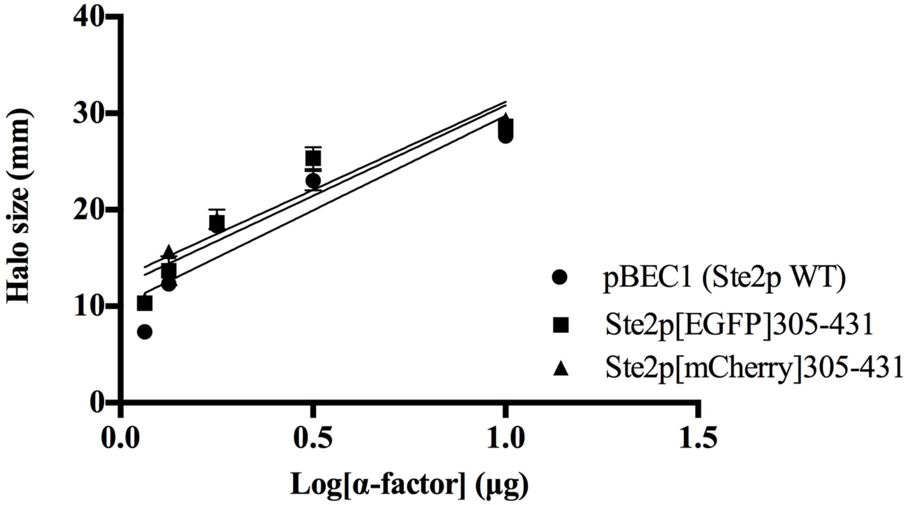

Figure 3.18 Biological assay of Ste2p constructs expressed from pBEC1. Wild-type Ste2p (●); Ste2p[EGFP]305-431, Ste2p receptor with EGFP (1-238) inserted between positions 304-305 (■); Ste2p[mCherry]305-431, Ste2p receptor with mCherry (1-237) inserted between positions 304-305 (▲).

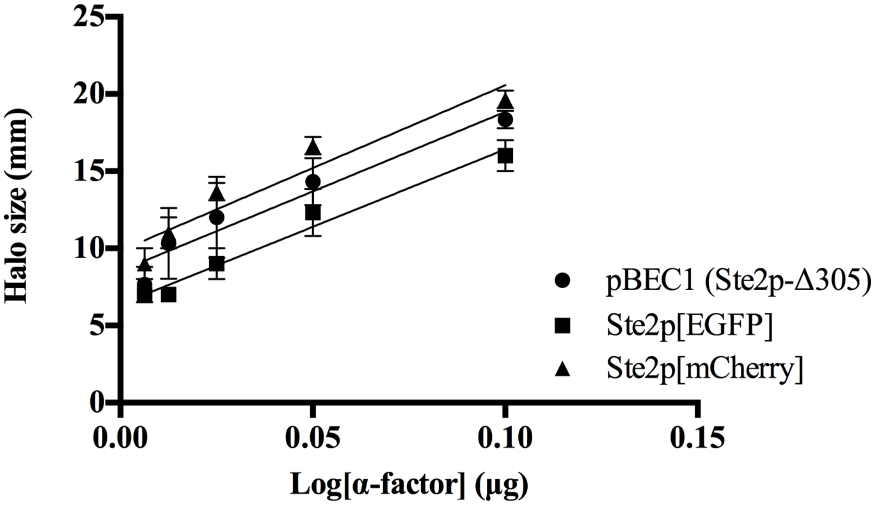

Figure 3.19 Biological assay of C-terminally truncated Ste2p constructs expressed from pBEC1. Ste2p-Δ305-431 (●); Ste2p[EGFP], C-terminally truncated Ste2p receptor with full-length EGFP (1-238) attached at position 304 (■); Ste2p[mCherry], C-terminally truncated Ste2p receptor with mCherry (1-237) attached at position 304 (▲).

Ste2p constructs fused with EGFP or EGFP fragments at position 304 were shown to be biologically active and responded to the pheromone, although the Ste2p[N-EGFP]305-431 was more sensitive to growth inhibition than the wild-type Ste2p and the Ste2p[EGFP]305-431 was less sensitive in comparison to the wild-type Ste2p (Figure 3.15, Figure 3.16, Table 3.2). The results of halo assay showed also that transformants expressing truncated receptors Ste2p-Δ305-431, Ste2p[N-EGFP], Ste2p[C-EGFP], Ste2p[EGFP] and Ste2p[mCherry] (Figures 3.17 and 3.19) were more responsive to pheromone-induced growth arrest. The amount of pheromone required for a 25 mm halo were calculated for Ste2p EGFP fusion constructs and the results showed that to create a 25 mm halo the pheromone required was about 5-fold less for Ste2p[N-EGFP] and Ste2p[C-EGFP] and two-fold less for Ste2p[EGFP] than that of the wild-type constructs (Table 3.2). Ste2p constructs fused with EGFP or mCherry fluorescent protein at position 304 were shown to be biologically active and responded to the pheromone. For full length constructs, Ste2p[EGFP]305-431 and Ste2p[mCherry]305-431 were compared with Ste2p WT from pBEC1 plasmid and all constructs created quite similar halos for different concentrations of pheromone (Figure 3.18). Ste2p[EGFP] and Ste2p[mCherry] were compared with C-terminally truncated Ste2p; Ste2p-Δ305-431; originating from pBEC1 plasmid. Ste2p[mCherry] was observed to be slightly more responsive to pheromone, whereas Ste2p[EGFP] was observed to be slightly less responsive (Figure 3.19). Pheromone Induced Growth Arrest Assay for Ste2p[N-mCherry] and Ste2p[C-mCherry] constructs was done after cloning these constructs into constitutively active double promoter plasmids.

Table 3.2 The amount of α-factor (μg) that yielded a 25mm halo zone for EGFP constructs.

Plasmid	μg α-factor corresponding to 25mm halo zone
pBEC1	0.28
pCL01	0.23
pBEC1[N-EGFP (1-158) inserted at 304]	0.16
pCL01[C-EGFP (159-238) inserted at 304]	0.17
pBEC1[N-EGFP (1-158) attached at 304]	0.06
pCL01[C-EGFP (159-238) attached at 304]	0.05
pBEC1[EGFP (1-238) inserted at 304]	0.49
pBEC1[EGFP (1-238) attached at 304]	0.12

3.1.6 Western blot experiment of Ste2p constructs

Protein expression of all the constructs was determined by western blotting using the protease-deficient BJS21. We used empty vector and cells expressing wild-type (WT) Ste2p as controls. Yeast cells were harvested and proteins were resolved by SDS-PAGE. The immunoblot was probed with affinity-purified antireceptor antiserum directed against the N-terminal domain of the Ste2p [178] and mCherry antibody (16D7, Life Technologies, NY, USA) and GFP Rabbit Serum Polyclonal antibody (Molecular Probes). An extract of Ste2Δ cells transformed with empty vector showed no band (data not shown). In Figure 3.20, the first lane contains membranes from cells expressing WT Ste2p receptor; the multiple bands observed at approximately 52 kDa are due to different glycosylated forms of the receptor as shown previously [182 183]. Lanes three to six show Ste2p[C-EGFP] (calc. M.W. 42 kDa), Ste2p[N-EGFP] (calc. M.W. 51 kDa), Ste2p[C-EGFP]305-431 (calc. M.W.57 kDa) and Ste2p[N-EGFP]305-431 (1-158) (calc. M.W. 66 kDa), respectively. The bands observed in the western blot for truncated Ste2p[C-EGFP] and Ste2p[N-EGFP] were below the WT Ste2p receptor band in accordance with their calculated molecular weights. The bands with full-length Ste2p receptors Ste2p[C-EGFP]305-431 and Ste2p[N-EGFP]305-431 with the inserted EGFP fragments shown at lanes 5 and 6 were above the WT Ste2p band, according to the calculated molecular weights. The multiple bands were likely due to the various glycosylated forms of Ste2p. In all lanes, higher bands corresponding to a dimeric state of Ste2p was observed. The last two lanes, 7 and 8 correspond to cells co-expressing either Ste2p[N-EGFP]/Ste2p[C-EGFP or Ste2p[C-EGFP]305-431/Ste2p[N-EGFP]305-431 from two different plasmids (Figure 3.20).

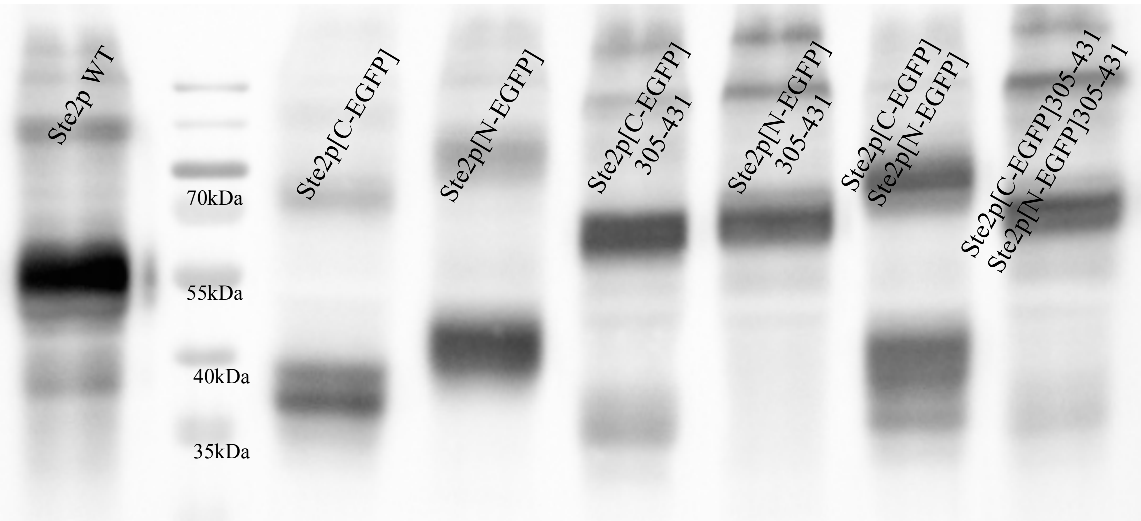

Figure 3.20 Western blot of the BJS21 cells expressing the constructs, the first lane is an extract of Ste2Δ cells expressing WT Ste2p receptor (52 kDa), the lanes three to six are extracts from cells expressing Ste2p[C-EGFP] (calc. ≈42 kDa), Ste2p[N-EGFP] (calc. ≈51 kDa), Ste2p[C-EGFP]305-431 (calc. ≈57 kDa) and Ste2p[N-EGFP]305-431 (calc. ≈66 kDa) respectively. Lane 7 shows cells co-expressing Ste2p[C-EGFP] and Ste2p[N-EGFP]; Lane 8 shows cells co-expressing Ste2p[C-EGFP]305-431 and Ste2p[N-EGFP]305-431. The proteins from lanes 1 to 8 were detected with antireceptor antiserum directed against the N-terminal domain of the α-factor receptor.

Figure 3.21 shows the immunoblot probed with GFP Rabbit Serum Polyclonal antibody and anti-FLAG antibody. First two lanes; extract of Ste2Δ cells and, extract of Ste2Δ cells expressing WT Ste2p receptor (52 kDa) from pBEC1 plasmid respectively; were probed with anti-FLAG antibody. Lanes four to seven show Ste2p[C-EGFP] (calc. M.W. 42 kDa), Ste2p[N-EGFP] (calc. M.W. 51 kDa), Ste2p[C-EGFP]305-431 (calc. M.W.57 kDa) and Ste2p[N-EGFP]305-431 (1-158) (calc. M.W. 66 kDa), respectively, last two empty lanes eight and nine represents extract of Ste2Δ cells transformed with empty plasmid (p424) and, extract of Ste2Δ cells expressing WT Ste2p receptor respectively. The multiple band patterns were also observed in the blot probed with GFP Rabbit Serum Polyclonal antibody and anti-FLAG antibody.

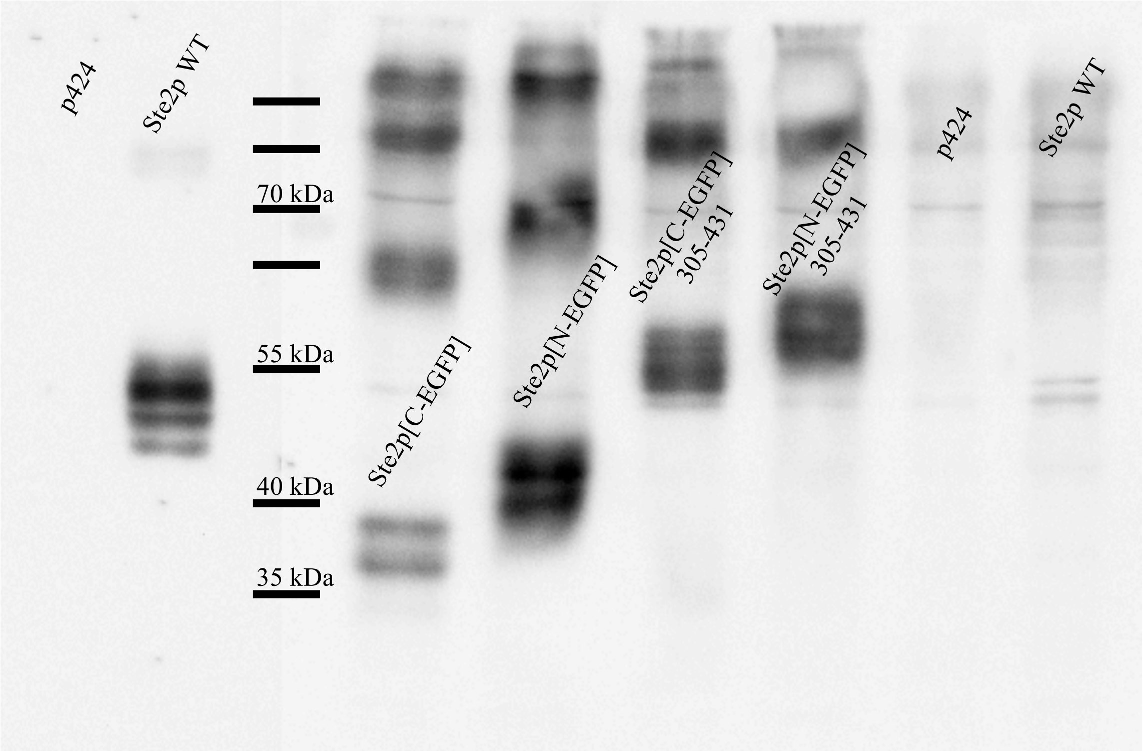

Figure 3.21 Western blot of the BJS21 cells expressing the constructs, the first lane is an extract of Ste2Δ cells, the second lane is an extract of Ste2Δ cells expressing WT Ste2p receptor (52 kDa), the lanes 4 to 7 are extracts from cells expressing Ste2p[C-EGFP] (calc. ≈42 kDa), Ste2p[N-EGFP] (calc. ≈51 kDa), Ste2p[C-EGFP]305-431 (calc. ≈57 kDa) and Ste2p[N-EGFP]305-431 (calc. ≈66 kDa) respectively. Lanes 8 and 9 are extracts of Ste2Δ cells transformed with empty plasmid and extract of Ste2Δ cells expressing WT Ste2p receptor (52 kDa) respectively. The proteins at lanes 1 and 2 were detected with anti-FLAG antibody and proteins from lanes 4 to 9 were detected with GFP Rabbit Serum Polyclonal antibody (Molecular Probes).

In Figure 3.22, the blot was detected using two primary antibodies; antireceptor antiserum directed against the N-terminal domain of the α-factor receptor and mCherry monoclonal antibody (16D7, Life Technologies, NY, USA) and two secondary antibodies; IRDye 680CW Goat anti-rabbit IGg secondary antibody (LI-COR, NE, USA) detected at 680nm and IRDye 800CW Goat anti-rat IGg secondary antibody detected at 800nm.

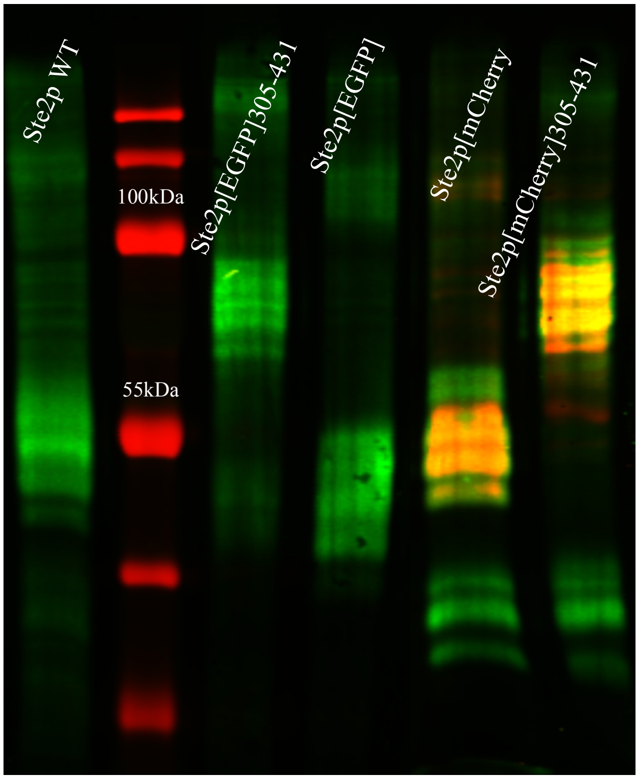

Figure 3.22 Western blot of the BJS21 cells expressing the constructs, the first lane is an extract of Ste2Δ cells expressing WT Ste2p receptor (52 kDa), the lanes three to six are extracts from cells expressing Ste2p[EGFP]305-431 (calc. ≈75 kDa), Ste2p[EGFP] (calc. ≈60 kDa), Ste2p[mCherry] (calc. ≈60 kDa) and Ste2p[mCherry]305-431 (calc. ≈75 kDa) respectively. The proteins from lanes 1 to 6 were detected with antireceptor antiserum directed against the N-terminal domain of the α-factor receptor (green channel), proteins at lanes 5 and 6 are also detected with mCherry monoclonal antibody (16D7, Life Technologies, NY, USA) (red channel) using LI-COR Odyssey CLx Infrared Imaging System.

The first lane on the blot contains membranes from cells expressing WT Ste2p receptor; the multiple bands observed at approximately 52 kDa are due to different glycosylated forms of the receptor [182] [183]. Lanes three to six show Ste2p[EGFP]305-431 (calc. M.W. 75 kDa), Ste2p[EGFP] (calc. M.W. 60 kDa), Ste2p[mCherry] (calc. M.W. 60 kDa) and Ste2p[mCherry]305-431 (calc. M.W. 75 kDa) respectively. The bands observed in the western blot for truncated Ste2p[EGFP] and Ste2p[mCherry], shown in lanes 4 and 5 are in accordance with their calculated molecular weights. The bands with full-length Ste2p receptors Ste2p[EGFP]305-431 and Ste2p[mCherry]305-431 with the inserted EGFP or mCherry shown at lanes 3 and 6 were above the WT Ste2p band, below 100 kDa protein ladder band in accordance with their calculated molecular weights. The multiple bands were likely due to the various glycosylated forms of Ste2p. Again in all lanes, higher bands corresponding to a dimeric state of Ste2p was observed (Figure 3.22).

Figure 3.23, represents the blot separated into two different channels. Blot a (left, green) shows Ste2p constructs detected with antireceptor antiserum directed against the N-terminal domain of the α-factor receptor and IRDye 680CW Goat anti-rabbit IGg secondary antibody (LI-COR, NE, USA) detected at 680nm. The first lane shows WT Ste2p receptor. Lanes three to six show after the empty lane shows Ste2p[EGFP]305-431, Ste2p[EGFP], Ste2p[mCherry] and Ste2p[mCherry]305-431 respectively as explained in Figure 3.22. Blot b (right, red) shows Ste2p constructs detected with mCherry monoclonal antibody and IRDye 800CW Goat anti-rat IGg secondary antibody detected at 800nm. The first lane shows WT Ste2p receptor, second lane shows protein ladder third and forth lanes correspond to Ste2p EGFP constructs. Lanes 1, 3 and 4 did not show any signal when detected using mCherry antibody also indicative of no cross-reactivity between the EGFP and mCherry antibody. Last two lanes show Ste2p[mCherry] and Ste2p[mCherry]305-431 respectively. The multiple bands patterns are due to different glycosylated forms of the receptor.

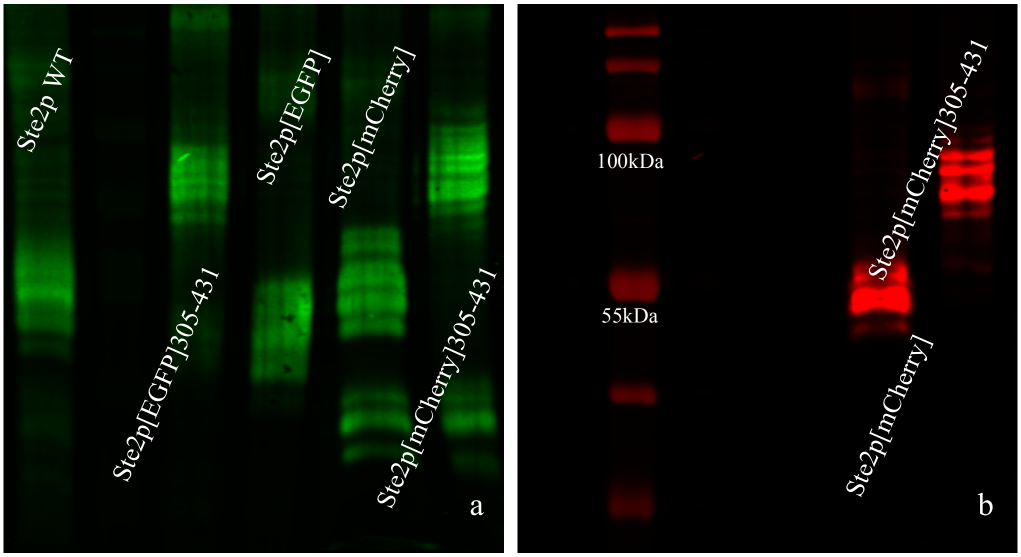

Figure 3.23 Western blot of the BJS21 cells expressing the Ste2p constructs detected at two separate channels (a) left blot shows Ste2p constructs detected with antireceptor antiserum directed against the N-terminal domain of the α-factor receptor primary antibody and IRDye 680CW Goat anti-rabbit IGg secondary antibody detected at 680nm (a) the right blot shows Ste2p constructs detected with mCherry monoclonal antibody and IRDye 800CW Goat anti-rat IGg secondary antibody detected at 800nm.

3.1.7 Saturation binding experiments

The expression levels were further evaluated by binding experiments whereby the K_d and B_max values indicating the affinity and number of receptors on the cell surface, respectively, can be determined by saturation binding assays (Figure 3.24, Table 3.3). The K_d value for cells expressing WT Ste2p protein was calculated from the binding curves to be 17 ± 2 nM. In the case of our co-expressed constructs, the K_d values for (Ste2p[N-EGFP]305-431/Ste2p[C-EGFP]305-431) was 5.8 ± 0.6 nM and for C-terminally truncated constructs, (Ste2p[N-EGFP] / Ste2p[C-EGFP]) the K_d was 12 ± 0.6 nM. Using the B_max value determined from the binding curves, the number of receptors per cell were calculated to be 6.7 $\times 10^3$ for cells expressing WT Ste2p protein, 1.4 $\times 10^3$ for Ste2p[N-EGFP]305-431/Ste2p[C-EGFP]305-431, and 5.1 $\times 10^3$ for Ste2p[N-EGFP]/Ste2p[C-EGFP] from DK102 cells. These K_d and B_max values indicated that receptors were expressed on the cell surface that were active in the sense of their binding the ligand α-factor.

Table 3.3 K_d, B_{max} and number of receptors at the plasma membrane calculated from the B_{max} for the constructs.

	K_d	B_{max}	# of receptors on plasma membrane
WT Ste2p	17.41±2	40554±2240	6.74 x 10^3
Ste2p[N-EGFP]305-431 / Ste2p[C-EGFP]305-431	5.8±0.6	8157±278	1.36 x 10^3
Ste2p[N-EGFP] / Ste2p[C-EGFP]	12.24±0.6	30489±550	5.07 x 10^3

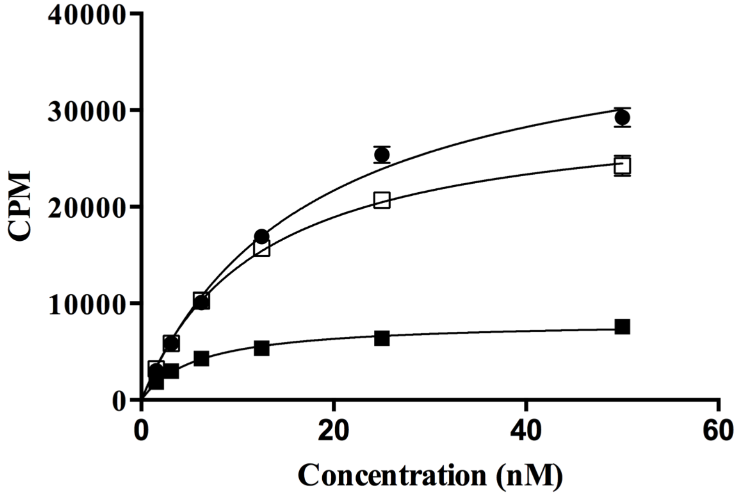

Figure 3.24 Saturation binding data of DK102 cells co-expressing the split EGFP receptor pairs. Cells expressing WT Ste2p receptor from pBEC1 vector (●); Cells co-expressing Ste2p[N-EGFP]305-431/Ste2p[C-EGFP]305-431, N-EGFP (1-158) or C-EGFP (159-238) inserted between positions 304-305 of the Ste2p receptor (■); Cells co-expressing Ste2p[N-EGFP]/Ste2p[C-EGFP], N-EGFP (1-158) or C-EGFP (159-238) attached at position 304 of C-terminally truncated Ste2p receptor (☐).

Ste2p constructs carrying EGFP split at 158-159 were biologically active and gave a BiFC signal. First part of the study focused on EGFP split at 158-159 and a full length EGFP appended or inserted at position 304 of Ste2p (See Table 1.1 for constructs used). These Ste2p constructs were expressed from pBEC1 or pCL01 plasmids carrying different auxotrophic markers in order to co-express the split EGFP constructs (Table 3.1).

3.2 Microscopy of cells expression Ste2p tagged with EGFP or split EGFP

Live cell imaging of yeast transformants was carried out without any fixation at room temperature using Leica SP2 Laser Scanning Confocal Microscope equipped with a Leica 63x/1.32 HCX PL APO Oil DIC objective. Cells were analyzed in single-track configurations in which the samples were excited by laser at 488 nm and the emission data were collected in the 505-550 nm range.

Photomultiplier tubes and cameras used in microscopy collect the data as grey pixels. All the images are then "pseudo-colored" according to their emission wavelength for presentation purposes.

3.2.1 Detection of monomers of full-length Ste2p tagged with EGFP

Ste2p receptor tagged with full length EGFP inserted between positions 304-305 (Ste2p[EGFP]305-431) showed a fluorescence signal on the membrane and intracellularly (Figure 3.25a). The intracellular signal could be due to trafficking of tagged Ste2p arising from the transport of receptors to the membrane and/or the signal arising from endocytosis of receptors internalized from the membrane.

To differentiate between endocytosis and transport of newly biosynthesized Ste2p, cells were treated with latrunculin A (LatA, 200 μM) for 30 min to block endocytosis [184, 185] or cycloheximide (60 μg/mL) for 30 min to prevent biosynthesis. Cells expressing Ste2p[EGFP]305-431 treated with latrunculin A (Figure 3.25 b) showed bright puncta on the plasma membrane (arrows in Figure 3.25b), whereas cells incubated with cycloheximide showed intracellular punctate pattern (arrows, Figure 3.25c) resembling the endocytotic vesicles [186]. These experiments indicated that the intracellular fluorescent signal in Figure 5a is due to trafficking of Ste2p to and from the plasma membrane.

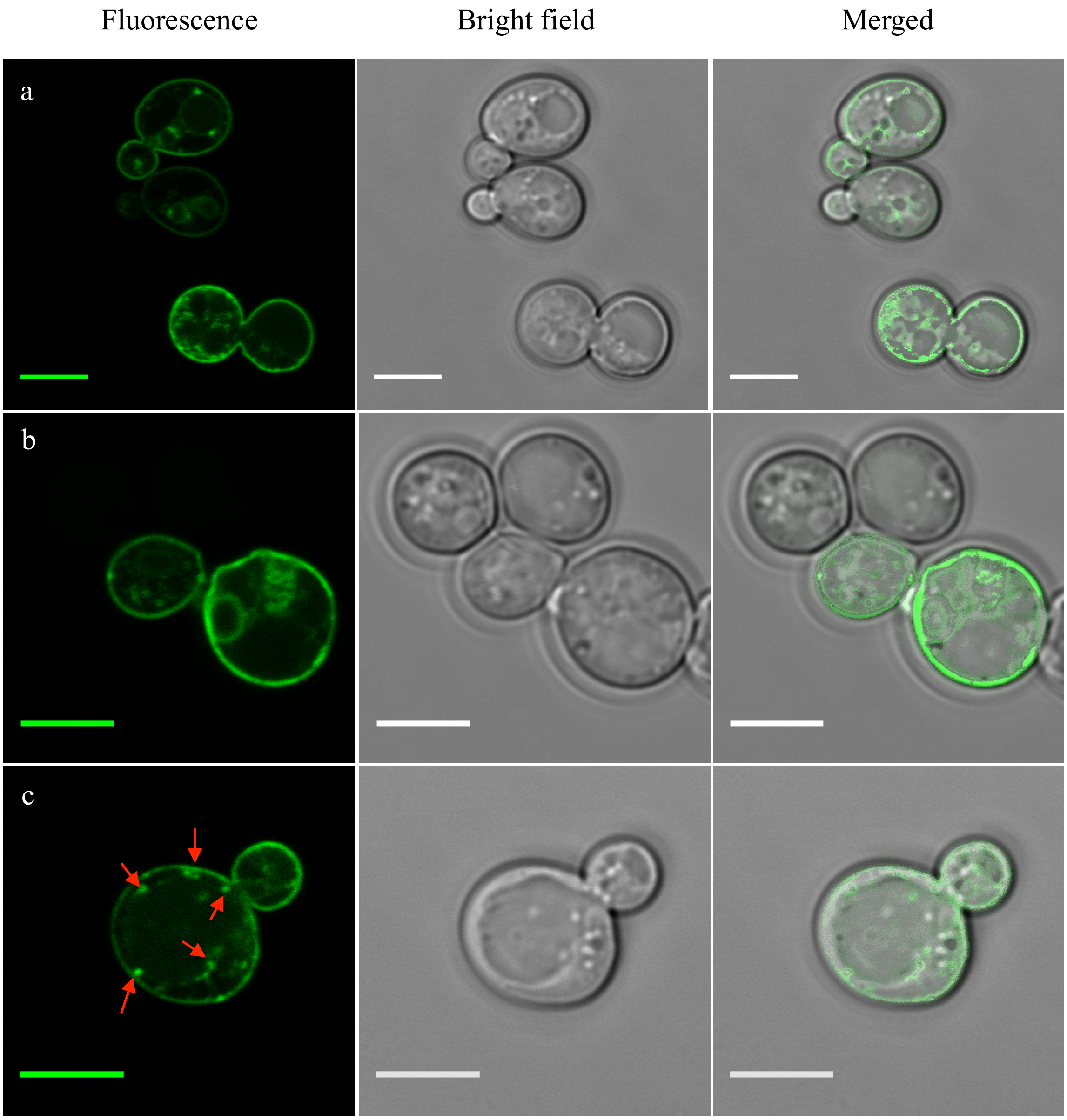

Figure 3.25 Cells expressing EGFP tagged full length Ste2p, scale bars correspond 5 μm length. **(a)** Shows cells expressing Ste2p[EGFP]305-431. **(b)** Shows cells expressing Ste2p[EGFP]305-431 treated with latrunculin A. **(c)** Shows cells expressing Ste2p[EGFP]305-431 treated with cycloheximide.

3.2.2 Detection of dimers of full-length Ste2p tagged with split EGFP

BiFC experiments were then undertaken to examine interaction between Ste2p molecules tagged with either the N-terminal or C-terminal portions of EGFP. Cells co-expression Ste2p[N-EGFP]305-431 and Ste2p[C-EGFP]305-431 are shown (Figure 3.26a). Expression of either construct by itself gave no fluorescent signal (data not shown). The signal observed on the plasma membrane suggested that Ste2p receptors are in a dimeric state on the membrane. An internal signal is also observed in Figure 3.26a (arrows). The BiFC signal can be explained by two mechanisms; either the receptors are dimerizing on the plasma membrane and being internalized as dimers (or oligomers), or/and the receptors are being transported to the membrane as dimers (or as oligomers).

We used latrunculin A and cycloheximide to determine the localization of the dimerization. Cells co-expressing Ste2p[N-EGFP]305-431 and Ste2p[N-EGFP]305-431 were incubated with latrunculin A (200 μM) for 30 minutes; the intracellular EGFP signal was almost completely lost and the fluorescent signal arising from dimer formation was observed mainly at the plasma membrane (Figure 3.26b). To determine whether the intracellular punctate signals arise from the dimerization of receptors during the biosynthesis and/or transport to the plasma membrane, cells were incubated with cycloheximide (60 μg/mL) for 30 min. The internal signal observed (Figure 3.26c) resembled that seen in Figure 3.26a. The observations shown in Figures 3.25 and 3.26 suggest that Ste2p receptors dimerize on the plasma membrane and internalize as dimers.

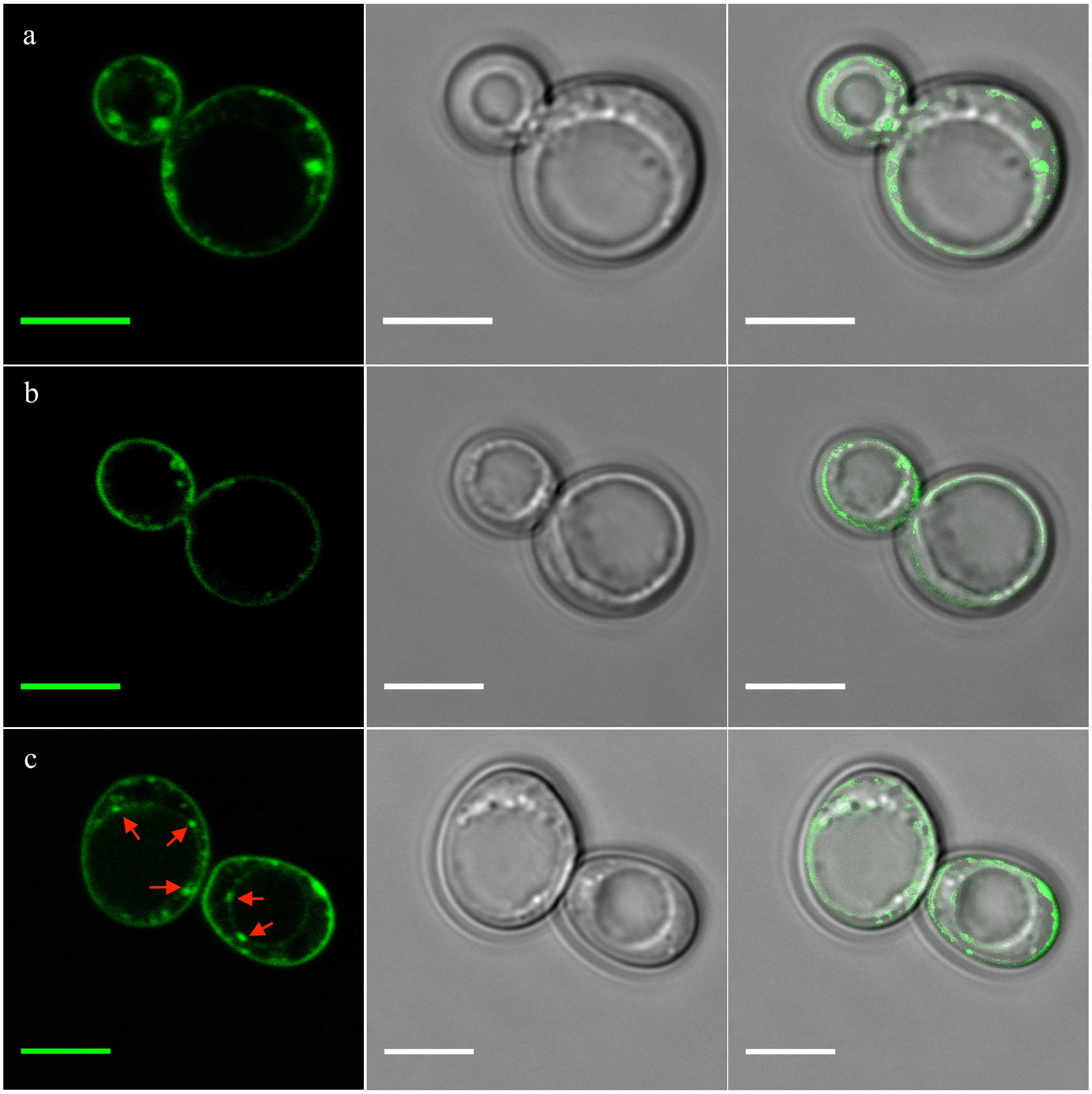

Figure 3.26 Cells co-expressing full length Ste2p tagged with either N-EGFP or C-EGFP, scale bars correspond 5 µm. **(a)** Shows cells co-expressing Ste2p[N-EGFP]305-431 / Ste2p[C-EGFP]305-431; Ste2p BiFC pair tagged with either N-EGFP (1-158) or C-EGFP (159-238) inserted between position 304-305. **(b)** Shows cells co-expressing Ste2p[N-EGFP]305-431 / Ste2p[C-EGFP]305-431 treated with latrunculin A, the internal signal arising from dimerization is almost completely lost. **(c)** Shows cells co-expressing Ste2p[N-EGFP]305-431 / Ste2p[C-EGFP]305-431 treated with cycloheximide, the internal puncta is shown with red arrows indicative of endocytic vesicles.

3.2.3 Detection of monomers of truncated Ste2p tagged with EGFP

C-terminally truncated Ste2p receptors were also used to test if the internal signal was due to endocytosis or trafficking to the plasma membrane, since these receptors lack a major endocytosis signal sequence found on the C-tail [187]; truncation of Ste2p receptors at the 304th residue of the C-terminal tail showed increased expression at the cell surface and retained the ability to bind agonist with high affinity and respond to pheromone [188].

Cells expressing C-terminally truncated Ste2p-Δ305-431 receptors tagged with full length EGFP are shown in Figure 3.27a. The fluorescence signal was observed both on the plasma membrane and intracellularly from truncated Ste2p[EGFP]. The intracellular signal may be interpreted as predominantly arising from the transport of newly synthesized receptor monomers to the membrane, because endocytosis is inhibited in this construct. This effect can further be observed by the comparison of fluorescence signal distribution and endocytotic puncta in Figure 3.25a (Ste2[EGFP]305-431) and Figure 3.27a (Ste2[EGFP]). The intracellular signal observed for full-length receptors (Figure 3.25a), arises from the two-way trafficking signal: the transport of receptors monomers to the membrane and endocytosis of receptor dimers from the membrane. In contrast the intracellular puncta observed in cells expressing C-terminally truncated receptors (Figure 3.27a) shows the signal arising predominantly from the synthesis and transport of receptor monomers to the plasma membrane. These cells expressing endocytosis deficient Ste2p[EGFP] construct were also treated with cycloheximide to block the protein synthesis and as a result the EGFP signal was observed only on the plasma membrane. That the signal was emanating from receptors trafficking to the cell membrane was further confirmed by treating cells expressing Ste2p[EGFP] with cycloheximide. When protein synthesis was blocked, the EGFP signal was observed only on the membrane, indicating the internal signal for the untreated cells arose from the biosynthesis and transport of newly synthesized receptor monomers to the membrane (Figure 3.27b).

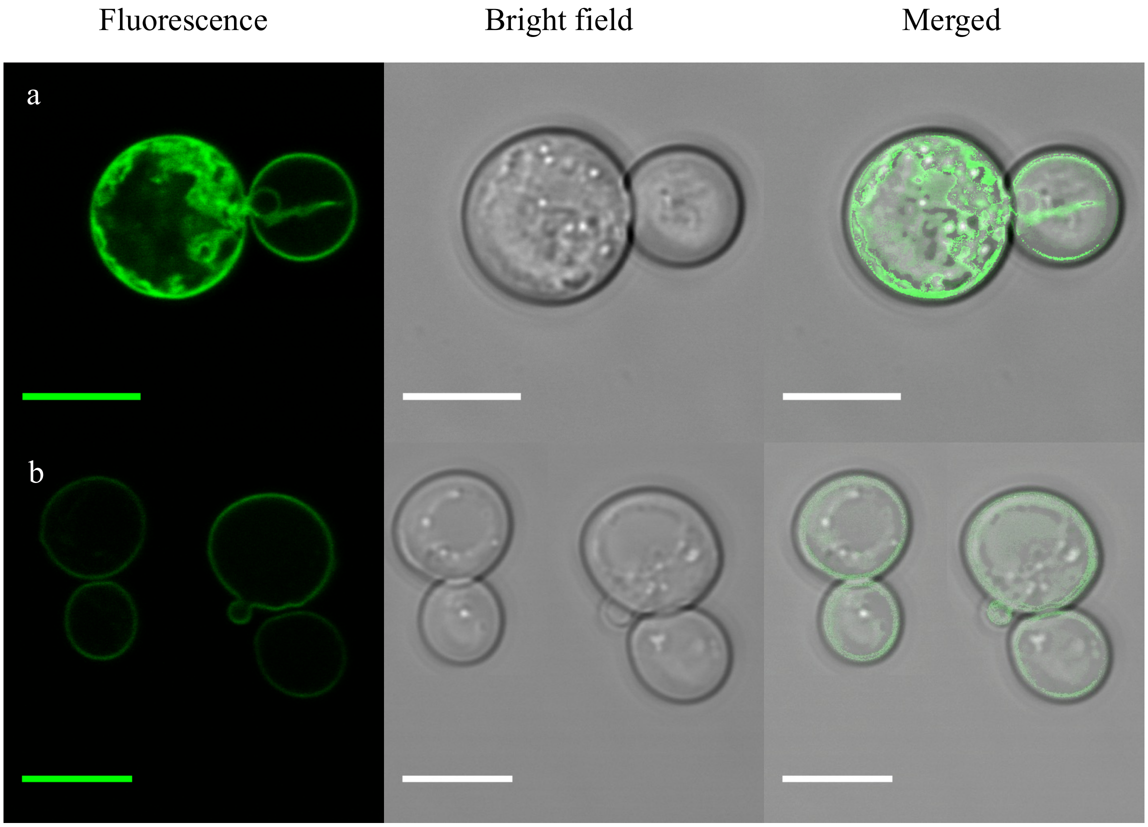

Figure 3.27 Cells expressing EGFP tagged C-terminally truncated Ste2p, scale bars correspond 5 µm. **(a)** Shows cells expressing Ste2p[EGFP]; C-terminally truncated Ste2p receptor tagged with full length EGFP attached at position 304. **(b)** Shows cells expressing Ste2p[EGFP] treated with cycloheximide. The internal EGFP signal was completely lost after blocking the protein synthesis.

3.2.4 Detection of dimers of truncated Ste2p tagged with split EGFP

The fluorescence signal observed in Figure 3.28 shows the dimerization of truncated Ste2p[N-EGFP] and truncated Ste2p[C-EGFP] at the cell membrane. Most strikingly, the dimerization signal was only observed on the plasma membrane and there was no detectable intracellular BiFC signal.

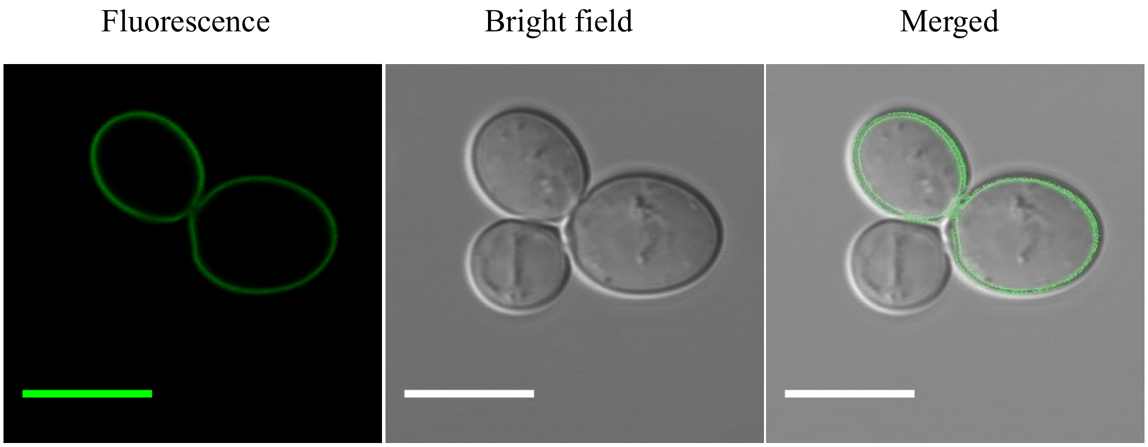

Figure 3.28 Cells co-expressing Ste2p[N-EGFP] / Ste2p[C-EGFP]; C-terminally truncated receptor tagged with either N-EGFP (1-158) or C-EGFP (159-238) attached to position 304, scale bars correspond 5 μm.

3.2.5 Detection of dimers of full-length and truncated Ste2p with spilt EGFP

To further probe the internalization mechanism, we imaged cells co-expressing full-length and truncated Ste2p. Cells co-expressing Ste2p[N-EGFP]305-431 / Ste2p[C-EGFP] (Figure 3.29a) or Ste2p[C-EGFP]305-431 / Ste2p[N-EGFP] (Figure 3.29b) showed an internal signal in contrast to the pair in which both receptors are C-terminally truncated, Ste2p[N-EGFP] / Ste2p[C-EGFP] (Figure 3.28). The full-length / truncated receptor pair was also treated with latrunculin A (Figure 3.29c) and cycloheximide (Figure 3.29d). In the case of latrunculin A treated cells, again the intracellular signal was almost completely lost. For the cells treated with cycloheximide, the bright endocytic vesicles can still be observed both intracellularly and adjacent to the plasma membrane.

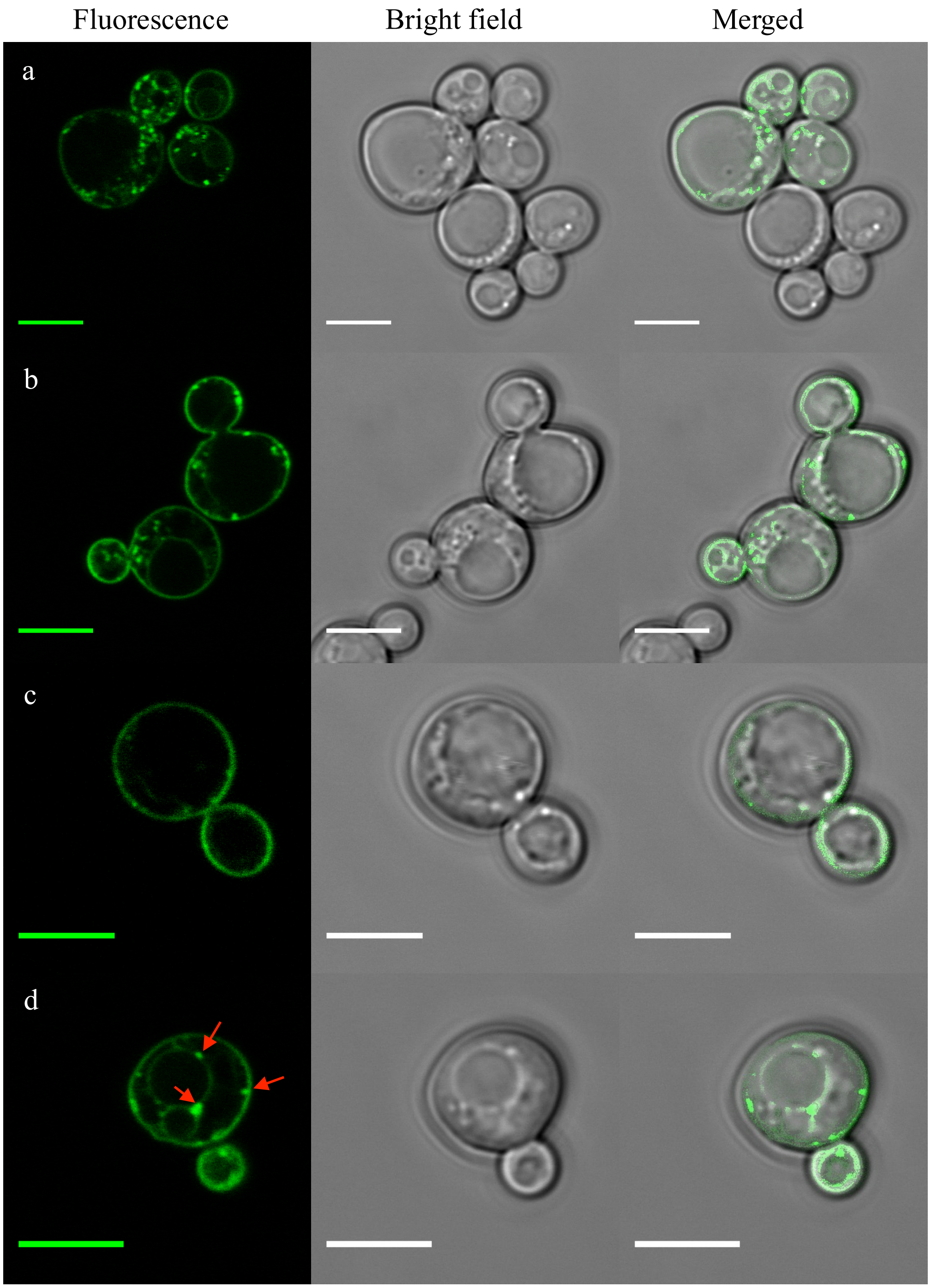

Figure 3.29 Cells co-expressing full length and C-terminally truncated Ste2p tagged with either N-EGFP or C-EGFP, scale bars correspond 5 µm length. **(a)** Shows cells co-expressing Ste2p[N-EGFP]305-431 / Ste2p[C-EGFP]. **(b)** Shows cells co-expressing Ste2p[C-EGFP]305-431 / Ste2p[N-EGFP]. **(c)** Shows the full length / truncated BiFC pair treated with latrunculin A, resulting with a signal loss intracellularly. **(d)** Shows the full length / truncated BiFC pair treated with cycloheximide, the red arrows show endocytotic vesicles at intracellular region.

In the first part of this study we demonstrated that labeling of Ste2p with EGFP fragments dissected between 158-159th residues resulted in a cellular fluorescence signal both for full length and C-terminally truncated receptors. The fluorescence signal was generated through the reassembly of fragments directed by the dimerization of yeast α-pheromone receptor Ste2p. We note that BiFC cannot distinguish between dimers and higher order oligomer formation.

Examination of truncated (at the 304th residue) and full-length receptors using a variety of techniques showed that Ste2p receptors dimerize mainly on the cell membrane and that the full-length receptor can be internalized as a dimer with a truncated receptor. In contrast, previous Ste2p dimerization studies carried out with C-terminally truncated receptors using FRET [64] or truncated and full-length receptors using BRET [130] did not show the location of dimerization. In addition, studies on full-length Ste2p endocytosis did not distinguish between monomer and dimer internalization [189]. Thus the present studies increase our understanding of GPCR receptor dimerization and internalization in the quiescent (non-ligand activated) state.

All Ste2p constructs fused with EGFP or EGFP fragments at position 304 were shown to be biologically active and responded to the pheromone (Figures 3.15 – 3.19). Ste2p[EGFP], Ste2p[N-EGFP] and Ste2p[C-EGFP] constructs showed greater growth response sensitivity which has been shown previously for truncated receptors [188, 190], due to the fact that the truncation of the C-terminal domain inhibits down regulation and such receptors are retained at the plasma membrane in a pheromone-responsive state [187, 188].

Protein expression of all the constructs was determined by western blotting (Figures 3.21 – 3.23). The bands observed in western blot for truncated receptors, Ste2p[N-EGFP] and Ste2p[C-EGFP] were slightly below Ste2p WT band and for full length receptors Ste2p[N-EGFP]305-431, Ste2p[C-EGFP]305-431 were slightly above the

WT band in accordance with their calculated molecular weights (Figures 3.21 – 3.23). Cells co-expressing the Ste2p[N-EGFP] / Ste2p[C-EGFP] pair and Ste2p[N-EGFP]305-431 / Ste2p[C-EGFP]305-431 pair were also harvested and multiple bands were observed in western blots corresponding to monomeric and dimeric states of the Ste2p receptor. The pattern in the gels indicates that both constructs are expressed in the cell providing a basis for measuring the BiFC of these co-expressed receptors.

The cell surface expression levels were evaluated from binding experiments with the K_d and B_{max} values, calculated from binding curves (Figure 3.24, Table 3.3). The B_{max} values showed that the cell surface expression levels of C-terminally truncated Ste2p constructs are higher compared to full length receptors. These data support previous reports [130, 188, 190] that showed C-terminally truncated constructs were found in greater amounts at the plasma membrane, in comparison to full length Ste2p constructs. Both pheromone induced growth arrest assay and saturation binding experiment indicated that receptors were expressed on the cell surface and they were active in the sense of their binding α-factor, the Ste2p receptor ligand.

One aim of this study was to determine where the receptor dimerization of a model GPCR occurs *in vivo* either at the plasma membrane or during transit to and from the membrane. To find an answer for this question we imaged cells expressing the constructs given in Table 3.1. To differentiate the internal signal between endocytosis and transport of newly biosynthesized Ste2p, cells were treated with latrunculin A to block endocytosis [184, 185] or cycloheximide to prevent biosynthesis.

Cells expressing Ste2p[EGFP]305-431 showed EGFP signal both on the plasma membrane and intracellularly (Figure 3.25a). When these cells were incubated with Latrunculin A, the cytosolic signal was observed (Figure 3.25b). Cycloheximide treated cells also showed cytosolic puncta resembling endocytic vesicles (Figure 3.25c). Thus, the images collected from cells expressing Ste2p[EGFP]305-431

(Figure 3.25) indicated that the intracellular signal is due to trafficking of Ste2p to and from the plasma membrane. These experiments with the full-length-EGFP receptor could not distinguish between trafficking of a monomer or dimers.

The fluorescence signal observed from cells co-expressing Ste2p[N-EGFP]305-431 and Ste2p[C-EGFP]305-431 is due to the receptor dimers, since either construct by itself had no fluorescence. The signal observed on the plasma membrane (Figure 3.26a) suggested that Ste2p receptors are in a dimeric state on the membrane. An internal signal, shown with red arrows in Figure 3.26a, was also observed. The intracellular BiFC signal can be explained by two mechanisms; either the receptors are dimerizing on the plasma membrane and being internalized as dimers (or higher order oligomers), and/or the receptors are being transported to the membrane as dimers (or as oligomers). To differentiate between these two mechanisms, cells co-expressing Ste2p[N-EGFP]305-431 and Ste2p[C-EGFP]305-431 were incubated with latrunculin A, which resulted an almost complete loss of the intracellular EGFP signal (Figure 3.26b). This observation suggested that cytosolic signal in Figure 3.26a arises from the trafficking of receptor dimer/oligomers from the plasma membrane. When cells were treated with cycloheximide, an internal signal similar to untreated cells was observed (Figure 3.26c) resembling endocytotic vesicles. The observations shown in Figures 3.25 and 3.26 suggest that Ste2p receptors dimerize on the plasma membrane and internalize as dimers.

The carboxyl tail of Ste2p receptor carries the DAKSS endocytosis signal. In this study, C-terminally truncated Ste2p-Δ305-431 receptor constructs were used to test if the internal signal was due to endocytosis or trafficking to the plasma membrane. The fluorescence signal was observed both on the plasma membrane and intracellularly in cells expressing Ste2p[EGFP] (Figure 3.27a). The internal EGFP signal may be interpreted as predominantly arising from the biosynthesis and transport of newly synthesized receptor monomers to the membrane, because endocytosis is prevented in this construct. This effect can further be observed by the comparison of fluorescence signal distribution and endocytotic puncta in Figure 3.25a (Ste2[EGFP]305-431) and Figure 3.27a (Ste2[EGFP]). The intracellular signal observed for full-length receptors (Figure 3.25a), arises from the two-way trafficking signal: the transport of receptors monomers to the membrane and endocytosis of receptor dimers from the membrane. In contrast the intracellular puncta observed in cells expressing C-terminally truncated receptors (Figure 3.27a) shows the signal arising predominantly from the synthesis and transport of receptor monomers to the plasma membrane which was further confirmed by treating cells expressing Ste2p[EGFP] with cycloheximide. When protein synthesis was inhibited, the EGFP signal was observed only on the membrane, indicating that the internal signal for the untreated cells arose from the biosynthesis and transport of newly synthesized receptor monomers to the membrane (Figure 3.27b).

The dimerization signal of the cells co-expressing Ste2p[N-EGFP] and Ste2p[C-EGFP] was only observed on the plasma membrane and there was no detectable intracellular BiFC signal (Figure 3.28). These results reinforce the conclusion that the truncated Ste2p-Δ305-431 receptors dimerize on the membrane; dimerization was not detected intracellularly.

Comparison of the fluorescence signal distribution from cells co-expressing Ste2p[N-EGFP]305-431 / Ste2p[C-EGFP]305-431 in Figure 3.26 and cells co-expressing Ste2p[N-EGFP] / Ste2p[C-EGFP] in Figure 3.28 indicated that the observed intracellular signal (Figure 3.26) was dependent on endocytosis of full-length receptors with an intact C-terminal domain.

When full length / truncated receptor pair was co-expressed, the reconstituted EGFP signal was observed both on the plasma membrane and intracellularly (Figure 3.29a, 3.29b) in contrast to the signal which was only observed on the plasma membrane from the cells co-expressing truncated / truncated (Ste2p[N-EGFP] / Ste2[C-EGFP]) pair (Figure 3.28). These results suggest that full length receptors act in a dominant-positive manner for internalization of endocytosis deficient C-terminally truncated Ste2p. This effect was noted previously when expressing two receptors, one deficient in endocytosis and the other being proficient [64]. Cells co-expressing full length / truncated receptor pair were also treated with latrunculin A and cycloheximide. In the case of latrunculin A, the intracellular signal was almost completely lost, whereas in the case of cycloheximide, the intracellular signal resembling endocytotic vesicles remained in the cytosol and adjacent to the plasma membrane. These data once more indicated that dimerization occurs on the plasma membrane and receptors internalize as dimers (or higher order oligomers).

The split-EGFP fusion proteins can be used for analysis of localization of Ste2p dimers in mutants and for determination of the influence of agonists and antagonists on dimerization. Additionally, the effects of post-translational modification, such as glycosylation or phosphorylation, can be examined using this system.

3.2.6 Conclusion of first part

The aim of this study was to determine where receptor dimerization of a model GPCR occurs *in vivo*: either at the plasma membrane or during transit to and from the membrane. We used a bimolecular fluorescence complementation assay with Ste2p incorporating split EGFP fragments and confocal laser microscopy. All the constructs were verified by sequencing, and the Ste2p receptors labeled with EGFP or EGFP fragments were shown to be biologically active. We showed that dimers of Ste2p were resident on the plasma membrane and internalized by a presumed endocytic route in live cells. The experimental procedure of BiFC requires dimer formation, but whether the receptors were also forming higher order aggregates could not be determined by the methods used. Fluorescent puncta presumed to represent endocytic vesicles containing Ste2p dimers were observed intracellularly in yeast cells expressing full-length receptors; however C-terminally truncated receptors as dimers were shown to be mostly localized on the membrane. The split-EGFP fusion proteins can be used for further analysis of localization of Ste2p mutant dimer formation. Additionally, effects of post-translational modifications or agonist and/or antagonist binding can be examined using split-EGFP constructs. Future experiments are being designed to distinguish between dimer or higher order oligomer formation during receptor biosynthesis, surface residence, and down regulation.

3.3 More than just a dimer: studying oligomerization of Ste2p

3.3.1 Construction of galactose inducible double promoter vectors

The pESC-TRP (carries a TRP1 yeast open reading frame as a selective maker) and pESC-URA (carries a URA3 yeast open reading frame as a selective maker) vectors (Agilent Technologies, CA, USA) were used for cloning Ste2p BiFC constructs for simultaneous expression through one plasmid. Other than the TRP1 and URA3 open reading frame, both plasmids have 2µ origin for yeast, pUC and f1 origins for bacteria and they carry the same multiple cloning regions. For yeast expression these plasmids are equipped with a divergent Gal1 – Gal10 promoter region, upstream of both multiple cloning sites and ADH1 and CYC1 terminators. These promoters induce the protein expression in Galactose medium, while keeping the expression repressed in Glucose medium.

For the simultaneous co-expression of two or more proteins, Ste2p constructs were cloned into pESC-TRP and pESC-URA double promoter vectors. The vector maps and multiple cloning regions of these vectors are given in Figure 3.30.

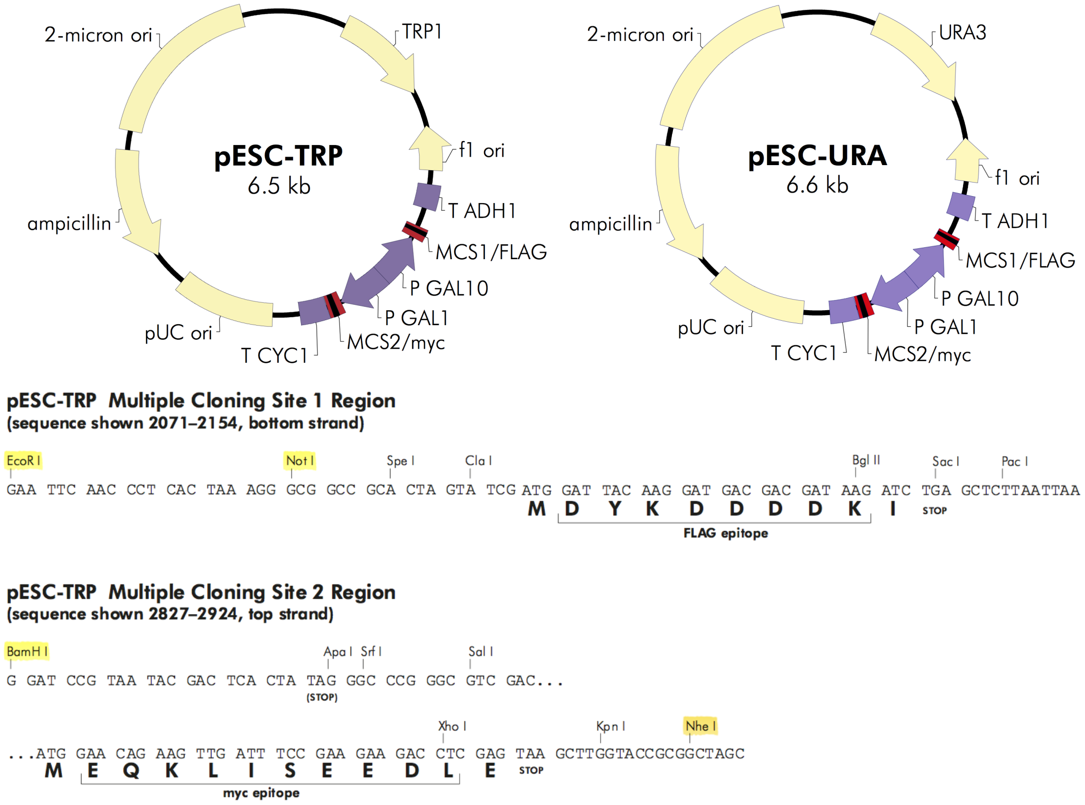
2-micron ori
TRP1
pESC-TRP
6.5 kb
f1 ori
T ADH1
MCS1/FLAG
P GAL10
P GAL1
MCS2/myc
T CYC1
pUC ori
ampicillin
2-micron ori
URA3
pESC-URA
6.6 kb
f1 ori
T ADH1
MCS1/FLAG
P GAL10
P GAL1
MCS2/myc
T CYC1
pUC ori
ampicillin
pESC-TRP Multiple Cloning Site 1 Region
(sequence shown 2071–2154, bottom strand)
EcoR I
Not I
Spe I
Cla I
Bgl II
Sac I
Pac I
GAA TTC AAC CCT CAC TAA AGG GCG GCC GCA CTA GTA TCG ATG GAT TAC AAG GAT GAC GAC GAT AAG ATC TGA GCTCTTAATTAA
M D Y K D D D D K I STOP
FLAG epitope
pESC-TRP Multiple Cloning Site 2 Region
(sequence shown 2827–2924, top strand)
BamH I
Apa I
Srf I
Sal I
G GAT CCG TAA TAC GAC TCA CTA TAG GGC CCG GGC GTC GAC...
(STOP)
Xho I
Kpn I
Nhe I
...ATG GAA CAG AAG TTG ATT TCC GAA GAA GAC CTC GAG TAA GCTTGGTACCGCGGCTAGC
M E Q K L I S E E D L E STOP
myc epitope

Figure 3.30 pESC-TRP and pESC-URA (Agilent Technologies, CA, USA) vector maps and their multiple cloning sites (MCS) sequences.

The Ste2p constructs were amplified with primers carrying 5’ EcoRI – 3’ NotI or 5’ BamHI – 3’ NheI restriction sites. The PCR products and pESC-TRP and pESC-URA vectors were let for digestion with the respective enzyme pairs and the products of digestion reaction were extracted from agarose gel (Figure 3.31).

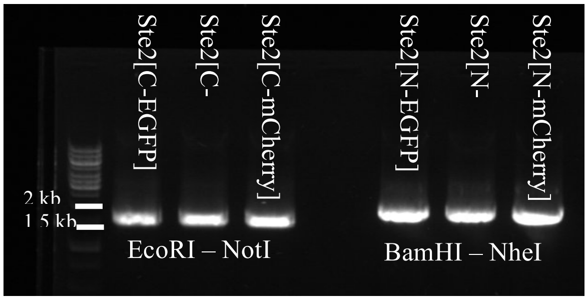
Ste2[C-EGFP]
Ste2[C-
Ste2[C-mCherry]
Ste2[N-EGFP]
Ste2[N-
Ste2[N-mCherry]
2 kb
1.5 kb
EcoRI – NotI
BamHI – NheI

Figure 3.31 Gel image for the amplified Ste2p constructs with either 5’ EcoRI – 3’ NotI primer pair or 5’ BamHI – 3’ NheI primer pair.

The Ste2p C-EGFP and C-mCherry constructs were cloned between EcoRI – NotI sites, Ste2p N-EGFP and N-mCherry constructs were cloned between BamHI – NheI sites. This way pESC-URA-STE2[C-EGFP] (pESC-U1) and pESC-URA-STE2[N-EGFP] (pESC-U2), pESC-URA-STE2[C-EGFP]305-431 (pESC-U3) and pESC-URA-STE2[N-EGFP]305-431 (pESC-U4) plasmids carrying Ste2p constructs tagged with EGFP fragments; pESC-TRP-STE2[C-mCherry] (pESC-T6) and pESC-TRP-STE2[N-mCherry] (pESC-T7) plasmids carrying Ste2p constructs tagged with mCherry fragments were constructed.

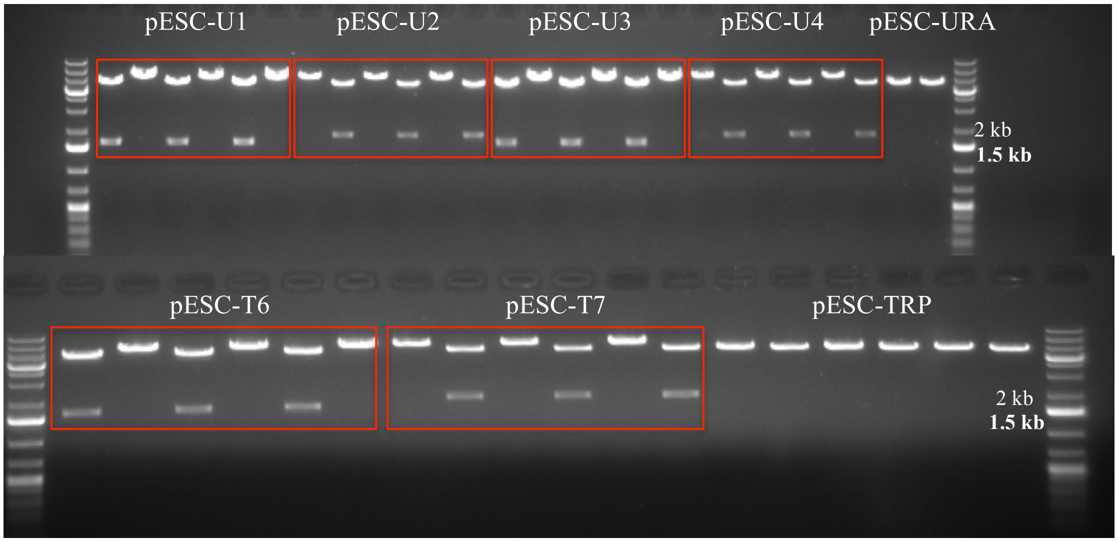

Figure 3.32 Three colonies were picked from each construct and each colony was digested with EcoRI – NotI (first lane), BamHI – NheI (second lane). Insert sizes were consistent with expected results.

The newly constructed plasmids carrying Ste2p constructs tagged with C-EGFP or C-mCherry were digested with BamHI – NheI enzyme pair and plasmids carrying Ste2p constructs tagged with N-EGFP and N-mCherry were digested with EcoRI – NotI (Figure 3.33) and extracted from agarose gel for cloning the complementary Ste2p construct into the empty multiple cloning site.

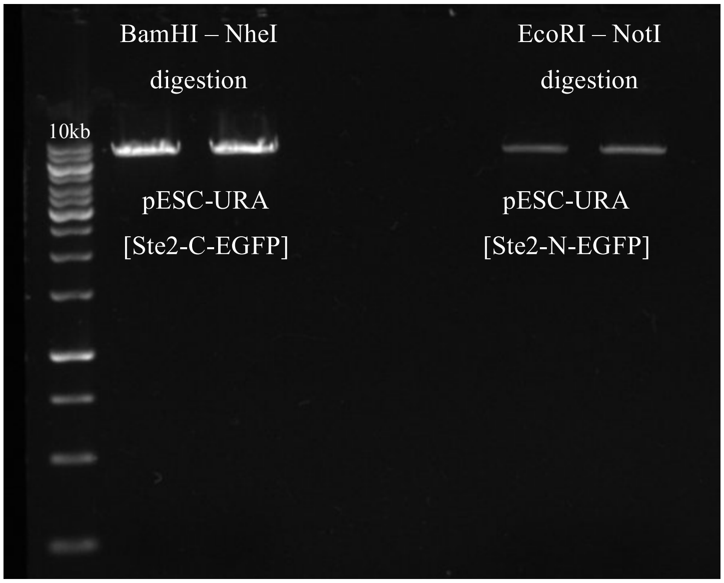

Figure 3.33 Digestion control of the inserts after the construction of pESC-URA-Ste2p[N-EGFP] and pESC-URA-Ste2p[C-EGFP] plasmids (left image). Digestion of pESC-URA-STE2[N-EGFP] and pESC-URA-STE2[C-EGFP] vectors for cloning the complementary Ste2p constructs; Ste2p[C-EGFP] and Ste2p[N-EGFP] respectively; into the empty cloning sites.

These linear pESC-URA and pESC-TRP based plasmids carrying Ste2p construct tagged with either N-EGFP or C-EGFP fragment were used for the ligation of complementary BiFC Ste2p construct into their empty multiple cloning site. Each plasmid obtained from the ligation reactions was digested with both EcoRI – NotI and BamHI – NheI enzyme pairs to verify the insertion of both Ste2p BiFC constructs. All Ste2p constructs tagged with N-EGFP (1-158) or N-mCherry (1-159) were cloned between BamHI and NheI restriction sites under the control of Gal1 promoter and CYC1 terminator; Ste2p constructs tagged with C-EGFP (159-238) and C-mCherry (160-237) were cloned between EcoRI and NotI under the control of Gal10 promoter and ADH1 terminator regions. Digestion controls of all these constructs were given in Figures 3.34 and 3.35.

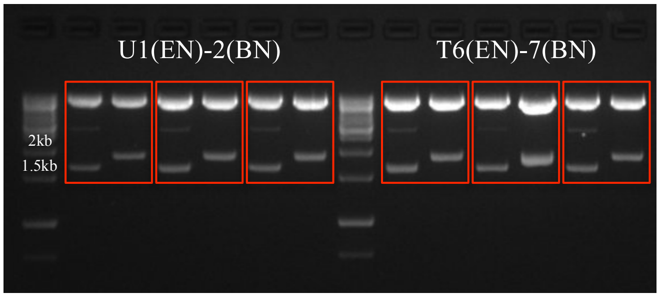
U1(EN)-2(BN)
T6(EN)-7(BN)
2kb
1.5kb

Figure 3.34 Digestion control of double promoter vectors for coexpression of complementary C-terminally truncated Ste2p constructs tagged with C-EGFP and N-EGFP (U12) and C-mCherry and N-mCherry (T67) from one plasmid. Each red box, represents EcoRI – NotI digestion (first lane) and BamHI – NheI digestion (second lane) of same plasmid. The sizes of Ste2p constructs are in accordance with the calculated values. STE2[C-EGFP] (1): 1614 bp, STE2[N-EGFP] (2): 1854 bp, STE2[C-mCherry] (6): 1611 bp, STE2[N-mCherry] (7): 1851 bp.

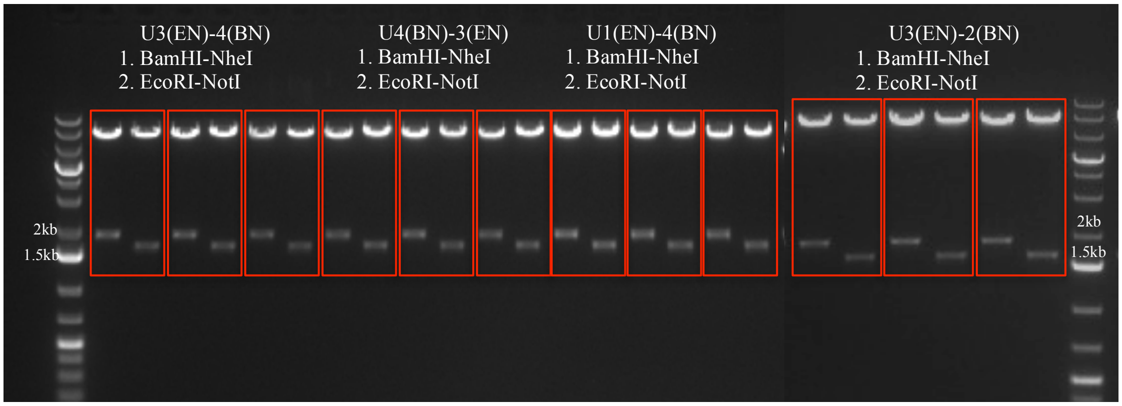
U3(EN)-4(BN)
1. BamHI-NheI
2. EcoRI-NotI
U4(BN)-3(EN)
1. BamHI-NheI
2. EcoRI-NotI
U1(EN)-4(BN)
1. BamHI-NheI
2. EcoRI-NotI
U3(EN)-2(BN)
1. BamHI-NheI
2. EcoRI-NotI
2kb
1.5kb
2kb
1.5kb

Figure 3.35 Digestion control of double promoter vectors for coexpression of complementary full length Ste2p constructs from one plasmid. In each red box, first lane represents BamHI – NheI digestion, second lane represents EcoRI – NotI digestion. The sizes of Ste2p constructs are in accordance with the calculated values. STE2[C-EGFP]305-431 (3): 1611 bp, STE2[N-EGFP]305-431 (4): 1851 bp, STE2[C-EGFP] (1): 1614 bp, STE2[N-EGFP] (2): 1854 bp.

All the plasmids constructed based on pESC double promoter vectors are given in Table 3.4.

Gal1 – Gal10 promoters are needed to be induced by galactose for the expression of the proteins using these plasmids, however in a glucose medium these promoters are repressed. Unfortunately, we were not able to grow the yeast transformants in the galactose medium (Appendix A). We first grew the yeast culture in glucose containing medium (Appendix A), then glucose containing medium was removed and cells were washed multiple times with water to get rid of any traces of glucose. The cultures were then resuspended in galactose medium and cells were imaged at several time intervals (1h – 3h – 9h – overnight – 48 h) neither growth nor any expression was observed.

Table 3.4 Abbreviated names of the Ste2p constructs (1st column) constructed from pESC vectors (2nd column) and the position of inserts (3rd and 4th columns).

Abbreviation	Origination plasmid	MCS1 (Gal10 – ADH1)	MCS2 (Gal1 – CYC1)
U1(EN)	pESC-URA	Ste2p[N-EGFP]	empty
U2(BN)	pESC-URA	empty	Ste2p[C-EGFP]
U3(EN)	pESC-URA	Ste2p[N-EGFP]305-431	empty
U4(BN)	pESC-URA	empty	Ste2p[C-EGFP]305-431
T6(EN)	pESC-TRP	Ste2p[N-mCherry]	empty
T7(BN)	pESC-TRP	empty	Ste2p[C-mCherry]
U12	pESC-URA	Ste2p[N-EGFP]	Ste2p[C-EGFP]
U34	pESC-URA	Ste2p[N-EGFP]305-431	Ste2p[C-EGFP]305-431
T67	pESC-TRP	Ste2p[N-mCherry]	Ste2p[C-mCherry]

Due to the failure of growth and expression from yeast cells in galactose medium, the medium was switched to another sugar source 1% raffinose with 1% galactose medium (Appendix A). Under these conditions cell growth and expression of Ste2p constructs from the plasmids was observed (Figures 3.15 – 18).

Unfortunately, yeast cells grow poorly in galactose medium broth. The expression of protein of interest from these vectors needs tedious strategies. Our Ste2p constructs originate from pBEC1 and pCL01 vectors, which are grown in glucose medium, hence studying the interaction of 3 or more proteins at the same time will eventually need a glucose medium. Furthermore, all the assays used throughout this study are optimized using glucose medium or plates. Taking into account all these limitations the galactose inducible Gal1-Gal10 promoter region on pESC vectors were switched with PGK1-TEF1 promoter region resulting in constitutively active expression vectors.

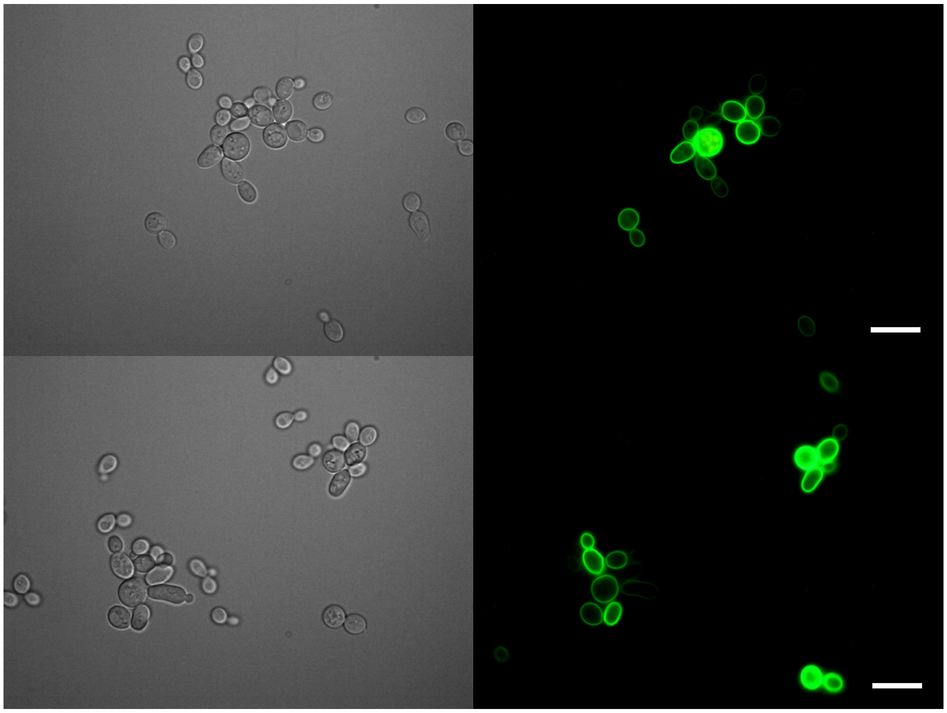

Figure 3.36 Bright field and fluorescent images of pESC-U12 vector, coexpression of Ste2p[N-EGFP] (1) and Ste2p[C-EGFP] (2), scale bars correspond 5 μm.

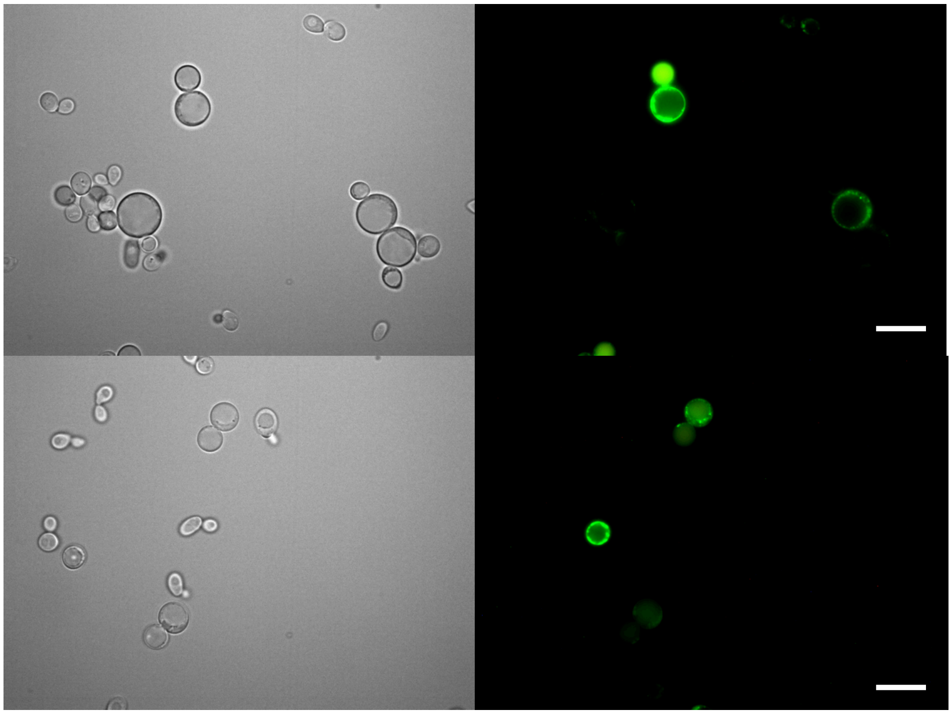

Figure 3.37 Bright field and fluorescent images of pESC-U43 vector, coexpression of Ste2p[N-EGFP]305-431 (3) and Ste2p[C-EGFP]305-431 (4), scale bars correspond 5 μm.

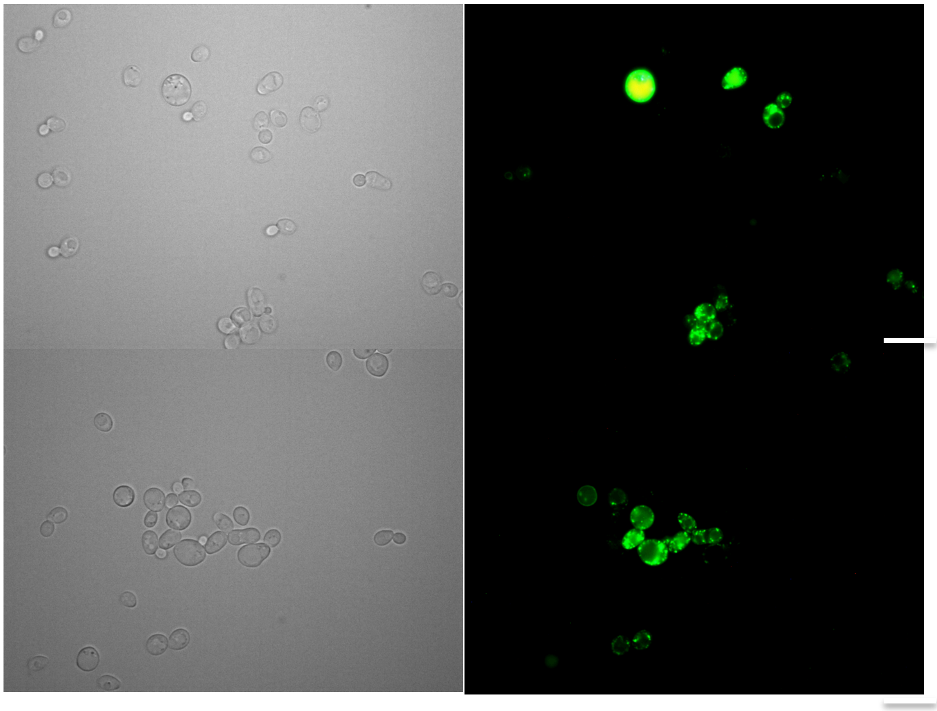

Figure 3.38 Bright field and fluorescent images of pESC-U23 vector, coexpression of Ste2p[C-EGFP] (2) and Ste2p[N-EGFP]305-431 (3), scale bars correspond 5 μm.

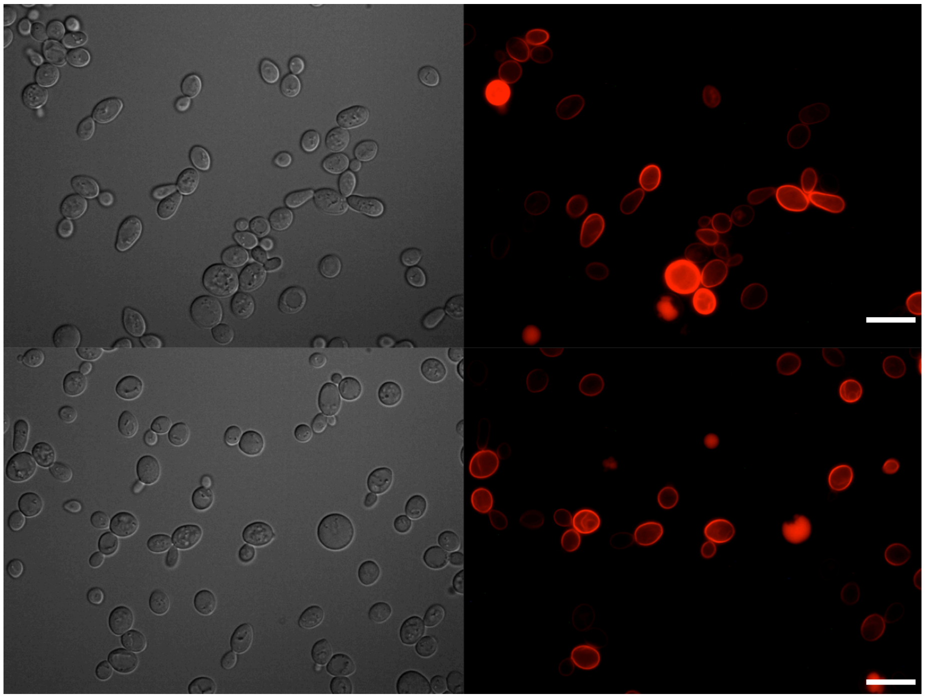

Figure 3.39 Bright field and fluorescent images of pESC-T67 vector, coexpression of Ste2p[N-mCherry] (6) and Ste2p[C-mCherry] (7), scale bars correspond 5 μm.

3.3.2 *Construction of constitutively active double promoter vectors*

For the coexpression of two or more proteins, Ste2p BiFC constructs; Ste2[N-EGFP] (pESC-U2), Ste2[C-EGFP] (pESC-U1), Ste2[N-EGFP]305-431 (pESC-U4), Ste2[C-EGFP]305-431 (pESC-U3); and Ste2[N-mCherry] (pESC-T7), Ste2[C-mCherry] (pESC-T6); were cloned into pESC-TRP and pESC-URA vectors. These double promoter vectors (Agilent Technologies, CA, USA) posses a Gal1 – Gal10 divergent promoter region at the upstream of the multiple cloning sites. These promoters induce protein expression in Galactose medium, while keeping the expression repressed in Glucose medium. Unfortunately, yeast cells grow poorly in Galactose medium broth and expression of protein of interest using galactose inducible promoters needs tedious procedures. All our previous constructs use constitutively active promoters on pBEC1 and pCL01 vectors, so Gal1 – Gal10 divergent promoter region of pESC vectors was decided to be switched with PGK1 – TEF1 promoter region.

This PGK1 – TEF1 divergent promoter region was amplified from pSP-G1 and pSP-G2 plasmids [172] (Figure 3.40).

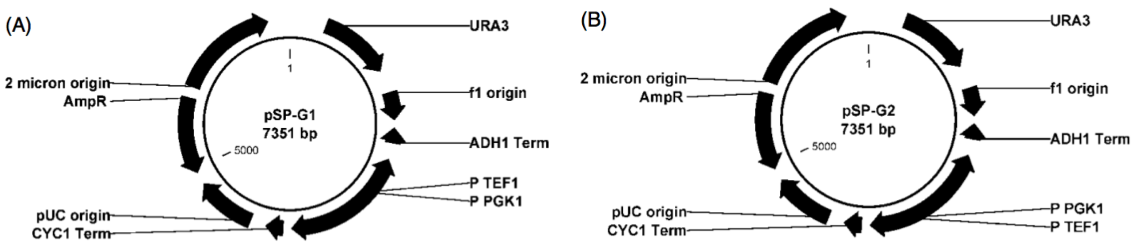
(A)
URA3
2 micron origin
AmpR
1
pSP-G1
7351 bp
5000
f1 origin
ADH1 Term
P TEF1
P PGK1
pUC origin
CYC1 Term
(B)
URA3
2 micron origin
AmpR
1
pSP-G2
7351 bp
5000
f1 origin
ADH1 Term
P PGK1
P TEF1
pUC origin
CYC1 Term

Figure 3.40 pSP-G1 (TEF1-PGK1) and pSP-G2 (PGK1-TEF1) vector maps.

So, the TEF1-PGK1 (G1) and PGK1-TEF1 (G2) promoter regions were amplified to carry EcoRI – BamHI sites on 5’ and 3’ termini respectively. The amplification of TEF1-PGK1 and PGK1-TEF1 regions from pSP-G1 and pSP-G2 were optimized using gradient PCR conditions at 5 different temperatures between 52 – 59 °C with and without addition of DMSO into the reaction mixture.

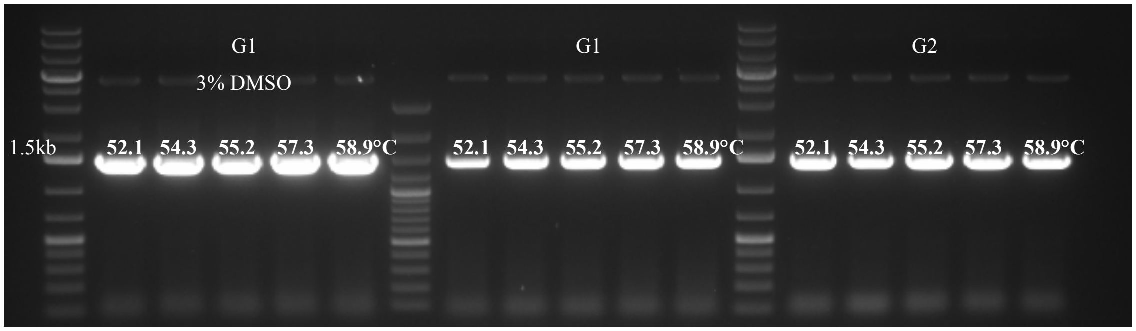
G1
3% DMSO
G1
G2
1.5kb
52.1
54.3
55.2
57.3
58.9°C
52.1
54.3
55.2
57.3
58.9°C
52.1
54.3
55.2
57.3
58.9°C

Figure 3.41 Agarose gel image of amplification product for PGK1-TEF1 and TEF1-PGK1 promoter region.

For the isolation of G1 and G2 sequences, PCR was upscaled to 50 µL using 55°C as annealing temperature. The reaction was purified with PCR purification kit and the product was left for digestion with EcoRI – BamHI restriction enzymes. Also, previously constructed pESC-URA based plasmid carrying Ste2p[N-EGFP] and Ste2p[C-EGFP] (pESC-U12); and pESC-TRP based plasmid carrying Ste2p[N-mCherry] and Ste2p[C-mCherry] (pESC-T67) were left for EcoRI – BamHI digestion. After the digestion, all 4 reactions were run and extracted from Low Melting Point Agarose Gel (1%) (Figure 3.42).

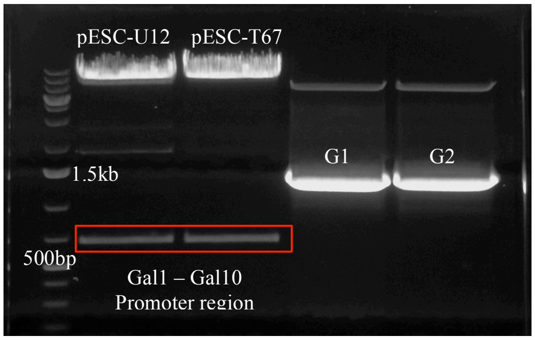
pESC-U12
pESC-T67
G1
G2
1.5kb
500bp
Gal1 – Gal10
Promoter region

Figure 3.42 Agarose gel image of EcoRI – BamHI digested U12 (Ste2p[N-EGFP], Ste2p[C-EGFP]), T67 (Ste2p[N-mCherry], Ste2p[C-mCherry]) constructs and PGK1 – TEF1 and TEF1 – PGK1 PCR products. The constitutively active double promoter region is right below 1.5 kb band as expected. Red box shows dropped Gal1 – Gal10 region.

Likewise, pESC-URA based plasmids, “U1” carrying Ste2[C-EGFP] on MCS1, “U2” carrying Ste2p[N-EGFP] on MCS2, pESC-TRP based plasmids, “U3” carrying Ste2[C-EGFP]305-431 on MCS1, “U4” carrying Ste2p[N-EGFP]305-431 on MCS2, pESC-TRP based plasmids “T6” carrying Ste2p[C-mCherry] on MCS1 and “T7” carrying Ste2p[N-mCherry] on its MCS2 were all digested with EcoRI – BamHI to drop the Gal1-Gal10 divergent promoter region. Figure 3.43 shows the agarose gel image of the digested vectors that are later extracted from gel.

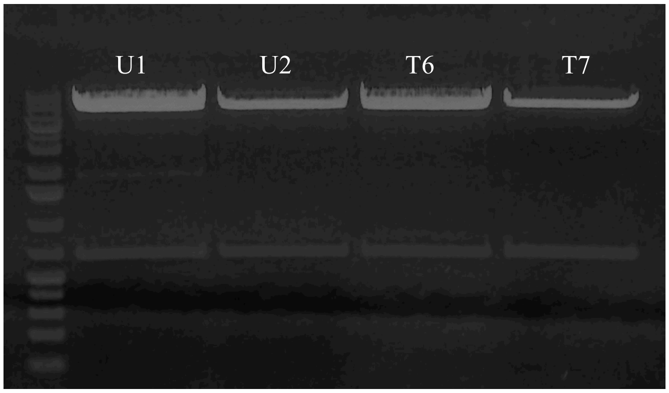

Figure 3.43 EcoRI-BamHI digestion of U1 (Ste2p[N-EGFP]), U2 (Ste2p[C-EGFP]), T6 (Ste2p[N-mCherry]), T7 (Ste2p[C-mCherry]) constructs to drop the Gal1-Gal10 promoter region.

All Ste2p BiFC constructs; U1, U2, U3, U4, T6, T7, U12, U34 and T67; were digested with EcoRI – BamHI enzymes to drop their Gal1 – Gal10 promoter region and were left for ligation with PGK1 – TEF1 or TEF1 – PGK1. Ligation reaction was directly used for transforming DH5α competent *E.coli*. Two-three colonies were picked from the LB plates with the appropriate antibiotic, grown overnight and the plasmids were isolated the following day. The plasmids were digested with appropriate restriction enzyme pair and digestion products were run on agarose gel to check the constructs carrying the correct insert size.

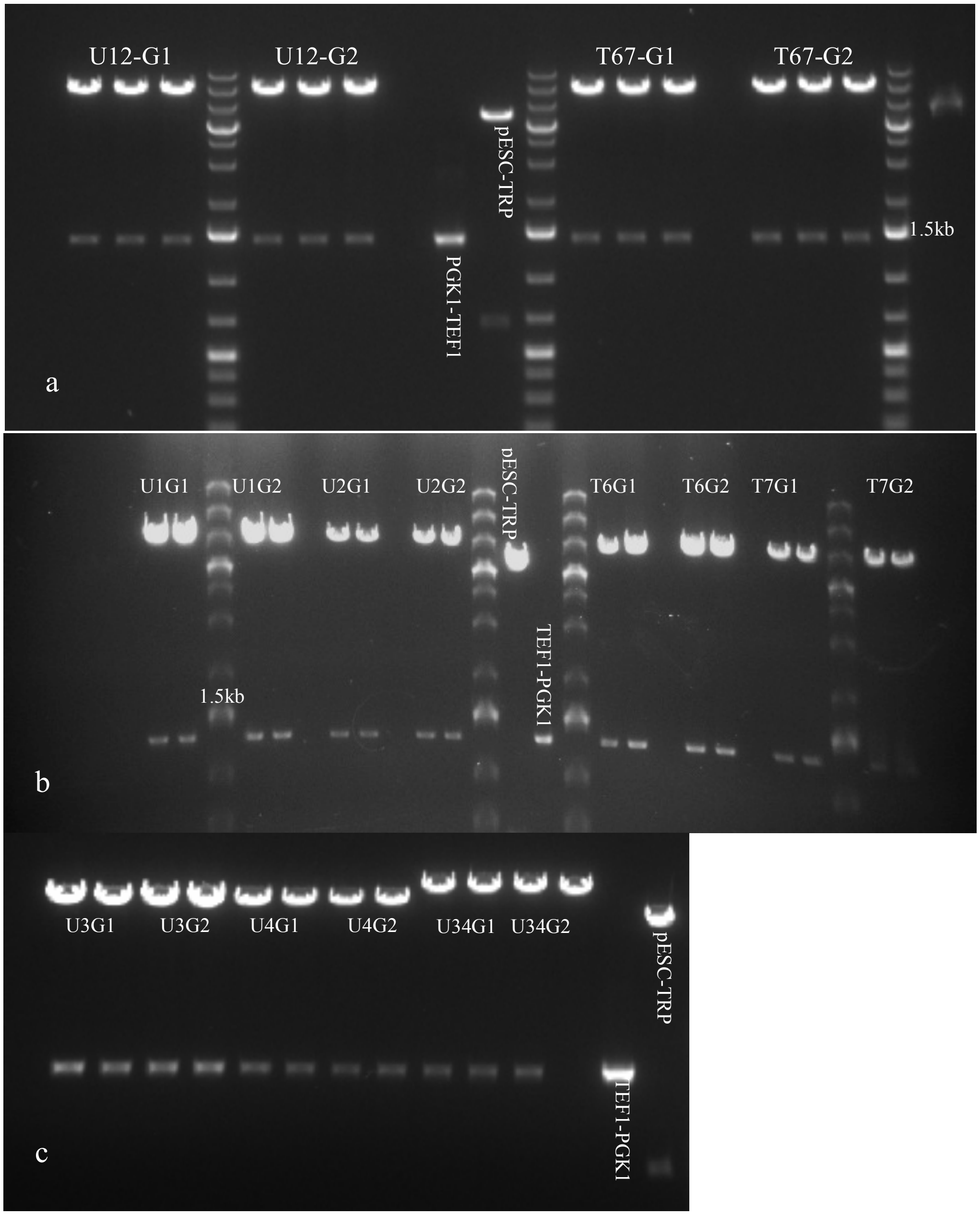
U12-G1
U12-G2
T67-G1
T67-G2
pESC-TRP
PGK1-TEF1
1.5kb
a
U1G1
U1G2
U2G1
U2G2
pESC-TRP
TEF1-PGK1
T6G1
T6G2
T7G1
T7G2
1.5kb
b
U3G1
U3G2
U4G1
U4G2
U34G1
U34G2
pESC-TRP
TEF1-PGK1
c

Figure 3.44 Agarose gel image of EcoRI – BamHI digestion control pESC-TRP and pESC-URA based constructs to verify correct TEF1-PGK1 (G1) or PGK1-TEF1 (G2) inserts. This new promoter region is expected around 1.5kb band, whereas the Gal1-Gal10 promoter region is approximately 670 base pairs. *(a)* pESC-URA based constructs carrying Ste2p[N-EGFP] (2) and Ste2p[C-EGFP] (1) at both MCS "U12" and pESC-TRP based constructs carrying Ste2p[N-mCherry] (7) and Ste2p[C-mCherry] (6) at both MCS "T67". (b) pESC-URA based constructs carrying Ste2p[N-EGFP] (2), Ste2p[C-EGFP] (1) at each MCS "U2" and "U1" and pESC-TRP based constructs carrying Ste2p[N-mCherry] (7), Ste2p[C-mCherry] (6) at each MCS "T7" and "T6". (c) pESC-URA based constructs carrying Ste2p[N-EGFP]305-431 (4), Ste2p[C-EGFP]305-431 (3) at each "U3" and "U4" or both "U34" MCS.

After the ligation of TEF1-PGK1 divergent promoter region, a preliminary imaging was done for U12 and T67 constructs and BiFC signal was observed from all transformants.

U12-G1 and U34-G1 constructs were also digested with NotI – NheI restriction enzymes to drop and also verify the size of whole MCS carrying both BiFC constructs; STE2[C-EGFP]-TEF1-PGK1-STE2[N-EGFP] and STE2[C-EGFP]305-431-TEF1-PGK1-STE2[N-EGFP]305-431 regions.

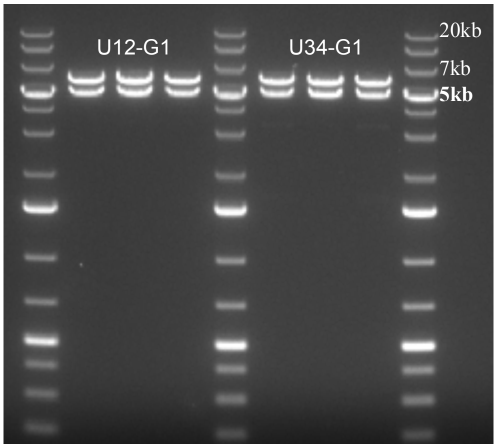

Figure 3.45 Agarose gel image for NotI – NheI digestion of U12G1 and U34G1 plasmids. The lower bands in first 3 lanes are STE2[C-EGFP]-TEF1-PGK1-STE2[N-EGFP] expected to show ≈ 5 kb DNA ladder band, upper bands are as expected ≈ 6kb. The lower bands in second 3 lanes group is STE2[C-EGFP]305-431-TEF1-PGK1-STE2[N-EGFP]305-431 construct again expected to show ≈ 5 kb DNA ladder band, likewise upper bands are as expected ≈ 6kb.

Using a similar cloning strategy, to create empty vectors Gal1 – Gal10 promoters on empty pESC-TRP and pESC-URA vectors were also switched with TEF1 – PGK1 (G1) PGK1 – TEF1 (G2) promoters.

Also, wild type Ste2p was amplified from pBEC1 plasmid to carry 5’ EcoRI – 3’ NotI and 5’ BamHI – 3’ NheI restriction sites and was cloned into both 1st and 2nd MCS of these new constitutively active double promoter vectors. These new empty vectors (TG1, TG2, UG1 and UG2) and constitutively active vectors expected to express wild type Ste2p were digested with restriction enzyme pairs and digestion products were run on agarose gel to check the inserts with correct size.

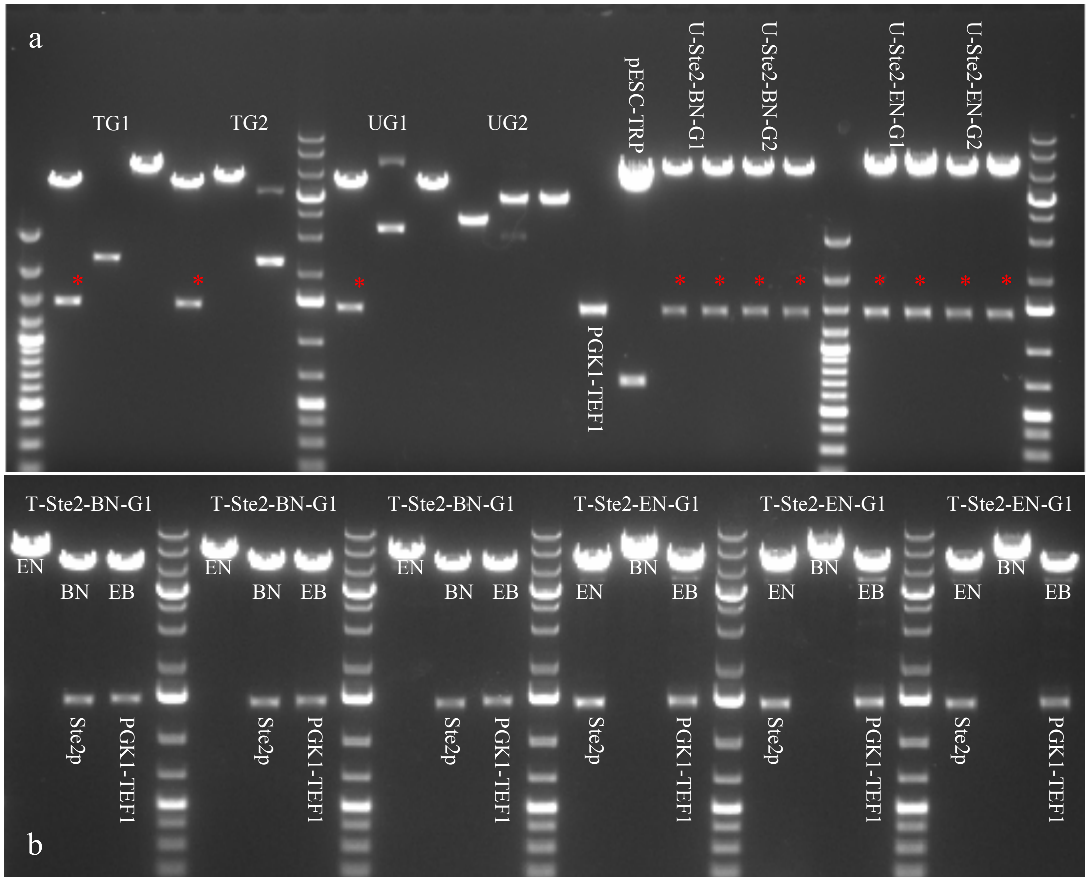
a
TG1
TG2
UG1
UG2
pESC-TRP
U-Ste2-BN-G1
U-Ste2-BN-G2
U-Ste2-EN-G1
U-Ste2-EN-G2
PGK1-TEF1
T-Ste2-BN-G1
T-Ste2-BN-G1
T-Ste2-BN-G1
T-Ste2-EN-G1
T-Ste2-EN-G1
T-Ste2-EN-G1
EN
BN
EB
Ste2p
PGK1-TEF1
b

Figure 3.46 Agarose gel image of constitutively active empty plasmids and constitutively active vectors carrying wild type Ste2p (a) EcoRI – BamHI digestion of constitutively active double promoter vectors with empty multiple cloning sites (TG1, TG2, UG1 and UG2) and constitutively active plasmids carrying wild type Ste2p in each MCS. The red asterix shows the correct TEF1 – PGK1 (G1) or PGK1 – TEF1 (G2) inserts as a band expected to be around 1.5kb ladder band. (b) Constitutively active plasmids originating from pESC-TRP plasmid carrying wild type Ste2p in each MCS. EcoRI – NotI (EN) band shows the insert at the 1st MCS, BamHI – NheI (BN) shows the insert at the 2nd MCS and EcoRI – BamHI (EB) shows the TEF1 – PGK1 or PGK1 – TEF1 promoter region.

As summary, new empty plasmids that carry constitutively active promoter region was constructed. Both EGFP and mCherry BiFC constructs were cloned into these new plasmids. Wild type Ste2 gene was cloned into these new plasmids to be used as the positive control during the biological assays. All constitutively active plasmids constructed in this part of study are given in Table 3.5.

Table 3.5 Constructed plasmids to study the interaction of 3 or more receptor. G1 stands for TEF1-PGK1 divergent promoter region, G2 stands for PGK1-TEF1 region.

Abbreviation	Plasmid	MCS1	MCS2
T-G1	pESC-TRP	empty	empty
T-G2	pESC-TRP	empty	empty
U-G1	pESC-URA	empty	empty
U-G2	pESC-URA	empty	empty
U-Ste2-EN-G1	pESC-URA	wild type Ste2p	empty
U-Ste2-BN-G1	pESC-URA	empty	wild type Ste2p
U-Ste2-EN-G2	pESC-URA	wild type Ste2p	empty
U-Ste2-BN-G2	pESC-URA	empty	wild type Ste2p
T-Ste2-EN-G1	pESC-TRP	wild type Ste2p	empty
T-Ste2-BN-G1	pESC-TRP	empty	wild type Ste2p
T-Ste2-EN-G2	pESC-TRP	wild type Ste2p	empty
T-Ste2-BN-G2	pESC-TRP	empty	wild type Ste2p
U1-G1	pESC-URA	Ste2p[N-EGFP]	empty
U1-G2	pESC-URA	Ste2p[N-EGFP]	empty
U2-G1	pESC-URA	empty	Ste2p[C-EGFP]
U2-G2	pESC-URA	empty	Ste2p[C-EGFP]
U3-G1	pESC-URA	Ste2p[N-EGFP] 305-431	empty
U3-G2	pESC-URA	Ste2p[N-EGFP] 305-431	empty
U4-G1	pESC-URA	empty	Ste2p[C-EGFP] 305-431
U4-G2	pESC-URA	empty	Ste2p[C-EGFP] 305-431
T6-G1	pESC-TRP	Ste2p[N-mCherry]	empty
T6-G2	pESC-TRP	Ste2p[N-mCherry]	empty
T7-G1	pESC-TRP	empty	Ste2p[C-mCherry]
T7-G2	pESC-TRP	empty	Ste2p[C-mCherry]
U12-G1	pESC-URA	Ste2p[N-EGFP]	Ste2p[C-EGFP]
U12-G2	pESC-URA	Ste2p[N-EGFP]	Ste2p[C-EGFP]
U34-G1	pESC-URA	Ste2p[N-EGFP] 305-431	Ste2p[C-EGFP] 305-431
U34-G2	pESC-URA	Ste2p[N-EGFP] 305-431	Ste2p[C-EGFP] 305-431
T67-G1	pESC-TRP	Ste2p[N-mCherry]	Ste2p[C-mCherry]
T67-G2	pESC-TRP	Ste2p[N-mCherry]	Ste2p[C-mCherry]

3.3.3 *Growth arrest assays of Ste2p constructs cloned into double promoter plasmids*

Pheromone induced growth arrest (Halo) assay was used to show that Ste2p constructs tagged with EGFP and mCherry fragments expressed from T-G1 and U-G1 plasmids are biologically functional. Halo assays were repeated at least three times for each of the plasmids and diameters of halos were plotted against logarithm of peptide concentration. The assay was quite reproducible as the variation in the inhibition zones was always within 2 mm for a given concentration.

DK102 cells expressing wild type Ste2p from T-G1 (TRP auxotrophic marker, TEF1 – PGK1 promoter region) and U-G1 (URA auxotrophic marker, TEF1 – PGK1 promoter region) plasmids were shown to respond to pheromone induced growth arrest assay. No halo was observed from the cells expressing empty constructs T-G1 and U-G1, whereas, a linear response of the halo size to the increasing concentration of α-factor was observed as shown in Figure 3.47.

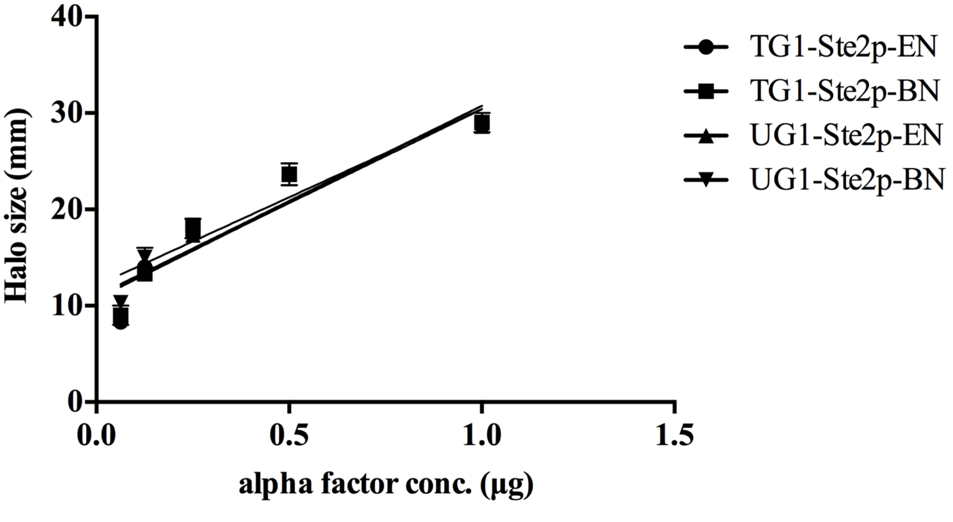

Figure 3.47 Biological assay of Ste2p constructs expressed from constitutively active double promoter plasmids. Wild-type Ste2p expressed from 1st MCS of TG1 plasmid (●), wild-type Ste2p expressed from 2nd MCS of TG1 plasmid (■), wild-type Ste2p expressed from 1st MCS of UG1 plasmid (▲), wild-type Ste2p expressed from 2nd MCS of UG1 plasmid (▼).

Wild type Ste2p were shown to be expressed at the cell surface and biologically functionally under control of TEF1 or PGK1 promoter, using T-G1 or U-G1 plasmids with different auxotrophies. All four constructs showed identical response to different concentrations of pheromone.

DK102 cells expressing C-terminally truncated Ste2p constructs; Ste2p[C-EGFP], Ste2p[N-EGFP], Ste2p[C-mCherry] and Ste2p[N-mCherry]; from either U-G1 or T-G1 plasmids were subjected to pheromone induced growth arrest assay (Figure 3.48).

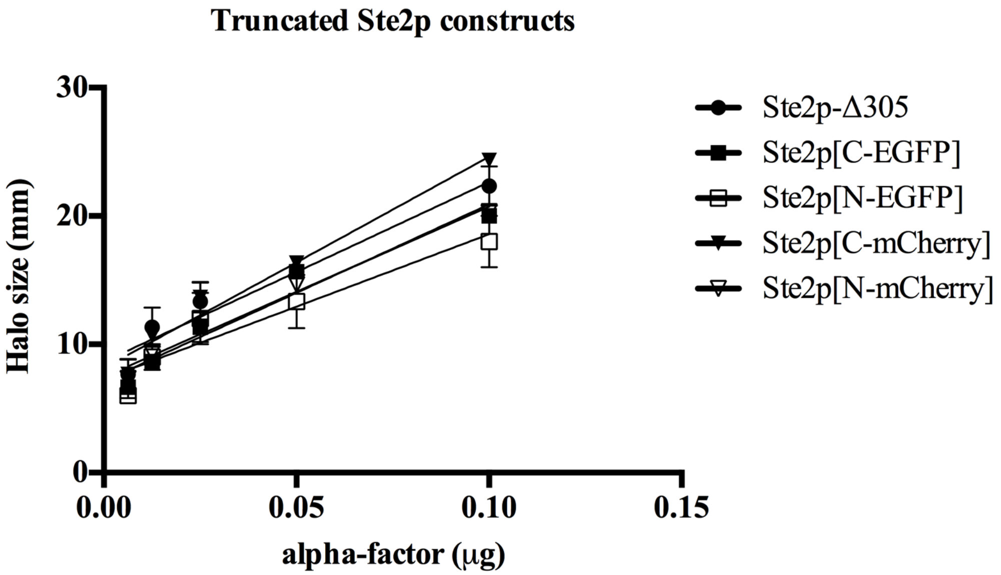

Figure 3.48 Biological assay of C-terminally truncated Ste2p constructs expressed from constitutively active double promoter plasmids. Ste2p-Δ305 expressed from 1st MCS of TG1 plasmid (●), Ste2p[C-EGFP] expressed from 1st MCS of UG1 plasmid (■), Ste2p[N-EGFP] expressed from 2nd MCS of UG1 plasmid (□), Ste2p[C-mCherry] expressed from 1st MCS of TG1 plasmid (▼), Ste2p[N-EGFP] expressed from 2nd MCS of UG1 plasmid (▽).

The results of halo assay showed that transformants expressing Ste2p-Δ305 and truncated receptors constructs, Ste2p[C-EGFP], Ste2p[N-EGFP], Ste2p[C-mCherry] and Ste2p[N-mCherry] (Figure 3.48) showed similar response to different concentrations of pheromone. Furthermore, as expected, all C-terminally truncated

Ste2p constructs were more responsive to pheromone-induced growth arrest, since they lack the down regulation domain found at the C-terminus of Ste2p receptor.

DK102 cells expressing Ste2p constructs with an intact C-terminus; Ste2p[C-EGFP]305-431, Ste2p[N-EGFP]305-431, from U-G1 plasmid were subjected to pheromone induced growth arrest assay (Figure 3.49).

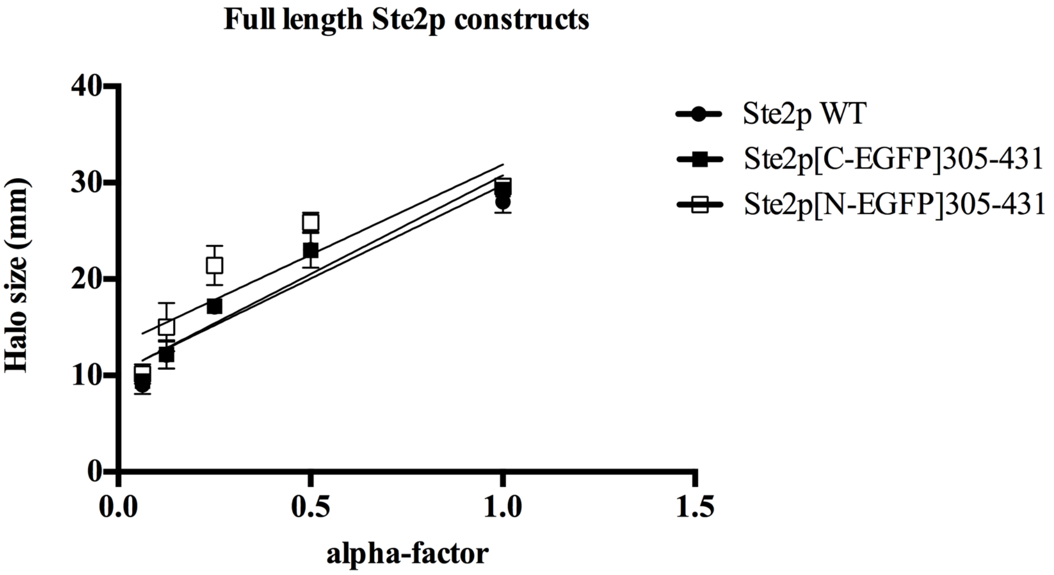

Figure 3.49 Biological assay of Ste2p constructs carrying an intact C-terminus expressed from constitutively active UG1 double promoter plasmids. Ste2p WT expressed from 1st MCS of UG1 plasmid (●), Ste2p[C-EGFP]305-431 expressed from 1st MCS of UG1 plasmid (■), Ste2p[N-EGFP]305-431 expressed from 2nd MCS of UG1 plasmid (□).

Ste2p constructs fused with EGFP fragments, inserted at position 304 were shown to be biologically active and responded to the pheromone quite similarly as DK102 cells expressing wild type Ste2p.

3.3.4 Western blot experiment of Ste2p constructs cloned into double promoter plasmid

These TEF1-PGK1 double promoter constructs were used in the transformation of BJS21 yeast strain. The transformant cells were harvested and proteins were resolved on SDS-PAGE. For the negative control 15µg of protein, for the positive controls 5µg of protein and for the BiFC constructs 15µg of protein were loaded on gel. The immunoblot was probed with affinity-purified antireceptor antiserum (1:15000) directed against the N-terminal domain of the Ste2p (Figure 3.59).

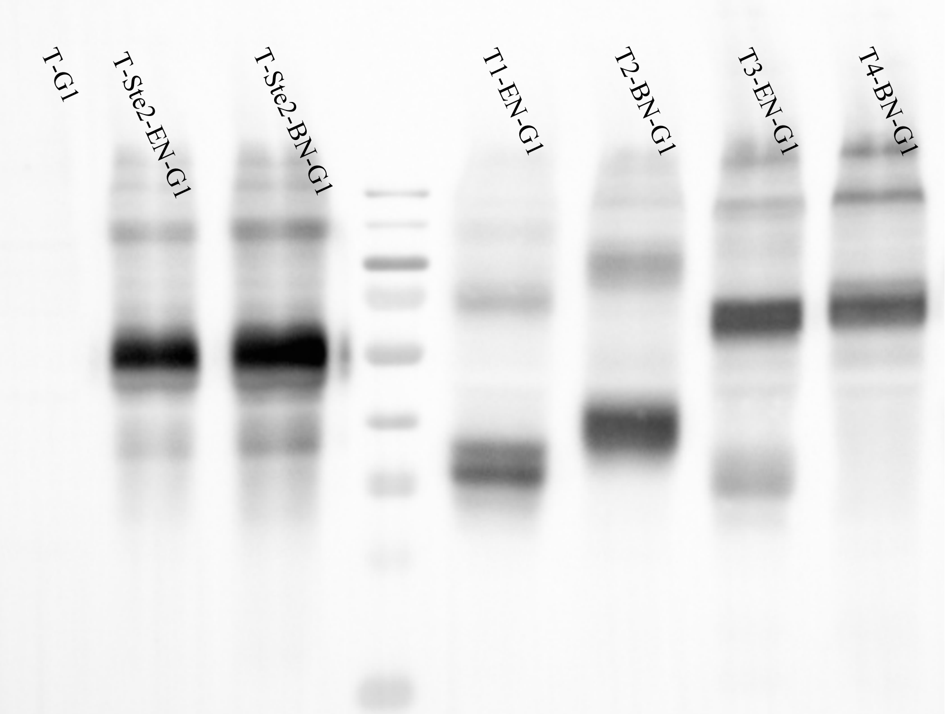

Figure 3.50 Western blot of the BJS21 cells expressing the constructs, the first lane is an extract of Ste2Δ cells expressing empty vector. The second lane is an extract of Ste2Δ cells expressing WT Ste2p receptor WT Ste2p (52 kDa) from the 1st MCS of T-G1 vector under TEF1 promoter. The third lane represents cells expressing WT Ste2p (52 kDa) from 2nd MCS of T-G1 vector under PGK1 promoter. Fourth lane is the protein marker. Fifth lane represents cells expressing Ste2p[C-EGFP] (calc. ≈42 kDa) under the control of TEF1. Sixth lane represents cells expressing Ste2p[N-EGFP] (calc. ≈51 kDa) under the control of PGK1 promoter. Seventh lane shows the transformants expressing Ste2p[C-EGFP]305-431 (calc. ≈57 kDa) from MCS1 of T-G1 vector, under the control of TEF1 promoter. Eight lane shows the transformants expressing Ste2p[N-EGFP]305-431 (calc. ≈66 kDa) from MCS2 of T-G1 vector, under the control of PGK1. The proteins from lanes 1 to 8 were detected with antireceptor antiserum directed against the N-terminal domain of the α-factor receptor.

Protein expression of all the constructs was determined by western blotting using the protease-deficient BJS21 (Figure 3.50). We used empty vector and cells expressing wild-type (WT) Ste2p as controls. Yeast cells were harvested and proteins were resolved by SDS-PAGE. The immunoblot was probed with affinity-purified antireceptor antiserum directed against the N-terminal domain of the Ste2p [178]. An extract of Ste2Δ cells transformed with empty vector showed no band. In Figure 3.50, the second and third lanes contains membranes from cells expressing WT Ste2p receptor; the multiple bands observed at approximately 52 kDa are due to different glycosylated forms of the receptor as shown previously [182 183]. Lanes five to eight show Ste2p[C-EGFP] (calc. M.W. 42 kDa), Ste2p[N-EGFP] (calc. M.W. 51 kDa), Ste2p[C-EGFP]305-431 (calc. M.W.57 kDa) and Ste2p[N-EGFP]305-431 (1-158) (calc. M.W. 66 kDa), respectively. The bands observed in the western blot for truncated Ste2p[C-EGFP] and Ste2p[N-EGFP were below the WT Ste2p receptor band in accordance with their calculated molecular weights. The bands with full-length Ste2p receptors Ste2p[C-EGFP]305-431 and Ste2p[N-EGFP]305-431 with the inserted EGFP fragments shown at lanes 7 and 8 were above the WT Ste2p band, according to the calculated molecular weights. The multiple bands were likely due to the various glycosylated forms of Ste2p. In all lanes, higher bands corresponding to a dimeric state of Ste2p was observed.

Figure 3.51 shows the Ste2p EGFP and mCherry BiFC constructs, and also the receptors tagged with full length EGFP and mCherry. The very first lane before protein size marker is the expression of WT Ste2p as a control. The third and forth lanes shows extracts of Ste2Δ cells expressing Ste2p[EGFP]305-431 (calc. M.W. 75 kDa) and Ste2p[EGFP] (calc. M.W. 60 kDa) from pBEC1 vector respectively. Lanes five to eight shows Ste2p EGFP and mCherry BiFC constructs. The ninth and tenth lanes shows extracts of Ste2Δ cells expressing Ste2p[mCherry] (calc. M.W. 60 kDa) and Ste2p[mCherry]305-431 (calc. M.W. 75 kDa) from pBEC1 vector respectively. The proteins from lanes 1 to 10 were detected with antireceptor antiserum directed against the N-terminal domain of the α-factor receptor, lanes 9 and 10 were also detected with mCherry antibody (16D7, Life Technologies, NY, USA).

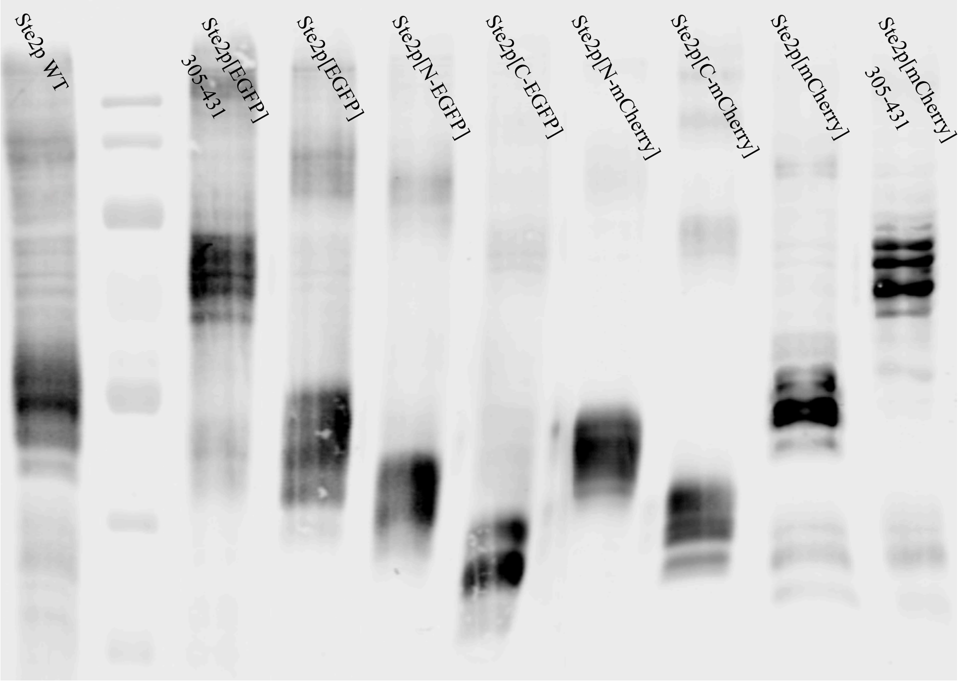

Figure 3.51 Western blot of the BJS21 cells expressing the constructs; the first lane is an extract of Ste2Δ cells expressing WT Ste2p receptor (52 kDa) from T-G1 vector. Second lane is the protein marker. The third lane represents cells expressing Ste2p[EGFP]305-431 (calc. ≈75 kDa) from pBEC1 vector. Forth lane represents cells expressing Ste2p[EGFP] (calc. ≈60 kDa) from pBEC1 plasmid. Fifth lane represents cells expressing Ste2p[N-EGFP] (calc. ≈51 kDa) from TG1 vector. Sixth lane shows the transformants expressing Ste2p[C-EGFP] (calc. ≈42 kDa) from T-G1 vector. Seventh lane represents cells expressing Ste2p[N-mCherry] (calc. ≈51 kDa) from TG1 vector. Eight lane shows the transformants expressing Ste2p[C-mCherry] (calc. ≈42 kDa) from T-G1 vector. Ninth lane shows the transformants expressing Ste2p[mCherry] (calc. ≈60 kDa) from pBEC1 plasmid. Tenth lane shows the transformants expressing Ste2p[mCherry]305-431 (calc. ≈75 kDa) from pBEC1 plasmid. The proteins from lanes 1 to 10 were detected with antireceptor antiserum directed against the N-terminal domain of the α-factor receptor; lanes 9 and 10 were also detected with mCherry antibody (16D7, Life Technologies, NY, USA).

As a summary, T-G1 and U-G1 plasmids were shown to functionally express wild type Ste2p, using pheromone induced growth arrest assay and these proteins were also resolved on SDS-PAGE. Then, the Ste2p constructs tagged with EGFP and mCherry fragments were shown to be biologically functional using pheromone induced growth arrest assay and also was shown to be correctly expressed by resolving these proteins on SDS-PAGE.

3.4 Imaging of higher Ste2p oligomers

3.4.1 Detection of oligomerization taking advantage of endocytosis

Examination of truncated (at the 304th residue) and full-length receptors using variety of techniques showed that Ste2p receptors dimerize mainly on the cell membrane and that the full-length receptor can be internalized as a dimer with a truncated receptor.

In our study, when full length / truncated receptor pair was co-expressed, the reconstituted EGFP signal was observed both on the plasma membrane and intracellularly (Figure 3.29a, 3.29b) in contrast to the signal which was only observed on the plasma membrane from the cells co-expressing truncated / truncated (Ste2p[N-EGFP] / Ste2[C-EGFP]) pair (Figure 3.28). These results suggest that full length receptors act in a dominant-positive manner for internalization of endocytosis deficient C-terminally truncated Ste2p. This effect was noted previously when expressing two receptors, one deficient in endocytosis and other being proficient [64].

Having shown the nature of the internal signal for the BiFC dimers, we raised the question "whether WT Ste2p act in a dominant-positive manner for internalization of a truncated BiFC pair?" For this we transformed DK102 cells with U12-G1 (Ste2p[N-EGFP] / Ste2p[C-EGFP], Table 3.5) and pBEC1 (WT Ste2p).

The fluorescence signal observed in Figure 3.52 shows the dimerization of truncated Ste2p[N-EGFP] and truncated Ste2p[C-EGFP] at the cell membrane. The fluorescence signal observed in the next image Figure 3.53 shows the cells expressing truncated Ste2p[N-EGFP], truncated Ste2p[C-EGFP] and WT Ste2p.

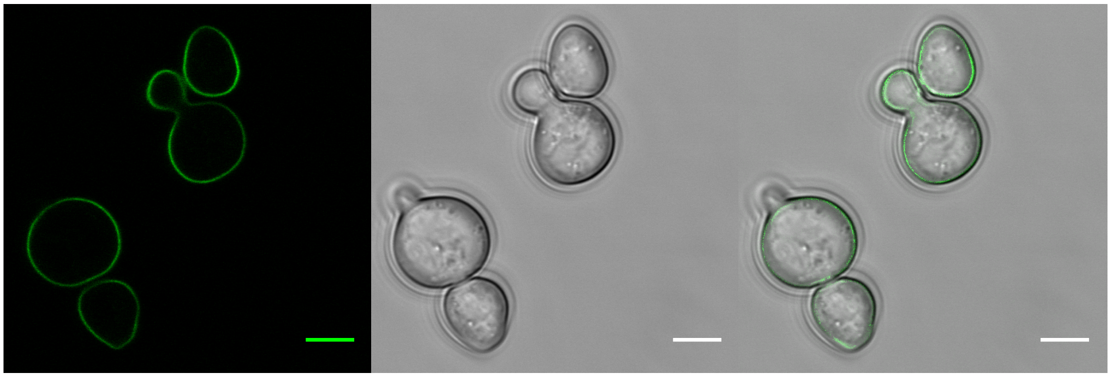

Figure 3.52 Cells co-expressing Ste2p[N-EGFP] / Ste2p[C-EGFP]; C-terminally truncated receptor tagged with either N-EGFP (1-158) or C-EGFP (159-238) attached to position 304, scale bars correspond 5 μm.

The dimerization signal of the cells co-expressing Ste2p[N-EGFP] and Ste2p[C-EGFP] was only observed on the plasma membrane and there was no detectable intracellular BiFC signal (Figures 3.52, 3.28).

Previously, with comparing the fluorescence signal distribution of cells co-expressing Ste2p[N-EGFP]305-431 / Ste2p[C-EGFP]305-431 (Figure 3.26) and cells co-expressing Ste2p[N-EGFP] / Ste2p[C-EGFP] (Figures 3.28, 3.52) we have shown that the fluorescence signal observed intracellularly (Figure 3.26) was dependent on endocytosis of full-length receptors with an intact C-terminal domain.

Furthermore, when full length / truncated receptor pair was co-expressed, the reconstituted EGFP signal was observed both on the plasma membrane and intracellularly (Figure 3.29a, 3.29b) in contrast to the signal which was only observed on the plasma membrane from the cells co-expressing truncated / truncated (Ste2p[N-EGFP] / Ste2[C-EGFP]) pair (Figures 3.28, 3.52).

Similarly, intracellular puncta resembling endocytotic vesicles, was observed in the cells co-expressing C-terminally truncated Ste2p BiFC pair; Ste2p[N-EGFP] /

Ste2p[C-EGFP] and Ste2p WT (Figure 3.53), suggesting the Ste2p WT is pulling down the dimer to the endocytotic pathway.

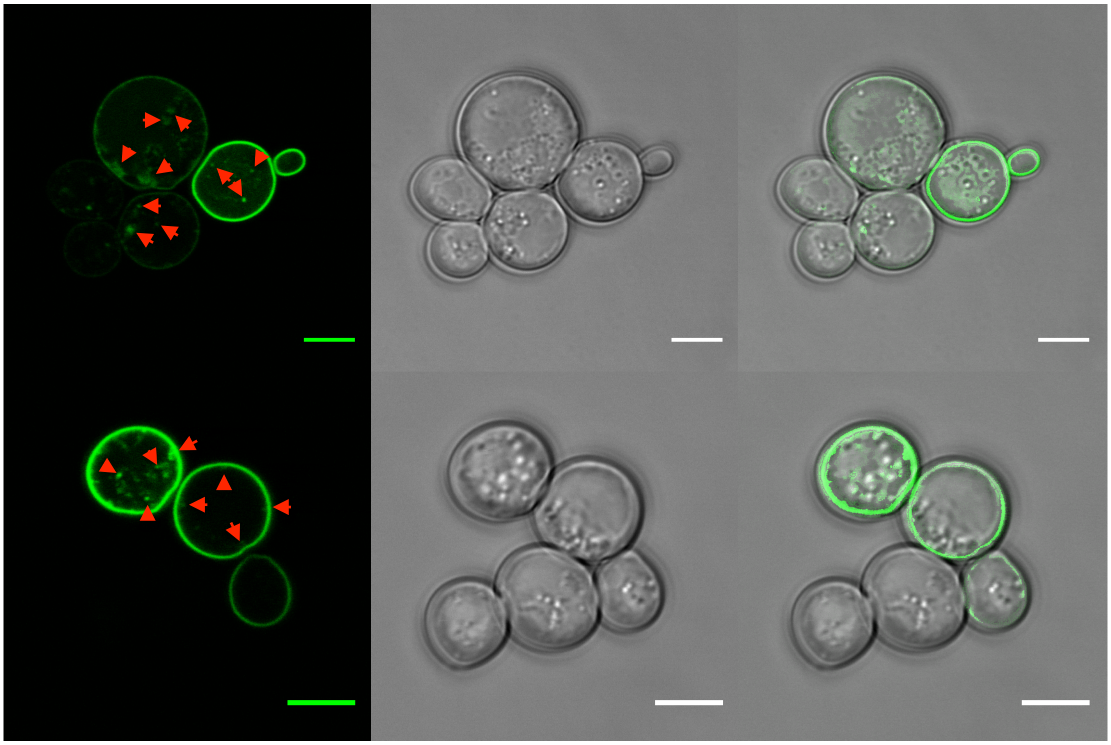

Figure 3.53 Cells co-expressing three Ste2p constructs; WT Ste2p and C-terminally truncated BiFC pair; Ste2p WT / Ste2p[N-EGFP] / Ste2p[C-EGFP]; the red arrows show endocytotic vesicles at intracellular region, scale bars correspond 5 µm length.

It was shown previously that Ste2p tagged with GFP localize to endocytic compartments in the absence of ligand, hence can be used to track endocytosis pathway [191]. So, we decided to use Ste2p[mCherry]305-431, to track the endocytosis of C-terminally truncated BiFC pair with colocalization experiments. Our hypothesis was if Ste2p is internalizing as three or more receptor oligomers, we should be able to observe colocalized intracellular puncta both at 488 nm (EGFP, green channel) and 543 nm (mCherry, red channel) excitation. So, we transformed DK102 cells to express Ste2p[mCherry]305-431 / Ste2p[N-EGFP] / Ste2p[C-EGFP] (Figure 3.54).

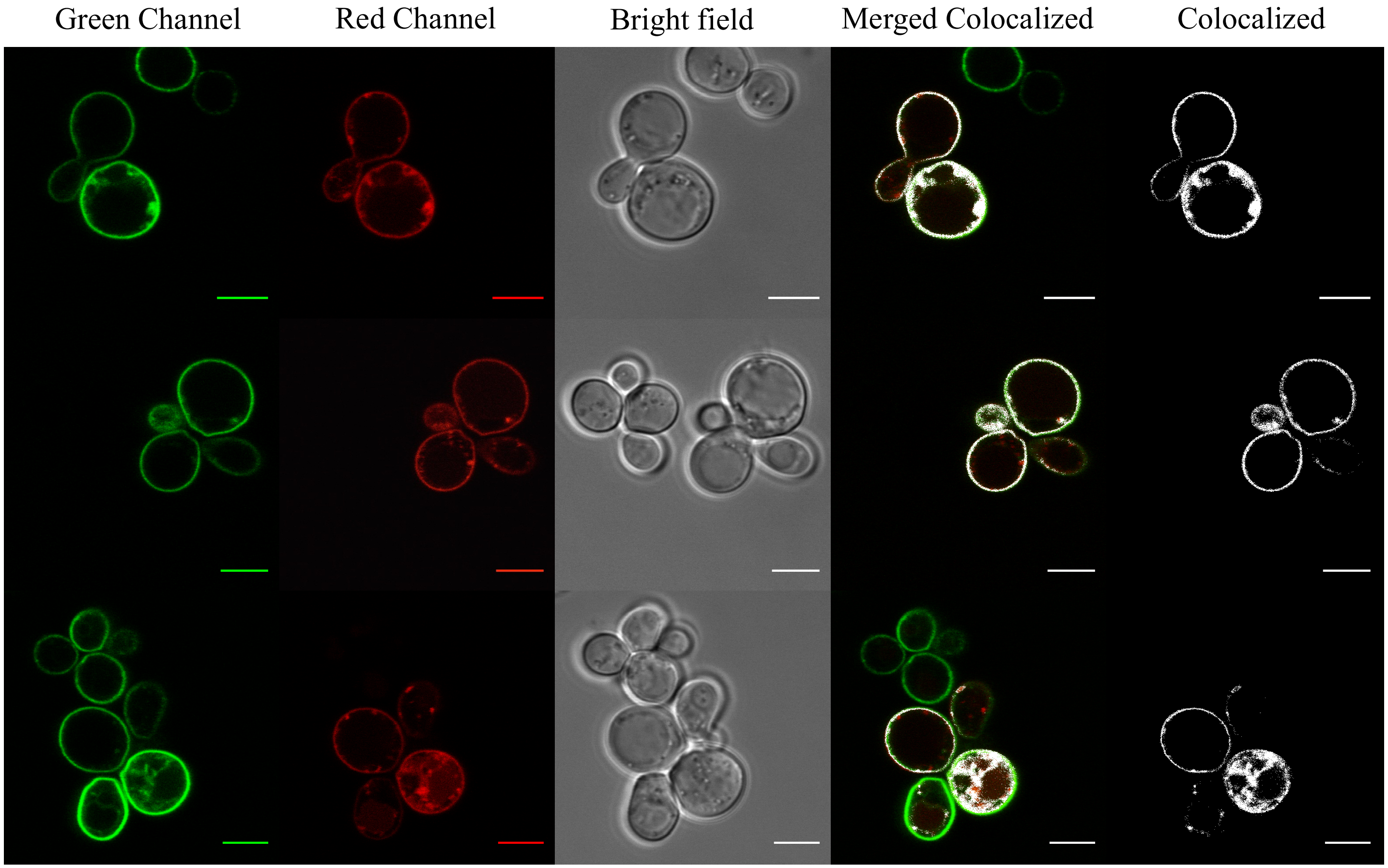
Green Channel
Red Channel
Bright field
Merged Colocalized
Colocalized

Figure 3.54 Cells co-expressing three Ste2p constructs; Ste2p[mCherry]305-431 and C-terminally truncated BiFC pair; Ste2p[N-EGFP] / Ste2p[C-EGFP]. Images from left to right shows cells excited with 488 nm laser (green channel), cells excited with 543 nm laser (red channel), bright field image, merged channels colocalized image (RGB) and colocalized image showing colocalization of signals from green and red channels. Scale bars correspond 5 μm length.

In figure 3.54, green channel shows the reconstituted EGFP signal as a result of the dimerization of C-terminally truncated Ste2p[N-EGFP] / Ste2p[C-EGFP] pair. These receptors lacking a major endocytosis signal sequence found on the C-tail [187] would be expected to stay as dimers only on the plasma membrane as shown previously (Figures 3.28, 3.52), yet the fluorescence signal was observed both on the plasma membrane and intracellularly resembling endocytotic vesicles. Red channel shows the fluorescence signal from monomeric Ste2p[mCherry]305-431 receptor, which was also observed both on the plasma membrane and intracellularly as expected. When green channel and red channel was merged, it was found out that the truncated BiFC pair; Ste2p[N-EGFP] and Ste2p[C-EGFP]; and Ste2p[mCherry]305-431 were colocalized both on the plasma membrane and also intracellularly resembling the endocytotic vesicles.

These results (Figures 3.53, 3.54) suggests that full length receptors act in a dominant-positive manner for internalization of not only as a dimer with another endocytosis deficient C-terminally truncated Ste2p, but the model GPCR Ste2p rather internalizes as an oligomeric state constituted of at least three receptors.

3.4.2 Detection of oligomerization using sensitized emission

Sensitized emission is the direct way of measuring FRET efficiency. In this method the donor fluorophore is excited and the emission signal is collected using a filter passing the light at acceptor emission region. Therefore, the collected signal is as a result of emission from the acceptor through a non-radiative energy transfer/excitation from the donor. For FRET analysis three sets of images are collected from the cells coexpressing both the donor and acceptor fluorophores. In the first image, the donor is excited and the emission is collected using filter set for the acceptor emission spectrum, which can be called FRET image. In the second image, the donor fluorophore is excited and the detection is done using filter detecting the donor emission, called donor image. Finally in the third image, acceptor fluorophore is excited and emission is detected using filter passing acceptor emission wavelength, called acceptor image. Two different sets of images are collected from cell expressing only the donor and only the acceptor. For the cells expressing only donor fluorophore, two images are collected, first image is collected using FRET settings and the second image is collected using donor settings (Figure 3.55a). From the cells expressing only the acceptor fluorophore, two images are collected, one at the FRET settings and the second at the acceptor settings (Figure 3.55b). These images are used for bleed-through for the calculations. Representative images for calculating FRET efficiency using sensitized emission is given in figure 3.56.

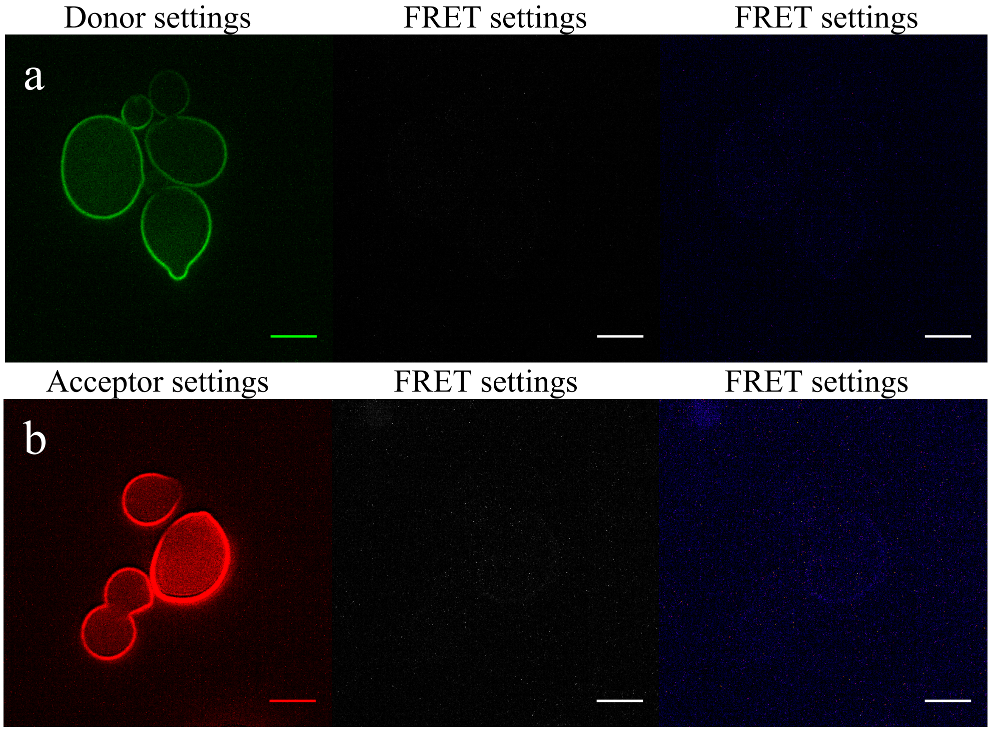

Figure 3.55 First image in both rows was taken at either donor (a) or acceptor (b) settings, the second image corresponds to FRET settings and finally the third image is the FRET image shown in “fire” settings under lookup tables in imageJ software for better visualization of bleed through (a) Yeast cells expressing only the donor; EGFP BiFC Ste2p pair (b) cells expressing only the acceptor; mCherry BiFC Ste2p pair. Scale bars correspond to 5 μm length.

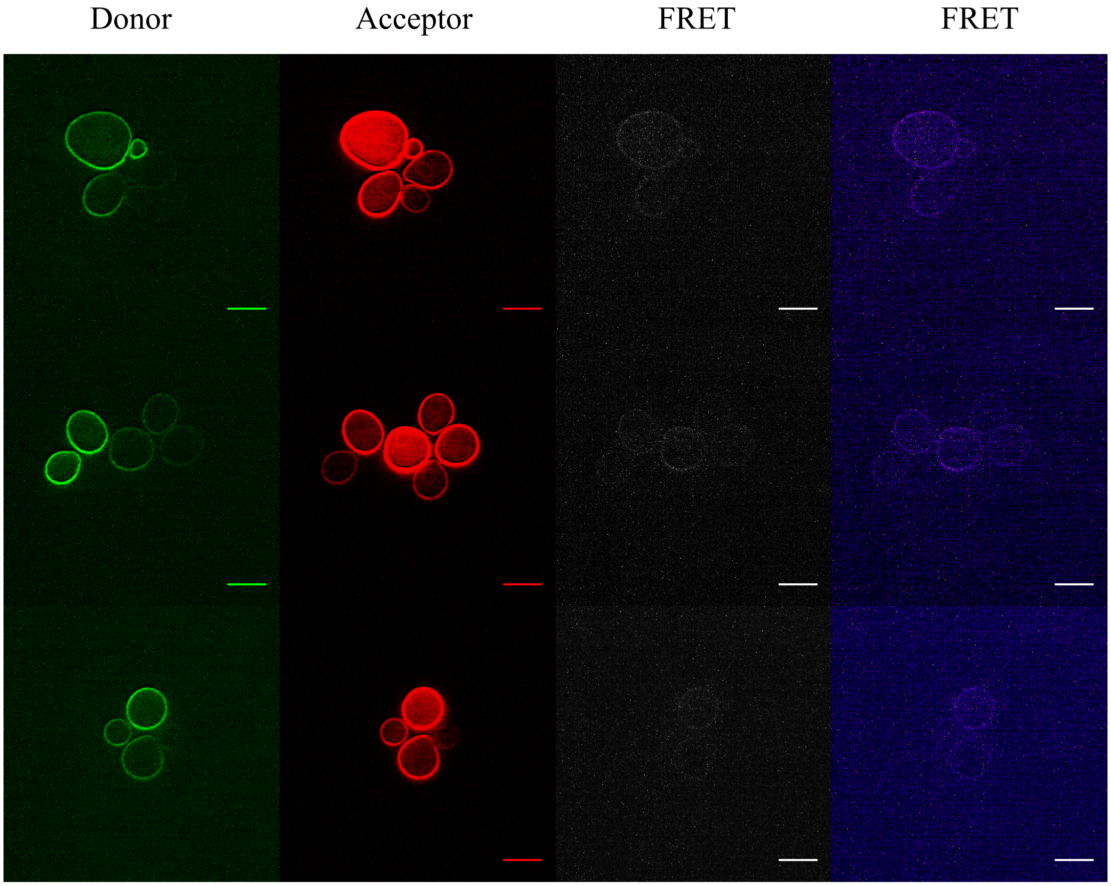

Figure 3.56 FRET image acquisition from cells coexpressing Ste2p EGFP BiFC pair and Ste2p mCherry BiFC pair. First column of images represent donor settings, second column represents acceptor settings, third column represents FRET settings, the fourth columns is “fire” representation of FRET image for better visualization of pixels. Scale bars correspond to 5 μm length.

3.4.3 Detection of oligomerization using acceptor photobleaching

The acceptor photobleaching fluorescence resonance energy transfer (FRET) method is widely used for monitoring molecular interactions in cells. This method of FRET, the efficiency relies on the donor signal ratio before and after the photobleaching of the acceptor. In the experimental setup, EGFP signal was collected using 488 nm led light and mCherry signal was collected using 590 nm led light. For acceptor photobleaching method, four sets of images were collected. In the first image, EGFP was excited at 488 nm light with 20% led power, in the second image mCherry was excited using 590 nm light with 20% led power, then for photobleaching the cells were irradiated for 2 minutes with 100% led power with 590 nm light. The third image was collected at 488 nm light again with 20% led power, this image is donor image after acceptor photobleaching and the acceptor image was collected as a forth image at 590 nm wavelength with 20% led power (Figure 3.56).

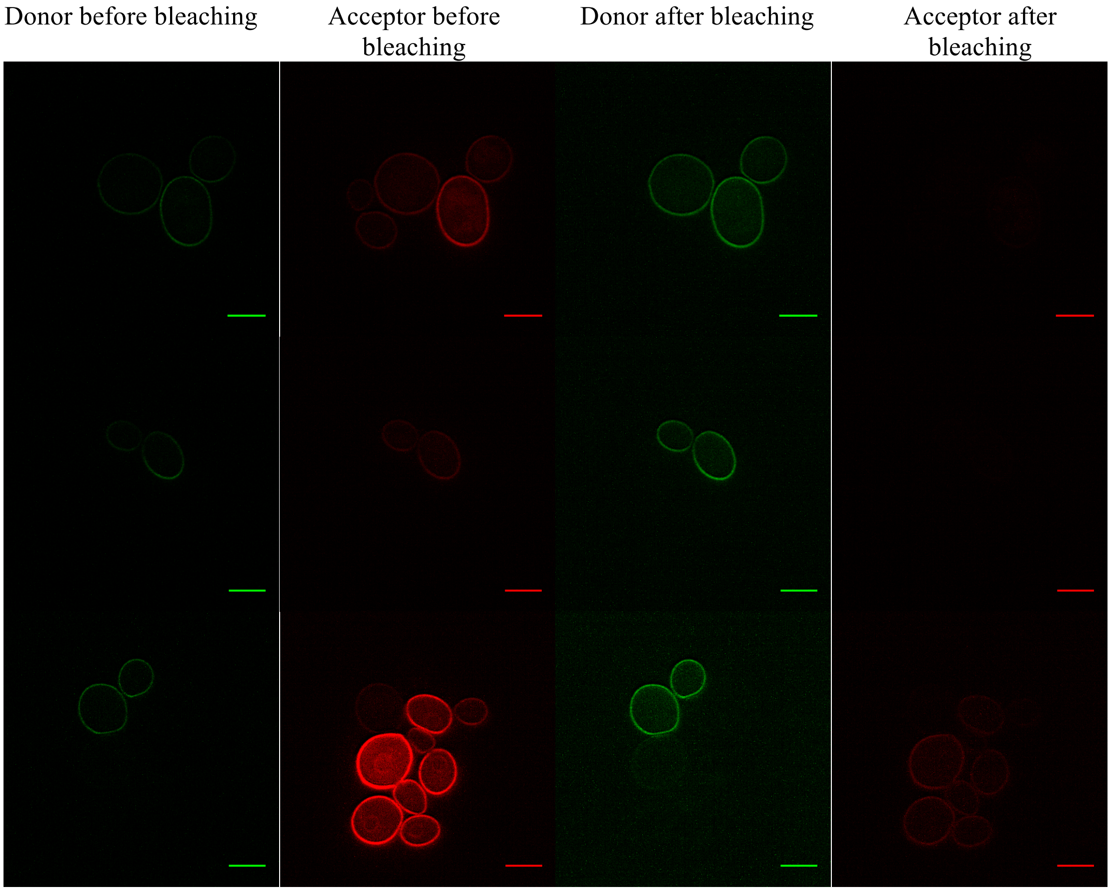

Figure 3.57 FRET data acquisition for acceptor photobleaching. First column shows donor signal before acceptor photobleaching; second column shows acceptor signal before photobleaching; third column shows donor after acceptor photobleaching, the forth column shows acceptor after bleaching. Scale bars correspond to 5 µm length.

Acceptor images collected before and after will be used during the calculation of FRET efficiency, for correction due to the possible partial bleaching and to correct the channel crosstalk. The preliminary data suggested that acceptor was almost completely bleached and there is an increase in the donor intensity after the photobleaching of the acceptor.

3.5 Conclusion to the second part

The second aim of this study was to determine whether the model GPCR interacts only as a homodimer or as higher homooligomeric structures with 3 or more proteins *in vivo*. For this, we used bimolecular fluorescence complementation (BiFC) assay with Ste2p incorporating split EGFP and split mCherry fragments, signal colocalization and Förster resonance energy transfer with confocal laser microscopy. All the constructs were verified by sequencing, and the Ste2p receptors labeled with EGFP, mCherry, EGFP or mCherry fragments were shown to be biologically active.

We showed that dimers of truncated Ste2p were resident on the plasma membrane but in the presence of a WT Ste2p, fluorescent puncta presumed to represent endocytic vesicles containing Ste2p BiFC dimer and a WT Ste2p were observed intracellularly in yeast cells, therefore indicating the interaction of at least 3 receptors.

Previously Ste2p receptor tagged with a fluorescent marker was shown to follow endocytic pathway. Three Ste2p constructs; EGFP BiFC dimer and a receptor tagged with mCherry were coexpressed in live cells to visualize the full-length receptor endocytosis. Ste2p with an intact C-tail tagged with mCherry was shown to switch on the endocytotic pathway for truncated receptor dimer; observed as colocalized puncta both in green and red channels intracellularly resembling endocytic vesicles. These results indicated that receptors interact at least as a 3 or more receptor oligomeric complex.

To study whether 4 receptors interact as a tetrameric complex, four Ste2p constructs were coexpressed in live cells; Ste2p EGFP BiFC pair and Ste2p mCherry BiFC pair. The reconstituted EGFP and mCherry signals were observed as colocalized signals on the plasma membrane, and signal was also observed in the FRET filter upon excitation of the donor. Furthermore, in the preliminary acceptor photobleaching data, number of pixels was significantly increased in the donor channel as a result of the photobleaching of acceptor, strongly suggesting that Ste2p interaction is at least as a tetrameric protein complex.

REFERENCES

[1] Gurevich, V. V., and Gurevich, E. V. (2008) GPCR monomers and oligomers: it takes all kinds, *Trends in neurosciences 31*, 74-81.

[2] McCudden, C. R., Hains, M. D., Kimple, R. J., Siderovski, D. P., and Willard, F. S. (2005) G-protein signaling: back to the future, *Cell Mol Life Sci 62*, 551-577.

[3] Gonzalez-Maeso, J. (2011) GPCR oligomers in pharmacology and signaling, *Molecular brain 4*, 20.

[4] Vilardaga, J. P., Agnati, L. F., Fuxe, K., and Ciruela, F. (2010) G-protein-coupled receptor heteromer dynamics, *J Cell Sci 123*, 4215-4220.

[5] Bunemann, M., Frank, M., and Lohse, M. J. (2003) Gi protein activation in intact cells involves subunit rearrangement rather than dissociation, *Proceedings of the National Academy of Sciences of the United States of America 100*, 16077-16082.

[6] Dohlman, H. G., and Thorner, J. W. (2001) Regulation of G protein-initiated signal transduction in yeast: paradigms and principles, *Annual review of biochemistry 70*, 703-754.

[7] Hall, R. A., Premont, R. T., and Lefkowitz, R. J. (1999) Heptahelical receptor signaling: beyond the G protein paradigm, *The Journal of cell biology 145*, 927-932.

[8] Neer, E. J. (1995) Heterotrimeric G proteins: organizers of transmembrane signals, *Cell 80*, 249-257.

[9] Offermanns, S. (2000) Mammalian G-protein function in vivo: new insights through altered gene expression, *Rev Physiol Biochem Pharmacol 140*, 63-133.

[10] Meigs, T. E., Fields, T. A., McKee, D. D., and Casey, P. J. (2001) Interaction of Galpha 12 and Galpha 13 with the cytoplasmic domain of cadherin provides a mechanism for beta -catenin release, *Proceedings of the National Academy of Sciences of the United States of America 98*, 519-524.

[11] Dohlman, H. G., and Thorner, J. (1997) RGS proteins and signaling by heterotrimeric G proteins, *The Journal of biological chemistry 272*, 3871-3874.

[12] Ross, E. M., and Wilkie, T. M. (2000) GTPase-activating proteins for heterotrimeric G proteins: regulators of G protein signaling (RGS) and RGS-like proteins, *Annual review of biochemistry 69*, 795-827.

[13] Burchett, S. A. (2000) Regulators of G protein signaling: a bestiary of modular protein binding domains, *J Neurochem 75*, 1335-1351.

[14] Fredriksson, R., and Schioth, H. B. (2005) The repertoire of G-protein-coupled receptors in fully sequenced genomes, *Molecular pharmacology 67*, 1414-1425.

[15] Whiteway, M., Hougan, L., Dignard, D., Thomas, D. Y., Bell, L., Saari, G. C., Grant, F. J., O'Hara, P., and MacKay, V. L. (1989) The STE4 and STE18 genes of yeast encode potential beta and gamma subunits of the mating factor receptor-coupled G protein, *Cell 56*, 467-477.

[16] Zhou, Z., Gartner, A., Cade, R., Ammerer, G., and Errede, B. (1993) Pheromone-induced signal transduction in Saccharomyces cerevisiae requires the sequential function of three protein kinases, *Molecular and cellular biology 13*, 2069-2080.

[17] Choi, K. Y., Satterberg, B., Lyons, D. M., and Elion, E. A. (1994) Ste5 tethers multiple protein kinases in the MAP kinase cascade required for mating in S. cerevisiae, *Cell 78*, 499-512.

[18] Dohlman, H. G., Apaniesk, D., Chen, Y., Song, J., and Nusskern, D. (1995) Inhibition of G-protein signaling by dominant gain-of-function mutations in Sst2p, a pheromone desensitization factor in Saccharomyces cerevisiae, *Molecular and cellular biology 15*, 3635-3643.

[19] Hicke, L., and Riezman, H. (1996) Ubiquitination of a yeast plasma membrane receptor signals its ligand-stimulated endocytosis, *Cell 84*, 277-287.

[20] Roth, A. F., and Davis, N. G. (1996) Ubiquitination of the yeast a-factor receptor, *The Journal of cell biology 134*, 661-674.

[21] Pausch, M. H. (1997) G-protein-coupled receptors in Saccharomyces cerevisiae: high-throughput screening assays for drug discovery, *Trends in biotechnology 15*, 487-494.

[22] Wang, Y., and Dohlman, H. G. (2004) Pheromone signaling mechanisms in yeast: a prototypical sex machine, *Science 306*, 1508-1509.

[23] Ozawa, A., Lindberg, I., Roth, B., and Kroeze, W. K. (2010) Deorphanization of novel peptides and their receptors, *The AAPS journal 12*, 378-384.

[24] Winzeler, E. A., Shoemaker, D. D., Astromoff, A., Liang, H., Anderson, K., Andre, B., Bangham, R., Benito, R., Boeke, J. D., Bussey, H., Chu, A. M., Connelly, C., Davis, K., Dietrich, F., Dow, S. W., El Bakkoury, M., Foury, F., Friend, S. H., Gentalen, E., Giaever, G., Hegemann, J. H., Jones, T., Laub, M., Liao, H., Liebundguth, N., Lockhart, D. J., Lucau-Danila, A., Lussier, M., M'Rabet, N., Menard, P., Mittmann, M., Pai, C., Rebischung, C., Revuelta, J. L., Riles, L., Roberts, C. J., Ross-MacDonald, P., Scherens, B., Snyder, M., Sookhai-Mahadeo, S., Storms, R. K., Veronneau, S., Voet, M., Volckaert, G., Ward, T. R., Wysocki, R., Yen, G. S., Yu, K., Zimmermann, K., Philippsen, P., Johnston, M., and Davis, R. W. (1999) Functional characterization of the S. cerevisiae genome by gene deletion and parallel analysis, *Science 285*, 901-906.

[25] Giaever, G., Chu, A. M., Ni, L., Connelly, C., Riles, L., Veronneau, S., Dow, S., Lucau-Danila, A., Anderson, K., Andre, B., Arkin, A. P., Astromoff, A., El-Bakkoury, M., Bangham, R., Benito, R., Brachat, S., Campanaro, S., Curtiss, M., Davis, K., Deutschbauer, A., Entian, K. D., Flaherty, P., Foury, F., Garfinkel, D. J., Gerstein, M., Gotte, D., Guldener, U., Hegemann, J. H., Hempel, S., Herman, Z., Jaramillo, D. F., Kelly, D. E., Kelly, S. L., Kotter, P., LaBonte, D., Lamb, D. C., Lan, N., Liang, H., Liao, H., Liu, L., Luo, C., Lussier, M., Mao, R., Menard, P., Ooi, S. L., Revuelta, J. L., Roberts, C. J., Rose, M., Ross-Macdonald, P., Scherens, B., Schimmack, G., Shafer, B., Shoemaker, D. D., Sookhai-Mahadeo, S., Storms, R. K., Strathern, J. N., Valle, G., Voet, M., Volckaert, G., Wang, C. Y., Ward, T. R., Wilhelmy, J., Winzeler, E. A., Yang, Y., Yen, G., Youngman, E., Yu, K., Bussey, H., Boeke, J. D., Snyder, M., Philippsen, P., Davis, R. W., and Johnston, M. (2002) Functional profiling of the Saccharomyces cerevisiae genome, *Nature 418*, 387-391.

[26] Global analysis of protein localization in budding yeast.

[27] Ghaemmaghami, S., Huh, W. K., Bower, K., Howson, R. W., Belle, A., Dephoure, N., O'Shea, E. K., and Weissman, J. S. (2003) Global analysis of protein expression in yeast, *Nature 425*, 737-741.

[28] Phizicky, E., Bastiaens, P. I., Zhu, H., Snyder, M., and Fields, S. (2003) Protein analysis on a proteomic scale, *Nature 422*, 208-215.

[29] Karlson, P., and Luscher, M. (1959) Pheromones: a new term for a class of biologically active substances, *Nature 183*, 55-56.

[30] Fuller, R. S., Sterne, R. E., and Thorner, J. (1988) Enzymes required for yeast prohormone processing, *Annu Rev Physiol 50*, 345-362.

[31] Caldwell, G. A., Naider, F., and Becker, J. M. (1995) Fungal lipopeptide mating pheromones: a model system for the study of protein prenylation, *Microbiol Rev 59*, 406-422.

[32] Blumer, K. J., and Thorner, J. (1991) Receptor-G protein signaling in yeast, *Annu Rev Physiol 53*, 37-57.

[33] Bender, A., and Sprague, G. F., Jr. (1986) Yeast peptide pheromones, a-factor and alpha-factor, activate a common response mechanism in their target cells, *Cell 47*, 929-937.

[34] Madden, K., and Snyder, M. (1998) Cell polarity and morphogenesis in budding yeast, *Annu Rev Microbiol 52*, 687-744.

[35] Sprague, G. F., Jr. (1991) Signal transduction in yeast mating: receptors, transcription factors, and the kinase connection, *Trends Genet 7*, 393-398.

[36] Madhani, H. D., Galitski, T., Lander, E. S., and Fink, G. R. (1999) Effectors of a developmental mitogen-activated protein kinase cascade revealed by expression signatures of signaling mutants, *Proceedings of the National Academy of Sciences of the United States of America 96*, 12530-12535.

[37] Roberts, C. J., Nelson, B., Marton, M. J., Stoughton, R., Meyer, M. R., Bennett, H. A., He, Y. D., Dai, H., Walker, W. L., Hughes, T. R., Tyers, M., Boone, C., and Friend, S. H. (2000) Signaling and circuitry of multiple MAPK pathways revealed by a matrix of global gene expression profiles, *Science 287*, 873-880.

[38] Elion, E. A., Trueheart, J., and Fink, G. R. (1995) Fus2 localizes near the site of cell fusion and is required for both cell fusion and nuclear alignment during zygote formation, *The Journal of cell biology 130*, 1283-1296.

[39] Heiman, M. G., and Walter, P. (2000) Prm1p, a pheromone-regulated multispanning membrane protein, facilitates plasma membrane fusion during yeast mating, *The Journal of cell biology 151*, 719-730.

[40] Stone, E. M., Heun, P., Laroche, T., Pillus, L., and Gasser, S. M. (2000) MAP kinase signaling induces nuclear reorganization in budding yeast, *Current biology : CB 10*, 373-382.

[41] Rose, M. D. (1996) Nuclear fusion in the yeast Saccharomyces cerevisiae, *Annu Rev Cell Dev Biol 12*, 663-695.

[42] Wittenberg, C., and Reed, S. I. (1996) Plugging it in: signaling circuits and the yeast cell cycle, *Current opinion in cell biology 8*, 223-230.

[43] Oehlen, L. J., Jeoung, D. I., and Cross, F. R. (1998) Cyclin-specific START events and the G1-phase specificity of arrest by mating factor in budding yeast, *Mol Gen Genet 258*, 183-198.

[44] Zheng, Y., Cerione, R., and Bender, A. (1994) Control of the yeast bud-site assembly GTPase Cdc42. Catalysis of guanine nucleotide exchange by Cdc24 and stimulation of GTPase activity by Bem3, *The Journal of biological chemistry 269*, 2369-2372.

[45] Johnson, D. I. (1999) Cdc42: An essential Rho-type GTPase controlling eukaryotic cell polarity, *Microbiol Mol Biol Rev 63*, 54-105.

[46] Drubin, D. G., and Nelson, W. J. (1996) Origins of cell polarity, *Cell 84*, 335-344.

[47] Cabib, E., Drgonova, J., and Drgon, T. (1998) Role of small G proteins in yeast cell polarization and wall biosynthesis, *Annual review of biochemistry 67*, 307-333.

[48] Chant, J. (1999) Cell polarity in yeast, *Annu Rev Cell Dev Biol 15*, 365-391.

[49] Pruyne, D., and Bretscher, A. (2000) Polarization of cell growth in yeast. I. Establishment and maintenance of polarity states, *J Cell Sci 113 (Pt 3)*, 365-375.

[50] Bishop, A. L., and Hall, A. (2000) Rho GTPases and their effector proteins, *The Biochemical journal 348 Pt 2*, 241-255.

[51] Butty, A. C., Pryciak, P. M., Huang, L. S., Herskowitz, I., and Peter, M. (1998) The role of Far1p in linking the heterotrimeric G protein to polarity establishment proteins during yeast mating, *Science 282*, 1511-1516.

[52] Nern, A., and Arkowitz, R. A. (2000) Nucleocytoplasmic shuttling of the Cdc42p exchange factor Cdc24p, *The Journal of cell biology 148*, 1115-1122.

[53] Chang, F., and Herskowitz, I. (1990) Identification of a gene necessary for cell cycle arrest by a negative growth factor of yeast: FAR1 is an inhibitor of a G1 cyclin, CLN2, *Cell 63*, 999-1011.

[54] Peter, M., and Herskowitz, I. (1994) Direct inhibition of the yeast cyclin-dependent kinase Cdc28-Cln by Far1, *Science 265*, 1228-1231.

[55] Shimada, Y., Gulli, M. P., and Peter, M. (2000) Nuclear sequestration of the exchange factor Cdc24 by Far1 regulates cell polarity during yeast mating, *Nat Cell Biol 2*, 117-124.

[56] Kozminski, K. G., Chen, A. J., Rodal, A. A., and Drubin, D. G. (2000) Functions and functional domains of the GTPase Cdc42p, *Molecular biology of the cell 11*, 339-354.

[57] Leberer, E., Dignard, D., Harcus, D., Thomas, D. Y., and Whiteway, M. (1992) The protein kinase homologue Ste20p is required to link the yeast pheromone response G-protein beta gamma subunits to downstream signalling components, *The EMBO journal 11*, 4815-4824.

[58] Ramer, S. W., and Davis, R. W. (1993) A dominant truncation allele identifies a gene, STE20, that encodes a putative protein kinase necessary for mating in Saccharomyces cerevisiae, *Proceedings of the National Academy of Sciences of the United States of America 90*, 452-456.

[59] Leeuw, T., Fourest-Lieuvin, A., Wu, C., Chenevert, J., Clark, K., Whiteway, M., Thomas, D. Y., and Leberer, E. (1995) Pheromone response in yeast: association of Bem1p with proteins of the MAP kinase cascade and actin, *Science 270*, 1210-1213.

[60] Cvrckova, F., De Virgilio, C., Manser, E., Pringle, J. R., and Nasmyth, K. (1995) Ste20-like protein kinases are required for normal localization of cell growth and for cytokinesis in budding yeast, *Genes Dev 9*, 1817-1830.

[61] Eby, J. J., Holly, S. P., van Drogen, F., Grishin, A. V., Peter, M., Drubin, D. G., and Blumer, K. J. (1998) Actin cytoskeleton organization regulated by the PAK family of protein kinases, *Current biology : CB 8*, 967-970.

[62] Weiss, E. L., Bishop, A. C., Shokat, K. M., and Drubin, D. G. (2000) Chemical genetic analysis of the budding-yeast p21-activated kinase Cla4p, *Nat Cell Biol 2*, 677-685.

[63] Leeuw, T., Wu, C., Schrag, J. D., Whiteway, M., Thomas, D. Y., and Leberer, E. (1998) Interaction of a G-protein beta-subunit with a conserved sequence in Ste20/PAK family protein kinases, *Nature 391*, 191-195.

[64] Overton, M. C., and Blumer, K. J. (2000) G-protein-coupled receptors function as oligomers in vivo, *Current biology : CB 10*, 341-344.

[65] Jackson, C. L., Konopka, J. B., and Hartwell, L. H. (1991) S. cerevisiae alpha pheromone receptors activate a novel signal transduction pathway for mating partner discrimination, *Cell 67*, 389-402.

[66] Wu, C., Whiteway, M., Thomas, D. Y., and Leberer, E. (1995) Molecular characterization of Ste20p, a potential mitogen-activated protein or extracellular signal-regulated kinase kinase (MEK) kinase kinase from Saccharomyces cerevisiae, *The Journal of biological chemistry 270*, 15984-15992.

[67] Drogen, F., O'Rourke, S. M., Stucke, V. M., Jaquenoud, M., Neiman, A. M., and Peter, M. (2000) Phosphorylation of the MEKK Ste11p by the PAK-like kinase Ste20p is required for MAP kinase signaling in vivo, *Current biology : CB 10*, 630-639.

[68] Neiman, A. M., and Herskowitz, I. (1994) Reconstitution of a yeast protein kinase cascade in vitro: activation of the yeast MEK homologue STE7 by STE11, *Proceedings of the National Academy of Sciences of the United States of America 91*, 3398-3402.

[69] Gartner, A., Nasmyth, K., and Ammerer, G. (1992) Signal transduction in Saccharomyces cerevisiae requires tyrosine and threonine phosphorylation of FUS3 and KSS1, *Genes Dev 6*, 1280-1292.

[70] Ma, D., Cook, J. G., and Thorner, J. (1995) Phosphorylation and localization of Kss1, a MAP kinase of the Saccharomyces cerevisiae pheromone response pathway, *Molecular biology of the cell 6*, 889-909.

[71] Errede, B., Gartner, A., Zhou, Z., Nasmyth, K., and Ammerer, G. (1993) MAP kinase-related FUS3 from S. cerevisiae is activated by STE7 in vitro, *Nature 362*, 261-264.

[72] Courchesne, W. E., Kunisawa, R., and Thorner, J. (1989) A putative protein kinase overcomes pheromone-induced arrest of cell cycling in S. cerevisiae, *Cell 58*, 1107-1119.

[73] Elion, E. A., Grisafi, P. L., and Fink, G. R. (1990) FUS3 encodes a cdc2+/CDC28-related kinase required for the transition from mitosis into conjugation, *Cell 60*, 649-664.

[74] Madhani, H. D., and Fink, G. R. (1998) The control of filamentous differentiation and virulence in fungi, *Trends Cell Biol 8*, 348-353.

[75] Mosch, H. U. (2000) Pseudohyphal development of Saccharomyces cerevisiae, *Contrib Microbiol 5*, 185-200.

[76] Gancedo, J. M. (2001) Control of pseudohyphae formation in Saccharomyces cerevisiae, *FEMS Microbiol Rev 25*, 107-123.

[77] Inouye, C., Dhillon, N., Durfee, T., Zambryski, P. C., and Thorner, J. (1997) Mutational analysis of STE5 in the yeast Saccharomyces cerevisiae: application of a differential interaction trap assay for examining protein-protein interactions, *Genetics 147*, 479-492.

[78] Choi, K. Y., Kranz, J. E., Mahanty, S. K., Park, K. S., and Elion, E. A. (1999) Characterization of Fus3 localization: active Fus3 localizes in complexes of varying size and specific activity, *Molecular biology of the cell 10*, 1553-1568.

[79] Pryciak, P. M., and Huntress, F. A. (1998) Membrane recruitment of the kinase cascade scaffold protein Ste5 by the Gbetagamma complex underlies activation of the yeast pheromone response pathway, *Genes Dev 12*, 2684-2697.

[80] Mahanty, S. K., Wang, Y., Farley, F. W., and Elion, E. A. (1999) Nuclear shuttling of yeast scaffold Ste5 is required for its recruitment to the plasma membrane and activation of the mating MAPK cascade, *Cell 98*, 501-512.

[81] Sette, C., Inouye, C. J., Stroschein, S. L., Iaquinta, P. J., and Thorner, J. (2000) Mutational analysis suggests that activation of the yeast pheromone response mitogen-activated protein kinase pathway involves conformational changes in the Ste5 scaffold protein, *Molecular biology of the cell 11*, 4033-4049.

[82] Whiteway, M. S., Wu, C., Leeuw, T., Clark, K., Fourest-Lieuvin, A., Thomas, D. Y., and Leberer, E. (1995) Association of the yeast pheromone response G

protein beta gamma subunits with the MAP kinase scaffold Ste5p, *Science 269*, 1572-1575.

[83] Inouye, C., Dhillon, N., and Thorner, J. (1997) Ste5 RING-H2 domain: role in Ste4-promoted oligomerization for yeast pheromone signaling, *Science 278*, 103-106.

[84] Feng, Y., Song, L. Y., Kincaid, E., Mahanty, S. K., and Elion, E. A. (1998) Functional binding between Gbeta and the LIM domain of Ste5 is required to activate the MEKK Ste11, *Current biology : CB 8*, 267-278.

[85] Yablonski, D., Marbach, I., and Levitzki, A. (1996) Dimerization of Ste5, a mitogen-activated protein kinase cascade scaffold protein, is required for signal transduction, *Proceedings of the National Academy of Sciences of the United States of America 93*, 13864-13869.

[86] Elion, E. A., Satterberg, B., and Kranz, J. E. (1993) FUS3 phosphorylates multiple components of the mating signal transduction cascade: evidence for STE12 and FAR1, *Molecular biology of the cell 4*, 495-510.

[87] Peter, M., Gartner, A., Horecka, J., Ammerer, G., and Herskowitz, I. (1993) FAR1 links the signal transduction pathway to the cell cycle machinery in yeast, *Cell 73*, 747-760.

[88] Kranz, J. E., Satterberg, B., and Elion, E. A. (1994) The MAP kinase Fus3 associates with and phosphorylates the upstream signaling component Ste5, *Genes Dev 8*, 313-327.

[89] Song, D., Dolan, J. W., Yuan, Y. L., and Fields, S. (1991) Pheromone-dependent phosphorylation of the yeast STE12 protein correlates with transcriptional activation, *Genes Dev 5*, 741-750.

[90] Hung, W., Olson, K. A., Breitkreutz, A., and Sadowski, I. (1997) Characterization of the basal and pheromone-stimulated phosphorylation states of Ste12p, *Eur J Biochem 245*, 241-251.

[91] Cook, J. G., Bardwell, L., Kron, S. J., and Thorner, J. (1996) Two novel targets of the MAP kinase Kss1 are negative regulators of invasive growth in the yeast Saccharomyces cerevisiae, *Genes Dev 10*, 2831-2848.

[92] Tedford, K., Kim, S., Sa, D., Stevens, K., and Tyers, M. (1997) Regulation of the mating pheromone and invasive growth responses in yeast by two MAP kinase substrates, *Current biology : CB 7*, 228-238.

[93] Olson, K. A., Nelson, C., Tai, G., Hung, W., Yong, C., Astell, C., and Sadowski, I. (2000) Two regulators of Ste12p inhibit pheromone-responsive transcription by separate mechanisms, *Molecular and cellular biology 20*, 4199-4209.

[94] Toda, T., Uno, I., Ishikawa, T., Powers, S., Kataoka, T., Broek, D., Cameron, S., Broach, J., Matsumoto, K., and Wigler, M. (1985) In yeast, RAS proteins are controlling elements of adenylate cyclase, *Cell 40*, 27-36.

[95] DeFeo-Jones, D., Scolnick, E. M., Koller, R., and Dhar, R. (1983) ras-Related gene sequences identified and isolated from Saccharomyces cerevisiae, *Nature 306*, 707-709.

[96] Powers, S., Kataoka, T., Fasano, O., Goldfarb, M., Strathern, J., Broach, J., and Wigler, M. (1984) Genes in S. cerevisiae encoding proteins with domains homologous to the mammalian ras proteins, *Cell 36*, 607-612.

[97] Kraakman, L., Lemaire, K., Ma, P., Teunissen, A. W., Donaton, M. C., Van Dijck, P., Winderickx, J., de Winde, J. H., and Thevelein, J. M. (1999) A Saccharomyces cerevisiae G-protein coupled receptor, Gpr1, is specifically required for glucose activation of the cAMP pathway during the transition to growth on glucose, *Mol Microbiol 32*, 1002-1012.

[98] Yun, C. W., Tamaki, H., Nakayama, R., Yamamoto, K., and Kumagai, H. (1998) Gpr1p, a putative G-protein coupled receptor, regulates glucose-dependent cellular cAMP level in yeast Saccharomyces cerevisiae, *Biochemical and biophysical research communications 252*, 29-33.

[99] Versele, M., Lemaire, K., and Thevelein, J. M. (2001) Sex and sugar in yeast: two distinct GPCR systems, *EMBO reports 2*, 574-579.

[100] Harashima, T., and Heitman, J. (2002) The Galpha protein Gpa2 controls yeast differentiation by interacting with kelch repeat proteins that mimic Gbeta subunits, *Molecular cell 10*, 163-173.

[101] Harashima, T., and Heitman, J. (2005) Galpha subunit Gpa2 recruits kelch repeat subunits that inhibit receptor-G protein coupling during cAMP-induced dimorphic transitions in Saccharomyces cerevisiae, *Molecular biology of the cell 16*, 4557-4571.

[102] Lohse, M. J. (2010) Dimerization in GPCR mobility and signaling, *Current opinion in pharmacology 10*, 53-58.

[103] Palczewski, K. (2010) Oligomeric forms of G protein-coupled receptors (GPCRs), *Trends in biochemical sciences 35*, 595-600.

[104] Ng, G. Y., O'Dowd, B. F., Lee, S. P., Chung, H. T., Brann, M. R., Seeman, P., and George, S. R. (1996) Dopamine D2 receptor dimers and receptor-blocking peptides, *Biochemical and biophysical research communications 227*, 200-204.

[105] Ciruela, F., Casado, V., Mallol, J., Canela, E. I., Lluis, C., and Franco, R. (1995) Immunological identification of A1 adenosine receptors in brain cortex, *Journal of neuroscience research 42*, 818-828.

[106] Agnati, L. F., Ferre, S., Lluis, C., Franco, R., and Fuxe, K. (2003) Molecular mechanisms and therapeutical implications of intramembrane receptor/receptor interactions among heptahelical receptors with examples from the striatopallidal GABA neurons, *Pharmacological reviews 55*, 509-550.

[107] Angers, S., Salahpour, A., and Bouvier, M. (2001) Biochemical and biophysical demonstration of GPCR oligomerization in mammalian cells, *Life sciences 68*, 2243-2250.

[108] Albizu, L., Cottet, M., Kralikova, M., Stoev, S., Seyer, R., Brabet, I., Roux, T., Bazin, H., Bourrier, E., Lamarque, L., Breton, C., Rives, M. L., Newman, A., Javitch, J., Trinquet, E., Manning, M., Pin, J. P., Mouillac, B., and Durroux, T. (2010) Time-resolved FRET between GPCR ligands reveals oligomers in native tissues, *Nature chemical biology 6*, 587-594.

[109] Shi, C., Paige, M. F., Maley, J., and Loewen, M. C. (2009) In vitro characterization of ligand-induced oligomerization of the S. cerevisiae G-protein coupled receptor, Ste2p, *Biochimica et biophysica acta 1790*, 1-7.

[110] Angers, S., Salahpour, A., and Bouvier, M. (2002) Dimerization: an emerging concept for G protein-coupled receptor ontogeny and function, *Annual review of pharmacology and toxicology 42*, 409-435.

[111] Lemmon, M. A., and Schlessinger, J. (2010) Cell signaling by receptor tyrosine kinases, *Cell 141*, 1117-1134.

[112] Weiss, A., and Schlessinger, J. (1998) Switching signals on or off by receptor dimerization, *Cell 94*, 277-280.

[113] Livnah, O., Stura, E. A., Middleton, S. A., Johnson, D. L., Jolliffe, L. K., and Wilson, I. A. (1999) Crystallographic evidence for preformed dimers of erythropoietin receptor before ligand activation, *Science 283*, 987-990.

[114] Remy, I., Wilson, I. A., and Michnick, S. W. (1999) Erythropoietin receptor activation by a ligand-induced conformation change, *Science 283*, 990-993.

[115] Tsuji, Y., Shimada, Y., Takeshita, T., Kajimura, N., Nomura, S., Sekiyama, N., Otomo, J., Usukura, J., Nakanishi, S., and Jingami, H. (2000) Cryptic dimer interface and domain organization of the extracellular region of metabotropic glutamate receptor subtype 1, *The Journal of biological chemistry 275*, 28144-28151.

[116] Reddy, P. S., and Corley, R. B. (1998) Assembly, sorting, and exit of oligomeric proteins from the endoplasmic reticulum, *Bioessays 20*, 546-554.

[117] White, J. H., Wise, A., Main, M. J., Green, A., Fraser, N. J., Disney, G. H., Barnes, A. A., Emson, P., Foord, S. M., and Marshall, F. H. (1998) Heterodimerization is required for the formation of a functional GABA(B) receptor, *Nature 396*, 679-682.

[118] Jones, K. A., Borowsky, B., Tamm, J. A., Craig, D. A., Durkin, M. M., Dai, M., Yao, W. J., Johnson, M., Gunwaldsen, C., Huang, L. Y., Tang, C., Shen, Q., Salon, J. A., Morse, K., Laz, T., Smith, K. E., Nagarathnam, D., Noble, S. A., Branchek, T. A., and Gerald, C. (1998) GABA(B) receptors function as a heteromeric assembly of the subunits GABA(B)R1 and GABA(B)R2, *Nature 396*, 674-679.

[119] Kaupmann, K., Malitschek, B., Schuler, V., Heid, J., Froestl, W., Beck, P., Mosbacher, J., Bischoff, S., Kulik, A., Shigemoto, R., Karschin, A., and Bettler, B. (1998) GABA(B)-receptor subtypes assemble into functional heteromeric complexes, *Nature 396*, 683-687.

[120] Kuner, R., Kohr, G., Grunewald, S., Eisenhardt, G., Bach, A., and Kornau, H. C. (1999) Role of heteromer formation in GABAB receptor function, *Science 283*, 74-77.

[121] Morello, J. P., Salahpour, A., Petaja-Repo, U. E., Laperriere, A., Lonergan, M., Arthus, M. F., Nabi, I. R., Bichet, D. G., and Bouvier, M. (2001) Association of calnexin with wild type and mutant AVPR2 that causes nephrogenic diabetes insipidus, *Biochemistry 40*, 6766-6775.

[122] Karpa, K. D., Lin, R., Kabbani, N., and Levenson, R. (2000) The dopamine D3 receptor interacts with itself and the truncated D3 splice variant d3nf: D3-D3nf interaction causes mislocalization of D3 receptors, *Molecular pharmacology 58*, 677-683.

[123] Fung, J. J., Deupi, X., Pardo, L., Yao, X. J., Velez-Ruiz, G. A., Devree, B. T., Sunahara, R. K., and Kobilka, B. K. (2009) Ligand-regulated oligomerization of beta(2)-adrenoceptors in a model lipid bilayer, *The EMBO journal 28*, 3315-3328.

[124] Vidi, P. A., Chen, J., Irudayaraj, J. M., and Watts, V. J. (2008) Adenosine A(2A) receptors assemble into higher-order oligomers at the plasma membrane, *FEBS Lett 582*, 3985-3990.

[125] Guo, W., Urizar, E., Kralikova, M., Mobarec, J. C., Shi, L., Filizola, M., and Javitch, J. A. (2008) Dopamine D2 receptors form higher order oligomers at physiological expression levels, *The EMBO journal 27*, 2293-2304.

[126] Golebiewska, U., Johnston, J. M., Devi, L., Filizola, M., and Scarlata, S. (2011) Differential response to morphine of the oligomeric state of mu-opioid in the presence of delta-opioid receptors, *Biochemistry 50*, 2829-2837.

[127] Pisterzi, L. F., Jansma, D. B., Georgiou, J., Woodside, M. J., Chou, J. T., Angers, S., Raicu, V., and Wells, J. W. (2010) Oligomeric size of the m2 muscarinic receptor in live cells as determined by quantitative fluorescence resonance energy transfer, *The Journal of biological chemistry 285*, 16723-16738.

[128] Patowary, S., Alvarez-Curto, E., Xu, T. R., Holz, J. D., Oliver, J. A., Milligan, G., and Raicu, V. (2013) The muscarinic M3 acetylcholine receptor exists as two differently sized complexes at the plasma membrane, *The Biochemical journal 452*, 303-312.

[129] Yesilaltay, A., and Jenness, D. D. (2000) Homo-oligomeric complexes of the yeast alpha-factor pheromone receptor are functional units of endocytosis, *Molecular biology of the cell 11*, 2873-2884.

[130] Gehret, A. U., Bajaj, A., Naider, F., and Dumont, M. E. (2006) Oligomerization of the yeast alpha-factor receptor: implications for dominant negative effects of mutant receptors, *The Journal of biological chemistry 281*, 20698-20714.

[131] Kim, H., Lee, B. K., Naider, F., and Becker, J. M. (2009) Identification of specific transmembrane residues and ligand-induced interface changes

involved in homo-dimer formation of a yeast G protein-coupled receptor, *Biochemistry 48*, 10976-10987.

[132] Gouldson, P. R., Higgs, C., Smith, R. E., Dean, M. K., Gkoutos, G. V., and Reynolds, C. A. (2000) Dimerization and domain swapping in G-protein-coupled receptors: a computational study, *Neuropsychopharmacology 23*, S60-77.

[133] Shimomura, O., Johnson, F. H., and Saiga, Y. (1962) Extraction, purification and properties of aequorin, a bioluminescent protein from the luminous hydromedusan, Aequorea, *J Cell Comp Physiol 59*, 223-239.

[134] Morise, H., Shimomura, O., Johnson, F. H., and Winant, J. (1974) Intermolecular energy transfer in the bioluminescent system of Aequorea, *Biochemistry 13*, 2656-2662.

[135] Prasher, D. C., Eckenrode, V. K., Ward, W. W., Prendergast, F. G., and Cormier, M. J. (1992) Primary structure of the Aequorea victoria green-fluorescent protein, *Gene 111*, 229-233.

[136] Chalfie, M., Tu, Y., Euskirchen, G., Ward, W. W., and Prasher, D. C. (1994) Green fluorescent protein as a marker for gene expression, *Science 263*, 802-805.

[137] Reid, B. G., and Flynn, G. C. (1997) Chromophore formation in green fluorescent protein, *Biochemistry 36*, 6786-6791.

[138] Day, R. N., and Davidson, M. W. (2009) The fluorescent protein palette: tools for cellular imaging, *Chemical Society reviews 38*, 2887-2921.

[139] Yang, F., Moss, L. G., and Phillips, G. N., Jr. (1996) The molecular structure of green fluorescent protein, *Nature biotechnology 14*, 1246-1251.

[140] Ormo, M., Cubitt, A. B., Kallio, K., Gross, L. A., Tsien, R. Y., and Remington, S. J. (1996) Crystal structure of the Aequorea victoria green fluorescent protein, *Science 273*, 1392-1395.

[141] Tsien, R. Y. (1998) The green fluorescent protein, *Annual review of biochemistry 67*, 509-544.

[142] Heim, R., Cubitt, A. B., and Tsien, R. Y. (1995) Improved green fluorescence, *Nature 373*, 663-664.

[143] Tsien, R. Y. (2005) Building and breeding molecules to spy on cells and tumors, *FEBS Lett 579*, 927-932.

[144] Shaner, N. C., Patterson, G. H., and Davidson, M. W. (2007) Advances in fluorescent protein technology, *J Cell Sci 120*, 4247-4260.

[145] Shcherbo, D., Murphy, C. S., Ermakova, G. V., Solovieva, E. A., Chepurnykh, T. V., Shcheglov, A. S., Verkhusha, V. V., Pletnev, V. Z., Hazelwood, K. L., Roche, P. M., Lukyanov, S., Zaraisky, A. G., Davidson, M. W., and Chudakov, D. M. (2009) Far-red fluorescent tags for protein imaging in living tissues, *The Biochemical journal 418*, 567-574.

[146] Matz, M. V., Fradkov, A. F., Labas, Y. A., Savitsky, A. P., Zaraisky, A. G., Markelov, M. L., and Lukyanov, S. A. (1999) Fluorescent proteins from nonbioluminescent Anthozoa species, *Nature biotechnology 17*, 969-973.

[147] Campbell, R. E., Tour, O., Palmer, A. E., Steinbach, P. A., Baird, G. S., Zacharias, D. A., and Tsien, R. Y. (2002) A monomeric red fluorescent protein, *Proceedings of the National Academy of Sciences of the United States of America 99*, 7877-7882.

[148] Shaner, N. C., Campbell, R. E., Steinbach, P. A., Giepmans, B. N., Palmer, A. E., and Tsien, R. Y. (2004) Improved monomeric red, orange and yellow fluorescent proteins derived from Discosoma sp. red fluorescent protein, *Nature biotechnology 22*, 1567-1572.

[149] Kerppola, T. K. (2009) Visualization of molecular interactions using bimolecular fluorescence complementation analysis: characteristics of protein fragment complementation, *Chemical Society reviews 38*, 2876-2886.

[150] Shekhawat, S. S., and Ghosh, I. (2011) Split-protein systems: beyond binary protein-protein interactions, *Current opinion in chemical biology 15*, 789-797.

[151] Frommer, W. B., Davidson, M. W., and Campbell, R. E. (2009) Genetically encoded biosensors based on engineered fluorescent proteins, *Chemical Society reviews 38*, 2833-2841.

[152] Johnsson, N., and Varshavsky, A. (1994) Split ubiquitin as a sensor of protein interactions in vivo, *Proceedings of the National Academy of Sciences of the United States of America 91*, 10340-10344.

[153] Barnard, E., McFerran, N. V., Trudgett, A., Nelson, J., and Timson, D. J. (2008) Detection and localisation of protein-protein interactions in

Saccharomyces cerevisiae using a split-GFP method, *Fungal genetics and biology : FG & B 45*, 597-604.

[154] Morell, M., Ventura, S., and Aviles, F. X. (2009) Protein complementation assays: approaches for the in vivo analysis of protein interactions, *FEBS Lett 583*, 1684-1691.

[155] Kerppola, T. K. (2006) Complementary methods for studies of protein interactions in living cells, *Nature methods 3*, 969-971.

[156] Kerppola, T. K. (2008) Bimolecular fluorescence complementation (BiFC) analysis as a probe of protein interactions in living cells, *Annu Rev Biophys 37*, 465-487.

[157] Hu, C. D., Chinenov, Y., and Kerppola, T. K. (2002) Visualization of interactions among bZIP and Rel family proteins in living cells using bimolecular fluorescence complementation, *Molecular cell 9*, 789-798.

[158] Hu, C. D., and Kerppola, T. K. (2003) Simultaneous visualization of multiple protein interactions in living cells using multicolor fluorescence complementation analysis, *Nature biotechnology 21*, 539-545.

[159] Robida, A. M., and Kerppola, T. K. (2009) Bimolecular fluorescence complementation analysis of inducible protein interactions: effects of factors affecting protein folding on fluorescent protein fragment association, *J Mol Biol 394*, 391-409.

[160] Laricchia-Robbio, L., Tamura, T., Karpova, T., Sprague, B. L., McNally, J. G., and Ozato, K. (2005) Partner-regulated interaction of IFN regulatory factor 8 with chromatin visualized in live macrophages, *Proceedings of the National Academy of Sciences of the United States of America 102*, 14368-14373.

[161] Ren, X., Vincenz, C., and Kerppola, T. K. (2008) Changes in the distributions and dynamics of polycomb repressive complexes during embryonic stem cell differentiation, *Molecular and cellular biology 28*, 2884-2895.

[162] Park, K., Yi, S. Y., Lee, C. S., Kim, K. E., Pai, H. S., Seol, D. W., Chung, B. H., and Kim, M. (2007) A split enhanced green fluorescent protein-based reporter in yeast two-hybrid system, *The protein journal 26*, 107-116.

[163] Sung, M. K., and Huh, W. K. (2007) Bimolecular fluorescence complementation analysis system for in vivo detection of protein-protein interaction in Saccharomyces cerevisiae, *Yeast 24*, 767-775.

[164] Förster, T. (1946) Energiewanderung und Fluoreszenz, *Die Naturwissenschaften 33*, 9.

[165] Förster, T. (1948) Zwischenmolekulare Energiewanderung und Fluoreszenz, *Annalen der Physik 2*, 20.

[166] Clegg, R. M. (1995) Fluorescence resonance energy transfer, *Curr Opin Biotechnol 6*, 103-110.

[167] Lakowicz, J. R. (2006) Principles of Fluorescence Spectroscopy (3rd Ed.), *Kluwer Academic/Plenum Publishers*.

[168] Dohlman, H. G., Goldsmith, P., Spiegel, A. M., and Thorner, J. (1993) Pheromone action regulates G-protein alpha-subunit myristoylation in the yeast Saccharomyces cerevisiae, *Proceedings of the National Academy of Sciences of the United States of America 90*, 9688-9692.

[169] Son, C. D., Sargsyan, H., Naider, F., and Becker, J. M. (2004) Identification of ligand binding regions of the Saccharomyces cerevisiae alpha-factor pheromone receptor by photoaffinity cross-linking, *Biochemistry 43*, 13193-13203.

[170] Sen, M., and Marsh, L. (1994) Noncontiguous domains of the alpha-factor receptor of yeasts confer ligand specificity, *The Journal of biological chemistry 269*, 968-973.

[171] Goldstein, A., L., McCusker, J., H. (1999) Three new dominant drug resistance cassettes for gene disruption in Saccharomyces cerevisiae, *Yeast 5*, 1541-1553.

[172] Partow, S., Siewers, V., Bjorn, S., Nielsen, J., and Maury, J. (2010) Characterization of different promoters for designing a new expression vector in Saccharomyces cerevisiae, *Yeast 27*, 955-964.

[173] Raths, S. K., Naider, F., and Becker, J. M. (1988) Peptide analogues compete with the binding of alpha-factor to its receptor in Saccharomyces cerevisiae, *The Journal of biological chemistry 263*, 17333-17341.

[174] Gietz, R. D., Schiestl, R. H., Willems, A. R., and Woods, R. A. (1995) Studies on the transformation of intact yeast cells by the LiAc/SS-DNA/PEG procedure, *Yeast 11*, 355-360.

[175] Zheng, L., Baumann, U., and Reymond, J. L. (2004) An efficient one-step site-directed and site-saturation mutagenesis protocol, *Nucleic acids research 32*, e115.

[176] Lee, B. K., Khare, S., Naider, F., and Becker, J. M. (2001) Identification of residues of the Saccharomyces cerevisiae G protein-coupled receptor contributing to alpha-factor pheromone binding, *The Journal of biological chemistry 276*, 37950-37961.

[177] Hoffman, G. A., Garrison, T. R., and Dohlman, H. G. (2002) Analysis of RGS proteins in Saccharomyces cerevisiae, *Methods Enzymol 344*, 617-631.

[178] Konopka, J. B., Jenness, D. D., and Hartwell, L. H. (1988) The C-terminus of the S. cerevisiae alpha-pheromone receptor mediates an adaptive response to pheromone, *Cell 54*, 609-620.

[179] Ozawa, T., and Umezawa, Y. (2001) Detection of protein-protein interactions in vivo based on protein splicing, *Current opinion in chemical biology 5*, 578-583.

[180] Ozawa, T., Takeuchi, T. M., Kaihara, A., Sato, M., and Umezawa, Y. (2001) Protein splicing-based reconstitution of split green fluorescent protein for monitoring protein-protein interactions in bacteria: improved sensitivity and reduced screening time, *Analytical chemistry 73*, 5866-5874.

[181] Overton, M. C., Chinault, S. L., and Blumer, K. J. (2003) Oligomerization, biogenesis, and signaling is promoted by a glycophorin A-like dimerization motif in transmembrane domain 1 of a yeast G protein-coupled receptor, *The Journal of biological chemistry 278*, 49369-49377.

[182] Hirschman, J. E., De Zutter, G. S., Simonds, W. F., and Jenness, D. D. (1997) The G beta gamma complex of the yeast pheromone response pathway. Subcellular fractionation and protein-protein interactions, *The Journal of biological chemistry 272*, 240-248.

[183] Mentesana, P. E., and Konopka, J. B. (2001) Mutational analysis of the role of N-glycosylation in alpha-factor receptor function, *Biochemistry 40*, 9685-9694.

[184] Ayscough, K. R., and Drubin, D. G. (1998) A role for the yeast actin cytoskeleton in pheromone receptor clustering and signalling, *Current biology : CB 8*, 927-930.

[185] Toshima, J. Y., Toshima, J., Kaksonen, M., Martin, A. C., King, D. S., and Drubin, D. G. (2006) Spatial dynamics of receptor-mediated endocytic trafficking in budding yeast revealed by using fluorescent alpha-factor derivatives, *Proceedings of the National Academy of Sciences of the United States of America 103*, 5793-5798.

[186] Walther, T. C., Brickner, J. H., Aguilar, P. S., Bernales, S., Pantoja, C., and Walter, P. (2006) Eisosomes mark static sites of endocytosis, *Nature 439*, 998-1003.

[187] Dosil, M., Schandel, K. A., Gupta, E., Jenness, D. D., and Konopka, J. B. (2000) The C terminus of the Saccharomyces cerevisiae alpha-factor receptor contributes to the formation of preactivation complexes with its cognate G protein, *Molecular and cellular biology 20*, 5321-5329.

[188] Kim, K. M., Lee, Y. H., Akal-Strader, A., Uddin, M. S., Hauser, M., Naider, F., and Becker, J. M. (2012) Multiple regulatory roles of the carboxy terminus of Ste2p a yeast GPCR, *Pharmacological research : the official journal of the Italian Pharmacological Society 65*, 31-40.

[189] Mulholland, J., Konopka, J., Singer-Kruger, B., Zerial, M., and Botstein, D. (1999) Visualization of receptor-mediated endocytosis in yeast, *Molecular biology of the cell 10*, 799-817.

[190] Chen, Q., and Konopka, J. B. (1996) Regulation of the G-protein-coupled alpha-factor pheromone receptor by phosphorylation, *Molecular and cellular biology 16*, 247-257.

[191] Chang, F. S., Han, G. S., Carman, G. M., and Blumer, K. J. (2005) A WASp-binding type II phosphatidylinositol 4-kinase required for actin polymerization-driven endosome motility, *The Journal of cell biology 171*, 133-142.

APPENDIX A

YEAST MEDIA PREPARATION

Composition of dropout mix (stock) for Media Lack of Tryptophane, Uracil, Tryptophane and Uracil (MLT, MLU and MLTU)

Table A.1 Composition of dropout mixture.

Component	Final concentration (g/L)
Adenine Sulfate	0.058
Arginine HCl	0.026
Asparagine	0.058
Aspartic Acid	0.14
Glutamic Acid	0.14
Histidine HCl	0.028
Isoleucine	0.028
Leucine	0.083
Lysine	0.042
Methionine	0.028
Phenylalanine	0.69
Serine	0.52
Threonine	0.28
Tyrosine	0.042
Tryptophan*	0.028
Valine	0.21
Uracil*	0.028

* Tryptophan and Uracil were not added to dropout mix. Tryptophan to give 0.028 g/L final concentration is added to prepare MLU, Uracil to give 0.028 g/L final concentration is added to prepare MLT.

All ingredients are weighed and combined in a dark bottle and mixed completely.

Dextrose Medium composition

Table A.2 Composition of Dextrose medium.

Component	Amount
Dextrose	20 g/L
Casamino Acids	10 g/L
YNB without Amino acids and Ammonium sulfate	1.7 g/L
Ammonium sulfate	5 g/L
Dropout mix	1.8 g/L

For Glucose solid agar plate preparation 20 g/L Agar is added to the media before sterilization by autoclaving at 121 °C for 20 minutes.

Galactose - Raffinose Medium composition

Table A.3 Composition of Galactose – Raffinose medium

Component	Amount
Galactose	10 g/L
Raffinose	10 g/L
Casamino Acids	10 g/L
YNB without Amino acids and Ammonium sulfate	1.7 g/L
Ammonium sulfate	5 g/L
Dropout mix	1.8 g/L

For Galactose – Raffinose solid agar plate preparation 20 g/L Agar is added to the media before sterilization by autoclaving at 121 °C for 20 minutes.

YEPD Media Composition

Table A.4 Composition of YEPD medium

Component	Amount
Yeast extract	10 g/L
Peptone	20 g/L
Dextrose	20g/L

For YEPD solid agar plate preparation 20 g/L Agar is added to the media before sterilization by autoclaving at 121 °C for 20 minutes.

APPENDIX B

BACTERIAL MEDIA PREPARATION

Luria-Bertani (LB) Medium

Table B.1 Composition of LB medium.

Component	Amount
Tryptone	10 g/L
Yeast extract	5 g/L
NaCl	5 g/L

For LB solid agar plate preparation 20 g/L Agar is added to the media before sterilization by autoclaving at 121 °C for 20 minutes.

Super Optimum Broth with catabolite repression (SOC)

Table B.2 Composition of SOC medium.

Component	Amount
Tryptone	20 g/L
Yeast Extract	5 g/L
NaCl	0.5 g/L
KCl	0.186 g/L
$MgCl_2$	0.952 g/L
$MgSO_4$	2.408 g/L
Dextrose	3.603 g/L

The pH was adjusted to 7.0 and medium was sterilized by autoclaving at 121 °C for 20 minutes and then sterile Mg^{2+} solution and glucose is added.

APPENDIX C

SOLUTIONS AND BUFFERS

10X Tris-Borate-EDTA (TBE) Buffer

Table C.1 Composition of 10X Tris-Borate-EDTA (TBE) Buffer

Component	Amount
Tris Base (890 mM)	108 g/L
Boric Acid (890 mM)	55 g/L
EDTA (20 mM)	40 mL/L

All ingredients were added to 800 mL of distilled water and volume was adjusted to 1L. For gel electrophoresis, the solution was diluted 1:10.

Single-stranded Carrier DNA (2 mg/mL)

200 mg of salmon sperm DNA (DNA Sodium Salt from salmon testes, Sigma D1626) was dissolved in 100 ml of TE buffer (Sigma, #93283) on a magnetic stirrer for 3-5 hours. 500 µL aliquots of the solution were prepared and stored in -20 °C.

1.0M Lithium Acetate Solution

Prepared as stock solution in distilled water. Final pH of the solution was adjusted to 8.4 – 8.9 then filter sterilized using 0.45 µm filter unit (Nalgene).

Polyethylene glycol (PEG 50% w/v)

50 mg of the polyethylene glycol (PEG) (Sigma, #P3640) was mixed with 35 ml of distilled water on a magnetic stirrer until it solved completely. Volume was adjusted to 100 mL and the solution was filter sterilized using 0.45 µm filter unit (Nalgene).

Preparation of SDS-PAGE Solutions

1.5 mM Tris pH 8.8, 0.4% SDS was prepared by adding 18 g Tris Base and 0.4 g SDS in 100 mL distilled water, pH was adjusted to 8.8 using HCl. 0.5 M Tris-HCL pH 6.8, 0.4% SDS was prepared by adding 6.055g Tris Base and 0.4 g SDS in 100 mL distilled water and pH was adjusted to 6.8 with HCl. 10% Ammonium Persulfate prepared by adding 1 g APS in 10mL water.

10X SDS Running Buffer

Table C.2 The composition of 10X SDS Running Buffer.

Component	Amount (g)
25mM Tris	30.3 g
20mM Glycine	188 g
SDS (1%)	10 g

All the components were added to 1 L of distilled H_2O pH was adjusted to 8.3.

6X Loading Buffer

Table C.3 The composition of 6X Loading Buffer

Components	Amount
0.5 M Tris HCl (pH 6.8)	1.2 mL
Glycerol	4.7 mL
SDS	1.2 g
Bromophenol Blue	6 mg
Distilled water	2.1 mL
β-Mercapto ethanol	50 µL (freshly added for 950µL)

SDS Polyacrylamide Gel

Table C.4 The composition of SDS Polyacrylamide gel

Components	Amounts in 10% Gel (4 minigels)	Amounts in 5% stacking Gel (2 minigels)
Distilled water	19.3 mL	4.8 mL
Tris	10 mL 1.5 M TRIS pH 8.8	2.0 mL 0.5 M TRIS pH 6.8
40% Acrylamide	9.9 mL	1.0 mL
50% Glycerol	240 µL	-
10% APS	240 µL	80 µL
TEMED	20 µL	8 µL

Coomassie Gel stain and destaining solution

Table C.5 The composition of Coomassie Gel stain and destaining solution

Components	Staining solution	Destaining Solution
Coomassie Brilliant Blue R-250	2.5 g	-
Ethanol	500 mL	165 mL
Ultrapure water	400 mL	785 mL
Acetic Acid	100 mL	50 mL

APPENDIX D

CODING SEQUENCES OF STE2 CONSTRUCTS

Ste2p[EGFP]305-451

```
ATGTCTGATGCGGCTCCTTCATTGAGCAATCTATTTTATGATCCAACGTATAATCCTGGTCAAAGCACCATTAACTACAC
TTCCATATATGGGAATGGATCTACCATCACTTTCGATGAGTTGCAAGGTTTAGTTAACAGTACTGTTACTCAGGCCATTA
TGTTTGGTGTCAGATGTGGTGCAGCTGCTTTGACTTTGATTGTCATGTGGATGACATCGAGAAGCAGAAAAACGCCGATT
TTCATTATCAACCAAGTTTCATTGTTTTTAATCATTTTGCATTCTGCACTCTATTTTAAATATTTACTGTCTAATTACTC
TTCAGTGACTTACGCTCTCACCGGATTTCCTCAGTTCATCAGTAGAGGTGACGTTCATGTTTATGGTGCTACAAATATAA
TTCAAGTCCTTCTTGTGGCTTCTATTGAGACTTCACTGGTGTTTCAGATAAAAGTTATTTTCACAGGCGACAACTTCAAA
AGGATAGGTTTGATGCTGACGTCGATATCTTTCACTTTAGGGATTGCTACAGTTACCATGTATTTTGTAAGCGCTGTTAA
AGGTATGATTGTGACTTATAATGATGTTAGTGCCACCCAAGATAAATACTTCAATGCATCCACAATTTTACTTGCATCCT
CAATAAACTTTATGTCATTTGTCCTGGTAGTTAAATTGATTTTAGCTATTAGATCAAGAAGATTCCTTGGTCTCAAGCAG
TTCGATAGTTTCCATATTTTACTCATAATGTCATGTCAATCTTTGTTGGTTCCATCGATAATATTCATCCTCGCATACAG
TTTGAAACCAAACCAGGGAACAGATGTCTTGACTACTGTTGCAACATTACTTGCTGTATTGTCTTTACCATTATCATCAA
TGTGGGCCACGGCTGCTAATAATGCATCCAAAATGGTGAGCAAGGGCGAGGAGCTGTTCACCGGGGTGGTGCCCATCCTG
GTCGAGCTGGACGGCGACGTAAACGGCCACAAGTTCAGCGTGTCCGGCGAGGGCGAGGGCGATGCCACCTACGGCAAGCT
GACCCTGAAGTTCATCTGCACCACCGGCAAGCTGCCCGTGCCCTGGCCCACCCTCGTGACCACCCTGACCTACGGCGTGC
AGTGCTTCAGCCGCTACCCCGACCACATGAAGCAGCACGACTTCTTCAAGTCCGCCATGCCCGAAGGCTACGTCCAGGAG
CGCACCATCTTCTTCAAGGACGACGGCAACTACAAGACCCGCGCCGAGGTGAAGTTCGAGGGCGACACCCTGGTGAACCG
CATCGAGCTGAAGGGCATCGACTTCAAGGAGGACGGCAACATCCTGGGGCACAAGCTGGAGTACAACTACAACAGCCACA
ACGTCTATATCATGGCCGACAAGCAGAAGAACGGCATCAAGGTGAACTTCAAGATCCGCCACAACATCGAGGACGGCAGC
GTGCAGCTCGCCGACCACTACCAGCAGAACACCCCCATCGGCGACGGCCCCGTGCTGCTGCCCGACAACCACTACCTGAG
CACCCAGTCCGCCCTGAGCAAAGACCCCAACGAGAAGCGCGATCACATGGTCCTGCTGGAGTTCGTGACCGCCGCCGGGA
TCACTCTCGGCATGGACGAGCTGTACAAGACAAACACAATTACTTCAGACTTTACAACATCCACAGATAGGTTTTATCCA
GGCACGCTGTCTAGCTTTCAAACTGATAGTATCAACAACGATGCTAAAAGCAGTCTCAGAAGTAGATTATATGACCTATA
TCCTAGAAGGAAGGAAACAACATCGGATAAACATTCGGAAAGAACTTTTGTTTCTGAGACTGCAGATGATATAGAGAAAA
ATCAGTTTTATCAGTTGCCCACACCTACGAGTTCAAAAAATACTAGGATAGGACCGTTTGCTGATGCAAGTTACAAAGAG
GGAGAAGTTGAACCCGTCGACATGTACACTCCCGATACGGCAGCTGATGAGGAAGCCAGAAAGTTCTGGACTGAAGATAA
TAATAATTTAgactacaaggacgacgatgacaagaccggtgtgccgcgcggcagcggcagcagccatcatcatcatcatc
Atagcagcggctaa
```

Figure D.1 Coding sequence of Ste2p[EGFP]305-451 construct. EGFP (1-238) sequence, highlighted with yellow is inserted between 912 – 913th residues inframe with the coding sequence corresponding to 304 – 305th positions on Ste2p receptor.

Ste2p[EGFP]305-431

```
ATGTCTGATGCGGCTCCTTCATTGAGCAATCTATTTTATGATCCAACGTATAATCCTGGTCAAAGCACCATTAACTACAC
TTCCATATATGGGAATGGATCTACCATCACTTTCGATGAGTTGCAAGGTTTAGTTAACAGTACTGTTACTCAGGCCATTA
TGTTTGGTGTCAGATGTGGTGCAGCTGCTTTGACTTTGATTGTCATGTGGATGACATCGAGAAGCAGAAAAACGCCGATT
TTCATTATCAACCAAGTTTCATTGTTTTTAATCATTTTGCATTCTGCACTCTATTTTAAATATTTACTGTCTAATTACTC
TTCAGTGACTTACGCTCTCACCGGATTTCCTCAGTTCATCAGTAGAGGTGACGTTCATGTTTATGGTGCTACAAATATAA
TTCAAGTCCTTCTTGTGGCTTCTATTGAGACTTCACTGGTGTTTCAGATAAAAGTTATTTTCACAGGCGACAACTTCAAA
AGGATAGGTTTGATGCTGACGTCGATATCTTTCACTTTAGGGATTGCTACAGTTACCATGTATTTTGTAAGCGCTGTTAA
AGGTATGATTGTGACTTATAATGATGTTAGTGCCACCCAAGATAAATACTTCAATGCATCCACAATTTTACTTGCATCCT
CAATAAACTTTATGTCATTTGTCCTGGTAGTTAAATTGATTTTAGCTATTAGATCAAGAAGATTCCTTGGTCTCAAGCAG
TTCGATAGTTTCCATATTTTACTCATAATGTCATGTCAATCTTTGTTGGTTCCATCGATAATATTCATCCTCGCATACAG
TTTGAAACCAAACCAGGGAACAGATGTCTTGACTACTGTTGCAACATTACTTGCTGTATTGTCTTTACCATTATCATCAA
TGTGGGCCACGGCTGCTAATAATGCATCCAAAATGGTGAGCAAGGGCGAGGAGCTGTTCACCGGGGTGGTGCCCATCCTG
GTCGAGCTGGACGGCGACGTAAACGGCCACAAGTTCAGCGTGTCCGGCGAGGGCGAGGGCGATGCCACCTACGGCAAGCT
GACCCTGAAGTTCATCTGCACCACCGGCAAGCTGCCCGTGCCCTGGCCCACCCTCGTGACCACCCTGACCTACGGCGTGC
AGTGCTTCAGCCGCTACCCCGACCACATGAAGCAGCACGACTTCTTCAAGTCCGCCATGCCCGAAGGCTACGTCCAGGAG
CGCACCATCTTCTTCAAGGACGACGGCAACTACAAGACCCGCGCCGAGGTGAAGTTCGAGGGCGACACCCTGGTGAACCG
CATCGAGCTGAAGGGCATCGACTTCAAGGAGGACGGCAACATCCTGGGGCACAAGCTGGAGTACAACTACAACAGCCACA
ACGTCTATATCATGGCCGACAAGCAGAAGAACGGCATCAAGGTGAACTTCAAGATCCGCCACAACATCGAGGACGGCAGC
GTGCAGCTCGCCGACCACTACCAGCAGAACACCCCCATCGGCGACGGCCCCGTGCTGCTGCCCGACAACCACTACCTGAG
CACCCAGTCCGCCCTGAGCAAAGACCCCAACGAGAAGCGCGATCACATGGTCCTGCTGGAGTTCGTGACCGCCGCCGGGA
TCACTCTCGGCATGGACGAGCTGTACAAGACAAACACAATTACTTCAGACTTTACAACATCCACAGATAGGTTTTATCCA
GGCACGCTGTCTAGCTTTCAAACTGATAGTATCAACAACGATGCTAAAAGCAGTCTCAGAAGTAGATTATATGACCTATA
TCCTAGAAGGAAGGAAACAACATCGGATAAACATTCGGAAAGAACTTTTGTTTCTGAGACTGCAGATGATATAGAGAAAA
ATCAGTTTTATCAGTTGCCCACACCTACGAGTTCAAAAAATACTAGGATAGGACCGTTTGCTGATGCAAGTTACAAAGAG
GGAGAAGTTGAACCCGTCGACATGTACACTCCCGATACGGCAGCTGATGAGGAAGCCAGAAAGTTCTGGACTGAAGATAA
TAATAATTTATAAgactacaaggacgacgatgacaagaccggtgtgccgcgcggcagcggcagcagccatcatcatcatc
atcatagcagcggctaa
```

Figure D.2 Coding sequence of Ste2p[EGFP]305-431 construct. EGFP (1-238) sequence, highlighted with yellow is inserted between 912 – 913th residues inframe with the coding sequence corresponding to 304 – 305th positions on Ste2p receptor, a "TAA" stop codon was inserted before FLAG™ and His$_6$ sequences at 1293rd position on STE2.

Ste2p[EGFP]

```
ATGTCTGATGCGGCTCCTTCATTGAGCAATCTATTTTATGATCCAACGTATAATCCTGGTCAAAGCACCATTAACTACAC
TTCCATATATGGGAATGGATCTACCATCACTTTCGATGAGTTGCAAGGTTTAGTTAACAGTACTGTTACTCAGGCCATTA
TGTTTGGTGTCAGATGTGGTGCAGCTGCTTTGACTTTGATTGTCATGTGGATGACATCGAGAAGCAGAAAAACGCCGATT
TTCATTATCAACCAAGTTTCATTGTTTTTAATCATTTTGCATTCTGCACTCTATTTTAAATATTTACTGTCTAATTACTC
TTCAGTGACTTACGCTCTCACCGGATTTCCTCAGTTCATCAGTAGAGGTGACGTTCATGTTTATGGTGCTACAAATATAA
TTCAAGTCCTTCTTGTGGCTTCTATTGAGACTTCACTGGTGTTTCAGATAAAAGTTATTTTCACAGGCGACAACTTCAAA
AGGATAGGTTTGATGCTGACGTCGATATCTTTCACTTTAGGGATTGCTACAGTTACCATGTATTTTGTAAGCGCTGTTAA
AGGTATGATTGTGACTTATAATGATGTTAGTGCCACCCAAGATAAATACTTCAATGCATCCACAATTTTACTTGCATCCT
CAATAAACTTTATGTCATTTGTCCTGGTAGTTAAATTGATTTTAGCTATTAGATCAAGAAGATTCCTTGGTCTCAAGCAG
TTCGATAGTTTCCATATTTTACTCATAATGTCATGTCAATCTTTGTTGGTTCCATCGATAATATTCATCCTCGCATACAG
TTTGAAACCAAACCAGGGAACAGATGTCTTGACTACTGTTGCAACATTACTTGCTGTATTGTCTTTACCATTATCATCAA
TGTGGGCCACGGCTGCTAATAATGCATCCAAAATGGTGAGCAAGGGCGAGGAGCTGTTCACCGGGGTGGTGCCCATCCTG
GTCGAGCTGGACGGCGACGTAAACGGCCACAAGTTCAGCGTGTCCGGCGAGGGCGAGGGCGATGCCACCTACGGCAAGCT
GACCCTGAAGTTCATCTGCACCACCGGCAAGCTGCCCGTGCCCTGGCCCACCCTCGTGACCACCCTGACCTACGGCGTGC
AGTGCTTCAGCCGCTACCCCGACCACATGAAGCAGCACGACTTCTTCAAGTCCGCCATGCCCGAAGGCTACGTCCAGGAG
CGCACCATCTTCTTCAAGGACGACGGCAACTACAAGACCCGCGCCGAGGTGAAGTTCGAGGGCGACACCCTGGTGAACCG
CATCGAGCTGAAGGGCATCGACTTCAAGGAGGACGGCAACATCCTGGGGCACAAGCTGGAGTACAACTACAACAGCCACA
ACGTCTATATCATGGCCGACAAGCAGAAGAACGGCATCAAGGTGAACTTCAAGATCCGCCACAACATCGAGGACGGCAGC
GTGCAGCTCGCCGACCACTACCAGCAGAACACCCCCATCGGCGACGGCCCCGTGCTGCTGCCCGACAACCACTACCTGAG
CACCCAGTCCGCCCTGAGCAAAGACCCCAACGAGAAGCGCGATCACATGGTCCTGCTGGAGTTCGTGACCGCCGCCGGGA
TCACTCTCGGCATGGACGAGCTGTACAAGTAAACAAACACAATTACTTCAGACTTTACAACATCCACAGATAGGTTTTAT
CCAGGCACGCTGTCTAGCTTTCAAACTGATAGTATCAACAACGATGCTAAAAGCAGTCTCAGAAGTAGATTATATGACCT
ATATCCTAGAAGGAAGGAAACAACATCGGATAAACATTCGGAAAGAACTTTTGTTTCTGAGACTGCAGATGATATAGAGA
AAAATCAGTTTTATCAGTTGCCCACACCTACGAGTTCAAAAAATACTAGGATAGGACCGTTTGCTGATGCAAGTTACAAA
GAGGGAGAAGTTGAACCCGTCGACATGTACACTCCCGATACGGCAGCTGATGAGGAAGCCAGAAAGTTCTGGACTGAAGA
TAATAATAATTTAgactacaaggacgacgatgacaagaccggtgtgccgcgcggcagcggcagcagccatcatcatcatc
atcatagcagcggctaa
```

Figure D.3 Coding sequence of Ste2[EGFP] construct. EGFP (1-238) sequence, highlighted with yellow, carrying a "TAA" stop codon was inserted between 912 – 913th residues inframe with the coding sequence, corresponding to 304 – 305th positions on Ste2p receptor.

Ste2p[N-EGFP]305-451

```
ATGTCTGATGCGGCTCCTTCATTGAGCAATCTATTTTATGATCCAACGTATAATCCTGGTCAAAGCACCATTAACTACAC
TTCCATATATGGGAATGGATCTACCATCACTTTCGATGAGTTGCAAGGTTTAGTTAACAGTACTGTTACTCAGGCCATTA
TGTTTGGTGTCAGATGTGGTGCAGCTGCTTTGACTTTGATTGTCATGTGGATGACATCGAGAAGCAGAAAAACGCCGATT
TTCATTATCAACCAAGTTTCATTGTTTTTAATCATTTTGCATTCTGCACTCTATTTTAAATATTTACTGTCTAATTACTC
TTCAGTGACTTACGCTCTCACCGGATTTCCTCAGTTCATCAGTAGAGGTGACGTTCATGTTTATGGTGCTACAAATATAA
TTCAAGTCCTTCTTGTGGCTTCTATTGAGACTTCACTGGTGTTTCAGATAAAAGTTATTTTCACAGGCGACAACTTCAAA
AGGATAGGTTTGATGCTGACGTCGATATCTTTCACTTTAGGGATTGCTACAGTTACCATGTATTTTGTAAGCGCTGTTAA
AGGTATGATTGTGACTTATAATGATGTTAGTGCCACCCAAGATAAATACTTCAATGCATCCACAATTTTACTTGCATCCT
CAATAAACTTTATGTCATTTGTCCTGGTAGTTAAATTGATTTTAGCTATTAGATCAAGAAGATTCCTTGGTCTCAAGCAG
TTCGATAGTTTCCATATTTTACTCATAATGTCATGTCAATCTTTGTTGGTTCCATCGATAATATTCATCCTCGCATACAG
TTTGAAACCAAACCAGGGAACAGATGTCTTGACTACTGTTGCAACATTACTTGCTGTATTGTCTTTACCATTATCATCAA
TGTGGGCCACGGCTGCTAATAATGCATCCAAAATGGTGAGCAAGGGCGAGGAGCTGTTCACCGGGGTGGTGCCCATCCTG
GTCGAGCTGGACGGCGACGTAAACGGCCACAAGTTCAGCGTGTCCGGCGAGGGCGAGGGCGATGCCACCTACGGCAAGCT
GACCCTGAAGTTCATCTGCACCACCGGCAAGCTGCCCGTGCCCTGGCCCACCCTCGTGACCACCCTGACCTACGGCGTGC
AGTGCTTCAGCCGCTACCCCGACCACATGAAGCAGCACGACTTCTTCAAGTCCGCCATGCCCGAAGGCTACGTCCAGGAG
CGCACCATCTTCTTCAAGGACGACGGCAACTACAAGACCCGCGCCGAGGTGAAGTTCGAGGGCGACACCCTGGTGAACCG
CATCGAGCTGAAGGGCATCGACTTCAAGGAGGACGGCAACATCCTGGGGCACAAGCTGGAGTACAACTACAACAGCCACA
ACGTCTATATCATGGCCGACAAGCAGACAAACACAATTACTTCAGACTTTACAACATCCACAGATAGGTTTTATCCAGGC
ACGCTGTCTAGCTTTCAAACTGATAGTATCAACAACGATGCTAAAAGCAGTCTCAGAAGTAGATTATATGACCTATATCC
TAGAAGGAAGGAAACAACATCGGATAAACATTCGGAAAGAACTTTTGTTTCTGAGACTGCAGATGATATAGAGAAAAATC
AGTTTTATCAGTTGCCCACACCTACGAGTTCAAAAAATACTAGGATAGGACCGTTTGCTGATGCAAGTTACAAAGAGGGA
GAAGTTGAACCCGTCGACATGTACACTCCCGATACGGCAGCTGATGAGGAAGCCAGAAAGTTCTGGACTGAAGATAATAA
TAATTTAgactacaaggacgacgatgacaagaccggtgtgccgcgcggcagcggcagcagccatcatcatcatcatcata
gcagcggctaa
```

Figure D.4 Coding sequence of Ste2p[N-EGFP]305-451 construct. N-EGFP (1-158) sequence, highlighted with yellow is inserted between 912 – 913th residues inframe with the coding sequence corresponding to 304 – 305th positions on Ste2p receptor.

Ste2p[N-EGFP]305-431

```
ATGTCTGATGCGGCTCCTTCATTGAGCAATCTATTTTATGATCCAACGTATAATCCTGGTCAAAGCACCATTAACTACAC
TTCCATATATGGGAATGGATCTACCATCACTTTCGATGAGTTGCAAGGTTTAGTTAACAGTACTGTTACTCAGGCCATTA
TGTTTGGTGTCAGATGTGGTGCAGCTGCTTTGACTTTGATTGTCATGTGGATGACATCGAGAAGCAGAAAAACGCCGATT
TTCATTATCAACCAAGTTTCATTGTTTTTAATCATTTTGCATTCTGCACTCTATTTTAAATATTTACTGTCTAATTACTC
TTCAGTGACTTACGCTCTCACCGGATTTCCTCAGTTCATCAGTAGAGGTGACGTTCATGTTTATGGTGCTACAAATATAA
TTCAAGTCCTTCTTGTGGCTTCTATTGAGACTTCACTGGTGTTTCAGATAAAAGTTATTTTCACAGGCGACAACTTCAAA
AGGATAGGTTTGATGCTGACGTCGATATCTTTCACTTTAGGGATTGCTACAGTTACCATGTATTTTGTAAGCGCTGTTAA
AGGTATGATTGTGACTTATAATGATGTTAGTGCCACCCAAGATAAATACTTCAATGCATCCACAATTTTACTTGCATCCT
CAATAAACTTTATGTCATTTGTCCTGGTAGTTAAATTGATTTTAGCTATTAGATCAAGAAGATTCCTTGGTCTCAAGCAG
TTCGATAGTTTCCATATTTTACTCATAATGTCATGTCAATCTTTGTTGGTTCCATCGATAATATTCATCCTCGCATACAG
TTTGAAACCAAACCAGGGAACAGATGTCTTGACTACTGTTGCAACATTACTTGCTGTATTGTCTTTACCATTATCATCAA
TGTGGGCCACGGCTGCTAATAATGCATCCAAAATGGTGAGCAAGGGCGAGGAGCTGTTCACCGGGGTGGTGCCCATCCTG
GTCGAGCTGGACGGCGACGTAAACGGCCACAAGTTCAGCGTGTCCGGCGAGGGCGAGGGCGATGCCACCTACGGCAAGCT
GACCCTGAAGTTCATCTGCACCACCGGCAAGCTGCCCGTGCCCTGGCCCACCCTCGTGACCACCCTGACCTACGGCGTGC
AGTGCTTCAGCCGCTACCCCGACCACATGAAGCAGCACGACTTCTTCAAGTCCGCCATGCCCGAAGGCTACGTCCAGGAG
CGCACCATCTTCTTCAAGGACGACGGCAACTACAAGACCCGCGCCGAGGTGAAGTTCGAGGGCGACACCCTGGTGAACCG
CATCGAGCTGAAGGGCATCGACTTCAAGGAGGACGGCAACATCCTGGGGCACAAGCTGGAGTACAACTACAACAGCCACA
ACGTCTATATCATGGCCGACAAGCAGACAAACACAATTACTTCAGACTTTACAACATCCACAGATAGGTTTTATCCAGGC
ACGCTGTCTAGCTTTCAAACTGATAGTATCAACAACGATGCTAAAAGCAGTCTCAGAAGTAGATTATATGACCTATATCC
TAGAAGGAAGGAAACAACATCGGATAAACATTCGGAAAGAACTTTTGTTTCTGAGACTGCAGATGATATAGAGAAAAATC
AGTTTTATCAGTTGCCCACACCTACGAGTTCAAAAAATACTAGGATAGGACCGTTTGCTGATGCAAGTTACAAAGAGGGA
GAAGTTGAACCCGTCGACATGTACACTCCCGATACGGCAGCTGATGAGGAAGCCAGAAAGTTCTGGACTGAAGATAATAA
TAATTTATAAgactacaaggacgacgatgacaagaccggtgtgccgcgcggcagcggcagcagccatcatcatcatcatc
atagcagcggctaa
```

Figure D.5 Coding sequence of Ste2p[N-EGFP]305-431 construct. N-EGFP (1-158) sequence, highlighted with yellow is inserted between 912 – 913th residues inframe with the coding sequence corresponding to 304 – 305th positions on Ste2p receptor, a "TAA" stop codon was inserted before FLAG™ and His$_6$ sequences at 1293rd position on STE2.

Ste2p[C-EGFP]305-451

```
ATGTCTGATGCGGCTCCTTCATTGAGCAATCTATTTTATGATCCAACGTATAATCCTGGTCAAAGCACCATTAACTACAC
TTCCATATATGGGAATGGATCTACCATCACTTTCGATGAGTTGCAAGGTTTAGTTAACAGTACTGTTACTCAGGCCATTA
TGTTTGGTGTCAGATGTGGTGCAGCTGCTTTGACTTTGATTGTCATGTGGATGACATCGAGAAGCAGAAAAACGCCGATT
TTCATTATCAACCAAGTTTCATTGTTTTTAATCATTTTGCATTCTGCACTCTATTTTAAATATTTACTGTCTAATTACTC
TTCAGTGACTTACGCTCTCACCGGATTTCCTCAGTTCATCAGTAGAGGTGACGTTCATGTTTATGGTGCTACAAATATAA
TTCAAGTCCTTCTTGTGGCTTCTATTGAGACTTCACTGGTGTTTCAGATAAAAGTTATTTTCACAGGCGACAACTTCAAA
AGGATAGGTTTGATGCTGACGTCGATATCTTTCACTTTAGGGATTGCTACAGTTACCATGTATTTTGTAAGCGCTGTTAA
AGGTATGATTGTGACTTATAATGATGTTAGTGCCACCCAAGATAAATACTTCAATGCATCCACAATTTTACTTGCATCCT
CAATAAACTTTATGTCATTTGTCCTGGTAGTTAAATTGATTTTAGCTATTAGATCAAGAAGATTCCTTGGTCTCAAGCAG
TTCGATAGTTTCCATATTTTACTCATAATGTCATGTCAATCTTTGTTGGTTCCATCGATAATATTCATCCTCGCATACAG
TTTGAAACCAAACCAGGGAACAGATGTCTTGACTACTGTTGCAACATTACTTGCTGTATTGTCTTTACCATTATCATCAA
TGTGGGCCACGGCTGCTAATAATGCATCCAAAAAGAACGGCATCAAGGTGAACTTCAAGATCCGCCACAACATCGAGGAC
GGCAGCGTGCAGCTCGCCGACCACTACCAGCAGAACACCCCCATCGGCGACGGCCCCGTGCTGCTGCCCGACAACCACTA
CCTGAGCACCCAGTCCGCCCTGAGCAAAGACCCCAACGAGAAGCGCGATCACATGGTCCTGCTGGAGTTCGTGACCGCCG
CCGGGATCACTCTCGGCATGGACGAGCTGTACAAGACAAACACAATTACTTCAGACTTTACAACATCCACAGATAGGTTT
TATCCAGGCACGCTGTCTAGCTTTCAAACTGATAGTATCAACAACGATGCTAAAAGCAGTCTCAGAAGTAGATTATATGA
CCTATATCCTAGAAGGAAGGAAACAACATCGGATAAACATTCGGAAAGAACTTTTGTTTCTGAGACTGCAGATGATATAG
AGAAAAATCAGTTTTATCAGTTGCCCACACCTACGAGTTCAAAAAATACTAGGATAGGACCGTTTGCTGATGCAAGTTAC
AAAGAGGGAGAAGTTGAACCCGTCGACATGTACACTCCCGATACGGCAGCTGATGAGGAAGCCAGAAAGTTCTGGACTGA
AGATAATAATAATTTAgactacaaggacgacgatgacaagaccggtgtgccgcgcggcagcggcagcagccatcatcatc
atcatcatagcagcggctaa
```

Figure D.6 Coding sequence of Ste2p[C-EGFP]305-451 construct. C-EGFP (159-238) sequence, highlighted with yellow is inserted between 912 – 913th residues inframe with the coding sequence corresponding to 304 – 305th positions on Ste2p receptor.

Ste2p[C-EGFP]305-431

```
ATGTCTGATGCGGCTCCTTCATTGAGCAATCTATTTTATGATCCAACGTATAATCCTGGTCAAAGCACCATTAACTACAC
TTCCATATATGGGAATGGATCTACCATCACTTTCGATGAGTTGCAAGGTTTAGTTAACAGTACTGTTACTCAGGCCATTA
TGTTTGGTGTCAGATGTGGTGCAGCTGCTTTGACTTTGATTGTCATGTGGATGACATCGAGAAGCAGAAAAACGCCGATT
TTCATTATCAACCAAGTTTCATTGTTTTTAATCATTTTGCATTCTGCACTCTATTTTAAATATTTACTGTCTAATTACTC
TTCAGTGACTTACGCTCTCACCGGATTTCCTCAGTTCATCAGTAGAGGTGACGTTCATGTTTATGGTGCTACAAATATAA
TTCAAGTCCTTCTTGTGGCTTCTATTGAGACTTCACTGGTGTTTCAGATAAAAGTTATTTTCACAGGCGACAACTTCAAA
AGGATAGGTTTGATGCTGACGTCGATATCTTTCACTTTAGGGATTGCTACAGTTACCATGTATTTTGTAAGCGCTGTTAA
AGGTATGATTGTGACTTATAATGATGTTAGTGCCACCCAAGATAAATACTTCAATGCATCCACAATTTTACTTGCATCCT
CAATAAACTTTATGTCATTTGTCCTGGTAGTTAAATTGATTTTAGCTATTAGATCAAGAAGATTCCTTGGTCTCAAGCAG
TTCGATAGTTTCCATATTTTACTCATAATGTCATGTCAATCTTTGTTGGTTCCATCGATAATATTCATCCTCGCATACAG
TTTGAAACCAAACCAGGGAACAGATGTCTTGACTACTGTTGCAACATTACTTGCTGTATTGTCTTTACCATTATCATCAA
TGTGGGCCACGGCTGCTAATAATGCATCCAAAAAGAACGGCATCAAGGTGAACTTCAAGATCCGCCACAACATCGAGGAC
GGCAGCGTGCAGCTCGCCGACCACTACCAGCAGAACACCCCCATCGGCGACGGCCCCGTGCTGCTGCCCGACAACCACTA
CCTGAGCACCCAGTCCGCCCTGAGCAAAGACCCCAACGAGAAGCGCGATCACATGGTCCTGCTGGAGTTCGTGACCGCCG
CCGGGATCACTCTCGGCATGGACGAGCTGTACAAGACAAACACAATTACTTCAGACTTTACAACATCCACAGATAGGTTT
TATCCAGGCACGCTGTCTAGCTTTCAAACTGATAGTATCAACAACGATGCTAAAAGCAGTCTCAGAAGTAGATTATATGA
CCTATATCCTAGAAGGAAGGAAACAACATCGGATAAACATTCGGAAAGAACTTTTGTTTCTGAGACTGCAGATGATATAG
AGAAAAATCAGTTTTATCAGTTGCCCACACCTACGAGTTCAAAAAATACTAGGATAGGACCGTTTGCTGATGCAAGTTAC
AAAGAGGGAGAAGTTGAACCCGTCGACATGTACACTCCCGATACGGCAGCTGATGAGGAAGCCAGAAAGTTCTGGACTGA
AGATAATAATAATTTATAAgactacaaggacgacgatgacaagaccggtgtgccgcgcggcagcggcagcagccatcatc
atcatcatcatagcagcggctaa
```

Figure D.7 Coding sequence of Ste2p[C-EGFP]305-431 construct. C-EGFP (159-238) sequence, highlighted with yellow is inserted between 912 – 913th residues inframe with the coding sequence corresponding to 304 – 305th positions on Ste2p receptor, a “TAA” stop codon was inserted before FLAG^{TM} and His$_6$ sequences at 1293rd position on STE2.

Ste2p[N-EGFP]

```
ATGTCTGATGCGGCTCCTTCATTGAGCAATCTATTTTATGATCCAACGTATAATCCTGGTCAAAGCACCATTAACTACAC
TTCCATATATGGGAATGGATCTACCATCACTTTCGATGAGTTGCAAGGTTTAGTTAACAGTACTGTTACTCAGGCCATTA
TGTTTGGTGTCAGATGTGGTGCAGCTGCTTTGACTTTGATTGTCATGTGGATGACATCGAGAAGCAGAAAAACGCCGATT
TTCATTATCAACCAAGTTTCATTGTTTTTAATCATTTTGCATTCTGCACTCTATTTTAAATATTTACTGTCTAATTACTC
TTCAGTGACTTACGCTCTCACCGGATTTCCTCAGTTCATCAGTAGAGGTGACGTTCATGTTTATGGTGCTACAAATATAA
TTCAAGTCCTTCTTGTGGCTTCTATTGAGACTTCACTGGTGTTTCAGATAAAAGTTATTTTCACAGGCGACAACTTCAAA
AGGATAGGTTTGATGCTGACGTCGATATCTTTCACTTTAGGGATTGCTACAGTTACCATGTATTTTGTAAGCGCTGTTAA
AGGTATGATTGTGACTTATAATGATGTTAGTGCCACCCAAGATAAATACTTCAATGCATCCACAATTTTACTTGCATCCT
CAATAAACTTTATGTCATTTGTCCTGGTAGTTAAATTGATTTTAGCTATTAGATCAAGAAGATTCCTTGGTCTCAAGCAG
TTCGATAGTTTCCATATTTTACTCATAATGTCATGTCAATCTTTGTTGGTTCCATCGATAATATTCATCCTCGCATACAG
TTTGAAACCAAACCAGGGAACAGATGTCTTGACTACTGTTGCAACATTACTTGCTGTATTGTCTTTACCATTATCATCAA
TGTGGGCCACGGCTGCTAATAATGCATCCAAAATGGTGAGCAAGGGCGAGGAGCTGTTCACCGGGGTGGTGCCCATCCTG
GTCGAGCTGGACGGCGACGTAAACGGCCACAAGTTCAGCGTGTCCGGCGAGGGCGAGGGCGATGCCACCTACGGCAAGCT
GACCCTGAAGTTCATCTGCACCACCGGCAAGCTGCCCGTGCCCTGGCCCACCCTCGTGACCACCCTGACCTACGGCGTGC
AGTGCTTCAGCCGCTACCCCGACCACATGAAGCAGCACGACTTCTTCAAGTCCGCCATGCCCGAAGGCTACGTCCAGGAG
CGCACCATCTTCTTCAAGGACGACGGCAACTACAAGACCCGCGCCGAGGTGAAGTTCGAGGGCGACACCCTGGTGAACCG
CATCGAGCTGAAGGGCATCGACTTCAAGGAGGACGGCAACATCCTGGGGCACAAGCTGGAGTACAACTACAACAGCCACA
ACGTCTATATCATGGCCGACAAGCAGTAAACAAACACAATTACTTCAGACTTTACAACATCCACAGATAGGTTTTATCCA
GGCACGCTGTCTAGCTTTCAAACTGATAGTATCAACAACGATGCTAAAAGCAGTCTCAGAAGTAGATTATATGACCTATA
TCCTAGAAGGAAGGAAACAACATCGGATAAACATTCGGAAAGAACTTTTGTTTCTGAGACTGCAGATGATATAGAGAAAA
ATCAGTTTTATCAGTTGCCCACACCTACGAGTTCAAAAAATACTAGGATAGGACCGTTTGCTGATGCAAGTTACAAAGAG
GGAGAAGTTGAACCCGTCGACATGTACACTCCCGATACGGCAGCTGATGAGGAAGCCAGAAAGTTCTGGACTGAAGATAA
TAATAATTTAgactacaaggacgacgatgacaagaccggtgtgccgcgcggcagcggcagcagccatcatcatcatcatc
atagcagcggctaa
```

Figure D.8 Coding sequence of Ste2p[N-EGFP] construct. N-EGFP (1-158) sequence, highlighted with yellow carrying a “TAA” stop codon was inserted between 912 – 913th residues inframe with the coding sequence, corresponding to 304 – 305th positions on Ste2p receptor.

Ste2p[C-EGFP]

```
ATGTCTGATGCGGCTCCTTCATTGAGCAATCTATTTTATGATCCAACGTATAATCCTGGTCAAAGCACCATTAACTACAC
TTCCATATATGGGAATGGATCTACCATCACTTTCGATGAGTTGCAAGGTTTAGTTAACAGTACTGTTACTCAGGCCATTA
TGTTTGGTGTCAGATGTGGTGCAGCTGCTTTGACTTTGATTGTCATGTGGATGACATCGAGAAGCAGAAAAACGCCGATT
TTCATTATCAACCAAGTTTCATTGTTTTTAATCATTTTGCATTCTGCACTCTATTTTAAATATTTACTGTCTAATTACTC
TTCAGTGACTTACGCTCTCACCGGATTTCCTCAGTTCATCAGTAGAGGTGACGTTCATGTTTATGGTGCTACAAATATAA
TTCAAGTCCTTCTTGTGGCTTCTATTGAGACTTCACTGGTGTTTCAGATAAAAGTTATTTTCACAGGCGACAACTTCAAA
AGGATAGGTTTGATGCTGACGTCGATATCTTTCACTTTAGGGATTGCTACAGTTACCATGTATTTTGTAAGCGCTGTTAA
AGGTATGATTGTGACTTATAATGATGTTAGTGCCACCCAAGATAAATACTTCAATGCATCCACAATTTTACTTGCATCCT
CAATAAACTTTATGTCATTTGTCCTGGTAGTTAAATTGATTTTAGCTATTAGATCAAGAAGATTCCTTGGTCTCAAGCAG
TTCGATAGTTTCCATATTTTACTCATAATGTCATGTCAATCTTTGTTGGTTCCATCGATAATATTCATCCTCGCATACAG
TTTGAAACCAAACCAGGGAACAGATGTCTTGACTACTGTTGCAACATTACTTGCTGTATTGTCTTTACCATTATCATCAA
TGTGGGCCACGGCTGCTAATAATGCATCCAAAAAGAACGGCATCAAGGTGAACTTCAAGATCCGCCACAACATCGAGGAC
GGCAGCGTGCAGCTCGCCGACCACTACCAGCAGAACACCCCCATCGGCGACGGCCCCGTGCTGCTGCCCGACAACCACTA
CCTGAGCACCCAGTCCGCCCTGAGCAAAGACCCCAACGAGAAGCGCGATCACATGGTCCTGCTGGAGTTCGTGACCGCCG
CCGGGATCACTCTCGGCATGGACGAGCTGTACAAGTAAACAAACACAATTACTTCAGACTTTACAACATCCACAGATAGG
TTTTATCCAGGCACGCTGTCTAGCTTTCAAACTGATAGTATCAACAACGATGCTAAAAGCAGTCTCAGAAGTAGATTATA
TGACCTATATCCTAGAAGGAAGGAAACAACATCGGATAAACATTCGGAAAGAACTTTTGTTTCTGAGACTGCAGATGATA
TAGAGAAAAATCAGTTTTATCAGTTGCCCACACCTACGAGTTCAAAAAATACTAGGATAGGACCGTTTGCTGATGCAAGT
TACAAAGAGGGAGAAGTTGAACCCGTCGACATGTACACTCCCGATACGGCAGCTGATGAGGAAGCCAGAAAGTTCTGGAC
TGAAGATAATAATAATTTAgactacaaggacgacgatgacaagaccggtgtgccgcgcggcagcggcagcagccatcatc
atcatcatcatagcagcggctaa
```

Figure D.7 Coding sequence of Ste2p[C-EGFP] construct. C-EGFP (159-238) sequence, highlighted with yellow carrying a "TAA" stop codon was inserted between 912 – 913th residues inframe with the coding sequence, corresponding to 304 – 305th positions on Ste2p receptor.

Ste2pG56/60L[EGFP]305-451

```
ATGTCTGATGCGGCTCCTTCATTGAGCAATCTATTTTATGATCCAACGTATAATCCTGGTCAAAGCACCATTAACTACAC
TTCCATATATGGGAATGGATCTACCATCACTTTCGATGAGTTGCAAGGTTTAGTTAACAGTACTGTTACTCAGGCCATTA
TGTTTCTTGTCAGATGTCTTGCAGCTGCTTTGACTTTGATTGTCATGTGGATGACATCGAGAAGCAGAAAAACGCCGATT
TTCATTATCAACCAAGTTTCATTGTTTTTAATCATTTTGCATTCTGCACTCTATTTTAAATATTTACTGTCTAATTACTC
TTCAGTGACTTACGCTCTCACCGGATTTCCTCAGTTCATCAGTAGAGGTGACGTTCATGTTTATGGTGCTACAAATATAA
TTCAAGTCCTTCTTGTGGCTTCTATTGAGACTTCACTGGTGTTTCAGATAAAAGTTATTTTCACAGGCGACAACTTCAAA
AGGATAGGTTTGATGCTGACGTCGATATCTTTCACTTTAGGGATTGCTACAGTTACCATGTATTTTGTAAGCGCTGTTAA
AGGTATGATTGTGACTTATAATGATGTTAGTGCCACCCAAGATAAATACTTCAATGCATCCACAATTTTACTTGCATCCT
CAATAAACTTTATGTCATTTGTCCTGGTAGTTAAATTGATTTTAGCTATTAGATCAAGAAGATTCCTTGGTCTCAAGCAG
TTCGATAGTTTCCATATTTTACTCATAATGTCATGTCAATCTTTGTTGGTTCCATCGATAATATTCATCCTCGCATACAG
TTTGAAACCAAACCAGGGAACAGATGTCTTGACTACTGTTGCAACATTACTTGCTGTATTGTCTTTACCATTATCATCAA
TGTGGGCCACGGCTGCTAATAATGCATCCAAAATGGTGAGCAAGGGCGAGGAGCTGTTCACCGGGGTGGTGCCCATCCTG
GTCGAGCTGGACGGCGACGTAAACGGCCACAAGTTCAGCGTGTCCGGCGAGGGCGAGGGCGATGCCACCTACGGCAAGCT
GACCCTGAAGTTCATCTGCACCACCGGCAAGCTGCCCGTGCCCTGGCCCACCCTCGTGACCACCCTGACCTACGGCGTGC
AGTGCTTCAGCCGCTACCCCGACCACATGAAGCAGCACGACTTCTTCAAGTCCGCCATGCCCGAAGGCTACGTCCAGGAG
CGCACCATCTTCTTCAAGGACGACGGCAACTACAAGACCCGCGCCGAGGTGAAGTTCGAGGGCGACACCCTGGTGAACCG
CATCGAGCTGAAGGGCATCGACTTCAAGGAGGACGGCAACATCCTGGGGCACAAGCTGGAGTACAACTACAACAGCCACA
ACGTCTATATCATGGCCGACAAGCAGAAGAACGGCATCAAGGTGAACTTCAAGATCCGCCACAACATCGAGGACGGCAGC
GTGCAGCTCGCCGACCACTACCAGCAGAACACCCCCATCGGCGACGGCCCCGTGCTGCTGCCCGACAACCACTACCTGAG
CACCCAGTCCGCCCTGAGCAAAGACCCCAACGAGAAGCGCGATCACATGGTCCTGCTGGAGTTCGTGACCGCCGCCGGGA
TCACTCTCGGCATGGACGAGCTGTACAAGACAAACACAATTACTTCAGACTTTACAACATCCACAGATAGGTTTTATCCA
GGCACGCTGTCTAGCTTTCAAACTGATAGTATCAACAACGATGCTAAAAGCAGTCTCAGAAGTAGATTATATGACCTATA
TCCTAGAAGGAAGGAAACAACATCGGATAAACATTCGGAAAGAACTTTTGTTTCTGAGACTGCAGATGATATAGAGAAAA
ATCAGTTTTATCAGTTGCCCACACCTACGAGTTCAAAAAATACTAGGATAGGACCGTTTGCTGATGCAAGTTACAAAGAG
GGAGAAGTTGAACCCGTCGACATGTACACTCCCGATACGGCAGCTGATGAGGAAGCCAGAAAGTTCTGGACTGAAGATAA
TAATAATTTAgactacaaggacgacgatgacaagaccggtgtgccgcgcggcagcggcagcagccatcatcatcatcatc
Atagcagcggctaa
```

Figure D.8 Coding sequence of Ste2pG56/60L[EGFP]305-451 construct. EGFP (1-238) sequence, highlighted with yellow is inserted between 912 – 913th residues inframe with the coding sequence corresponding to 304 – 305th positions on Ste2p receptor. Red letters show inserted mutations.

Ste2pG56/60L[N-EGFP]305-451

```
ATGTCTGATGCGGCTCCTTCATTGAGCAATCTATTTTATGATCCAACGTATAATCCTGGTCAAAGCACCATTAACTACAC
TTCCATATATGGGAATGGATCTACCATCACTTTCGATGAGTTGCAAGGTTTAGTTAACAGTACTGTTACTCAGGCCATTA
TGTTTCTTGTCAGATGTCTTGCAGCTGCTTTGACTTTGATTGTCATGTGGATGACATCGAGAAGCAGAAAAACGCCGATT
TTCATTATCAACCAAGTTTCATTGTTTTTAATCATTTTGCATTCTGCACTCTATTTTAAATATTTACTGTCTAATTACTC
TTCAGTGACTTACGCTCTCACCGGATTTCCTCAGTTCATCAGTAGAGGTGACGTTCATGTTTATGGTGCTACAAATATAA
TTCAAGTCCTTCTTGTGGCTTCTATTGAGACTTCACTGGTGTTTCAGATAAAAGTTATTTTCACAGGCGACAACTTCAAA
AGGATAGGTTTGATGCTGACGTCGATATCTTTCACTTTAGGGATTGCTACAGTTACCATGTATTTTGTAAGCGCTGTTAA
AGGTATGATTGTGACTTATAATGATGTTAGTGCCACCCAAGATAAATACTTCAATGCATCCACAATTTTACTTGCATCCT
CAATAAACTTTATGTCATTTGTCCTGGTAGTTAAATTGATTTTAGCTATTAGATCAAGAAGATTCCTTGGTCTCAAGCAG
TTCGATAGTTTCCATATTTTACTCATAATGTCATGTCAATCTTTGTTGGTTCCATCGATAATATTCATCCTCGCATACAG
TTTGAAACCAAACCAGGGAACAGATGTCTTGACTACTGTTGCAACATTACTTGCTGTATTGTCTTTACCATTATCATCAA
TGTGGGCCACGGCTGCTAATAATGCATCCAAAATGGTGAGCAAGGGCGAGGAGCTGTTCACCGGGGTGGTGCCCATCCTG
GTCGAGCTGGACGGCGACGTAAACGGCCACAAGTTCAGCGTGTCCGGCGAGGGCGAGGGCGATGCCACCTACGGCAAGCT
GACCCTGAAGTTCATCTGCACCACCGGCAAGCTGCCCGTGCCCTGGCCCACCCTCGTGACCACCCTGACCTACGGCGTGC
AGTGCTTCAGCCGCTACCCCGACCACATGAAGCAGCACGACTTCTTCAAGTCCGCCATGCCCGAAGGCTACGTCCAGGAG
CGCACCATCTTCTTCAAGGACGACGGCAACTACAAGACCCGCGCCGAGGTGAAGTTCGAGGGCGACACCCTGGTGAACCG
CATCGAGCTGAAGGGCATCGACTTCAAGGAGGACGGCAACATCCTGGGGCACAAGCTGGAGTACAACTACAACAGCCACA
ACGTCTATATCATGGCCGACAAGCAGACAAACACAATTACTTCAGACTTTACAACATCCACAGATAGGTTTTATCCAGGC
ACGCTGTCTAGCTTTCAAACTGATAGTATCAACAACGATGCTAAAAGCAGTCTCAGAAGTAGATTATATGACCTATATCC
TAGAAGGAAGGAAACAACATCGGATAAACATTCGGAAAGAACTTTTGTTTCTGAGACTGCAGATGATATAGAGAAAAATC
AGTTTTATCAGTTGCCCACACCTACGAGTTCAAAAAATACTAGGATAGGACCGTTTGCTGATGCAAGTTACAAAGAGGGA
GAAGTTGAACCCGTCGACATGTACACTCCCGATACGGCAGCTGATGAGGAAGCCAGAAAGTTCTGGACTGAAGATAATAA
TAATTTAgactacaaggacgacgatgacaagaccggtgtgccgcgcggcagcggcagcagccatcatcatcatcatcata
gcagcggctaa
```

Figure D.9 Coding sequence of Ste2pG56/60L[N-EGFP]305-451 construct. N-EGFP (1-158) sequence, highlighted with yellow is inserted between 912 – 913th residues inframe with the coding sequence corresponding to 304 – 305th positions on Ste2p receptor. Red letters show inserted mutations.

Ste2pG56/60L[C-EGFP]305-451

```
ATGTCTGATGCGGCTCCTTCATTGAGCAATCTATTTTATGATCCAACGTATAATCCTGGTCAAAGCACCATTAACTACAC
TTCCATATATGGGAATGGATCTACCATCACTTTCGATGAGTTGCAAGGTTTAGTTAACAGTACTGTTACTCAGGCCATTA
TGTTTCTTGTCAGATGTCTTGCAGCTGCTTTGACTTTGATTGTCATGTGGATGACATCGAGAAGCAGAAAAACGCCGATT
TTCATTATCAACCAAGTTTCATTGTTTTTAATCATTTTGCATTCTGCACTCTATTTTAAATATTTACTGTCTAATTACTC
TTCAGTGACTTACGCTCTCACCGGATTTCCTCAGTTCATCAGTAGAGGTGACGTTCATGTTTATGGTGCTACAAATATAA
TTCAAGTCCTTCTTGTGGCTTCTATTGAGACTTCACTGGTGTTTCAGATAAAAGTTATTTTCACAGGCGACAACTTCAAA
AGGATAGGTTTGATGCTGACGTCGATATCTTTCACTTTAGGGATTGCTACAGTTACCATGTATTTTGTAAGCGCTGTTAA
AGGTATGATTGTGACTTATAATGATGTTAGTGCCACCCAAGATAAATACTTCAATGCATCCACAATTTTACTTGCATCCT
CAATAAACTTTATGTCATTTGTCCTGGTAGTTAAATTGATTTTAGCTATTAGATCAAGAAGATTCCTTGGTCTCAAGCAG
TTCGATAGTTTCCATATTTTACTCATAATGTCATGTCAATCTTTGTTGGTTCCATCGATAATATTCATCCTCGCATACAG
TTTGAAACCAAACCAGGGAACAGATGTCTTGACTACTGTTGCAACATTACTTGCTGTATTGTCTTTACCATTATCATCAA
TGTGGGCCACGGCTGCTAATAATGCATCCAAAAAGAACGGCATCAAGGTGAACTTCAAGATCCGCCACAACATCGAGGAC
GGCAGCGTGCAGCTCGCCGACCACTACCAGCAGAACACCCCCATCGGCGACGGCCCCGTGCTGCTGCCCGACAACCACTA
CCTGAGCACCCAGTCCGCCCTGAGCAAAGACCCCAACGAGAAGCGCGATCACATGGTCCTGCTGGAGTTCGTGACCGCCG
CCGGGATCACTCTCGGCATGGACGAGCTGTACAAGACAAACACAATTACTTCAGACTTTACAACATCCACAGATAGGTTT
TATCCAGGCACGCTGTCTAGCTTTCAAACTGATAGTATCAACAACGATGCTAAAAGCAGTCTCAGAAGTAGATTATATGA
CCTATATCCTAGAAGGAAGGAAACAACATCGGATAAACATTCGGAAAGAACTTTTGTTTCTGAGACTGCAGATGATATAG
AGAAAAATCAGTTTTATCAGTTGCCCACACCTACGAGTTCAAAAAATACTAGGATAGGACCGTTTGCTGATGCAAGTTAC
AAAGAGGGAGAAGTTGAACCCGTCGACATGTACACTCCCGATACGGCAGCTGATGAGGAAGCCAGAAAGTTCTGGACTGA
AGATAATAATAATTTAgactacaaggacgacgatgacaagaccggtgtgccgcgcggcagcggcagcagccatcatcatc
atcatcatagcagcggctaa
```

Figure D.10 Coding sequence of Ste2pG56/60L[C-EGFP]305-451 construct. C-EGFP (159-238) sequence, highlighted with yellow is inserted between 912 – 913th residues inframe with the coding sequence corresponding to 304 – 305th positions on Ste2p receptor. Red letters show inserted mutations.

Ste2pP290D[EGFP]305-431

```
ATGTCTGATGCGGCTCCTTCATTGAGCAATCTATTTTATGATCCAACGTATAATCCTGGTCAAAGCACCATTAACTACAC
TTCCATATATGGGAATGGATCTACCATCACTTTCGATGAGTTGCAAGGTTTAGTTAACAGTACTGTTACTCAGGCCATTA
TGTTTGGTGTCAGATGTGGTGCAGCTGCTTTGACTTTGATTGTCATGTGGATGACATCGAGAAGCAGAAAAACGCCGATT
TTCATTATCAACCAAGTTTCATTGTTTTTAATCATTTTGCATTCTGCACTCTATTTTAAATATTTACTGTCTAATTACTC
TTCAGTGACTTACGCTCTCACCGGATTTCCTCAGTTCATCAGTAGAGGTGACGTTCATGTTTATGGTGCTACAAATATAA
TTCAAGTCCTTCTTGTGGCTTCTATTGAGACTTCACTGGTGTTTCAGATAAAAGTTATTTTCACAGGCGACAACTTCAAA
AGGATAGGTTTGATGCTGACGTCGATATCTTTCACTTTAGGGATTGCTACAGTTACCATGTATTTTGTAAGCGCTGTTAA
AGGTATGATTGTGACTTATAATGATGTTAGTGCCACCCAAGATAAATACTTCAATGCATCCACAATTTTACTTGCATCCT
CAATAAACTTTATGTCATTTGTCCTGGTAGTTAAATTGATTTTAGCTATTAGATCAAGAAGATTCCTTGGTCTCAAGCAG
TTCGATAGTTTCCATATTTTACTCATAATGTCATGTCAATCTTTGTTGGTTCCATCGATAATATTCATCCTCGCATACAG
TTTGAAACCAAACCAGGGAACAGATGTCTTGACTACTGTTGCAACATTACTTGCTGTATTGTCTTTAGATTTATCATCAA
TGTGGGCCACGGCTGCTAATAATGCATCCAAAATGGTGAGCAAGGGCGAGGAGCTGTTCACCGGGGTGGTGCCCATCCTG
GTCGAGCTGGACGGCGACGTAAACGGCCACAAGTTCAGCGTGTCCGGCGAGGGCGAGGGCGATGCCACCTACGGCAAGCT
GACCCTGAAGTTCATCTGCACCACCGGCAAGCTGCCCGTGCCCTGGCCCACCCTCGTGACCACCCTGACCTACGGCGTGC
AGTGCTTCAGCCGCTACCCCGACCACATGAAGCAGCACGACTTCTTCAAGTCCGCCATGCCCGAAGGCTACGTCCAGGAG
CGCACCATCTTCTTCAAGGACGACGGCAACTACAAGACCCGCGCCGAGGTGAAGTTCGAGGGCGACACCCTGGTGAACCG
CATCGAGCTGAAGGGCATCGACTTCAAGGAGGACGGCAACATCCTGGGGCACAAGCTGGAGTACAACTACAACAGCCACA
ACGTCTATATCATGGCCGACAAGCAGAAGAACGGCATCAAGGTGAACTTCAAGATCCGCCACAACATCGAGGACGGCAGC
GTGCAGCTCGCCGACCACTACCAGCAGAACACCCCCATCGGCGACGGCCCCGTGCTGCTGCCCGACAACCACTACCTGAG
CACCCAGTCCGCCCTGAGCAAAGACCCCAACGAGAAGCGCGATCACATGGTCCTGCTGGAGTTCGTGACCGCCGCCGGGA
TCACTCTCGGCATGGACGAGCTGTACAAGACAAACACAATTACTTCAGACTTTACAACATCCACAGATAGGTTTTATCCA
GGCACGCTGTCTAGCTTTCAAACTGATAGTATCAACAACGATGCTAAAAGCAGTCTCAGAAGTAGATTATATGACCTATA
TCCTAGAAGGAAGGAAACAACATCGGATAAACATTCGGAAAGAACTTTTGTTTCTGAGACTGCAGATGATATAGAGAAAA
ATCAGTTTTATCAGTTGCCCACACCTACGAGTTCAAAAAATACTAGGATAGGACCGTTTGCTGATGCAAGTTACAAAGAG
GGAGAAGTTGAACCCGTCGACATGTACACTCCCGATACGGCAGCTGATGAGGAAGCCAGAAAGTTCTGGACTGAAGATAA
TAATAATTTATAAgactacaaggacgacgatgacaagaccggtgtgccgcgcggcagcggcagcagccatcatcatcatc
atcatagcagcggctaa
```

Figure D.2 Coding sequence of Ste2p[EGFP]305-431 construct. EGFP (1-238) sequence, highlighted with yellow is inserted between 912 – 913th residues inframe with the coding sequence corresponding to 304 – 305th positions on Ste2p receptor, a "TAA" stop codon was inserted before FLAG™ and His_6 sequences at 1293rd position on STE2.

Ste2pP290D[EGFP]

```
ATGTCTGATGCGGCTCCTTCATTGAGCAATCTATTTTATGATCCAACGTATAATCCTGGTCAAAGCACCATTAACTACAC
TTCCATATATGGGAATGGATCTACCATCACTTTCGATGAGTTGCAAGGTTTAGTTAACAGTACTGTTACTCAGGCCATTA
TGTTTGGTGTCAGATGTGGTGCAGCTGCTTTGACTTTGATTGTCATGTGGATGACATCGAGAAGCAGAAAAACGCCGATT
TTCATTATCAACCAAGTTTCATTGTTTTTAATCATTTTGCATTCTGCACTCTATTTTAAATATTTACTGTCTAATTACTC
TTCAGTGACTTACGCTCTCACCGGATTTCCTCAGTTCATCAGTAGAGGTGACGTTCATGTTTATGGTGCTACAAATATAA
TTCAAGTCCTTCTTGTGGCTTCTATTGAGACTTCACTGGTGTTTCAGATAAAAGTTATTTTCACAGGCGACAACTTCAAA
AGGATAGGTTTGATGCTGACGTCGATATCTTTCACTTTAGGGATTGCTACAGTTACCATGTATTTTGTAAGCGCTGTTAA
AGGTATGATTGTGACTTATAATGATGTTAGTGCCACCCAAGATAAATACTTCAATGCATCCACAATTTTACTTGCATCCT
CAATAAACTTTATGTCATTTGTCCTGGTAGTTAAATTGATTTTAGCTATTAGATCAAGAAGATTCCTTGGTCTCAAGCAG
TTCGATAGTTTCCATATTTTACTCATAATGTCATGTCAATCTTTGTTGGTTCCATCGATAATATTCATCCTCGCATACAG
TTTGAAACCAAACCAGGGAACAGATGTCTTGACTACTGTTGCAACATTACTTGCTGTATTGTCTTTAGATTTATCATCAA
TGTGGGCCACGGCTGCTAATAATGCATCCAAAATGGTGAGCAAGGGCGAGGAGCTGTTCACCGGGGTGGTGCCCATCCTG
GTCGAGCTGGACGGCGACGTAAACGGCCACAAGTTCAGCGTGTCCGGCGAGGGCGAGGGCGATGCCACCTACGGCAAGCT
GACCCTGAAGTTCATCTGCACCACCGGCAAGCTGCCCGTGCCCTGGCCCACCCTCGTGACCACCCTGACCTACGGCGTGC
AGTGCTTCAGCCGCTACCCCGACCACATGAAGCAGCACGACTTCTTCAAGTCCGCCATGCCCGAAGGCTACGTCCAGGAG
CGCACCATCTTCTTCAAGGACGACGGCAACTACAAGACCCGCGCCGAGGTGAAGTTCGAGGGCGACACCCTGGTGAACCG
CATCGAGCTGAAGGGCATCGACTTCAAGGAGGACGGCAACATCCTGGGGCACAAGCTGGAGTACAACTACAACAGCCACA
ACGTCTATATCATGGCCGACAAGCAGAAGAACGGCATCAAGGTGAACTTCAAGATCCGCCACAACATCGAGGACGGCAGC
GTGCAGCTCGCCGACCACTACCAGCAGAACACCCCCATCGGCGACGGCCCCGTGCTGCTGCCCGACAACCACTACCTGAG
CACCCAGTCCGCCCTGAGCAAAGACCCCAACGAGAAGCGCGATCACATGGTCCTGCTGGAGTTCGTGACCGCCGCCGGGA
TCACTCTCGGCATGGACGAGCTGTACAAGTAAACAAACACAATTACTTCAGACTTTACAACATCCACAGATAGGTTTTAT
CCAGGCACGCTGTCTAGCTTTCAAACTGATAGTATCAACAACGATGCTAAAAGCAGTCTCAGAAGTAGATTATATGACCT
ATATCCTAGAAGGAAGGAAACAACATCGGATAAACATTCGGAAAGAACTTTTGTTTCTGAGACTGCAGATGATATAGAGA
AAAATCAGTTTTATCAGTTGCCCACACCTACGAGTTCAAAAAATACTAGGATAGGACCGTTTGCTGATGCAAGTTACAAA
GAGGGAGAAGTTGAACCCGTCGACATGTACACTCCCGATACGGCAGCTGATGAGGAAGCCAGAAAGTTCTGGACTGAAGA
TAATAATAATTTAgactacaaggacgacgatgacaagaccggtgtgccgcgcggcagcggcagcagccatcatcatcatc
atcatagcagcggctaa
```

Figure D.3 Coding sequence of Ste2[EGFP] construct. EGFP (1-238) sequence, highlighted with yellow, carrying a “TAA” stop codon was inserted between 912 – 913th residues inframe with the coding sequence, corresponding to 304 – 305th positions on Ste2p receptor.

Ste2pP290D[N-EGFP]305-431

```
ATGTCTGATGCGGCTCCTTCATTGAGCAATCTATTTTATGATCCAACGTATAATCCTGGTCAAAGCACCATTAACTACAC
TTCCATATATGGGAATGGATCTACCATCACTTTCGATGAGTTGCAAGGTTTAGTTAACAGTACTGTTACTCAGGCCATTA
TGTTTGGTGTCAGATGTGGTGCAGCTGCTTTGACTTTGATTGTCATGTGGATGACATCGAGAAGCAGAAAAACGCCGATT
TTCATTATCAACCAAGTTTCATTGTTTTTAATCATTTTGCATTCTGCACTCTATTTTAAATATTTACTGTCTAATTACTC
TTCAGTGACTTACGCTCTCACCGGATTTCCTCAGTTCATCAGTAGAGGTGACGTTCATGTTTATGGTGCTACAAATATAA
TTCAAGTCCTTCTTGTGGCTTCTATTGAGACTTCACTGGTGTTTCAGATAAAAGTTATTTTCACAGGCGACAACTTCAAA
AGGATAGGTTTGATGCTGACGTCGATATCTTTCACTTTAGGGATTGCTACAGTTACCATGTATTTTGTAAGCGCTGTTAA
AGGTATGATTGTGACTTATAATGATGTTAGTGCCACCCAAGATAAATACTTCAATGCATCCACAATTTTACTTGCATCCT
CAATAAACTTTATGTCATTTGTCCTGGTAGTTAAATTGATTTTAGCTATTAGATCAAGAAGATTCCTTGGTCTCAAGCAG
TTCGATAGTTTCCATATTTTACTCATAATGTCATGTCAATCTTTGTTGGTTCCATCGATAATATTCATCCTCGCATACAG
TTTGAAACCAAACCAGGGAACAGATGTCTTGACTACTGTTGCAACATTACTTGCTGTATTGTCTTTAGATTTATCATCAA
TGTGGGCCACGGCTGCTAATAATGCATCCAAAATGGTGAGCAAGGGCGAGGAGCTGTTCACCGGGGTGGTGCCCATCCTG
GTCGAGCTGGACGGCGACGTAAACGGCCACAAGTTCAGCGTGTCCGGCGAGGGCGAGGGCGATGCCACCTACGGCAAGCT
GACCCTGAAGTTCATCTGCACCACCGGCAAGCTGCCCGTGCCCTGGCCCACCCTCGTGACCACCCTGACCTACGGCGTGC
AGTGCTTCAGCCGCTACCCCGACCACATGAAGCAGCACGACTTCTTCAAGTCCGCCATGCCCGAAGGCTACGTCCAGGAG
CGCACCATCTTCTTCAAGGACGACGGCAACTACAAGACCCGCGCCGAGGTGAAGTTCGAGGGCGACACCCTGGTGAACCG
CATCGAGCTGAAGGGCATCGACTTCAAGGAGGACGGCAACATCCTGGGGCACAAGCTGGAGTACAACTACAACAGCCACA
ACGTCTATATCATGGCCGACAAGCAGACAAACACAATTACTTCAGACTTTACAACATCCACAGATAGGTTTTATCCAGGC
ACGCTGTCTAGCTTTCAAACTGATAGTATCAACAACGATGCTAAAAGCAGTCTCAGAAGTAGATTATATGACCTATATCC
TAGAAGGAAGGAAACAACATCGGATAAACATTCGGAAAGAACTTTTGTTTCTGAGACTGCAGATGATATAGAGAAAAATC
AGTTTTATCAGTTGCCCACACCTACGAGTTCAAAAAATACTAGGATAGGACCGTTTGCTGATGCAAGTTACAAAGAGGGA
GAAGTTGAACCCGTCGACATGTACACTCCCGATACGGCAGCTGATGAGGAAGCCAGAAAGTTCTGGACTGAAGATAATAA
TAATTTATAAgactacaaggacgacgatgacaagaccggtgtgccgcgcggcagcggcagcagccatcatcatcatcatc
atagcagcggctaa
```

Figure D.5 Coding sequence of Ste2p[N-EGFP]305-431 construct. N-EGFP (1-158) sequence, highlighted with yellow is inserted between 912 – 913th residues inframe with the coding sequence corresponding to 304 – 305th positions on Ste2p receptor, a "TAA" stop codon was inserted before FLAG^{TM} and His$_6$ sequences at 1293rd position on STE2.

Ste2pP290D[C-EGFP]305-431

```
ATGTCTGATGCGGCTCCTTCATTGAGCAATCTATTTTATGATCCAACGTATAATCCTGGTCAAAGCACCATTAACTACAC
TTCCATATATGGGAATGGATCTACCATCACTTTCGATGAGTTGCAAGGTTTAGTTAACAGTACTGTTACTCAGGCCATTA
TGTTTGGTGTCAGATGTGGTGCAGCTGCTTTGACTTTGATTGTCATGTGGATGACATCGAGAAGCAGAAAAACGCCGATT
TTCATTATCAACCAAGTTTCATTGTTTTTAATCATTTTGCATTCTGCACTCTATTTTAAATATTTACTGTCTAATTACTC
TTCAGTGACTTACGCTCTCACCGGATTTCCTCAGTTCATCAGTAGAGGTGACGTTCATGTTTATGGTGCTACAAATATAA
TTCAAGTCCTTCTTGTGGCTTCTATTGAGACTTCACTGGTGTTTCAGATAAAAGTTATTTTCACAGGCGACAACTTCAAA
AGGATAGGTTTGATGCTGACGTCGATATCTTTCACTTTAGGGATTGCTACAGTTACCATGTATTTTGTAAGCGCTGTTAA
AGGTATGATTGTGACTTATAATGATGTTAGTGCCACCCAAGATAAATACTTCAATGCATCCACAATTTTACTTGCATCCT
CAATAAACTTTATGTCATTTGTCCTGGTAGTTAAATTGATTTTAGCTATTAGATCAAGAAGATTCCTTGGTCTCAAGCAG
TTCGATAGTTTCCATATTTTACTCATAATGTCATGTCAATCTTTGTTGGTTCCATCGATAATATTCATCCTCGCATACAG
TTTGAAACCAAACCAGGGAACAGATGTCTTGACTACTGTTGCAACATTACTTGCTGTATTGTCTTTAGATTTATCATCAA
TGTGGGCCACGGCTGCTAATAATGCATCCAAAAAGAACGGCATCAAGGTGAACTTCAAGATCCGCCACAACATCGAGGAC
GGCAGCGTGCAGCTCGCCGACCACTACCAGCAGAACACCCCCATCGGCGACGGCCCCGTGCTGCTGCCCGACAACCACTA
CCTGAGCACCCAGTCCGCCCTGAGCAAAGACCCCAACGAGAAGCGCGATCACATGGTCCTGCTGGAGTTCGTGACCGCCG
CCGGGATCACTCTCGGCATGGACGAGCTGTACAAGACAAACACAATTACTTCAGACTTTACAACATCCACAGATAGGTTT
TATCCAGGCACGCTGTCTAGCTTTCAAACTGATAGTATCAACAACGATGCTAAAAGCAGTCTCAGAAGTAGATTATATGA
CCTATATCCTAGAAGGAAGGAAACAACATCGGATAAACATTCGGAAAGAACTTTTGTTTCTGAGACTGCAGATGATATAG
AGAAAAATCAGTTTTATCAGTTGCCCACACCTACGAGTTCAAAAAATACTAGGATAGGACCGTTTGCTGATGCAAGTTAC
AAAGAGGGAGAAGTTGAACCCGTCGACATGTACACTCCCGATACGGCAGCTGATGAGGAAGCCAGAAAGTTCTGGACTGA
AGATAATAATAATTTATAAgactacaaggacgacgatgacaagaccggtgtgccgcgcggcagcggcagcagccatcatc
atcatcatcatagcagcggctaa
```

Figure D.7 Coding sequence of Ste2p[C-EGFP]305-431 construct. C-EGFP (159-238) sequence, highlighted with yellow is inserted between 912 – 913th residues inframe with the coding sequence corresponding to 304 – 305th positions on Ste2p receptor, a “TAA” stop codon was inserted before FLAG™ and His_6 sequences at 1293rd position on STE2.

Ste2pP290D[N-EGFP]

```
ATGTCTGATGCGGCTCCTTCATTGAGCAATCTATTTTATGATCCAACGTATAATCCTGGTCAAAGCACCATTAACTACAC
TTCCATATATGGGAATGGATCTACCATCACTTTCGATGAGTTGCAAGGTTTAGTTAACAGTACTGTTACTCAGGCCATTA
TGTTTGGTGTCAGATGTGGTGCAGCTGCTTTGACTTTGATTGTCATGTGGATGACATCGAGAAGCAGAAAAACGCCGATT
TTCATTATCAACCAAGTTTCATTGTTTTTAATCATTTTGCATTCTGCACTCTATTTTAAATATTTACTGTCTAATTACTC
TTCAGTGACTTACGCTCTCACCGGATTTCCTCAGTTCATCAGTAGAGGTGACGTTCATGTTTATGGTGCTACAAATATAA
TTCAAGTCCTTCTTGTGGCTTCTATTGAGACTTCACTGGTGTTTCAGATAAAAGTTATTTTCACAGGCGACAACTTCAAA
AGGATAGGTTTGATGCTGACGTCGATATCTTTCACTTTAGGGATTGCTACAGTTACCATGTATTTTGTAAGCGCTGTTAA
AGGTATGATTGTGACTTATAATGATGTTAGTGCCACCCAAGATAAATACTTCAATGCATCCACAATTTTACTTGCATCCT
CAATAAACTTTATGTCATTTGTCCTGGTAGTTAAATTGATTTTAGCTATTAGATCAAGAAGATTCCTTGGTCTCAAGCAG
TTCGATAGTTTCCATATTTTACTCATAATGTCATGTCAATCTTTGTTGGTTCCATCGATAATATTCATCCTCGCATACAG
TTTGAAACCAAACCAGGGAACAGATGTCTTGACTACTGTTGCAACATTACTTGCTGTATTGTCTTTAGATTTATCATCAA
TGTGGGCCACGGCTGCTAATAATGCATCCAAAATGGTGAGCAAGGGCGAGGAGCTGTTCACCGGGGTGGTGCCCATCCTG
GTCGAGCTGGACGGCGACGTAAACGGCCACAAGTTCAGCGTGTCCGGCGAGGGCGAGGGCGATGCCACCTACGGCAAGCT
GACCCTGAAGTTCATCTGCACCACCGGCAAGCTGCCCGTGCCCTGGCCCACCCTCGTGACCACCCTGACCTACGGCGTGC
AGTGCTTCAGCCGCTACCCCGACCACATGAAGCAGCACGACTTCTTCAAGTCCGCCATGCCCGAAGGCTACGTCCAGGAG
CGCACCATCTTCTTCAAGGACGACGGCAACTACAAGACCCGCGCCGAGGTGAAGTTCGAGGGCGACACCCTGGTGAACCG
CATCGAGCTGAAGGGCATCGACTTCAAGGAGGACGGCAACATCCTGGGGCACAAGCTGGAGTACAACTACAACAGCCACA
ACGTCTATATCATGGCCGACAAGCAGTAAACAAACACAATTACTTCAGACTTTACAACATCCACAGATAGGTTTTATCCA
GGCACGCTGTCTAGCTTTCAAACTGATAGTATCAACAACGATGCTAAAAGCAGTCTCAGAAGTAGATTATATGACCTATA
TCCTAGAAGGAAGGAAACAACATCGGATAAACATTCGGAAAGAACTTTTGTTTCTGAGACTGCAGATGATATAGAGAAAA
ATCAGTTTTATCAGTTGCCCACACCTACGAGTTCAAAAAATACTAGGATAGGACCGTTTGCTGATGCAAGTTACAAAGAG
GGAGAAGTTGAACCCGTCGACATGTACACTCCCGATACGGCAGCTGATGAGGAAGCCAGAAAGTTCTGGACTGAAGATAA
TAATAATTTAgactacaaggacgacgatgacaagaccggtgtgccgcgcggcagcggcagcagccatcatcatcatcatc
atagcagcggctaa
```

Figure D.8 Coding sequence of Ste2p[N-EGFP] construct. N-EGFP (1-158) sequence, highlighted with yellow carrying a “TAA” stop codon was inserted between 912 – 913th residues inframe with the coding sequence, corresponding to 304 – 305th positions on Ste2p receptor.

Ste2pP290D[C-EGFP]

```
ATGTCTGATGCGGCTCCTTCATTGAGCAATCTATTTTATGATCCAACGTATAATCCTGGTCAAAGCACCATTAACTACAC
TTCCATATATGGGAATGGATCTACCATCACTTTCGATGAGTTGCAAGGTTTAGTTAACAGTACTGTTACTCAGGCCATTA
TGTTTGGTGTCAGATGTGGTGCAGCTGCTTTGACTTTGATTGTCATGTGGATGACATCGAGAAGCAGAAAAACGCCGATT
TTCATTATCAACCAAGTTTCATTGTTTTTAATCATTTTGCATTCTGCACTCTATTTTAAATATTTACTGTCTAATTACTC
TTCAGTGACTTACGCTCTCACCGGATTTCCTCAGTTCATCAGTAGAGGTGACGTTCATGTTTATGGTGCTACAAATATAA
TTCAAGTCCTTCTTGTGGCTTCTATTGAGACTTCACTGGTGTTTCAGATAAAAGTTATTTTCACAGGCGACAACTTCAAA
AGGATAGGTTTGATGCTGACGTCGATATCTTTCACTTTAGGGATTGCTACAGTTACCATGTATTTTGTAAGCGCTGTTAA
AGGTATGATTGTGACTTATAATGATGTTAGTGCCACCCAAGATAAATACTTCAATGCATCCACAATTTTACTTGCATCCT
CAATAAACTTTATGTCATTTGTCCTGGTAGTTAAATTGATTTTAGCTATTAGATCAAGAAGATTCCTTGGTCTCAAGCAG
TTCGATAGTTTCCATATTTTACTCATAATGTCATGTCAATCTTTGTTGGTTCCATCGATAATATTCATCCTCGCATACAG
TTTGAAACCAAACCAGGGAACAGATGTCTTGACTACTGTTGCAACATTACTTGCTGTATTGTCTTTAGATTTATCATCAA
TGTGGGCCACGGCTGCTAATAATGCATCCAAAAAGAACGGCATCAAGGTGAACTTCAAGATCCGCCACAACATCGAGGAC
GGCAGCGTGCAGCTCGCCGACCACTACCAGCAGAACACCCCCATCGGCGACGGCCCCGTGCTGCTGCCCGACAACCACTA
CCTGAGCACCCAGTCCGCCCTGAGCAAAGACCCCAACGAGAAGCGCGATCACATGGTCCTGCTGGAGTTCGTGACCGCCG
CCGGGATCACTCTCGGCATGGACGAGCTGTACAAGTAAACAAACACAATTACTTCAGACTTTACAACATCCACAGATAGG
TTTTATCCAGGCACGCTGTCTAGCTTTCAAACTGATAGTATCAACAACGATGCTAAAAGCAGTCTCAGAAGTAGATTATA
TGACCTATATCCTAGAAGGAAGGAAACAACATCGGATAAACATTCGGAAAGAACTTTTGTTTCTGAGACTGCAGATGATA
TAGAGAAAAATCAGTTTTATCAGTTGCCCACACCTACGAGTTCAAAAAATACTAGGATAGGACCGTTTGCTGATGCAAGT
TACAAAGAGGGAGAAGTTGAACCCGTCGACATGTACACTCCCGATACGGCAGCTGATGAGGAAGCCAGAAAGTTCTGGAC
TGAAGATAATAATAATTTAgactacaaggacgacgatgacaagaccggtgtgccgcgcggcagcggcagcagccatcatc
atcatcatcatagcagcggctaa
```

Figure D.7 Coding sequence of Ste2p[C-EGFP] construct. C-EGFP (159-238) sequence, highlighted with yellow carrying a “TAA” stop codon was inserted between 912 – 913th residues inframe with the coding sequence, corresponding to 304 – 305th positions on Ste2p receptor.

Ste2p[mCherry]305-451

```
ATGTCTGATGCGGCTCCTTCATTGAGCAATCTATTTTATGATCCAACGTATAATCCTGGTCAAAGCACCATTAACTACAC
TTCCATATATGGGAATGGATCTACCATCACTTTCGATGAGTTGCAAGGTTTAGTTAACAGTACTGTTACTCAGGCCATTA
TGTTTGGTGTCAGATGTGGTGCAGCTGCTTTGACTTTGATTGTCATGTGGATGACATCGAGAAGCAGAAAAACGCCGATT
TTCATTATCAACCAAGTTTCATTGTTTTTAATCATTTTGCATTCTGCACTCTATTTTAAATATTTACTGTCTAATTACTC
TTCAGTGACTTACGCTCTCACCGGATTTCCTCAGTTCATCAGTAGAGGTGACGTTCATGTTTATGGTGCTACAAATATAA
TTCAAGTCCTTCTTGTGGCTTCTATTGAGACTTCACTGGTGTTTCAGATAAAAGTTATTTTCACAGGCGACAACTTCAAA
AGGATAGGTTTGATGCTGACGTCGATATCTTTCACTTTAGGGATTGCTACAGTTACCATGTATTTTGTAAGCGCTGTTAA
AGGTATGATTGTGACTTATAATGATGTTAGTGCCACCCAAGATAAATACTTCAATGCATCCACAATTTTACTTGCATCCT
CAATAAACTTTATGTCATTTGTCCTGGTAGTTAAATTGATTTTAGCTATTAGATCAAGAAGATTCCTTGGTCTCAAGCAG
TTCGATAGTTTCCATATTTTACTCATAATGTCATGTCAATCTTTGTTGGTTCCATCGATAATATTCATCCTCGCATACAG
TTTGAAACCAAACCAGGGAACAGATGTCTTGACTACTGTTGCAACATTACTTGCTGTATTGTCTTTACCATTATCATCAA
TGTGGGCCACGGCTGCTAATAATGCATCCAAAatggtgagcaagggcgaggaggataacatggccatcatcaaggagttc
atgcgcttcaaggtgcacatggagggctccgtgaacggccacgagttcgagatcgagggcgagggcgagggccgcccctа
cgagggcacccagaccgccaagctgaaggtgaccaagggtggccccctgcccttcgcctgggacatcctgtcccctcagt
tcatgtacggctccaaggcctacgtgaagcaccccgccgacatccccgactacttgaagctgtccttccccgagggcttc
aagtgggagcgcgtgatgaacttcgaggacggcggcgtggtgaccgtgacccaggactcctccctgcaggacggcgagtt
catctacaaggtgaagctgcgcggcaccaacttcccctccgacggccccgtaatgcagaagaagaccatgggctgggagg
cctcctccgagcggatgtaccccgaggacggcgccctgaagggcgagatcaagcagaggctgaagctgaaggacggcggc
cactacgacgctgaggtcaagaccacctacaaggccaagaagcccgtgcagctgcccggcgcctacaacgtcaacatcaa
gttggacatcacctcccacaacgaggactacaccatcgtggaacagtacgaacgcgccgagggccgccactccaccggcg
gcatggacgagctgtacaagACAAACACAATTACTTCAGACTTTACAACATCCACAGATAGGTTTTATCCAGGCACGCTG
TCTAGCTTTCAAACTGATAGTATCAACAACGATGCTAAAAGCAGTCTCAGAAGTAGATTATATGACCTATATCCTAGAAG
GAAGGAAACAACATCGGATAAACATTCGGAAAGAACTTTTGTTTCTGAGACTGCAGATGATATAGAGAAAAATCAGTTTT
ATCAGTTGCCCACACCTACGAGTTCAAAAAATACTAGGATAGGACCGTTTGCTGATGCAAGTTACAAAGAGGGAGAAGTT
GAACCCGTCGACATGTACACTCCCGATACGGCAGCTGATGAGGAAGCCAGAAAGTTCTGGACTGAAGATAATAATAATTT
Agactacaaggacgacgatgacaagaccggtgtgccgcgcggcagcggcagcagccatcatcatcatcatcatagcagcg
gctaa
```

Figure D.11 Coding sequence of Ste2p[mCherry]305-451 construct. mCherry (1-237) sequence, highlighted with red is inserted between 912 – 913th residues inframe with the coding sequence corresponding to 304 – 305th positions on Ste2p receptor. , a “TAA” stop codon was inserted before FLAG$^{\text{TM}}$ and His$_6$ sequences at 1293rd position on STE2.

Ste2p[mCherry]305-431

```
ATGTCTGATGCGGCTCCTTCATTGAGCAATCTATTTTATGATCCAACGTATAATCCTGGTCAAAGCACCATTAACTACAC
TTCCATATATGGGAATGGATCTACCATCACTTTCGATGAGTTGCAAGGTTTAGTTAACAGTACTGTTACTCAGGCCATTA
TGTTTGGTGTCAGATGTGGTGCAGCTGCTTTGACTTTGATTGTCATGTGGATGACATCGAGAAGCAGAAAAACGCCGATT
TTCATTATCAACCAAGTTTCATTGTTTTTAATCATTTTGCATTCTGCACTCTATTTTAAATATTTACTGTCTAATTACTC
TTCAGTGACTTACGCTCTCACCGGATTTCCTCAGTTCATCAGTAGAGGTGACGTTCATGTTTATGGTGCTACAAATATAA
TTCAAGTCCTTCTTGTGGCTTCTATTGAGACTTCACTGGTGTTTCAGATAAAAGTTATTTTCACAGGCGACAACTTCAAA
AGGATAGGTTTGATGCTGACGTCGATATCTTTCACTTTAGGGATTGCTACAGTTACCATGTATTTTGTAAGCGCTGTTAA
AGGTATGATTGTGACTTATAATGATGTTAGTGCCACCCAAGATAAATACTTCAATGCATCCACAATTTTACTTGCATCCT
CAATAAACTTTATGTCATTTGTCCTGGTAGTTAAATTGATTTTAGCTATTAGATCAAGAAGATTCCTTGGTCTCAAGCAG
TTCGATAGTTTCCATATTTTACTCATAATGTCATGTCAATCTTTGTTGGTTCCATCGATAATATTCATCCTCGCATACAG
TTTGAAACCAAACCAGGGAACAGATGTCTTGACTACTGTTGCAACATTACTTGCTGTATTGTCTTTACCATTATCATCAA
TGTGGGCCACGGCTGCTAATAATGCATCCAAAatggtgagcaagggcgaggaggataacatggccatcatcaaggagttc
atgcgcttcaaggtgcacatggagggctccgtgaacggccacgagttcgagatcgagggcgagggcgagggccgcccta
cgagggcacccagaccgccaagctgaaggtgaccaagggtggccccctgcccttcgcctgggacatcctgtcccctcagt
tcatgtacggctccaaggcctacgtgaagcaccccgccgacatccccgactacttgaagctgtccttccccgagggcttc
aagtgggagcgcgtgatgaacttcgaggacggcggcgtggtgaccgtgacccaggactcctccctgcaggacggcgagtt
catctacaaggtgaagctgcgcggcaccaacttcccctccgacggccccgtaatgcagaagaagaccatgggctgggagg
cctcctccgagcggatgtaccccgaggacggcgccctgaagggcgagatcaagcagaggctgaagctgaaggacggcggc
cactacgacgctgaggtcaagaccacctacaaggccaagaagcccgtgcagctgcccggcgcctacaacgtcaacatcaa
gttggacatcacctcccacaacgaggactacaccatcgtggaacagtacgaacgcgccgagggccgccactccaccggcg
gcatggacgagctgtacaagACAAACACAATTACTTCAGACTTTACAACATCCACAGATAGGTTTTATCCAGGCACGCTG
TCTAGCTTTCAAACTGATAGTATCAACAACGATGCTAAAAGCAGTCTCAGAAGTAGATTATATGACCTATATCCTAGAAG
GAAGGAAACAACATCGGATAAACATTCGGAAAGAACTTTTGTTTCTGAGACTGCAGATGATATAGAGAAAAATCAGTTTT
ATCAGTTGCCCACACCTACGAGTTCAAAAAATACTAGGATAGGACCGTTTGCTGATGCAAGTTACAAAGAGGGAGAAGTT
GAACCCGTCGACATGTACACTCCCGATACGGCAGCTGATGAGGAAGCCAGAAAGTTCTGGACTGAAGATAATAATAATTT
Ataa
```

Figure D.12 Coding sequence of Ste2p[mCherry]305-451 construct. mCherry (1-237) sequence, highlighted with red is inserted between 912 – 913th residues inframe with the coding sequence corresponding to 304 – 305th positions on Ste2p receptor, a “TAA” stop codon was inserted before FLAG^{TM} and His$_6$ sequences at 1293rd position on STE2.

Ste2p[mCherry]

```
ATGTCTGATGCGGCTCCTTCATTGAGCAATCTATTTTATGATCCAACGTATAATCCTGGTCAAAGCACCATTAACTACAC
TTCCATATATGGGAATGGATCTACCATCACTTTCGATGAGTTGCAAGGTTTAGTTAACAGTACTGTTACTCAGGCCATTA
TGTTTGGTGTCAGATGTGGTGCAGCTGCTTTGACTTTGATTGTCATGTGGATGACATCGAGAAGCAGAAAAACGCCGATT
TTCATTATCAACCAAGTTTCATTGTTTTTAATCATTTTGCATTCTGCACTCTATTTTAAATATTTACTGTCTAATTACTC
TTCAGTGACTTACGCTCTCACCGGATTTCCTCAGTTCATCAGTAGAGGTGACGTTCATGTTTATGGTGCTACAAATATAA
TTCAAGTCCTTCTTGTGGCTTCTATTGAGACTTCACTGGTGTTTCAGATAAAAGTTATTTTCACAGGCGACAACTTCAAA
AGGATAGGTTTGATGCTGACGTCGATATCTTTCACTTTAGGGATTGCTACAGTTACCATGTATTTTGTAAGCGCTGTTAA
AGGTATGATTGTGACTTATAATGATGTTAGTGCCACCCAAGATAAATACTTCAATGCATCCACAATTTTACTTGCATCCT
CAATAAACTTTATGTCATTTGTCCTGGTAGTTAAATTGATTTTAGCTATTAGATCAAGAAGATTCCTTGGTCTCAAGCAG
TTCGATAGTTTCCATATTTTACTCATAATGTCATGTCAATCTTTGTTGGTTCCATCGATAATATTCATCCTCGCATACAG
TTTGAAACCAAACCAGGGAACAGATGTCTTGACTACTGTTGCAACATTACTTGCTGTATTGTCTTTACCATTATCATCAA
TGTGGGCCACGGCTGCTAATAATGCATCCAAAatggtgagcaagggcgaggaggataacatggccatcatcaaggagttc
atgcgcttcaaggtgcacatggagggctccgtgaacggccacgagttcgagatcgagggcgagggcgagggccgcccccta
cgagggcacccagaccgccaagctgaaggtgaccaagggtggccccctgcccttcgcctgggacatcctgtcccctcagt
tcatgtacggctccaaggcctacgtgaagcaccccgccgacatccccgactacttgaagctgtccttccccgagggcttc
aagtgggagcgcgtgatgaacttcgaggacggcggcgtggtgaccgtgacccaggactcctccctgcaggacggcgagtt
catctacaaggtgaagctgcgcggcaccaacttcccctccgacggccccgtaatgcagaagaagaccatgggctgggagg
cctcctccgagcggatgtaccccgaggacggcgccctgaagggcgagatcaagcagaggctgaagctgaaggacggcggc
cactacgacgctgaggtcaagaccacctacaaggccaagaagcccgtgcagctgcccggcgcctacaacgtcaacatcaa
gttggacatcacctcccacaacgaggactacaccatcgtggaacagtacgaacgcgccgagggccgccactccaccggcg
gcatggacgagctgtacaagTAG
```

Figure D.13 Coding sequence of Ste2[mCherry] construct. mCherry (1-237) sequence, highlighted with red, carrying a “TAA” stop codon was inserted between 912 – 913th residues inframe with the coding sequence, corresponding to 304 – 305th positions on Ste2p receptor.

Ste2p[N-mCherry]

```
ATGTCTGATGCGGCTCCTTCATTGAGCAATCTATTTTATGATCCAACGTATAATCCTGGTCAAAGCACCATTAACTACAC
TTCCATATATGGGAATGGATCTACCATCACTTTCGATGAGTTGCAAGGTTTAGTTAACAGTACTGTTACTCAGGCCATTA
TGTTTGGTGTCAGATGTGGTGCAGCTGCTTTGACTTTGATTGTCATGTGGATGACATCGAGAAGCAGAAAAACGCCGATT
TTCATTATCAACCAAGTTTCATTGTTTTTAATCATTTTGCATTCTGCACTCTATTTTAAATATTTACTGTCTAATTACTC
TTCAGTGACTTACGCTCTCACCGGATTTCCTCAGTTCATCAGTAGAGGTGACGTTCATGTTTATGGTGCTACAAATATAA
TTCAAGTCCTTCTTGTGGCTTCTATTGAGACTTCACTGGTGTTTCAGATAAAAGTTATTTTCACAGGCGACAACTTCAAA
AGGATAGGTTTGATGCTGACGTCGATATCTTTCACTTTAGGGATTGCTACAGTTACCATGTATTTTGTAAGCGCTGTTAA
AGGTATGATTGTGACTTATAATGATGTTAGTGCCACCCAAGATAAATACTTCAATGCATCCACAATTTTACTTGCATCCT
CAATAAACTTTATGTCATTTGTCCTGGTAGTTAAATTGATTTTAGCTATTAGATCAAGAAGATTCCTTGGTCTCAAGCAG
TTCGATAGTTTCCATATTTTACTCATAATGTCATGTCAATCTTTGTTGGTTCCATCGATAATATTCATCCTCGCATACAG
TTTGAAACCAAACCAGGGAACAGATGTCTTGACTACTGTTGCAACATTACTTGCTGTATTGTCTTTACCATTATCATCAA
TGTGGGCCACGGCTGCTAATAATGCATCCAAAatggtgagcaagggcgaggaggataacatggccatcatcaaggagttc
atgcgcttcaaggtgcacatggagggctccgtgaacggccacgagttcgagatcgagggcgagggcgagggccgcccta
cgagggcacccagaccgccaagctgaaggtgaccaagggtggccccctgcccttcgcctgggacatcctgtcccctcagt
tcatgtacggctccaaggcctacgtgaagcaccccgccgacatccccgactacttgaagctgtccttccccgagggcttc
aagtgggagcgcgtgatgaacttcgaggacggcggcgtggtgaccgtgacccaggactcctccctgcaggacggcgagtt
catctacaaggtgaagctgcgcggcaccaacttcccctccgacggccccgtaatgcagaagaagaccatgggctgggagg
cctcctccgagcggatgtaccccgaggactag
```

Figure D.14 Coding sequence of Ste2p[N-mCherry] construct. N-mCherry (1-159) sequence, highlighted with red carrying a “TAG” stop codon was inserted between 912 – 913th residues inframe with the coding sequence, corresponding to 304 – 305th positions on Ste2p receptor.

Ste2p[C-mCherry]

```
ATGTCTGATGCGGCTCCTTCATTGAGCAATCTATTTTATGATCCAACGTATAATCCTGGTCAAAGCACCATTAACTACAC
TTCCATATATGGGAATGGATCTACCATCACTTTCGATGAGTTGCAAGGTTTAGTTAACAGTACTGTTACTCAGGCCATTA
TGTTTGGTGTCAGATGTGGTGCAGCTGCTTTGACTTTGATTGTCATGTGGATGACATCGAGAAGCAGAAAAACGCCGATT
TTCATTATCAACCAAGTTTCATTGTTTTTAATCATTTTGCATTCTGCACTCTATTTTAAATATTTACTGTCTAATTACTC
TTCAGTGACTTACGCTCTCACCGGATTTCCTCAGTTCATCAGTAGAGGTGACGTTCATGTTTATGGTGCTACAAATATAA
TTCAAGTCCTTCTTGTGGCTTCTATTGAGACTTCACTGGTGTTTCAGATAAAAGTTATTTTCACAGGCGACAACTTCAAA
AGGATAGGTTTGATGCTGACGTCGATATCTTTCACTTTAGGGATTGCTACAGTTACCATGTATTTTGTAAGCGCTGTTAA
AGGTATGATTGTGACTTATAATGATGTTAGTGCCACCCAAGATAAATACTTCAATGCATCCACAATTTTACTTGCATCCT
CAATAAACTTTATGTCATTTGTCCTGGTAGTTAAATTGATTTTAGCTATTAGATCAAGAAGATTCCTTGGTCTCAAGCAG
TTCGATAGTTTCCATATTTTACTCATAATGTCATGTCAATCTTTGTTGGTTCCATCGATAATATTCATCCTCGCATACAG
TTTGAAACCAAACCAGGGAACAGATGTCTTGACTACTGTTGCAACATTACTTGCTGTATTGTCTTTACCATTATCATCAA
TGTGGGCCACGGCTGCTAATAATGCATCCAAAggcgccctgaagggcgagatcaagcagaggctgaagctgaaggacggc
ggccactacgacgctgaggtcaagaccacctacaaggccaagaagcccgtgcagctgcccggcgcctacaacgtcaacat
caagttggacatcacctcccacaacgaggactacaccatcgtggaacagtacgaacgcgccgagggccgccactccaccg
gcggcatggacgagctgtacaagtag
```

Figure D.15 Coding sequence of Ste2p[C-mCherry] construct. C-mCherry (160-237) sequence, highlighted with red carrying a “TAA” stop codon was inserted between 912 – 913th residues inframe with the coding sequence, corresponding to 304 – 305th positions on Ste2p receptor.

VITA

Orkun CEVHEROGLU

Work: Orta Doğu Teknik Üniversitesi, Fen-Edebiyat Fakültesi, Biyolojik Bilimler
Bölümü, No:253, 06800 Çankaya, Ankara, TURKEY
Mobile: +90 (532) 396 54 96
Email: ocevheroglu@gmail.com

Education

Middle East Technical University, Department of Biotechnology, Ankara, TURKEY ▪ PhD. program, Graduate School of Applied Sciences, Department of Biotechnology **Thesis title: More than just a dimer: Detection of G-protein coupled receptor oligomers using fluorescent protein reassembly of Ste2p, a yeast pheromone.**	Feb. 2008	Sep. 2015
Middle East Technical University, Department of Chemistry Ankara, TURKEY ▪ MSc program, Graduate School of Applied Sciences, Department of Chemistry (CGPA: 3.71/4.00) **Thesis title: Unexpected Cyclization of Dipyridyl-glycoluril in the Presence of Formaldehyde and Strong Acid: A New Scaffold with a Potential as an Anion Receptor.**	Sep. 2002	Aug. 2005
Middle East Technical University, Department of Chemistry, Ankara, TURKEY ▪ BSc. program, Faculty of Arts and Sciences, Department of Chemistry (CGPA: 3.46/4.00)	Sep. 1998	June 2002
TED Ankara College Foundation High School Ankara, TURKEY	Sep. 1995	June 1998

Experience

University of Tennessee, Knoxville, Knoxville, TN, USA ▪ Research specialist II	Sep. 2014	Apr. 2015
University of Tennessee, Knoxville, Knoxville, TN, USA ▪ PhD. scholar at Turkish Academy of Sciences, 2214/A program	Oct. 2013	Sep. 2014
Genera Biotechnology, Ankara, TURKEY ▪ Founding partner R&D on "Fluorescent tumor and neuronal markers for surgery", supported by Republic of Turkey Ministry of Science, Industry and Technology.	Dec. 2012	Dec. 2013
Middle East Technical University, Department of Biological Sciences, Ankara, TURKEY ▪ Research specialist Turkish Academy of Sciences, Grant no: 110T414 researcher.	June 2011	Sep. 2013
PCI Pharmaceuticals and Chemicals Co., Ankara, TURKEY ▪ Founding partner Product licensing and registration at Republic of Turkey, Ministry of Health and Presidency of Pharmaceuticals and Medicals.	June 2006	Oct. 2010
Middle East Technical University, Department of Chemistry, Ankara, TURKEY ▪ Research and Teaching Assistant.	Sep. 2002	Mar. 2011
Technischen Universität Darmstadt, Department of Chemistry, Darmstadt, Germany ▪ Workshop on “Coordination, Catalysis and Supramolecular Chemistry”.	Sep. 2001	Sep. 2001
Pfizer Manufacturing Italy, Rome, ITALY ▪ Intern	June 2001	Sep. 2001

Honors and awards

- Turkish Academy of Sciences 2214/A program scholarship for 12 months.

List of publications

- Cevheroglu, O., Becker, J.M., Son, C.D., More than just a dimer: Detection of G-protein coupled receptor oligomers using resonance energy transfer and fluorescent protein reassembly of Ste2p, a yeast pheromone, *manuscript in preparation*.

- More than just a dimer: Detection of G-protein coupled receptor oligomers using fluorescent protein reassembly of Ste2p, a yeast pheromone, 2015, PhD. thesis.

- Cevheroglu, O., Kumas, G., Hauser, M., Becker, J.M., Son, C.D., Detection of G Protein-Coupled Receptor Dimers Using Enhanced Green Fluorescent Protein Reassembly of Ste2p, A Yeast Pheromone Receptor, *manuscript submitted*.

- Unexpected Cyclization of Dipyridyl-glycoluril in the Presence of. Formaldehyde and Strong Acid: A New Scaffold with a Potential as a. Receptor, 2005, MSc. thesis.

- Saki, N.; Icli, B.; Cevheroglu, O, Akkaya, E.U., Unexpected Cyclization of Dipyridyl-glycoluril in the Presence of Formaldehyde and Strong Acid: A New Scaffold with a Potential as a Receptor. *"J. Inc. Phen. Macrocycl. Chem. "*, 55, (2006), p.219.